Universiteit Gent
Faculteit Ingenieurswetenschappen en Architectuur
Vakgroep Informatietechnologie

Stochastic Macromodeling for Efficient and Accurate Variability Analysis of Modern High-Speed Circuits

Stochastische Macromodellering voor Efficiënte en Nauwkeurige Variabiliteitsanalyse van Moderne Hogesnelheidsschakelingen

Domenico Spina

Universiteit Gent
Faculteit Ingenieurswetenschappen en Architectuur
Vakgroep Informatietechnologie

Promotoren: prof. dr. ir. Tom Dhaene
              prof. dr. ir. Luc Knockaert
              prof. dr. ing. Giulio Antonini

Universiteit Gent
Faculteit Ingenieurswetenschappen en Architectuur

Vakgroep Informatietechnologie
Gaston Crommenlaan 8 bus 201, B-9050 Gent, België

Tel.: +32-9-331.49.00
Fax.: +32-9-331.48.99

Università degli Studi dell'Aquila
Dipartimento di Ingegneria Industriale e
dell'Informazione e di Economia

Stochastic Macromodeling for Efficient and Accurate Variability Analysis of Modern High-Speed Circuits

Macromodellizazione Stocastica per una Efficiente ed Accurata Analisi di Variabilità di Moderni Circuiti ad Alta Velocità

Domenico Spina

SSD: ING-IND/31

Università degli Studi dell'Aquila
Dipartimento di Ingegneria Industriale e
dell'Informazione e di Economia

Coordinatore del corso:	prof. dr. ing. Giuseppe Ferri
Direttori di tesi:	prof. dr. ir. Tom Dhaene
	prof. dr. ir. Luc Knockaert
	prof. dr. ing. Giulio Antonini

Università degli Studi dell'Aquila

Dipartimento di Ingegneria Industriale e dell'Informazione e di Economia
Via G. Gronchi 18, 67100, LAquila, Italia

Acknowledgements

Alessandro, Tijana, Amparo, Adriàn, Conchi, Endre, Visnja, to the "Lost in Ghent" Nerea, Alfonso, Dani, Pepe, Olga, Michela, Raffaele, Teresa, Minerva, Diego, Tiago, Nathalia, Pedro, Ilaria. I want to thanks you all for each beer drinking, park barbecuing, Withecat dancing, Graslei chips eating, surprise partying moment that we spent together. I actually know that this list is way incomplete, but you are in it anyway and you know it (in my defense I am terrible at names!). Plus, being with you I am learning Spanish! Toma! Almost last, but not least, a special mention goes to the "superheroes" that I met during these years: a big thank you to "Mari" for the many dinners followed by endless talks when you listened to my ramblings over and over (and I can talk a lot!) and for being always ready to help me. I wish to thank "Tash", that I met in my ancient days as Erasmus student, when I was the mysterious Italian flat mate. Even if I woke you up several times laughing at Friends (the serial not the people) in the middle of the night and I shocked you hanging my strange colored underwear (by the way I threw them all) you were a friend to me since the beginning of this adventure and you are the kindest and nicest person that I met. To il "Maestro Supremo", pride of Ortona, ambassador of Abruzzo, the man who has been my flat mate for almost three years and yet survived to tell it, thanks for the countless hours spent doing funny jokes (even in dialect), for creating a small Abruzzo fortress in the foreign land of Ghent and for being such a nice friend. However, I will never forgive you for cooking arrosticini in the apartment while I was in Italy!

A special thanks goes out to all my old friends in Italy: Piero, Chiara, Elia, Maurizio, Francesco, Leonardo, Eleonora, Marilina, Lucia, Fratta, Sara, Silvia, Roberta, Davide, Dario, Massimo, Sabina, Luca, Vala, Enza, Mario and the Roseto gang and many others that I know since eons ago. Together we saw "things many people wouldn't believe: attack ships on fire off the shoulder of Orion and c-beams glitter in the dark near the Tannhauser Gate" (yes we are a bit nerdy inside). Together we faced many life changing phases from high school to adult life. I promise that my "verbo" will be with you for many more years and in the meantime I will try to work on my synthesis skills (but never ask me again to tell you the Silmarillon!).

Dulcis in fundo, I wish to thank "la mia piccolina"! You made these years legen... wait for it ... dary! In the last years, you made me laugh so hard that I actually had pain in the jar, I can always count on you (I hate that you are al-most always right!) and we even invented a new language that from now on will be known as Spanitalish and that we speak every day. Sei proprio una persona speziale!

Finally, I wish to thank my wonderful family starting with my grandfather Tonino, my aunts, uncles and cousins that have always been there for me with their love, guidance, and support. In particular, I dedicate this PhD thesis to my parents and brothers: I want to thank Maurizio and Rossella for their constant love, support and encouragement even in the most difficult periods of my life. They made me into the man I am today. Many thanks to my brother Fabrizio for growing up with me and sharing many wonderful moments, I wish you all the best for your future now that you are starting your own family! Finally, I wish to thank my younger

brothers Paolo and Daniele: I know that I taught you everything you know and I was such a good big brother, but with brothers like you it has been easy! P.S.: next time I will crush you at DOTA!

Infine, voglio ringraziare la mia meravigliosa famiglia iniziando da mio nonno Tonino, le mie zie, zii e cugini che sono sempre stati presenti nella mia vita con il loro amore, i loro consigli ed il loro supporto. In particolare, dedico questa tesi di dottorato ai miei genitori e fratelli: voglio ringraziare Maurizio e Rossella per il loro costante amore, supporto ed incoraggiamento che non è mai mancato anche nei periodi più difficili della mia vita. Grazie a loro sono diventato l'uomo che sono oggi. Mille grazie a mio fratello Fabrizio per essere cresciuto con me ed aver condiviso molti momenti meravigliosi, ti faccio i miei migliori auguri per il futuro ora che stai creando la tua nuova famiglia! Infine, voglio ringraziare i miei fratellini Paolo and Daniele: so di avervi insegnato tutto ciò che sapete e che sono stato un fratello maggiore fantastico, ma con fratelli come voi è stato facile! P.S.: la prossima volta vi distruggerò a DOTA!

Gent, August 2014
Domenico Spina

Table of Contents

List of Acronyms

B

BIBO	bounded-input bounded-output

C

CAD	computer aided design
CDF	cumulative distribution function

E

EM	electromagnetic
EMC	electromagnetic compatibility

I

IC	integrated circuits
I/O	inputs/outputs

M

MC	Monte Carlo
MEMS	micro electro-mechanical systems
MNA	modified nodal analysis
MOR	model order reduction
MOVF	Multivariate Orthonormal Vector Fitting Technique

O

| ODE | ordinary differential equations |

P

PA	power amplifier
PC	Polynomial Chaos
PDF	probability density function
PEEC	Partial Element Equivalent Circuit
PRIMA	passive reduced-order interconnect macromodeling algorithm

Q

| quasi-LPV | quasi-linear parameter-varying |

R

| RF | radio frequency |
| RMS | root mean square |

S

SC	Stochastic Collocation
SI	signal integrity
SVD	singular value decomposition

T

TEM	transverse electromagnetic
THD	total harmonic distortion
TFT	Transfer Function Trajectory
TL	transmission line

TLT	transmission line theory
TPW	trajectory piecewise

V

VF	Vector Fitting

Samenvatting
– Summary in Dutch –

De toenemende vraag naar hogere prestaties van geïntegreerde schakelingen (IC's) leidt onvermijdelijk naar signalen met hogere bandbreedtes. Omwille van nieuwe geavanceerde productiemogelijkheden worden deze ICs steeds kleiner, en ook de dichtheid hiervan wordt aanzienlijk verhoogd. De afgelopen jaren is het analyseren van de variabiliteitseffecten van geometrische en elektrische parameters op de prestaties van moderne ICs steeds belangrijker geworden. Parametervariabiliteit is inderdaad een belangrijke oorzaak voor de verminderde prestaties van ICs, omdat het invloed heeft op belangrijke eigenschappen zoals koppeling, vertraging en overspraak. Verschillende oorzaken van variabiliteit zijn bv. routerings- of ontwerpsonzekerheden en veranderingen in hun werkingsomstandigheden als gevolg van temperatuurschommelingen. De toleranties van het productieproces zijn hierbij van groot belang. Een onvermijdelijk gevolg van het fabricageproces is dat er onderlinge afwijkingen bestaan tussen componenten die ontwikkeld zijn volgens hetzelfde ontwerp.

Om de effecten van parametervariabiliteit op de prestatie van schakelingen in rekening te brengen, kan men de werking van moderne ICs als een toevalsveranderlijke beschouwen tijdens de ontwerpfase. Vervolgens kan men een statistische analyse uitvoeren om de integriteit van het signaal van moderne ICs te beoordelen. Dit wordt doorgaans uitgevoerd met behulp van Monte Carlo (MC)-gebaseerde methoden. De MC analyse wordt beschouwd als de standaardaanpak voor variabiliteitsanalyse dankzij zijn robuustheid, nauwkeurigheid en eenvoud van implementatie. Het belangrijkste nadeel van deze werkwijze is de langzame convergentie die de ontwerpers ertoe dwingt om een groot aantal simulaties uit te voeren vooraleer er betrouwbare resultaten verkregen worden. Doordat simulaties van moderne ICs vaak computationeel duur zijn, is de hoge rekentijd van de MC analyse een belangrijke hinderpaal. De belangstelling voor efficiënte en nauwkeurige variabiliteitsanalysetechnieken is de afgelopen jaren drastisch toegenomen, omwille van het feit dat een korte marktintroductietijd en een first-time-right aanpak essentieel zijn. Dit is belangrijk in een sterk concurrerende markt die vele categorieën van de moderne elektronische componenten omvat.

Het doel van dit proefschrift is het ontwikkelen van innovatieve technieken voor efficiënte en nauwkeurige variabiliteitsanalyse van moderne hogesnelheids ICs, gebruik makend van geschikte stochastische macromodellen. In dit proefschrift wordt een stochastisch macromodel gedefinieerd als een wiskundig model

dat het invoer-uitvoer systeemgedrag van een generiek systeem beschrijft. Dit ge-
drag is dan functie van n of meerdere systeemparameters die fungeren als toevals-
veranderlijken. Het berekenen van geschikte stochastische macromodellen laat
toe om de variabiliteitsanalyse nauwkeurig en efficiënt uit te voeren, aangezien
het aantal simulaties drastisch wordt gereduceerd ten opzichte van de MC analyse.
De stochastische macromodelingstechnieken die in dit proefschrift worden behan-
deld zijn gebaseerd op een Polynomiale Chaos (PC) ontwikkeling of de Stochas-
tische Collocatie (SC) methode. De PC-gebaseerde modelleringsaanpak beoogt
het uitdrukken van een stochastisch proces als een reeks orthogonale basisfunc-
ties met geschikte coëfficiënten. Dit geeft een analytische voorstelling weer van
de systeemvariabiliteit ten opzichte van de toevalsveranderlijken in kwestie. De
SC-methodes benaderen de ongekende stochastische oplossing door functies te in-
terpoleren in de stochastische ruimte. Hierdoor verkrijgt men een hoge nauwkeu-
righeid en efficiëntie bij het schatten van de systeemvariabiliteit. De implementatie
is even eenvoudig als de methodes die gebaseerd zijn op bemonstering, zoals de
MC analyse.

Dit proefschrift is als volgt opgebouwd: Hoofdstuk 1 geeft een algemene in-
troductie van het doctoraatswerk waarbij de context en motivatie voor dit werk be-
sproken wordt. Hoofdstuk 2 beschrijft de basisbegrippen van kansrekening die no-
dig zijn om het wiskundig kader van dit proefschrift te begrijpen. Dit geeft tevens
een overzicht van state-of-the-art technieken om de variabiliteit analyse uit te voe-
ren. In het bijzonder wordt de trage convergentie van de MC methode bestudeerd.
Hieruit blijkt dat het schatten van de variabiliteitseigenschappen via de MC me-
thode voor complexe hogesnelheids IC's duur is, zowel in termen van het geheu-
gen als rekentijd. Daaruit volgt de noodzaak voor efficiënte en nauwkeurige ma-
cromodelingstechnieken die op maat gebouwd zijn voor de variabiliteitsanalyse.
De eerste model-gedreven stochastische macromodelingstechniek die ontwikkeld
werd tijdens mijn onderzoek staat beschreven in hoofdstuk 3. De voorgestelde
methode is gebaseerd op het berekenen van univariate macromodellen voor de
overdrachtsfuncties van het systeem, en op de PC expansie van de desbetreffende
toestands-ruimte matrices. De toepassing van de PC-expansie wordt uitgebreid
naar algemene passieve multipoortschakelen (zoals interconnecties, filters, con-
nectoren, etc.), die voorheen enkel aangenomen werden voor discrete components
en transmissielijnen met meerdere geleiders. Hoofdstuk 4 omvat een vergelijking
van drie verschillende state-of-the-art technieken die gebruikt worden voor va-
riabiliteitsanalyse van lineaire en passieve multipoortsystemen. Deze vergelijking
focust zich op de unieke eigenschappen van elektromagnetische (EM) systeemmo-
dellering. In het bijzonder worden de prestaties van de PC-gebaseerde techniek in
hoofdstuk 3 vergeleken met de SC-gebaseerde aanpak. In deze studie wordt voor-
gesteld om state-of-the-art adaptieve bemonsteringstechnieken te gebruiken die de
SC-gebaseerd modellen bouwen, als alternatief voor een schaarse bemonstering
van de parameterruimte. Inderdaad, de adaptieve bemonsteringstechnieken laten
toe om de berekening van SC-gebaseerde modellen te automatiseren, waardoor de
bemonstering van de parameterruimte niet overgelaten wordt aan de ontwerper.
Verder wordt een nieuwe SC gebaseerde methode voorgesteld die nieuwe interpo-

latieschemas gebruikt op basis van amplitude- en frequentieschalingcoëfficiënten. De stochastische macromodelingstechniek beschreven in hoofdstuk 5 is gebaseerd op een niet-intrusieve toepassing van de PC expansie: het macromodel wordt verkregen door de toepassing van de PC-expansie op het invoer- en uitvoersniveau in plaats van de tussenliggende toestands-ruimte modellen zoals voorgesteld werd in hoofdstuk 3. Dit leidt tot een efficiëntere procedure om modellen te bouwen. Bovendien maakt de voorgestelde techniek het mogelijk om de stabiliteit te handhaven en de passiviteit van de berekende PC-gebaseerde macromodel te controleren. De toepassing van de PC expansie op systemen die beschreven worden door een groot aantal vergelijkingen (zoals degene die verkregen worden via EM methoden) is niet triviaal. In hoofdstuk 6 wordt een nieuwe stochastische macromodelingstechniek voorgesteld om dit probleem aan te pakken. Deze aanpak is gebaseerd op een geschikte combinatie van model-orde reductie en PC-technieken, waardoor het uiteindelijke model met gereduceerde orde nauwkeurige stochastische berekeningen en variabiliteitsanalyses kan uitvoeren. Vervolgens wordt in hoofdstuk 7 een stochastische macromodelingstechniek voorgesteld, die geschikt is voor de variabiliteitsanalyse van niet-lineaire systemen. De voorgestelde aanpak is gebaseerd op een combinatie van de overdrachtsfunctie trajectorie methode en de PC expansie, en kan worden toegepast om een breed gamma van niet-lineaire systemen te bestuderen. Bovendien kan een hiërarchische benadering worden gebruikt om de complexiteit van de modellering te verminderen. De voorgestelde methode laat toe om de variabiliteitsanalyse nauwkeurig en met verhoogde efficiëntie uit te voeren ten opzichte van de MC analyse. Tenslotte wordt in het aanhangsel (appendix) een techniek voorgesteld om parametrische gevoeligheidsanalyses van transmissielijnen met meerdere geleiders uit te voeren. Dit resultaat werd ontwikkeld in de vroege fase van mijn onderzoek. Variabiliteitsanalyse en gevoeligheidsanalyse zijn complementair: het eerste schat de gevolgen van de variabiliteit van geometrische of elektrische parameters op de circuitprestaties, terwijl het tweede de parameters onderscheidt die een sterker effect hebben op de prestaties van de schakeling.

Summary

The increasing demand for performance of integrated circuits (ICs) pushes operation to higher signal bandwidths, while rapid advances in manufacturing capabilities have significantly reduced the feature size and increased the density of these devices. In this scenario, the analysis of the effects of geometrical and electrical parameters variability on the performance of the modern ICs (variability analysis) has become crucial in the recent years. Indeed, parameters variability is a primary source of degradation of the ICs performances, since it can affect important characteristics such as coupling, delay and crosstalk. Different sources of variability are present, like routing/layout uncertainties and changes of a device operating conditions due to temperature fluctuation, but the tolerances of the manufacturing process rank among one of the major ones. Fundamentally, as a result of the manufacturing process, a mismatch is introduced between devices that are designed to be the same.

As a result, the response of modern ICs can be considered as a random process during the design phase, in order to take into account the effects of parameters variability on the circuits performances. In this framework, a statistical analysis is required for the assessment of signal integrity of modern ICs, which is typically performed using Monte Carlo (MC)-based methods. The MC analysis is considered the standard approach for variability analysis thanks to its robustness, accuracy and ease of implementation. The main drawback of this method is constituted by its slow convergence rate, that forces the designers to perform a large number of simulations to obtain reliable results. Since simulations of modern ICs are often computationally expensive, considering that both the operative bandwidth and complexity of modern electrical systems are constantly increasing, the high computational time required by the MC analysis is a clear limitation. Hence, the interest for efficient and accurate variability analysis techniques increased dramatically in the recent years, considering that short time-to-market and first-time-right approach are fundamental in the highly competitive market of many categories of modern electronic devices.

The goal of this PhD thesis is developing innovative techniques for efficient and accurate variability analysis of modern high-speed ICs, via the calculation of suitable stochastic macromodels. In this PhD thesis, a stochastic macromodel is defined as a mathematical model of a generic system which describes the system behavior as seen from its inputs/outputs (I/O) ports, when one or more of the systems parameters are random variables. The computation of suitable stochastic macromodel allows to perform the variability analysis with accuracy and effi-

ciency, since the number of simulations needed to obtain statistical information is drastically reduced with respect to the MC analysis. In particular, the stochastic macromodeling techniques presented in this PhD thesis are based on the Polynomial Chaos (PC) expansion or on the Stochastic Collocation (SC) methods. The PC-based modeling approach aims at expressing a stochastic process as a series of orthogonal basis functions with suitable coefficients and gives an analytical representation of the variability of the system with respect to the random variables under consideration. The SC methods approximate the unknown stochastic solution by functions interpolation in the stochastic space offering high accuracy and efficiency in estimating system variability features as well as easy implementation as sampling-based methods like the MC analysis.

This PhD thesis is organized as follows: Chapter 1 gives a general introduction of the PhD work discussing the context as well as the motivation for this work. Chapter 2 describes the basic notions on probability theory necessary to understand the mathematical framework of this PhD dissertation and presents an overview of the state-of-the-art techniques for the variability analysis. In particular, the slow converge rate of the MC method is studied, proving that the estimation of variability features for complex high-speed ICs performed via MC method is expensive, both in terms of memory and computational time. Hence, the need for efficient and accurate macromodeling techniques tailored for the variability analysis becomes evident. The first model-driven stochastic macromodeling technique developed during my research activity is described in Chapter 3. The proposed method is based on the calculation of root macromodels of the system transfer functions and on the PC expansion of the corresponding state-space matrices. It extends to general passive multiport circuits (such as interconnections, filters, connectors, etc.) the application of the PC expansion, previously adopted only for lumped elements and multiconductor transmission lines. Chapter 4 proposes a comparative study of three different state-of-the-art techniques for the variability analysis of linear and passive multiport systems. The proposed comparison focus on the unique features of electromagnetic (EM) system modeling. In particular, the performances of the PC-based technique described in Chapter 3 are compared with respect to SC-based approaches. In this framework, the presented study proposes the adoption of state-of-the art adaptive sampling schemes to build SC-based model instead of using sparse sampling in the parameters space. Indeed, adaptive sampling schemes allow to increase the automatization of the SC-based models generation procedure, since the sampling of the parameters space is not chosen by the designer. Furthermore, a new SC-based method that uses novel interpolation schemes based on amplitude and frequency scaling coefficients is presented. The stochastic macromodeling technique described in Chapter 5 is based on a non-intrusive application of the PC expansion: the macromodel is obtained through the application of the PC expansion at an input-output level without intermediate state-space models as for the technique presented in Chapter 3, adopting an efficient model-building procedure. Furthermore, the proposed technique allows to enforce the stability and check the passivity of the calculated PC-based macromodel. The application of the PC expansion to systems described by a large number of equations, such

as the ones resulting by means of EM methods is not trivial. In Chapter 6, it is presented a new stochastic macromodeling technique that tackles this issue. It is based on a suitable combination of model order reduction and PC techniques, generating a final reduced-order model able to accurately end efficiently perform stochastic computations and variability analysis. Next, a stochastic macromodeling technique suitable for the variability analysis of nonlinear systems is presented in Chapter 7. The proposed approach, based on the combination of the Transfer Function Trajectory method and of the PC expansion, can be applied to study a broad range of nonlinear systems. Furthermore, a hierarchical approach can be used to reduce the modeling complexity. The proposed method allows to perform the variability analysis with accuracy and improved efficiency with respect to the MC analysis. Finally, in the Appendix is presented a technique for the parametric sensitivity analysis of multiconductor transmission lines developed in the early phase of my research. Variability analysis and sensitivity analysis are complementary: the first estimates the effects of the variability of geometrical or electrical parameters on the circuits performances, while the second individuates the parameters which variations have a stronger effect on the circuit performances.

1
Introduction

The co-founder of Intel Corporation Gordon Moore published in 1965 a study on the long-term evolution of integrated circuits: by recognizing a trend in integrated circuit complexity, Gordon Moore predicted that the available memory and calculation speed of microprocessors would have an exponential growth, doubling every year [1]. This prediction became famous as Moore's Law and with a small correction in the growth rate (doubling every 18 months) is still valid today [2]. Nowadays, micro-electronic circuits are widespread in the modern society and are used in a incredibly high number of activities: communication (smartphones), entertainment and scientific research (personal computer), spatial exploration (satellites) are just few examples.

This incredible diffusion was mainly supported by the progresses in the manufacturing process that allowed the integration on a single chip of different heterogeneous functional blocks, like digital, analog, micro electro-mechanical systems (MEMS), and radio frequency (RF) devices. Furthermore, it was possible to reduce the size of modern micro-electronic circuits and to increase the number of components on a single chip thanks to the miniaturization of the manufacturing process in the sub-micrometer region. However, no progress is attained without a cost. Realizing such miniaturized electronic circuit is extremely complex, expensive, and time-consuming. Mass production and a 24-hours production cycle are the only way to reduce the costs and to introduce ICs in the market at a competitive price. Furthermore, the miniaturization in the nanometer region increased functionality, portability and computational power of modern ICs, but also made impossible to modify or repair them once produced.

Hence, robust design of modern ICs is fundamental, especially considering that the impact of the effects of geometrical or electrical parameters variability on the ICs performance became increasingly relevant in the nanometer region [3]-[6]. Different sources of variability are present, like routing/layout uncertainties and changes of a device operating conditions due to temperature fluctuation, but the tolerances of the manufacturing process rank among one of the major ones. Fundamentally, as a result of the manufacturing process, a mismatch is introduced between devices that are designed to be the same. Furthermore, process variations affect different phases of the manufacturing process, such as etching, lithography, polishing [5]. Typical examples of process variations are random dopant fluctuation effects, line edge and width roughness, fixed charges in the gate dielectric and interface roughness [6]. Note that, process induced mismatch significantly threatens the efficiency of both digital circuits, by influencing their timing closure [5], and analog ones, since matched devices and differential signal paths are fundamental for most high-performance analog circuits [7].

In this scenario, design tools for the variability analysis of integrated circuits are fundamental for a robust and successful design. In the context of this PhD thesis, variability analysis means the analysis of the effects of geometrical or electrical parameters variability on the ICs performance. The MC-based methods represent the standard approach for variability analysis thanks to their accuracy and ease of implementation. The key of MC method [8] is to simulate a circuit, using suitable EM simulators such as ADS Momentum[1] or circuit simulators such as PSpice[2], for a large set of samples of the random parameters, chosen according to their pertinent distributions, collecting all the data, and computing the statistics and variability analysis based on the large dataset so obtained. However, it can be proved that accuracy of the results of the variability analysis performed with a MC method depends on the inverse square root of the number of simulations performed. Since simulations are often computationally expensive due to the increased complexity of systems, MC has a very high computational cost. Recently, new approaches, based on the PC expansion and SC methods, have emerged to perform variability analysis as an efficient alternative to the computationally cumbersome MC-based techniques. The PC-based modeling approach expands a stochastic process in terms of orthogonal polynomials, giving an analytical representation of the variability of the system with respect to the random variables under consideration [9]. Conversely, the SC-based approach approximates the unknown stochastic solution by interpolation functions in the stochastic space [9].

The goal of this PhD thesis is to develop innovative PC-based or SC-based macromodeling techniques suitable for efficient and accurate variability analysis of modern high-speed ICs (reffered as stochastic macromodeling). Macromodel-

---

[1]Momentum EEsof EDA, Agilent Technologies, Santa Rosa, CA.
[2]Cadence Design Systems, San Jose, California

ing techniques compute a mathematical model of a generic system that describes the system behavior as seen from its I/O ports, while no information is retained on its internal structure. In particular, the systems considered in this PhD thesis are circuits which time- or frequency-domain behavior depends by a set of geometrical (for example a conductor width or length) or electrical (like the dielectric permittivity) parameters varying in a suitable range, called design or parameters space, according to a probability distribution, see Fig. 1.1.

Furthermore, two main approaches exist in the literature for computing macromodels: data-driven and model-driven. The first computes the macromodel starting from a set of data describing the I/O response of the system in the frequency- or time-domain, while the latter consider an existing set of equations describing the system I/O response (i.e. the Telegrapher's equations, state-space representations, etc) as a starting point to build the macromodel. The variability analysis techniques presented in this PhD thesis are developed using both the approaches.

However, modern high-speed ICs are formed by heterogeneous devices and components. Each type of device or component (mixers, connectors, operational amplifiers, filters, etc) has his unique characteristics and corresponding set of specifications that the designer must satisfy. Considering the huge differences in I/O behaviors, frequency bandwidth and design constraints of the different modern ICs, it is important to specify which circuits can be described with a specific macromodeling technique. Note that, it is possible to categorize the different types of electric and electronic components in broad classes, based on some general criteria, as follows:

- Information transmission: *analog* circuits convey information through changes in the current, voltage, or frequency of a continuous time-varying signal called analog signal. Analog devices include operational amplifiers, voltage regulators, modulators and mixers. Circuits where voltage or current signals can assume only a finite numbers of discrete values (or levels) are called *digital* circuits. Binary (two-levels) digital circuits are the most common and each level is interpreted as one of two different states: 0/1, on/off, true/false. Boolean logic, that is the foundation of digital electronics and computer processing, is implemented via digital circuits using logic gates, realized with transistors.

- Energy transmission: *passive* devices [10] cannot generate more energy than they can absorb through their electrical ports. Passivity conditions for devices described by admittance, impedance and scattering parameters can be found in [10]. Examples of passive components are resistors, capacitors, inductors, and transformers. Conversely, a device that can generate more energy than it can absorb through its electrical ports is called *active*. Note that, active devices must relies on a source of energy. Active devices include

transistors and operational amplifiers.

- Response to input signals: a circuit is called *linear* if it obeys the superposition principle. Basically, when a linear combination of the (voltage or current) signals $x_1(t)$ and $x_2(t)$ is applied to the circuit input ports, the output signal is the linear combination of the outputs due to the signals $x_1(t)$ and $x_2(t)$ applied separately. Hence, any steady-state output of the circuit for a sinusoidal input of frequency f_0 is also sinusoidal with frequency f_0. Linear circuits can be analyzed in the frequency-domain using the Fourier analysis and the Laplace transform. Furthermore, linear time-invariant systems (the I/O response to any input signal is independent by the particular time instant chosen to apply the input signal) are completely defined in the time-domain by their impulse response, and by their transfer function in the Laplace-domain. Conversely, the superposition principle is not valid for *nonlinear* circuits. Hence, the output of a nonlinear circuit for a linear combination of input signals is not equal to the linear combination of the input signals applied separately. As a consequence, the spectrum of the output signal can have components in a different frequency range with respect to the spectrum of the input signal. A mixer is the typical example of this behavior, due to the intermodulation distortion. Nonlinear circuits are typically studied in the time-domain, even if frequency-domain analysis techniques, such as the Harmonic Balance [11], can be applied under specific conditions. However, if a transistor is polarized in its nearly linear region and a relatively small signal is applied to it, a linear approximation (small-signal approximation) can be used to describe its I/O behavior, see Fig. 1.2. Since transistors are the basic "building block" of many electronic devices such as operational amplifiers, linear analysis techniques can be used in analyzing many circuits with nonlinear components when the signal levels are small.

- Electrical length: the *lumped* model approximation can be used if the following relation can be applied: $L << \lambda$, where L represents the characteristic length of the circuit and λ is its operating wavelength (or the smaller wavelength in the circuit frequency bandwidth). Under this condition, the EM energy can be considered concentrated in the components of the circuit that are assumed to be connected by perfectly conducting wires. However, circuits which electrical properties, such as resistance, capacitance and inductance, are distributed continuously throughout the materials of the circuit are called *distributed*. Circuits that can be studied with the transmission line (TL) model [12] fall in this category.

Clearly, any electric or electronic device falls in multiple categories: a microstrip line is a distributed, linear and passive circuit, while a typical operational amplifier is a lumped, nonlinear and active device.

Finally, the performances of modern ICs, are highly influenced by the operating frequency bandwidth. The type of model that can be applied to describe a circuit changes drastically increasing its frequency bandwidth, when second order effects, such as crosstalk, reflection, delay and coupling, become increasingly important. In conclusion, the increasing demand for performance from ICs pushes operation to higher signal bandwidths, while rapid advances in manufacturing capabilities have significantly reduced the feature size and increased the density of these devices. In this scenario, the analysis of the effects of geometrical or electrical parameters variability on the ICs performance is fundamental.

1.1 Research contributions

This PhD thesis proposes innovative PC-based or SC-based macromodeling techniques suitable for efficient and accurate variability analysis of modern high-speed circuits. In particular, the variability analysis is performed for two distinct categories of circuits: linear and passive systems and nonlinear (typically active) ones. Linear and passive systems will be analyzed in the frequency-domain by computing a stochastic macromodel of their transfer function, that can be expressed by means of different representations e.g. scattering, impedance or admittance parameters, while nonlinear circuits will be studied in the time-domain. Each technique developed during my PhD research is described in a dedicated chapter by

- indicating the sampling strategy adopted to build the macromodel;

- detailing the procedure to build the desired stochastic macromodel;

- discussing the characteristics of the proposed macromodeling strategy;

- validating the accuracy and efficiency of the variability analysis performed with the proposed approach by means of comparison with state-of-the-art techniques for the variability analysis for suitable numerical examples.

In particular, Chapter 2 gives to the reader the basic notions on probability theory as well as an overview of the state-of-the-art techniques for the variability analysis. Chapters $3 - 6$ describe the stochastic macromodeling techniques developed for linear and passive systems, and Chapter 7 for nonlinear ones. Finally, in the Appendix it is presented a technique for the parametric sensitivity analysis of multiconductor transmission lines developed in the early phase of my research. A brief description of each chapter is presented here with their contribution in the overall research as shown in Fig. 1.3.
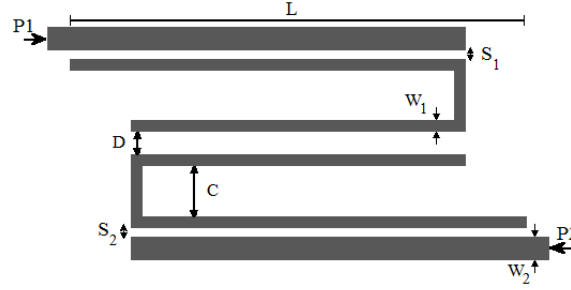
(a) Layout of an hairpin filter.
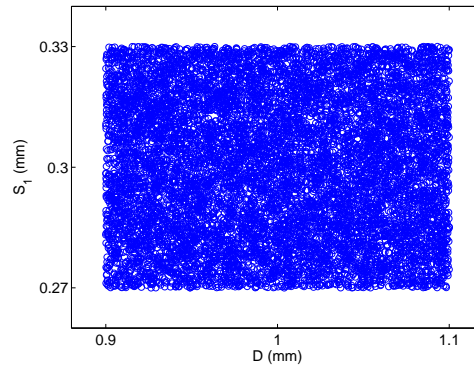
(b) Representation of the parameters space.
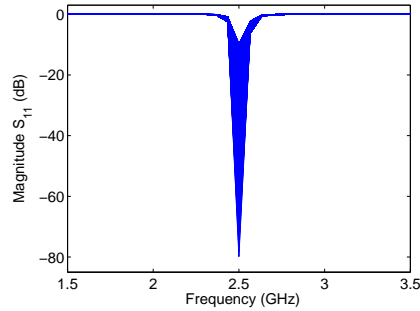
(c) Effect of the parameter variability on the hairpin
filter frequency response.

Figure 1.1: The spacings D and S_1 of a bandpass hairpin filter are considered random variables with uniform distribution. The blue circles ($\circ$) in Fig. 1.1b represent a discrete set of 10000 values of the parameters D and S_1 taken accordingly to the uniform distribution. The blue lines in Fig. 1.1c represent the element S_{11} of the filter scattering parameters obtained for each set of values of the the parameters D and S_1. It is evident that the filter scattering parameters are random quantities themselves and must be described in statistical terms.
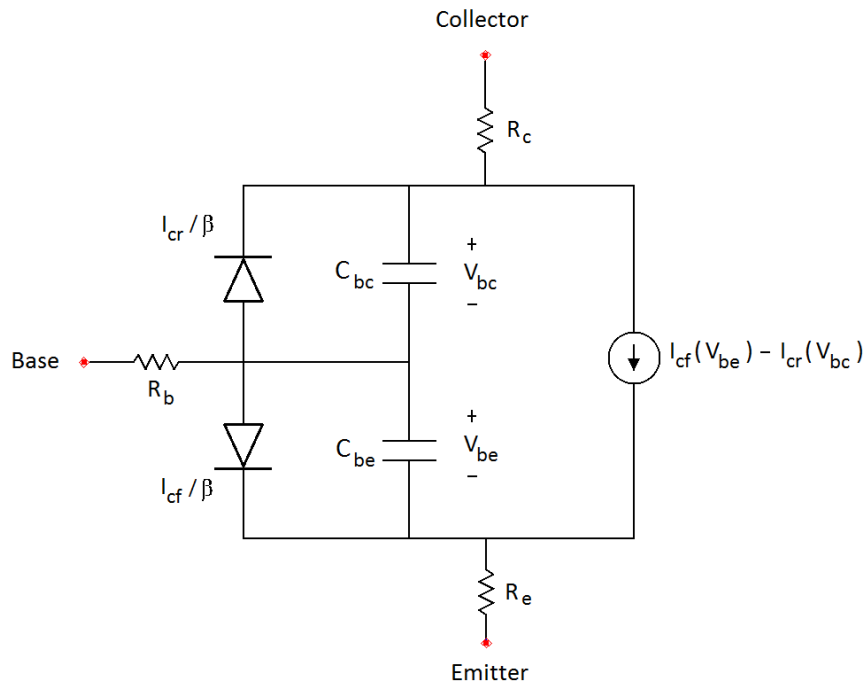
(a) Large signal model of a bipolar junction transistor.
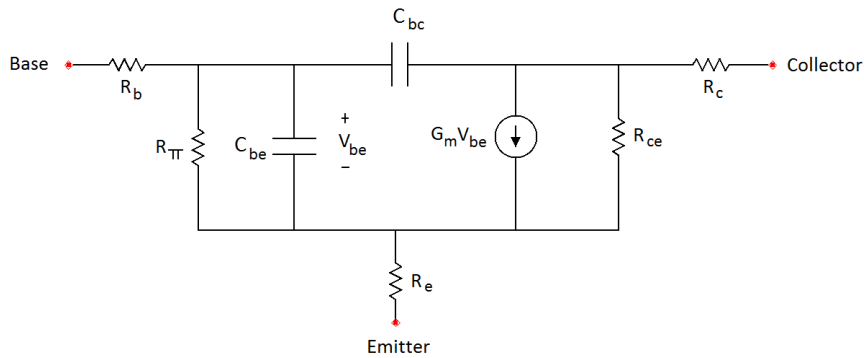
(b) Small signal model of a bipolar junction transistor.

Figure 1.2: Fig. 1.2a show a large signal circuit equivalent for a bipolar junction transistor. The capacitances C_{be} and C_{bc} have both depletion and diffusion components. Often a second pair of diodes is included to account for base leakage current at low base-to-emitter voltage [13]. A small signal hybrid-pi equivalent circuit for a bipolar junction transistor is shown in Fig. 1.2b. This is a linearization of the large signal model in Fig. 1.2a that simplifies the circuit analysis [13].

Macromodeling for Efficient and Accurate Variability Analysis

Introduction

Ch. 2: Probability Theory and Variability Analysis.

Stochastic Macromodeling Linear and Passive Devices

Data Driven

Ch. 3: Variability Analysis of Multiport Systems via PC
Expansion.

Ch. 4: A Comparative Study of PC and SC Methods for
Variability Analysis of Multiport Systems.

Ch. 5: PC-Based Macromodeling of Multiport Systems
using an Input-Output Approach.

Model Driven

Ch. 6: Efficient Variability Analysis of Electromagnetic
Systems via PC and Model Order Reduction.

Stochastic Macromodeling Nonlinear Devices

Ch. 7: Stochastic Macromodeling of Nonlinear Systems via
PC Expansion and Transfer Function Trajectories.

Appendix

Time-Domain Green's Function-Based Parametric Sensitivity
Analysis of Multiconductor Transmission Lines.

Figure 1.3: Research contribution.

Chapter 2

At first, this Chapter gives the basic notions of probability necessary to understand the mathematical framework of the PhD dissertation. In particular, the concepts of random variables and stochastic process are discussed here. Next, a brief overview of the state-of-the-art variability analysis techniques are described in the rest of the Chapter. In particular, the properties of the MC analysis, PC expansion and SC methods are presented here with particular focus on the strategy adopted to characterize the stochastic process under study (sampling-based for the MC, interpolation-based for the SC methods, approximation as a summation of suitable polynomial functions for the PC expansion) and on the sampling strategy required by each technique. The information presented in this Chapter are fundamental for the rest of the PhD dissertation.

Chapter 3

In this Chapter is described the first data-driven stochastic macromodeling technique developed during my research activity. It extends to general linear and passive multiport circuits (such as interconnections, filters, connectors, etc.) the application of the PC expansion, previously adopted only for lumped elements and multiconductor transmission lines. The proposed technique is based on the calculation of root macromodels of the system transfer functions and on the PC expansion of the corresponding state-space matrices. This transfer function may be expressed in terms of e.g. scattering, impedance or admittance parameters, as such making it applicable to a large range of systems. The accuracy and efficiency of the proposed method are validated by means of comparison with the standard MC approach.

Chapter 4

A comparative study of three main techniques used to build stochastic models to perform variability analysis of general linear and passive multiport systems is presented in this Chapter: the PC-based technique described in Chapter 3, a SC method based on standard interpolation schemes, a new SC-based method that uses novel interpolation schemes based on amplitude and frequency scaling coefficients. The proposed study evaluates not only the accuracy and efficiency of the different methods in estimating system variability features, but also describes:

- the order estimation and sampling strategy adopted;

- the capability to preserve the physical properties of the system under study;

- the computational cost to build the stochastic macromodel.

Indeed, using efficient sampling strategies is of paramount importance since the simulations of complex EM systems are time consuming. Performing stable time-domain simulations requires that the physical properties of stability and passivity of the stochastic macromodel are guaranteed. Finally, the compactness and computational efficiency of the stochastic macromodel are important indicators of the performances of the different variability analysis methods.

Chapter 5

An innovative PC-based technique to build stochastic frequency-domain macro-models of generic linear multiport systems is presented. Differently on the technique presented in Chapter 3, a non-intrusive approach is used to calculate a macromodel of the system transfer function including its statistical properties, making it tailored for variability analysis. The combination of the modeling power of the Vector Fitting algorithm with the PC expansion applied at an input-output level allows to accurately and efficiently describe the system variability features. Finally, the stability of the proposed macromodel can be guaranteed and the passivity can be verified by means of classical approaches. Thanks to its versatility and automated order selection, the proposed technique is suitable to be applied to a large range of complex modern electrical systems (e.g. filters, interconnections).

Chapter 6

The application of the MC method to complex high-speed systems analyzed by means of EM methods, that usually produce very large systems of equations which are expensive to solve, is often computationally very expensive. However, a PC-based macromodeling approach, such as the one described in Chapter 3, can not be efficiently used for systems described by very large systems of equations. Indeed, the calculation of the PC expansion for such systems would lead to an augmented system of such a high dimension that the computational cost required to solve it may compromise the efficiency of the PC expansion with respect to the MC analysis.

This Chapter proposes a novel method for the variability analysis of systems described by a large numbers of equations based on combinations of a PC expansion of the original system matrices and model order reduction techniques. The novel proposed method first calculates a set of reduced order models with common order using a common compact projection matrix and then computes the PC expansion of the reduced models. The proposed technique is flexible, since the transfer function of a generic multiport system can be expressed by different representations and it allows to use different MOR techniques to calculate the reduced systems. Finally, it is presented a discussion of the performances of the

proposed method with respect to different variability analysis techniques that propose a combination of a PC expansion of the original system matrices and model order reduction techniques.

Chapter 7

A novel approach is presented in this Chapter to perform variability analysis of nonlinear systems. The versatility of the method makes it suitable for the analysis of complex nonlinear electronic systems, since a hierarchical approach can be used to reduce the modeling complexity. The proposed technique is a variation-aware extension of the Transfer Function Trajectory method by means of the PC expansion. The proposed method allows to perform the variability analysis with good accuracy and improved efficiency compared to MC analysis. Previously developed state-of-the-art PC-based techniques for the variability analysis of nonlinear electronic devices have been limited to specific types of circuits (namely oscillators and DC/DC converters) and to the evaluation of the effects of variability of macromodels embedded in nonlinear circuits.

Appendix

Variability analysis and sensitivity analysis are complementary: the first estimates the effects of the variability of geometrical or electrical parameters on the circuits performances, while the second individuates the parameters which variations have a stronger effect on the circuit performances. A new parametric macromodeling technique for lossy and dispersive multiconductor transmission lines providing sensitivity information over the entire design space is proposed in this Appendix. Parametric macromodels are multivariate models describing the complex behavior of EM systems with respect to several geometrical (i.e. width or length of conductors) or electrical (i.e. dielectric permittivity) design parameters and the frequency (or time). Parametric macromodels which provide sensitivity information are well suited for design space exploration, design optimization and crosstalk analysis. In particular, the proposed technique can handle multiple design parameters, such as substrate or geometrical layout features, and provides time-domain sensitivity information for voltages and currents at the ports of the lines. It is derived from the dyadic Green's function of the 1-D wave propagation problem. The rational nature of the Green's function permits the generation of a time–domain macromodel for the computation of transient voltage and current sensitivities with respect to both electrical and physical parameters, completely avoiding similarity transformation and it is suited to generate state-space models and synthesize equivalent circuits, which can be easily embedded into conventional SPICE-like solvers.

1.2 Publications

The research results obtained during this PhD research have been published in scientific journals and presented at a series of international conferences. The following list provides an overview of the publications during my PhD research.

1.2.1 Publications in international journals (listed in the Science Citation Index [3])

1. **Domenico Spina**, Francesco Ferranti, Giulio Antonini, Tom Dhaene, Luc Knockaert. *Time-Domain Green's Function-Based Parametric Sensitivity Analysis of Multiconductor Transmission Lines.* Published in IEEE Transactions on Components, Packaging and Manufacturing Technology, 2(9):1510–1517, Sept. 2012.

2. **Domenico Spina**, Francesco Ferranti, Tom Dhaene, Luc Knockaert, Giulio Antonini, Dries Vande Ginste. *Variability Analysis of Multiport Systems via Polynomial Chaos Expansion.* Published in IEEE Transactions on Microwave Theory and Techniques, 60(8):2329–2338, Aug. 2012.

3. **Domenico Spina**, Francesco Ferranti, Giulio Antonini, Tom Dhaene, Luc Knockaert. *Efficient Variability Analysis of Electromagnetic Systems via Polynomial Chaos and Model Order Reduction.* Published in IEEE Transactions on Components, Packaging and Manufacturing Technology, 4(6):1038–1051, Jun. 2014.

4. **Domenico Spina**, Dimitri De Jonghe, Dirk Deschrijver, Georges Gielen, Luc Knockaert, Tom Dhaene. *Stochastic Macromodeling of Nonlinear Systems via Polynomial Chaos Expansion and Transfer Function Trajectories.* Published in IEEE Transactions on Microwave Theory and Techniques, 62(7):1454–1460, Jul. 2014.

5. **Domenico Spina**, Francesco Ferranti, Tom Dhaene, Luc Knockaert, Giulio Antonini. *Polynomial Chaos-Based Macromodeling of Multiport Systems using an Input-Output Approach.* Submitted to International Journal of Numerical Modelling: Electronic Networks, Devices and Fields, 2014.

6. **Domenico Spina**, Krishnan Chemmangat, Francesco Ferranti, Tom Dhaene, Luc Knockaert and Flavio G. Canavero. *A Comparative Study of Polynomial*

---

[3]The publications listed are recognized as 'A1 publications', according to the following definition used by Ghent University: A1 publications are articles listed in the Science Citation Index, the Social Science Citation Index or the Arts and Humanities Citation Index of the ISI Web of Science, restricted to contributions listed as article, review, letter, note or proceedings paper.

Chaos and Stochastic Collocation Methods for Variability Analysis of Multiport Systems. Submitted to International Journal of Numerical Modelling: Electronic Networks, Devices and Fields, 2014.

1.2.2 Publications in international conferences (listed in the Science Citation Index [4])

1. **Domenico Spina**, Francesco Ferranti, Giulio Antonini, Tom Dhaene, Luc Knockaert. *Time-domain parametric sensitivity analysis of multiconductor transmission lines.* Published in proceedings of the 15th IEEE workshop on signal propagation on interconnects (SPI), 2011, pages 125–128, Naples, Italy, 2011.

2. **Domenico Spina**, Francesco Ferranti, Giulio Antonini, Tom Dhaene, Luc Knockaert. *Non Intrusive Polynomial Chaos-based Stochastic Macromodeling of Multiport Systems* Accepted for the 18th IEEE workshop on signal propagation on interconnects (SPI), 2014, Ghent, Belgium, 2014.

1.2.3 Publications in other international conferences

1. **Domenico Spina**, Francesco Ferranti, Tom Dhaene, Luc Knockaert, Giulio Antonini. *Polynomial chaos based variability analysis of multiport systems.* Published in proceedings of the International Conference on Synthesis, Modeling, Analysis and Simulation Methods and Applications to Circuit Design (SMACD), 2012, pages 245–248, Sevilla, Spain, 2012.

---

[4]The publications listed are recognized as 'P1 publications', according to the following definition used by Ghent University: P1 publications are proceedings listed in the Conference Proceedings Citation Index - Science or Conference Proceedings Citation Index - Social Science and Humanities of the ISI Web of Science, restricted to contributions listed as article, review, letter, note or proceedings paper, except for publications that are classified as A1.

References

[1] G. E. Moore. *Cramming more components onto integrated circuits*. Electronics, 38(8):114–117, Apr. 1965.

[2] S. B. Dhia, M. Ramdani, E. Sicard. *Electromagnetic Compatibility of Integrated Circuits: Techniques for Low Emission and Susceptibility*. Springer, 2006.

[3] G. A. Abdelmalek, R. Ziani, M. Laghrouchec. *Testing and fault tolerance of integrated circuits*. AASRJ Special Issue, 4(5), Sep. 2012.

[4] A. Nieuwoudt and Y. Massoud. *On the Impact of Process Variations for Carbon Nanotube Bundles for VLSI Interconnect*. IEEE Trans. Electron Devices, 54(3):446–455, Mar. 2007.

[5] F. Gong, X. Liu, H. Yu, S. H. D. Tan, J. Ren, and L. He. *A Fast Non-Monte-Carlo Yield Analysis and Optimization by Stochastic Orthogonal Polynomials*. ACM Transactions on Design Automation of Electronic Systems (TODAES), 17(1), Jan. 2012.

[6] E. Maricau, G. Gielen. *Analog IC Reliability in Nanometer CMOS*. Springer, 2013.

[7] M. Onabajo, J. Silva-Martinez. *Analog Circuit Design for Process Variation-Resilient Systems-on-a-Chip*. Springer, 2012.

[8] G. S. Fishman. *Monte Carlo: Concepts, Algorithms, and Applications*. Springer-Verlag, New York, 1996.

[9] M. S. Eldred. *Recent advance in non-intrusive polynomial-chaos and stochastic collocation methods for uncertainty analysis and design*. In Proc. 50th AIAA/ASME/ASCE/AHS/ASC Structures, Structural Dynamics, and Materials Conference, Palm Springs, California, May 2009.

[10] B. D. O. Anderson, S. Vongpanitlerd. *Network Analysis and Synthesis – A Modern Systems Approach*. Prentice-Hall, Englewood Cliffs, NJ, 1973.

[11] M. Nakhla and J. Vlach. *A piecewise harmonic balance technique for determination of periodic response of nonlinear systems*. IEEE Trans. Circuits Syst., 23(2):85–91, Feb. 1976.

[12] R. R. Paul. *Analysis of Multiconductor Transmission Lines*. New York: Wiley, 1994.

[13] S. A. Maas. *The RF and microwave circuit design cookbook*. Artech House, Boston, 1998.

2

Probability Theory and Variability Analysis

In the first part of this Chapter, namely Sections 2.1 - 2.3, a brief overview of probability theory is given. Far from giving a complete and exhaustive description of this domain of mathematics, the main aim of the proposed study is to describe the basic notion and vocabulary of probability theory, necessary to understand the mathematical framework of the PhD dissertation. The information included in Sections 2.1 - 2.3 are inspired by [1]. Next, an overview of the three main state-of-the-art variability analysis techniques, namely MC, PC and SC, is given in the rest of the Chapter. In particular, the focus of the following discussion is on the strategy adopted by each method to characterize the stochastic process under study (sampling-based for the MC, interpolation-based for the SC methods, approximation as a summation of suitable polynomial functions for the PC expansion) and on the sampling strategy used.

2.1 Random Variables

A probability space associated with a random phenomenon can be defined as a triple $(\Omega, \mathcal{F}, \mathbb{P})$. The sample space Ω is the set of all possible outcomes and an event can be defined as a subset of Ω containing outcomes $\omega \in \Omega$. The set of events defines the σ-algebra $\mathcal{F}$ associated with Ω. The probability measure $\mathbb{P}$ is a

function which associates a number $\mathbb{P}(A)$ to each set $A \in \mathcal{F}$ which follows the Kolmogorov axioms:

$$\mathbb{P}(A) \geq 0 \quad \forall A \in \mathcal{F} \tag{2.1}$$

$$\mathbb{P}(\Omega) = 1 \tag{2.2}$$

$$\mathbb{P}(A \cup B) = \mathbb{P}(A) + \mathbb{P}(B) \quad \forall A, B \in \mathcal{F}, A \cap B = \emptyset \tag{2.3}$$

where $A \cap B = \emptyset$ indicates two disjoint events.

A real random variable x is a mapping $x : \Omega \rightarrow D_x \in \mathbb{R}$. Hence, a random variable x assigns a real value to each outcome $\omega \in \Omega$. The random variable x is called discrete if D_x is a discrete (possibly infinite) set, otherwise x is called continuous. The rest of this study will focus on the properties continuous random variables, since the variability analysis techniques proposed in this PhD thesis consider only this type of variables.

A continuous random variable is completely defined by its cumulative distribution function (CDF) and probability density function (PDF). The CDF represents the probability that the random variable x is less or equal to the value X:

$$F_x(X) = \mathbb{P}(x \leq X) \tag{2.4}$$

Since the CDF is a probability, it must satisfy the following conditions:

$$0 \leq F_x(X) \leq 1 \text{ for } -\infty < X < \infty \tag{2.5}$$

$$F_x(-\infty) = 0 \text{ and } F_x(\infty) = 1 \tag{2.6}$$

$$\mathbb{P}(X_1 < x \leq X_2) = F_x(X_2) - F_x(X_1) \tag{2.7}$$

The PDF is defined as:

$$f_x(X) = \lim_{h \to 0, h > 0} \mathbb{P}(X \leq x \leq X + h) \tag{2.8}$$

and it can be computed as:

$$f_x(X) = \frac{dF_x(X)}{dX} \tag{2.9}$$

Hence, the probability that the random variable x assumes a value in the interval $(a, b) \in D_x$ can be expressed in function of the PDF as:

$$\mathbb{P}(a < x < b) = \int_a^b f_x(X)\, dX \tag{2.10}$$

A random variable x is said to have a finite moment of order $p \geq 1$ if $E\left[|x|^p\right] < \infty$ and the p-th moment of x is defined by $E\left[x^p\right]$, where the symbol $E\left[\cdot\right]$ indicates

the mathematical expectation. Important moments of x are the mean value, the variance and the standard deviation that are respectively defined as:

$$\mu_x = E\left[x\right] = \int_{D_x} X f_x\left(X\right) dX \tag{2.11}$$

$$\sigma_x^2 = E\left[\left(x - \mu_x\right)^2\right] \tag{2.12}$$

$$\sigma_x = \sqrt{\sigma_x^2} \tag{2.13}$$

Finally, the expectation operator defines an inner product on the vectorial space $L^2\left(\Omega, \mathcal{F}, \mathbb{P}\right)$ composed of real random variables with finite second moment $E\left[x^2\right] < \infty$:

$$<x, y> = E\left[xy\right] \tag{2.14}$$

Hence, the vectorial space $L^2\left(\Omega, \mathcal{F}, \mathbb{P}\right)$ equipped with the inner product (2.14) is a Hilbert space. In particular, two random variables x and y are said orthogonal if and only if $E\left[xy\right] = 0$.

2.1.1 Example: Uniform Random Variable

A random variable x with continuous uniform distribution is characterized by the following PDF:

$$f_x\left(X\right) = \begin{cases} \frac{1}{b-a} & \text{for } a \leq X \leq b \\ 0 & \text{for } X < a \text{ or } X > b \end{cases} \tag{2.15}$$

where the parameters a and b are the minimum and maximum value, respectively, of the support of x. The probability distribution is called uniform because all intervals of the same length on the distribution support are equally probable. The corresponding CDF is:

$$F_x\left(X\right) = \begin{cases} 0 & \text{for } X < a \\ \frac{X-a}{b-a} & \text{for } a \leq X < b \\ 1 & \text{for } X \geq b \end{cases} \tag{2.16}$$

Finally, the mean and the variance can be expressed as a function of the parameters a and b as:

$$\mu_x = \frac{1}{2}\left(a + b\right) \tag{2.17}$$

$$\sigma_x^2 = \frac{1}{12}\left(b - a\right)^2 \tag{2.18}$$

2.2 Random Vectors

The events A and B are independent if the occurrence of B does not affect the probability of occurrence of A:

$$\mathbb{P}\left(A|B\right) = \frac{\mathbb{P}\left(A \cap B\right)}{\mathbb{P}\left(B\right)} = \mathbb{P}\left(A\right) \tag{2.19}$$

where $\mathbb{P}\left(A|B\right)$ is the conditional probability of the event A with respect to the event B. Hence, it is easy to prove from (2.19) that the events A and B are independent if and only if:

$$\mathbb{P}\left(A \cap B\right) = \mathbb{P}\left(A\right)\mathbb{P}\left(B\right) \tag{2.20}$$

Similarly, two random variables are independent if they convey no information about each other. Hence, the assessment of the probability distribution of each random variable is not changed by information received on the other. Formally, two random variables x_1 and x_2 are independent if and only if:

$$\mathbb{P}\left((x_1 \in A) \cap (x_2 \in B)\right) = \mathbb{P}\left(x_1 \in A\right)\mathbb{P}\left(x_2 \in B\right) \quad \forall A, B \in \mathcal{F} \tag{2.21}$$

A set of random variables $x_1, \ldots, x_N$ is mutually independent if the relation (2.21) is valid for all the subsets of the random variables $x_1, \ldots, x_N$. The covariance of the random variables x_1 and x_2 provides a measure of the strength of the correlation between the two random variables considered and is defined as:

$$Cov\left[x_1, x_2\right] = E\left[(x_1 - \mu_{x_1})(x_2 - \mu_{x_2})\right] = E\left[(x_1 x_2)\right] - E\left[(x_1)\right]E\left[(x_2)\right] \tag{2.22}$$

If the covariance of two random variables is zero, the variables are called uncorrelated. It is possible to prove that if two random variables are independent they are uncorrelated, while the reverse is not true.

The vector $\boldsymbol{x} = [x_1, \ldots, x_N]$ is a N-dimensional random vector if its components are random variables. Hence, the random vector $\boldsymbol{x}$ is a mapping $\boldsymbol{x} : \boldsymbol{\Omega} \rightarrow \boldsymbol{D_x} \in \mathbb{R}^N$. Moments like mean and standard deviation of the random vector $\boldsymbol{x}$ are the vectors containing the corresponding moment of each component:

$$\boldsymbol{\mu_x} = [\mu_{x_1}, \ldots, \mu_{x_N}] \tag{2.23}$$

$$\boldsymbol{\sigma_x} = [\sigma_{x_1}, \ldots, \sigma_{x_N}] \tag{2.24}$$

The covariance matrix $\boldsymbol{C}$ of $\boldsymbol{x}$ is a square matrix formed by the following elements:

$$C_{i,j} = Cov\left[x_i, x_j\right] \text{ for } i, j = 1, \ldots, N \tag{2.25}$$

A vector of continuous random variables is completely defined by its joint CDF:

$$F_{\boldsymbol{x}}\left(X_1, \ldots, X_N\right) = \mathbb{P}\left(x_1 \leq X_1, \ldots, x_N \leq X_N\right) \tag{2.26}$$

and its joint PDF:

$$\mathbb{P}\left(a_1 < x_1 < b_1, \ldots, a_N < x_N < b_N\right) =$$
$$\int_{a_N}^{b_N} \cdots \int_{a_1}^{b_1} f_{\boldsymbol{x}}\left(X_1, \ldots, X_N\right) dX_1 \ldots dX_N \quad (2.27)$$

It is important to notice that, if the components of the random vector $\boldsymbol{x}$ are independent, than the joint CDF and PDF are the product of the CDFs and of PDFs of the single random variables, respectively, as:

$$F_{\boldsymbol{x}}\left(X_1, \ldots X_N\right) = \prod_{i=1}^{N} F_{x_i}\left(X_i\right) \quad (2.28)$$

$$f_{\boldsymbol{x}}\left(X_1, \ldots X_N\right) = \prod_{i=1}^{N} f_{x_i}\left(X_i\right) \quad (2.29)$$

2.2.1 Example: Vector of Gaussian Random Variables

Gaussian random vectors, indicated with $\boldsymbol{x} \sim \mathcal{N}\left(\boldsymbol{\mu_x}, \boldsymbol{C}\right)$, are defined by the following joint PDF:

$$f_{\boldsymbol{x}} = (2\pi)^{\frac{N}{2}} \, det(\boldsymbol{C})^{-\frac{1}{2}} \exp\left(-\frac{1}{2}\left(\boldsymbol{x} - \boldsymbol{\mu_x}\right)^T \boldsymbol{C}^{-1}\left(\boldsymbol{x} - \boldsymbol{\mu_x}\right)\right) \quad (2.30)$$

For the particular case of Gaussian random vectors, if the random variables are uncorrelated, then they are also independent and (2.30) becomes:

$$f_{\boldsymbol{x}} = \prod_{i=1}^{N} \frac{1}{\sqrt{2\pi}\sigma_{x_i}} \exp\left(-\frac{(x_i - \mu_{x_i})^2}{2\sigma_{x_i}^2}\right) \quad (2.31)$$

2.3 Stochastic Process

A stochastic process $H\left(t, \boldsymbol{x}\right)$ is a collection of random variables $\boldsymbol{x}$ defined on the same probability space $(\Omega, \mathcal{F}, \mathbb{P})$. The index $t \in T$ represents the time and the stochastic process $H\left(t, \boldsymbol{x}\right)$ is called discrete-time process, if $T \subseteq \mathbb{N}$, or continuous-time process, if T is not countable. Typically, $T = [a, b]$ with $a, b \in \mathbb{N}$ and $T = \mathbb{R}_+ = [0, \infty]$, respectively.

Each generic stochastic process can be considered as a function of the variables $t \in T$ and $\omega \in \Omega$. Indeed, for each fixed value of time $t = \bar{t}$ the stochastic process $H\left(\bar{t}, \boldsymbol{x}\right)$ is a random variable, and for every fixed $\omega = \bar{\omega}$ the stochastic process is a deterministic function of time called trajectory of the stochastic process.

Defining a notion of probability density function for a stochastic process is not easy. Usually, only a family of finite-dimensional distribution is considered that

corresponds to a finite set of time instants t_i for $i = 1, \ldots, G$ with $G \subseteq \mathbb{N}$, where for each t_i the stochastic process $H(t_i, \boldsymbol{x})$ is a random variable.

A second order process is a real-valued stochastic process $H(t, \boldsymbol{x})$ for $t \geq 0$ with $E\left[H(t, \boldsymbol{x})^2\right] < \infty \quad \forall t \in T$. The mean, the variance and the autocovariance function of a second order process are respectively defined as:

$$\mu_H(t) = E\left[H(t, \boldsymbol{x})\right] \tag{2.32}$$

$$\sigma_H^2(t) = E\left[\left(H(t, \boldsymbol{x}) - \mu_H\right)^2\right] \tag{2.33}$$

$$C_H(t_1, t_2) = Cov\left[H(t_1, \boldsymbol{x}) H(t_2, \boldsymbol{x})\right] \tag{2.34}$$

2.3.1   Example: Continuous Stochastic Process

Let us suppose that $\lambda \in \mathbb{R}$, and x_1, x_2 are independent random variables such that

- $\mu_{x_1} = 0$ and $E\left[x_1^2\right] < \infty$,

- x_2 is uniformly distributed on $[0, 2\pi]$.

The stochastic process

$$H(t, \boldsymbol{x}) = x_1 cos(x_2 + \lambda t) \tag{2.35}$$

is a second order process with

$$\mu_H(t) = 0 \tag{2.36}$$

$$C_H(t_1, t_2) = \frac{1}{2} E\left[x_1^2\right] cos(\lambda(t_2 - t_1)) \tag{2.37}$$

2.4   Monte Carlo Method

In Section 2.3, it was introduced the notion of stochastic process $H(t, \boldsymbol{x})$ in the time domain. Since frequency-domain analysis is essential for many electronic circuits, it is immediate to introduce the notion of stochastic process in the frequency-domain $H(f, \boldsymbol{x})$ as a function of the frequency f and of the random variables considered. The variability analysis techniques presented in this Chapter can be applied to both time- or frequency-domain stochastic process. Hence, the explicit dependency on time or frequency of the stochastic processes considered is omitted in the notation used in the rest of the Chapter.

The MC method or analysis is a statistical evaluation tool that relies on repeatedly solving a problem by using a large set of values of the random variables involved. In the context of this PhD thesis, the problem is the analysis of the effects of geometrical or electrical parameters variability on the performance of the circuit under study. In particular, Computer Aided Design (CAD) tools, such as

EM simulators, will be used to analyze the particular IC considered. Since the MC method represents the standard approach for variability analysis thanks to its accuracy, robustness and ease of implementation, it will be used as a reference to evaluate the accuracy and efficiency of the techniques presented in this PhD thesis.

At first, the MC analysis requires to individuate the random parameters of interest and their distribution. It is important to remark that the identification of the random variables involved in the stochastic process under exam is a fundamental preliminary step required to be able to perform the variability analysis with any technique. For the purpose of this PhD thesis, it will be assumed that the distribution of the random variables of interest is known. Next, it is necessary to compute a large set of samples of the chosen random parameters according to their distribution. However, truly random samples are not always required for the MC method to be accurate and different computational algorithms can be used to generate deterministic pseudo-random sequences [2]. For the purpose of this work, the samples needed are generated using suitable pseudo-random generators in MAT-LAB[1]. Now, it is possible to simulate the IC under study via CAD tools for each sample obtained for the chosen random parameters. This step of the MC analysis represents its main drawback for the application of this variability analysis method to modern high-speed ICs. Indeed simulating such circuits is often expensive, considering that both the operative bandwidth and complexity of modern electrical systems are constantly increasing. Due to the large number of simulations required to obtained accurate results, as it will be described in the following, the MC analysis has a really high computational time. Finally, it is possible to collect and analyze the results obtained so far to compute statistical information.

In the rest of this Section, it will be described the accuracy of the MC method in estimating statistical information according to the number of samples considered in the analysis. Let us suppose that we want to compute via MC analysis the mean $\mu(Y)$ of the stochastic process $Y(\boldsymbol{x})$, that depends on N random variables included in the vector $\boldsymbol{x}$, see equation (2.32). Without loss of generality, we suppose that the random variables $\boldsymbol{x}$ are independent and uniformly distributed. Hence, equation (2.32) requires to calculate a suitable multidimensional integral defined on the N-dimensional unit hypercube [2, 3]. The mean of $Y(\boldsymbol{x})$ can be computed using the MC method as [2]:

$$\mu(Y)_{MC} = \frac{1}{K} \sum_{k=1}^{K} Y_k \qquad (2.38)$$

where $Y_k = Y(\boldsymbol{x}_k)$ for $k = 1, \ldots, K$. Next, it is possible to prove that the estimator (2.38) is unbiased:

$$E\left[\mu(Y)_{MC}\right] = \mu(Y) \qquad (2.39)$$

---

[1] The Mathworks, Inc., Natick

and, since Y_k for $k = 1, \ldots, K$ are independent identically distributed, it converges almost surely to the exact value $\mu(Y)$ as [3]:

$$\lim_{K \to \infty} \mathbb{P}\left(\mu(Y)_{MC} = \mu(Y)\right) = 1 \tag{2.40}$$

Finally, the variance of the estimator (2.38) can be expressed with respect to the variance $\sigma(Y)^2$ of the stochastic process $Y(\boldsymbol{x})$ as [3]:

$$\sigma^2(\mu(Y)_{MC}) = \frac{\sigma^2(Y)}{K} \tag{2.41}$$

It is important to notice that the statistic computed on samples sets, including equation (2.38), are random quantities. Indeed, performing a MC analysis with the same number of samples K for different values of the random variables $\boldsymbol{x}$ would produce different values of (2.38). An important measure of the accuracy of estimation (2.38) is given by the confidence interval $100(1 - \alpha)\%$: the mean $\mu(Y)$ of the stochastic process $Y(\boldsymbol{x})$ lies inside the range individuated by the confidence interval with approximated probability $(1 - \alpha)$, where $0 < \alpha < 1$.

Under fairly general conditions [2], it is possible to prove that:

$$\lim_{K \to \infty} \mathbb{P}\left(Estim \leq \beta\right) = F_{\mathcal{N}}(\beta) \tag{2.42}$$

where

$$Estim = \frac{\mu(Y)_{MC} - \mu(Y)}{\sqrt{\frac{\sigma^2(Y)}{K}}} \tag{2.43}$$

and $F_{\mathcal{N}}$ is the CDF of the normal distribution (Gaussian distribution with zero mean and unitary standard deviation). Equivalently, the quantity $Estim$ converges in distribution to a random variables with normal distribution for $N \to \infty$. An asymptotically valid confidence interval for (2.38) is

$$100(1 - \alpha)\% =$$

$$\left[\mu(Y)_{MC} - F_{\mathcal{N}}^{-1}\left(1 - \frac{\alpha}{2}\right)\sqrt{\frac{\sigma^2(Y)}{K}}, \ \mu(Y)_{MC} + F_{\mathcal{N}}^{-1}\left(1 - \frac{\alpha}{2}\right)\sqrt{\frac{\sigma^2(Y)}{K}}\right] \tag{2.44}$$

However, the variance $\sigma(Y)^2$ of the stochastic process $Y(\boldsymbol{x})$ in (2.44) is unknown. A strongly consistent estimator of $\sigma(Y)^2$ can be computed using the MC analysis as [2]:

$$\sigma(Y)_{MC}^2 = \frac{1}{K - 1} \sum_{k=1}^{K} (Y_k - \mu(Y)_{MC})^2 \tag{2.45}$$

Note that, the use of (2.45) in (2.44) introduces a sampling-based error. The MC analysis can be used to estimate higher order moments, even if with a slower convergence rate with respect to the mean, since the variance of the related estimators is usually large.

Equation (2.44) allows to point out two important characteristics of the MC method:

- the MC analysis has a slow convergence rate with respect to the number K of simulations performed, since the confidence interval (2.44) depends on the inverse square root of K;

- the convergence rate of the MC analysis does not depend on the number N of random variables considered, making the MC method particularly suitable in performing the variability analysis with respect to an high number of parameters.

Concluding, the MC method is straightforward to implement, robust and accurate, but has a slow convergence rate with respect to the number of simulations performed. Since simulations of complex high speed ICs are expensive, the MC method has a really high computational time.

2.5 Polynomial Chaos expansion

A stochastic process $Y(\boldsymbol{\xi})$ with finite variance can be expanded as a series of orthogonal polynomials with suitable coefficients as [4]

$$Y(\boldsymbol{\xi}) = \sum_{i=0}^{\infty} \alpha_i \varphi_i(\boldsymbol{\xi}) \tag{2.46}$$

where $\varphi_i(\boldsymbol{\xi})$ are the corresponding orthogonal polynomials depending on the vector of normalized random variables $\boldsymbol{\xi}$ and the coefficients α_i are called PC coefficients. Regarding the polynomials, the following orthogonality condition is satisfied [5]

$$< \varphi_i(\boldsymbol{\xi}), \varphi_j(\boldsymbol{\xi}) > = \int_{\boldsymbol{\Omega}} \varphi_i(\boldsymbol{\xi}) \varphi_j(\boldsymbol{\xi}) W(\boldsymbol{\xi}) d\boldsymbol{\xi} = a_i \delta_{ij} \tag{2.47}$$

where a_i are positive numbers, δ_{ij} is the Kronecker delta and $W(\boldsymbol{\xi})$, called weighting function in the theory of orthogonal polynomials [6], is a probability measure with support $\boldsymbol{\Omega}$. The construction of the PC expansion (2.46) entails a three-step process:

- Calculating the orthogonal polynomials $\varphi_i(\boldsymbol{\xi})$.

- Truncating the series to a finite order.

- Computing the PC coefficients α_i.

If the stochastic process $Y(\boldsymbol{\xi})$ is composed of independent random variables, the identification of the orthogonal polynomials, also called basis functions, is straightforward: the global uncertainty PDF is the product of the PDFs of the single random variables. In this case, the weighting function can be written as

$$W(\boldsymbol{\xi}) = \prod_{i=1}^{N} W_i(\xi_i) \tag{2.48}$$

where N is the number of random variables. Therefore, due to the orthogonality relation (2.47), the basis functions $\varphi_i(\boldsymbol{\xi})$ can be calculated as product combinations of orthogonal polynomials corresponding to each individual random variable ξ_i [7]. Using the so called "total order expansion" [8], (2.46) can be truncated to a limited number of M basis functions as

$$\varphi_j(\boldsymbol{\xi}) = \prod_{k=1}^{N} \phi_{i_k}(\xi_k) \quad \text{with} \quad \sum_{k=1}^{N} i_k \leq P \quad \text{and} \quad 0 \leq j \leq M \tag{2.49}$$

where $\phi_{i_k}(\xi_k)$ represents the polynomial function of degree i corresponding to the random variable ξ_k and P is the highest degree of the polynomials used in the truncated PC expansion (called order of the expansion in the rest of this PhD thesis). It is easy to show [8] that the total number of basis functions $M+1$ used in the PC expansion is

$$M + 1 = \frac{(N+P)!}{N!P!} \tag{2.50}$$

Note that for random variables with specific PDFs (indicated in the sequel as standard distributions) the basis functions are the polynomials of the Wiener-Askey scheme [6], as shown in Table 2.1. For example, in the Gaussian PDF case the basis functions are the Hermite polynomials, and in the uniform PDF case the basis functions are the Legendre polynomials. The optimality of the polynomials of the Wiener-Askey scheme is guaranteed as their weighting function $W(\boldsymbol{\xi})$ corresponds to the PDF of the associated random variable, when placed in a standard form [5, 6]. Due to this property, an exponential convergence rate can be achieved [5]. Furthermore, optimal basis functions can be calculated numerically for independent random variables with arbitrary PDFs following the approach described in [5].

In the general case of correlated random variables with arbitrary PDFs, the basis functions can be calculated following the approach described in [5, 7, 8]. In this case, decorrelation can be obtained via a variable transformation, such as the Nataf transformation [9] or the Karhunen-Loéve expansion [10] and the convergence rate of the PC expansion may not be exponential.

After determination of the basis functions, (2.46) is truncated as follows

$$Y(\boldsymbol{\xi}) \approx \sum_{i=0}^{M} \alpha_i \varphi_i(\boldsymbol{\xi}) \tag{2.51}$$

Next, the $M + 1$ PC coefficients α_i must be computed. Two main approaches exist in the literature to compute the PC coefficients: the spectral projection and the linear regression technique [8]. The first approach projects the stochastic process on each basis function, requiring the evaluation of the following multidimensional integral

$$\alpha_i = \frac{1}{<\varphi_i(\boldsymbol{\xi}), \varphi_i(\boldsymbol{\xi})>} \int_{\boldsymbol{\Omega}} Y(\boldsymbol{\xi})\varphi_i(\boldsymbol{\xi})W(\boldsymbol{\xi})d\boldsymbol{\xi} \tag{2.52}$$

for each coefficient of the PC expansion. The second approach calculates all the PC coefficients solving a least-square system [8]

$$\boldsymbol{\Psi}\boldsymbol{\alpha} = \boldsymbol{R} \tag{2.53}$$

Equation (2.53) is calculated with respect to an initial set of discrete samples of the normalized random variables $\boldsymbol{\xi}$, indicated as $\left[\boldsymbol{\xi}_j\right]_{j=1}^{K}$. The $j-$th row of the matrix $\boldsymbol{\Psi}$ contains the multivariate polynomial basis evaluated at $\boldsymbol{\xi}_j$ and the matrix $\boldsymbol{R}$ represents the corresponding set of stochastic process values.

The main advantage of the PC expansion is the analytical representation of the system variability. For example, the mean μ and the variance σ^2 of the stochastic process Y can be written as [8]

$$\mu = \alpha_0 \tag{2.54}$$

$$\sigma^2 = \sum_{i=1}^{M} \alpha_i^2 < \varphi_i(\boldsymbol{\xi}), \varphi_i(\boldsymbol{\xi}) > \tag{2.55}$$

Apart from all moments, also stochastic functions of $Y(\boldsymbol{\xi})$, such as the PDF and the CDF, can be computed following standard analytical formulas or numerical schemes [1].

If the stochastic process under study is written in a matrix form $\boldsymbol{Y}(\boldsymbol{\xi})$, the PC coefficient must be calculated for each entry of $\boldsymbol{Y}(\boldsymbol{\xi})$. In this case, (2.51) can be written as

$$\boldsymbol{Y}(\boldsymbol{\xi}) \approx \sum_{i=0}^{M} \boldsymbol{\alpha}_i\varphi_i(\boldsymbol{\xi}) \tag{2.56}$$

Random variables	Polynomial	Support range
Gaussian	Hermite	$[-\infty, \infty]$
Uniform	Legendre	$[-1, 1]$
Beta	Jacobi	$[-1, 1]$
Gamma	Laguerre	$[0, \infty]$

Table 2.1: Polynomials of the Wiener-Askey scheme for continuous random variables [6].

where $\boldsymbol{\alpha}_i$ is the matrix of PC coefficients for the i-th polynomial basis and has the same size of $\boldsymbol{Y}(\boldsymbol{\xi})$. For a complete reference to PC theory, the reader is referred to [4] – [8].

2.6   Stochastic Collocation methods

The basic idea of the SC approach is to approximate the unknown stochastic solution by interpolation functions in the stochastic space. The interpolation is constructed by repeatedly solving (sampling) the deterministic problem at a pre-determined set of nodes in the stochastic space. E.g., a stochastic process $\mathbf{Y}(\boldsymbol{\xi})$ can be expressed as:

$$\mathbf{Y}(\boldsymbol{\xi}) = \sum_{i=1}^{Q} \mathbf{Y}(\boldsymbol{\xi}_i) L_i(\boldsymbol{\xi}) \tag{2.57}$$

where $\boldsymbol{\xi}$ denote the stochastic parameters and $\{L_i(\boldsymbol{\xi})\}_{n=1}^{N}$ represents the interpolation basis functions. Hence, the computational effort required for the collocation approach depends on the number of support nodes used for constructing the interpolation. Once the interpolation scheme has been selected, no estimation of the order of the basis functions is needed. As a result, the key issue for this approach is the selection of the support nodes, such that using the minimal number of nodes one achieves a good approximation.

For example, if the Lagrange interpolation scheme is chosen, the element L_i in (2.57) for a one-dimensional interpolation can be expressed as

$$L_i(\xi) = \prod_{i=1, \ i \neq j}^{Q} \frac{\xi - \xi_i}{\xi_j - \xi_i} \tag{2.58}$$

where L_i is equal to 1 for $\xi = \xi_j$ and is equal to 0 for $\xi = \xi_i$. Next, for interpolation in multiple dimensions, a tensor-product approach can be used and equation (2.57) becomes

$$\mathbf{Y}(\boldsymbol{\xi}) = \sum_{i_1=1}^{Q_{k_1}} \cdots \sum_{i_N=1}^{Q_{k_N}} \mathbf{Y}\left(\boldsymbol{\xi}_{i_1}^{k_1}, \ldots, \boldsymbol{\xi}_{i_N}^{k_N}\right) \left(L_{i_1}^{k_1} \otimes \cdots \otimes L_{i_N}^{k_N}\right) \tag{2.59}$$

where $\boldsymbol{\xi}_i^k$ is the $i-$th node in the $k-$th direction and the total number of nodes used in (2.59) is

$$\prod_{n=1}^{N} Q_{k_n} \tag{2.60}$$

Obviously, the adoption of the full tensor-product approach is not efficient with respect to the number of random variables N. Hence, the adoption of Smolyak sparse grids [11–13] to choose the collocation points allows to drastically reduce

the total number of nodes used in the interpolation while preserving a high level of accuracy.

The stochastic moments can be computed by means of analytical formulas and then very efficiently, once the analytical form of the interpolation kernel functions $\{L_i(\boldsymbol{\xi})\}_{n=1}^N$ and probability measure $W(\boldsymbol{\xi})$ has been decided. Indeed, the $m-$th moment of $\mathbf{Y}(\boldsymbol{\xi})$ can be expressed as:

$$\mu_m\left(\mathbf{Y}\left(\boldsymbol{\xi}\right)\right) = \mathbb{E}\left[\mathbf{Y}^m\left(\boldsymbol{\xi}\right)\right] = \int_\Omega \mathbf{Y}^m\left(\boldsymbol{\xi}\right) W\left(\boldsymbol{\xi}\right) d\boldsymbol{\xi} \qquad (2.61)$$

where $W\left(\boldsymbol{\xi}\right)$ is a probability measure with support Ω. Let us assume that the interpolation kernel functions $\{L_i\left(\boldsymbol{\xi}\right)\}_{n=1}^N$ only depend on the stochastic space grid points and their computation does not require the solution of a linear system to impose an interpolation constraint. Therefore, interpolating systems, matrices or scalars does not make any difference for these interpolation kernel functions.

References

[1] A. Papoulis. *Probability, Random Variables and Stochastic Processes.* McGraw-Hill College, 1991.

[2] G. S. Fishman. *Monte Carlo: Concepts, Algorithms, and Applications.* Springer-Verlag, New York, 1996.

[3] A. Singhee, R. A. Rutenbar. *Why Quasi-Monte Carlo is Better Than Monte Carlo or Latin Hypercube Sampling for Statistical Circuit Analysis,.* IEEE Trans. Comput.-Aided Design Integr. Circuits Syst., 29(11):1763–1776, Nov. 2010.

[4] G. Blatman and B. Sudret. *An adaptive algorithm to build up sparse polynomial chaos expansions for stochastic finite element analysis.* Probabilistic Engineering Mechanics, 25(2):183 – 197, Apr. 2010.

[5] J. A. S. Witteveen and H. Bijl. *Modeling Arbitrary Uncertainties Using Gram-Schmidt Polynomial Chaos.* In Proc. 44th AIAA Aerospace Sciences Meeting and Exhibit, number AIAA-2006-0896, Palm Springs, California, Jan. 2006.

[6] D. Xiu and G. E. Karniadakis. *The Wiener-Askey Polynomial Chaos for Stochastic Differential Equations.* SIAM J. Sci. Comput., 24(2):619–644, Apr. 2002.

[7] C. Soize and R. Ghanem. *PHYSICAL SYSTEMS WITH RANDOM UNCERTAINTIES: CHAOS REPRESENTATIONS WITH ARBITRARY PROBABILITY MEASURE.* SIAM J. SCI. COMPUT., 26(2):395–410, Jul. 2004.

[8] M. S. Eldred. *Recent advance in non-intrusive polynomial-chaos and stochastic collocation methods for uncertainty analysis and design.* In Proc. 50th AIAA/ASME/ASCE/AHS/ASC Structures, Structural Dynamics, and Materials Conference, Palm Springs, California, May 2009.

[9] A. Der-Kiureghian and P. L. Liu. *Structural Reliability Under Incomplete Probability Information,.* J. Eng. Mech., ASCE, 112(1):85–104, Jan. 1986.

[10] M. Loeve. *Probability Theory.* Springer-Verlag, 4-th edition, 1977.

[11] V. Barthelmann, E. Novak, and K. Ritter. *High dimensional polynomial interpolation on sparse grid.* Adv. Comput. Math., Mar. 2000.

[12] E. Novak and K. Ritter. *High dimensional integration of smooth functions over cubes.* Numer. Math., Nov. 1996.

[13] E. Novak and K. Ritter. *Simple cubature formulas with high polynomial exactness*. Construct. Approx., 15(4):499–522, Oct. 1999.

3

Variability Analysis of Multiport Systems via Polynomial Chaos Expansion

In this chapter, the first model-driven stochastic macromodeling technique developed during my research activity is presented. It is based on the calculation of root macromodels of the system transfer functions and on the PC expansion of the corresponding state-space matrices. It extends to general passive multiport circuits (such as interconnections, filters, connectors, etc.) the application of the PC expansion, previously adopted only for lumped elements and multiconductor transmission lines.

<p align="center">⋆ ⋆ ⋆</p>

D. Spina, F. Ferranti, T. Dhaene, L. Knockaert, G. Antonini, D. Vande Ginste

Abstract We present a novel technique to perform variability analysis of multiport systems. The versatility of the proposed technique makes it suitable for the analysis of different types of modern electrical systems. The proposed method, based

on the calculation of a set of univariate macromodels and on the use of the PC expansion, produces a macromodel of the transfer function of the multiport system including its statistical properties. The accuracy and the significant speed-up with respect to the classical MC analysis are verified by means of two numerical examples.

3.1   Introduction

The increasing demand for performance from ICs pushes operation to higher signal bandwidths, while rapid advances in manufacturing capabilities have significantly reduced the feature size and increased the density of these devices. In this scenario, the analysis of the effects of geometrical or electrical parameters variability on the ICs performance is fundamental.

The standard approach for variability analysis is the MC method. MC gives accurate results and its implementation is straightforward, but it requires a large number of simulations. Since simulations are often computationally expensive due to the increased complexity of systems, MC has a very high computational cost. Recently, a new approach, based on the PC expansion, has emerged to perform variability analysis as an efficient alternative to the computationally cumbersome MC-based techniques. The PC-based modeling approach expands a stochastic process in terms of orthogonal polynomials, giving an analytical representation of the variability of the system with respect to the random variables under consideration [1]. Over the recent years, techniques were developed to study the stochastic variations of electrical circuits by means of the PC expansion. These techniques were tailored to handle specific systems, namely multiconductor transmission lines [2] - [4] and lumped elements circuits [5], [6].

Instead, the variability analysis technique presented in this chapter can be applied to any generic multiport system, if the linear system can be described by a state-space model. The starting point of the proposed technique is the evaluation of the system transfer function on a discrete set of frequencies and geometrical or physical parameters chosen for the variability analysis. The transfer function of the system in the frequency-domain can be expressed in different forms (e.g. scattering, impedance or admittance parameters), making the proposed method applicable to a large range of microwave systems. Next, a univariate frequency-domain macromodel is computed using the Vector Fitting (VF) technique [7] - [9] for each combination of the discretized design parameters. In this chapter, we refer to these initial univariate macromodels as *root macromodels*. Afterwards, a state-space realization is obtained for each *root macromodel*, allowing to calculate the PC model with respect to the random variables under consideration.

The main advantage of this new approach is clear: the PC-model of the state-space matrices is able to describe the statistical properties of the system over the

entire frequency range of the chosen samples. Furthermore, the PC model of the system transfer function can be calculated for each frequency of interest by combining the PC model of the state-space matrices with the existing deterministic equations for systems expressed in state-space form. Finally, the corresponding PC expansion of the ports voltage and current can be easily obtained from the PC representation of the system transfer function.

3.2   Variability analysis of Multiport Systems

3.2.1   Transfer function PC modeling

The starting point of our approach is the description of a multiport system with a generic linear input-output representation in state-space form:

$$(s\boldsymbol{I} - \boldsymbol{A}(\boldsymbol{\xi}))\,\boldsymbol{X}(s,\boldsymbol{\xi}) = \boldsymbol{B}(\boldsymbol{\xi}) \tag{3.1}$$

$$\boldsymbol{Y}(s,\boldsymbol{\xi}) = \boldsymbol{C}(\boldsymbol{\xi})\boldsymbol{X}(s,\boldsymbol{\xi}) + \boldsymbol{D}(\boldsymbol{\xi}) \tag{3.2}$$

where the dependency on a vector of random variables $\boldsymbol{\xi}$ is explicitly indicated. The goal is to calculate the PC expansion in the form (see Section 2.5)

$$\boldsymbol{Y} \approx \sum_{i=0}^{M} \boldsymbol{\alpha}_i \varphi_i(\boldsymbol{\xi}) \tag{3.3}$$

of the state-space variables $\boldsymbol{X}$ and, consequently, of the output $\boldsymbol{Y}$, starting from the PC expansion of the state-space matrices. The reader is referred to Section 2.5 for a complete overview about the properties of the PC expansion.

Without loss of generality, for ease of notation, the random variables of the stochastic process $\boldsymbol{Y}$ are chosen as independent and the corresponding PDFs are standard distributions. Hence, the basis functions $\varphi_i(\boldsymbol{\xi})$ are the polynomials of the Wiener-Askey scheme [10]. Note, however, that (3.1) and (3.2) can also be calculated for the general case of correlated random variables with arbitrary distributions, using the techniques described in Section 2.5.

In what follows, we will demonstrate that, to achieve our goal, it is necessary to:

- Decide on the number of basis functions M in (3.3).

- Compute the PC coefficients of the state-space matrices.

- Calculate and solve an equivalent linear system for the coefficients of the PC expansion of $\boldsymbol{X}$.

- Combine the obtained results in a suitable way in order to obtain the PC expansion of $\boldsymbol{Y}$.

Since, for practical applications, the highest degree of the polynomials used in the PC expansion (3.3) can be limited between two and five [2], [10], the number of basis functions M in our approach is chosen upfront according to (2.50):

$$M + 1 = \frac{(N + P)!}{N!P!}$$

where N is the number of random variables and P is the highest degree of the polynomials used in the PC expansion (3.3).

Next, the PC coefficients are computed by means of the linear regression approach solving a suitable least-square system in the form [1]

$$\boldsymbol{\Psi}\boldsymbol{\alpha} = \boldsymbol{R} \tag{3.4}$$

Hence, the equivalent matrices $\boldsymbol{\Psi}$ and $\boldsymbol{R}$ must be built for the state-space matrices in (3.1), (3.2).

The first step is the computation of K univariate frequency-domain macromodels, called *root macromodels* [11], [12]. This is done by invoking the VF algorithm K times, i.e., for a discrete set of values of the normalized random variables $\left[\boldsymbol{\xi}_j\right]_{j=1}^{K}$, each time using L frequency samples $[f_l]_{l=1}^{L}$. A simple pole-flipping scheme is used to enforce stability [7]. Afterwards, a state-space realization is obtained for each stable *root macromodel* $[\boldsymbol{A}_j, \boldsymbol{B}_j, \boldsymbol{C}_j, \boldsymbol{D}_j]_{j=1}^{K}$ using a realization technique. The realization technique used to convert a pole-residue model to a state-space form has an influence on the smoothness of the state-space matrices with respect to the design parameters and, therefore, on the accuracy of the final PC model. We use a standard Gilbert realization [13] in our approach.

Note that all K realizations of all state-space matrices must have the same dimensions to build the matrix $\boldsymbol{R}$. This requirement can easily be satisfied if one considers that the range of variation of each random variable is relatively small. Therefore, the VF algorithm is applied first to estimate the maximum number of poles needed for the rational modeling by computing the poles at the corner points of the discrete set of initial data, and afterwards to build the corresponding *root macromodels* using this number of poles. Finally, ordering the basis functions and the state-space matrices computed for each $\boldsymbol{\xi}_j$, an equivalent equation (3.4) can be obtained for each state-space matrix. Let us suppose that T poles are needed to build each *root macromodel*, then the matrices $\boldsymbol{\Psi}$, $\boldsymbol{\alpha}$ and $\boldsymbol{R}$ of equation (3.4) calculated for the state-space matrix $\boldsymbol{A}$ can be written as

$$\boldsymbol{\Psi} = \begin{bmatrix} \boldsymbol{\varphi}_0\left(\boldsymbol{\xi}_1\right) & \cdots & \boldsymbol{\varphi}_M\left(\boldsymbol{\xi}_1\right) \\ \vdots & \vdots & \vdots \\ \boldsymbol{\varphi}_0\left(\boldsymbol{\xi}_K\right) & \cdots & \boldsymbol{\varphi}_M\left(\boldsymbol{\xi}_K\right) \end{bmatrix}$$

$$\boldsymbol{\alpha} = \begin{bmatrix} \boldsymbol{A}_0 \\ \vdots \\ \boldsymbol{A}_M \end{bmatrix} \tag{3.5}$$

$$\boldsymbol{R} = \begin{bmatrix} \boldsymbol{A}\left(\boldsymbol{\xi}_1\right) \\ \vdots \\ \boldsymbol{A}\left(\boldsymbol{\xi}_K\right) \end{bmatrix}$$

where $\boldsymbol{\varphi}_i\left(\boldsymbol{\xi}_j\right)$ is the product of the identity matrix $\boldsymbol{I}^{T \times T}$ with the $i-$th basis function $[\varphi_i]_{i=1}^M$ calculated for the $j-$th sample of $\left[\boldsymbol{\xi}_j\right]_{j=1}^K$, the symbol $\boldsymbol{A}_i$, $i = 0, \cdots, M$, represents the $i-$th PC coefficient matrix, while $\boldsymbol{A}\left(\boldsymbol{\xi}_j\right)$ is the $\boldsymbol{A}$ matrix calculated for $\left[\boldsymbol{\xi}_j\right]_{j=1}^K$. Equation (3.4) for the state-space matrices can be solved in a least squares sense using an element-wise, column-wise or matrix-wise approach. Note that, the linear system in the form (3.5) must be overdermined to be solved in a least-square sense. In [1] it is recommended to use a number of samples equal to the double of the basis function used, i.e., $K \approx 2\left(M + 1\right)$.

At this point, we have obtained the representation of the state-space matrices in the form (3.3), using an a priori estimation of the expansion order and the linear regression method to calculate the PC coefficients, which are from now on denoted as $\boldsymbol{A}_i$, $\boldsymbol{B}_i$, $\boldsymbol{C}_i$, $\boldsymbol{D}_i$, $i = 0, ..., M$. Using (3.3) to express the state-space matrices, the state-vector and the output, (3.1) and (3.2) can be rewritten as

$$s \sum_{j=0}^M \boldsymbol{X}_j(s)\varphi_j(\boldsymbol{\xi}) = \sum_{i=0}^M \sum_{j=0}^M \boldsymbol{A}_i \boldsymbol{X}_j(s)\varphi_i(\boldsymbol{\xi})\varphi_j(\boldsymbol{\xi}) + \sum_{i=0}^M \boldsymbol{B}_i \varphi_i(\boldsymbol{\xi}) \tag{3.6}$$

$$\sum_{j=0}^M \boldsymbol{Y}_j(s)\varphi_j(\boldsymbol{\xi}) = \sum_{i=0}^M \sum_{j=0}^M \boldsymbol{C}_i \boldsymbol{X}_j(s)\varphi_i(\boldsymbol{\xi})\varphi_j(\boldsymbol{\xi}) + \sum_{i=0}^M \boldsymbol{D}_i \varphi_i(\boldsymbol{\xi}) \tag{3.7}$$

where the only unknowns are the matrices of PC coefficients $\boldsymbol{X}_j(s)$ for the state-vector, and $\boldsymbol{Y}_j(s)$ for the output. Next we calculate the desired state-vector coefficients solving a corresponding linear system of the form

$$\boldsymbol{\Phi}_X \boldsymbol{X}_\alpha = \boldsymbol{B}_\alpha \tag{3.8}$$

where $\boldsymbol{B}_\alpha$ is the matrix containing all PC coefficients of the $\boldsymbol{B}$ matrix, $\boldsymbol{X}_\alpha$ is the matrix containing all unknown PC coefficients and $\boldsymbol{\Phi}_X$ is a matrix containing weighted scalar products as discussed in what follows. Equation (3.8) can be obtained by projecting (3.6) on the basis functions of the PC expansion. To explain

how (3.8) is built, let us for simplicity assume that the state-space matrices depend on one random variable and two basis functions are used for the PC expansion. The extension to the case of multiple random variables and higher order of expansion is straightforward. Furthermore, the explicit dependency on the vector $\boldsymbol{\xi}$ is omitted in the following equations, for the sake of clarity. In this simplified case, equation (3.6) can be rewritten as

$$
\begin{aligned}
s\boldsymbol{X}_0\varphi_0 + s\boldsymbol{X}_1\varphi_1 = {} & \boldsymbol{A}_0\boldsymbol{X}_0\varphi_0\varphi_0 \\
& + \boldsymbol{A}_1\boldsymbol{X}_0\varphi_1\varphi_0 + \boldsymbol{A}_0\boldsymbol{X}_1\varphi_0\varphi_1 + \boldsymbol{A}_1\boldsymbol{X}_1\varphi_1\varphi_1 \\
& + \boldsymbol{B}_0\varphi_0 + \boldsymbol{B}_1\varphi_1 \quad (3.9)
\end{aligned}
$$

Due to the orthogonality relation (2.47), projection of (3.9) onto the first basis function φ_0, yields

$$
\begin{aligned}
s\boldsymbol{X}_0 < \varphi_0, \varphi_0 >= {} & \\
& \boldsymbol{A}_0\boldsymbol{X}_0 < \varphi_0\varphi_0, \varphi_0 > + \boldsymbol{A}_1\boldsymbol{X}_0 < \varphi_1\varphi_0, \varphi_0 > \\
& + \boldsymbol{A}_0\boldsymbol{X}_1 < \varphi_0\varphi_1, \varphi_0 > + \boldsymbol{A}_1\boldsymbol{X}_1 < \varphi_1\varphi_1, \varphi_0 > \\
& + \boldsymbol{B}_0 < \varphi_0, \varphi_0 > \quad (3.10)
\end{aligned}
$$

Similarly, projecting (3.9) onto the second basis function φ_1, we obtain

$$
\begin{aligned}
s\boldsymbol{X}_1 < \varphi_1, \varphi_1 >= {} & \\
& \boldsymbol{A}_0\boldsymbol{X}_0 < \varphi_0\varphi_0, \varphi_1 > + \boldsymbol{A}_1\boldsymbol{X}_0 < \varphi_1\varphi_0, \varphi_1 > \\
& + \boldsymbol{A}_0\boldsymbol{X}_1 < \varphi_0\varphi_1, \varphi_1 > + \boldsymbol{A}_1\boldsymbol{X}_1 < \varphi_1\varphi_1, \varphi_1 > \\
& + \boldsymbol{B}_1 < \varphi_1, \varphi_1 > \quad (3.11)
\end{aligned}
$$

Upon calculation of the scalar products in (3.10) and (3.11), a matrix equation in the form (3.8) is obtained:

$$
\begin{pmatrix} \boldsymbol{\Phi}_{X00} & \boldsymbol{\Phi}_{X01} \\ \boldsymbol{\Phi}_{X10} & \boldsymbol{\Phi}_{X11} \end{pmatrix} \begin{pmatrix} \boldsymbol{X}_0 \\ \boldsymbol{X}_1 \end{pmatrix} = \begin{pmatrix} \boldsymbol{B}_0 \\ \boldsymbol{B}_1 \end{pmatrix} \tag{3.12}
$$

where

$$
\begin{aligned}
\boldsymbol{\Phi}_{X00} &= s\boldsymbol{I} - \boldsymbol{A}_0 \frac{< \varphi_0\varphi_0, \varphi_0 >}{< \varphi_0, \varphi_0 >} - \boldsymbol{A}_1 \frac{< \varphi_1\varphi_0, \varphi_0 >}{< \varphi_0, \varphi_0 >} \\
\boldsymbol{\Phi}_{X01} &= -\boldsymbol{A}_0 \frac{< \varphi_0\varphi_1, \varphi_0 >}{< \varphi_0, \varphi_0 >} - \boldsymbol{A}_1 \frac{< \varphi_1\varphi_1, \varphi_0 >}{< \varphi_0, \varphi_0 >} \\
\boldsymbol{\Phi}_{X10} &= -\boldsymbol{A}_0 \frac{< \varphi_0\varphi_1, \varphi_1 >}{< \varphi_1, \varphi_1 >} - \boldsymbol{A}_1 \frac{< \varphi_1\varphi_0, \varphi_1 >}{< \varphi_1, \varphi_1 >} \\
\boldsymbol{\Phi}_{X11} &= s\boldsymbol{I} - \boldsymbol{A}_0 \frac{< \varphi_0\varphi_1, \varphi_1 >}{< \varphi_1, \varphi_1 >} - \boldsymbol{A}_1 \frac{< \varphi_1\varphi_1, \varphi_1 >}{< \varphi_1, \varphi_1 >}
\end{aligned} \tag{3.13}
$$
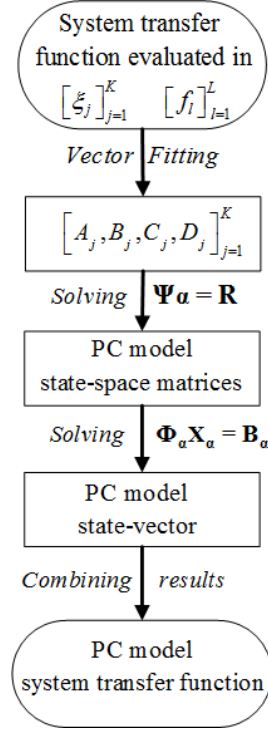
Figure 3.1: Flow chart of the proposed modeling strategy.

and $\boldsymbol{I}$ is the identity matrix. Note that solving (3.12) for different frequency samples does not require renewed calculation of the scalar products in (3.13). Finally, it is now possible to directly compute the PC coefficients of the output $\boldsymbol{Y}_j(s)$. Indeed, because of the orthogonality relation (2.47), projecting equation (3.7) onto the basis functions $\varphi_p(\boldsymbol{\xi})$, $p = 0, ..., M$, leads to

$$
\begin{aligned}
&\boldsymbol{Y}_p(s) < \varphi_p(\boldsymbol{\xi}), \varphi_p(\boldsymbol{\xi}) >= \\
&\sum_{i=0}^{M} \sum_{j=0}^{M} \boldsymbol{C}_i \boldsymbol{X}_j(s) < \varphi_i(\boldsymbol{\xi}) \varphi_j(\boldsymbol{\xi}), \varphi_p(\boldsymbol{\xi}) > + \boldsymbol{D}_p < \varphi_p(\boldsymbol{\xi}), \varphi_p(\boldsymbol{\xi}) >
\end{aligned}
\tag{3.14}
$$

where all the scalar products were already pre-computed in the previous step in order to build the matrix $\boldsymbol{\Phi}_X$.

The proposed PC-based approach aims at performing frequency-domain variability analysis on a large range of microwave systems (e.g. filters, connectors, non-uniform transmission lines), overcoming the limitation of the previously developed PC-based technique [2] - [6], that were tailored to handle specific systems. This appealing characteristic of the proposed PC-based method is obtained by ap-

plying the PC expansion to a state-space representation of the multiport systems. This approach has two main advantages:

- the system transfer function can be expressed in several forms such as scattering, impedance or admittance parameters;

- the PC model of the state-space representation is frequency independent; however, it allows to describe the system in a large frequency range, see (3.6), (3.7).

Indeed, the frequency-dependent PC expansion of the system transfer function can be calculated for every frequency of interest $f' \in [f_1, f_L]$, by solving the linear system (3.8) for $s = j2\pi f'$ and applying the results obtained in (3.14). To solve (3.8), it is only required to compute the projection of (3.6) onto each basis function. We remark that these projections are frequency-independent and can be calculated upfront. The proposed modeling strategy is summarized in Fig. 3.1.

3.2.2 Port Voltages and Currents PC modeling

In this Section, we describe how to compute the PC expansion of the port voltages and currents starting from the PC expansion of the transfer function of the multiport system. We suppose that the terminations are linear and independent of the random variables $\boldsymbol{\xi}$. For ease of notation, the dependency on the Laplace variable s and the random variables $\boldsymbol{\xi}$ are omitted in the following equations. For a multiport system described by its impedance parameters $\boldsymbol{Z}$, the following relation applies [14]:

$$\tilde{\boldsymbol{V}} = \boldsymbol{Z}\tilde{\boldsymbol{I}} \tag{3.15}$$

where the symbol $\tilde{\boldsymbol{V}}$ is used for the port voltages and $\tilde{\boldsymbol{I}}$ for the port currents. We introduce the terminations of the lines to solve (3.15). In case of linear loads, we have

$$\tilde{\boldsymbol{I}} = \boldsymbol{I}_s - \boldsymbol{G}\tilde{\boldsymbol{V}} - s\boldsymbol{C}\tilde{\boldsymbol{V}} \tag{3.16}$$

where $\boldsymbol{I}_s$ is the vector of the source currents, while the matrices $\boldsymbol{G}$ and $\boldsymbol{C}$ describe linear resistive and capacitive lumped elements at the ports of the system. Substituting (3.16) in (3.15) gives

$$\tilde{\boldsymbol{V}} + \boldsymbol{Z}\left(\boldsymbol{G} + s\boldsymbol{C}\right)\tilde{\boldsymbol{V}} = \boldsymbol{Z}\boldsymbol{I}_s \tag{3.17}$$

In (3.17) only $\boldsymbol{Z}$ and $\tilde{\boldsymbol{V}}$ depend on the random variables $\boldsymbol{\xi}$ and therefore application of the PC expansion leads to

$$\sum_{i=0}^{M} \tilde{\boldsymbol{V}}_i \varphi_i(\boldsymbol{\xi}) + \sum_{i=0}^{M}\sum_{j=0}^{M} \boldsymbol{Z}_j\left(\boldsymbol{G} + s\boldsymbol{C}\right)\tilde{\boldsymbol{V}}_i \varphi_i(\boldsymbol{\xi})\varphi_j(\boldsymbol{\xi}) = \sum_{j=0}^{M} \boldsymbol{Z}_j \boldsymbol{I}_s \varphi_j(\boldsymbol{\xi}) \tag{3.18}$$

where $\tilde{V}_i$ represents the vector containing the $i-$th PC coefficients of the port voltages and Z_j is a matrix containing the $j-$th PC coefficients of the impedance parameters. The desired PC coefficients for the port voltages are again obtained by projecting equation (3.18) onto the basis functions $\varphi_p(\boldsymbol{\xi})$, $p = 0,...,M$, as follows:

$$\tilde{V}_p < \varphi_p(\boldsymbol{\xi}), \varphi_p(\boldsymbol{\xi}) > +$$
$$\sum_{i=0}^{M}\sum_{j=0}^{M} Z_j \left(G + sC\right) \tilde{V}_i < \varphi_i(\boldsymbol{\xi})\varphi_j(\boldsymbol{\xi}), \varphi_p(\boldsymbol{\xi}) >=$$
$$Z_p I_s < \varphi_p(\boldsymbol{\xi}), \varphi_p(\boldsymbol{\xi}) > \quad (3.19)$$

As before, the scalar products are already known, because they were pre-computed during the calculation of the matrix $\boldsymbol{\Phi}_X$. Therefore, the p-th PC coefficient vector of the port voltages can be calculated immediately from (3.19). Once the PC expansion for the port voltages is calculated, the corresponding expression for the port currents can be obtained directly expressing (3.16) with respect to the chosen basis functions, as follows:

$$\sum_{i=0}^{M} \tilde{I}_i\varphi_i(\boldsymbol{\xi}) = I_s - \sum_{i=0}^{M} G\tilde{V}_i\varphi_i(\boldsymbol{\xi}) - s\sum_{i=0}^{M} C\tilde{V}_i\varphi_i(\boldsymbol{\xi}) \qquad (3.20)$$

Similar relations apply in the case of admittance and scattering parameters, as illustrated in the next Section.

3.3   Numerical Examples

In this Section, the proposed technique is applied to two different structures. In each example, the scattering parameters of the structure, calculated with respect to a reference impedance of 50 Ω, are considered as a stochastic process with respect to two or three independent random variables ($N = 2$ or $N = 3$) with uniform PDFs. The corresponding basis functions are products of the Legendre polynomials [15] and are shown in Table 3.1[1] for $M = 5$ and $P = 2$, while the weighting function (2.48) is

$$W(\boldsymbol{\xi}) = \begin{cases} 2^{-N}, & |\xi_i| \leq 1, \quad i = 1, ..., N \\ 0, & elsewhere \end{cases} \qquad (3.21)$$

The proposed PC-based method and the MC method are compared to validate the efficiency and accuracy of our novel technique. In each example, the scalar products in (3.8) are calculated analytically on beforehand. The simulations are

---

[1]Based on the fact that $\int_{-1}^{1} P_n(x)^2 dx = 2/(2n+1)$ where $P_n(x)$ are the Legendre polynomials.

performed with MATLAB $2010a$ on a computer with an Intel(R) Core(TM) i3 processor and 4 GB RAM.

index i	i-th basis function φ_i	$< \varphi_i, \varphi_i >$
0	1	1
1	ξ_1	$\frac{1}{3}$
2	ξ_2	$\frac{1}{3}$
3	$\frac{1}{2}\left(3\xi_1^2 - 1\right)$	$\frac{1}{5}$
4	$\xi_1\xi_2$	$\frac{1}{9}$
5	$\frac{1}{2}\left(3\xi_2^2 - 1\right)$	$\frac{1}{5}$

Table 3.1: Legendre polynomials products for two independent random variables, with $M = 5$ and $P = 2$ [3].

3.3.1   Transmission line

In this first example, a lossy microstrip line of length 8 cm is modeled within the frequency range $[0 - 4]$ GHz. Its cross section is shown in Fig. 3.2. The copper line has width $w = 160$ μm, thickness $t = 15$ μm and conductivity $\sigma = 5.8 \cdot 10^7$ S/m. The dielectric is SiO_2 of thickness $h = 180$ μm with relative permittivity $\epsilon_r = 3.9$ and loss tangent $tan\delta = 0.001$.

The length and width of the conductor and the dielectric relative permittivity are considered as independent random variables with a uniform PDF, varying within a range of $\pm5\%$ with respect to the central value mentioned previously. We note that the choice of a line length as parameter for the variability analysis is particularly meaningful because:

- it causes a shift of the resonances of the microstrip, see Fig. 3.3, since a total variation of 0.8 cm in the line length is considered during the variability analysis;

- it cannot be modeled using the techniques described in [2] - [4], since they start from a stochastic model of the per-unit-length parameters for the variability analysis.

The scattering parameters are evaluated using a quasi-analytical model [16] over a grid composed of $4 \times 4 \times 4$ (L, w, ϵ_r) samples for all the random variables and 101 samples for the frequency. The frequency samples are divided in two groups: modeling points (51 samples), used to calculate the state-space representation of the scattering parameters, and validation points (50 samples), used to verify the accuracy of the PC-model with respect to the MC analysis.

The state-space matrices are calculated using the VF algorithm, targeting -50 dB as maximum absolute model error between the scattering parameters and the corresponding *root macromodels* in order to estimate the required number of poles. The PC expansion is calculated using $P = 2$ and $M = 9$, according to (2.50). In Table 3.2 the computational time needed for the MC analysis (performed using 10000 (L, w, ϵ_r) samples for the validation frequencies) and the proposed PC-based technique is reported. Additionally, for the proposed PC method, the computational time needed to calculate the initial samples and to build the polynomial model of the scattering parameters is shown. The comparison in Table 3.2 illustrates the significant efficiency gain of the proposed technique.

To calculate the port voltages and currents variability, we use a frequency-domain Thévenin voltage source of 1 V with a source impedance of 50 Ω. The line is also terminated by 50 Ω.

The proposed PC-based technique has an excellent accuracy compared with the classical MC analysis in computing system variability features, as shown in Figs. 3.4 - 3.7. In particular, Figs. 3.4, 3.5 show the mean and the standard deviation of the real part of the element S_{12}, Fig. 3.6 describes the PDF and the CDF of S_{11} at 1.24 GHz and Fig. 3.7 shows the standard deviation of the imaginary part of the current at the output port of the microstrip. Similar results can be obtained for the other entries of the scattering matrix and for the port signals.
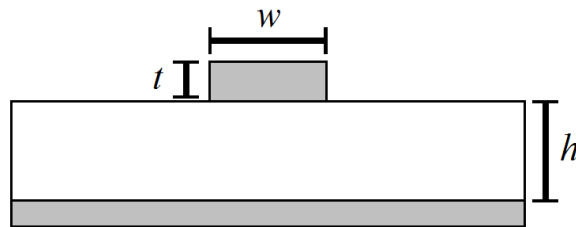
Figure 3.2: Example 3.3.1. Cross section of the lossy microstrip.
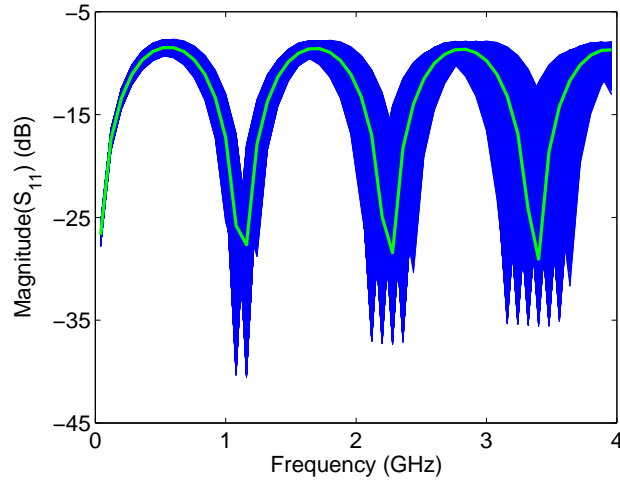
Figure 3.3: Example 3.3.1. Variability of the magnitude of S_{11}. The thick green line corresponds to the central value for L, w and ϵ_r, while the blue lines are the results of MC simulations.
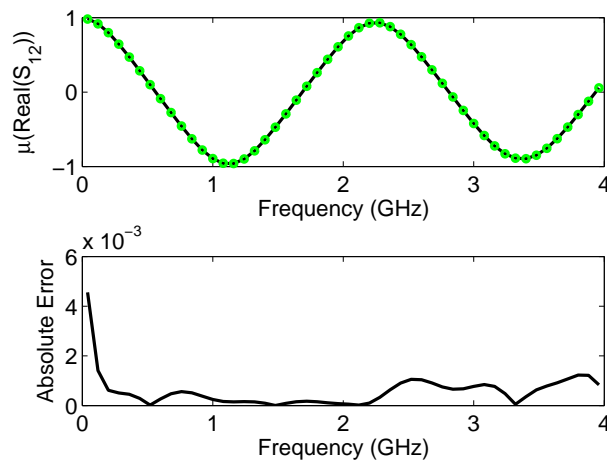
Figure 3.4: Example 3.3.1. The top plot shows a comparison between the mean of the real part of S_{12} obtained with the MC analysis (full black line) and the proposed PC-based method (green circles: ($\circ$)) for the validation frequencies. The lower plot shows the absolute error between the two values.

Figure 3.5: Example 3.3.1. The top plot shows a comparison between the standard deviation of the real part of S_{12} obtained with the MC analysis (full black line) and the proposed PC-based method (green circles: (○)) for the validation frequencies. The lower plot shows the absolute error between the two values.
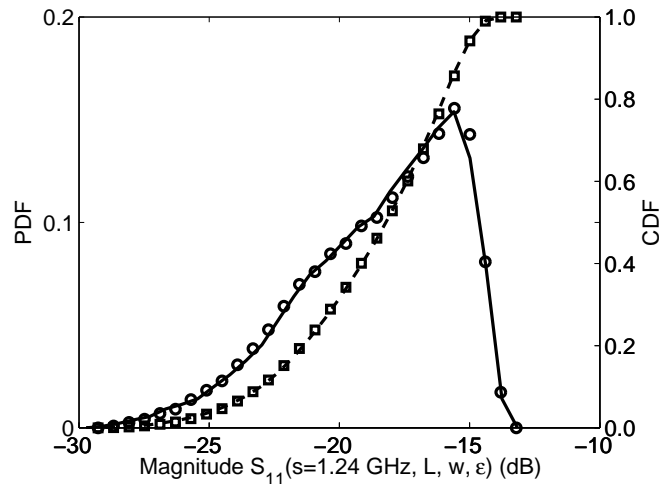
Figure 3.6: Example 3.3.1. PDF and CDF of the magnitude of S_{11} at 1.24 GHz. Full black line: PDF computed using the novel technique; Dashed black line: CDF computed using the novel technique; Circles (○): PDF computed using MC technique; Squares (□): CDF computed using MC technique.

Technique	Computational time
Monte Carlo Analysis (10000 samples)	152.1 s
PC-based technique	7.43 s
Details PC-based technique	Computational time
Initial simulations (64 samples)	0.97 s
PC model scattering parameters	6.46 s

Table 3.2: Example 3.3.1. Efficiency of the Proposed PC-based Technique.
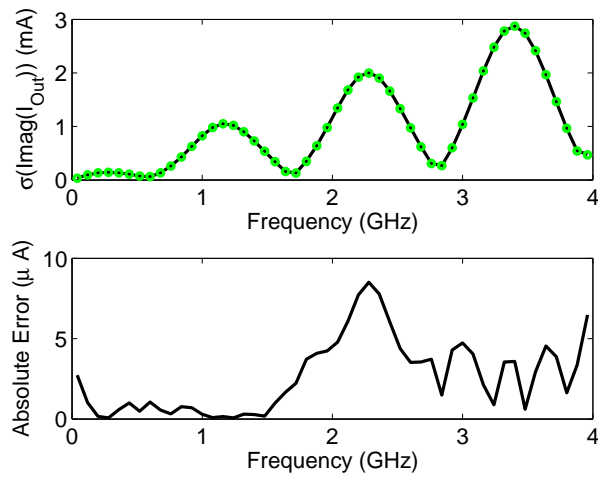
Figure 3.7: Example 3.3.1. The top plot shows a comparison between the standard deviation of the imaginary part of the current at the output port of the microstrip obtained with the MC analysis (full black line) and the proposed PC-based method (green circles: (○)) for the validation frequencies. The lower plot shows the absolute error between the two values.

3.3.2   Double Folded Stub Microstrip Bandstop Filter

In this second example, a double folded stub microstrip bandstop filter [11] has been modeled within the frequency range $[4.75 - 20.25]$ GHz. Its layout is shown in Fig. 3.8.

The substrate is 0.1270 mm thick with a relative dielectric constant $\epsilon_r = 9.9$ and a loss tangent $tan\delta = 0.003$. The length L and the distance S are considered independent random variables with a uniform PDF, varying in a range of $\pm 10\%$ with respect to the central value $L_0 = 2.1946$ mm and $S_0 = 0.1219$ mm, respectively. The scattering parameters are evaluated using the program ADS Momentum over a grid composed of 6×6 (L, S) samples for the geometrical parameters and 62 samples for the frequency. Then, the frequency samples are divided in two groups: modeling points (31 samples) and validation points (31 samples). In this example, the scattering parameters show a high variability with respect to (L, S), as shown in Fig. 3.9.

As in the previous example, VF is used to construct the *root macromodels* for the modeling points, and the accuracy target was again set at -50 dB. The PC expansion is calculated using $P = 3$ and $M = 9$, according to (2.50).

The comparison between the computational time needed for the MC analysis performed using 10000 (L, S) samples for the validation points and the proposed PC-based technique is shown in Table 3.3, demonstrating the efficiency of the proposed PC-based method. In Fig. 3.10 it is shown an example of the convergence rate of the MC analysis in computing the system variability features; note how the choice of the sample size for the MC analysis affects the accuracy.

In order to evaluate the variability of the port voltages and currents, the filter is excited by a frequency-domain Thévenin voltage source of 1 V with a source impedance of 50 Ω and the filter is terminated on a 50 Ω impedance.

Figures 3.11 - 3.14 show the accuracy of the proposed PC-based technique compared to the classical MC analysis in computing system variability features. In particular, Figs. 3.11 and 3.12 show the mean and the standard deviation of the

*Figure 3.8: Example 3.3.2. Geometry of the double folded stub microstrip bandstop filter.*
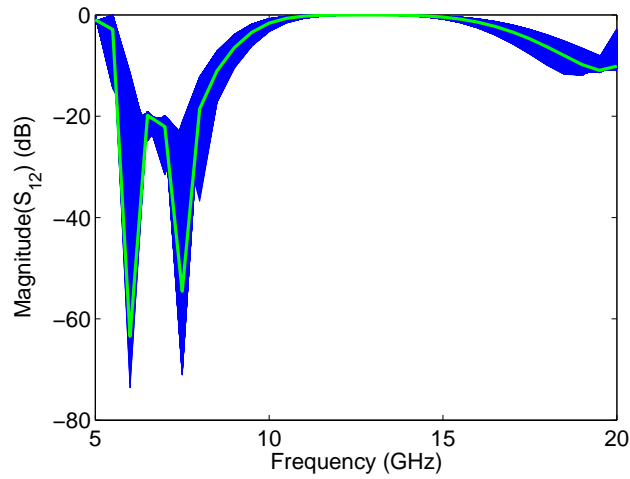
Figure 3.9: Example 3.3.2. Variability of the magnitude of S_{12}. The thick green line corresponds to the central value for S and L, while the blue lines are the results of MC simulations.
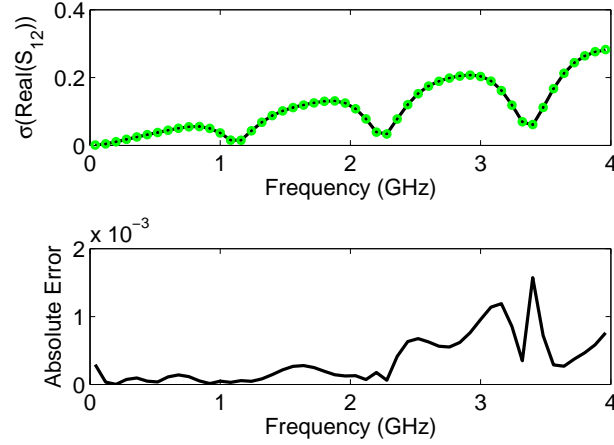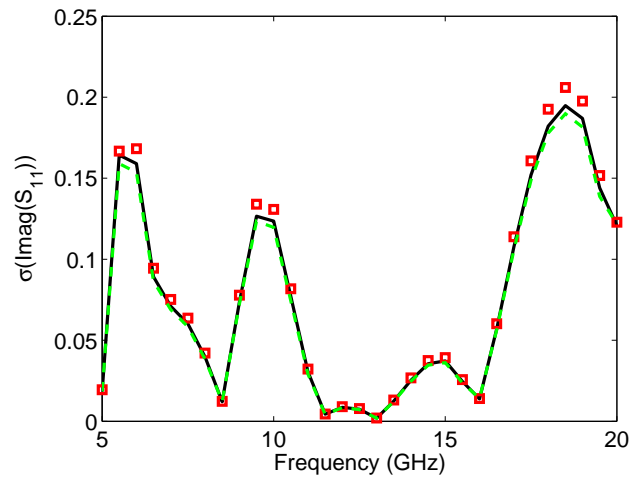

Figure 3.10: Example 3.3.2. Standard deviation of imaginary part of S_{11} obtained with the MC analysis using different sample size. Full black line: standard deviation computed using 10000 samples; Dashed green line: standard deviation computed using 1000 samples; Squares ($\square$): standard deviation computed using 100 samples.

Technique	Computational time
Monte Carlo Analysis (10000 samples)	$253\ h$, $22\ min$, $37.2\ s$
PC-based technique	$54\ min$ $56.88\ s$
Details PC-based technique	Computational time
Initial EM simulations (36 samples, ADS)	$54\ min$ $43.76\ s$
PC model scattering parameters	$13.12\ s$

Table 3.3: Example 3.3.2. Efficiency of the Proposed PC-based Technique.

real part of the element S_{22}, Fig. 3.13 describes the PDF and the CDF of S_{12} at 7.5 GHz and Fig. 3.14 shows the standard deviation of the imaginary part of the voltage at the output port of the filter. Similar results can be obtained for all other entries of the scattering matrix and for the port signals.

3.4   Conclusions

In this chapter, an innovative technique for efficient variability analysis of general multiport systems, such as interconnections, filters, connectors, etc., is presented. It is based on the calculation of *root macromodels* of the system transfer functions and on the PC expansion of the corresponding state-space matrices. The approach allows a representation of the transfer function including its statistical properties. This transfer function may be expressed in terms of e.g. scattering, impedance or admittance parameters, as such making it applicable to a large range of systems. The accuracy and efficiency of the proposed method are validated by means of comparison with the standard MC approach, and this for two distinct illustrative examples.
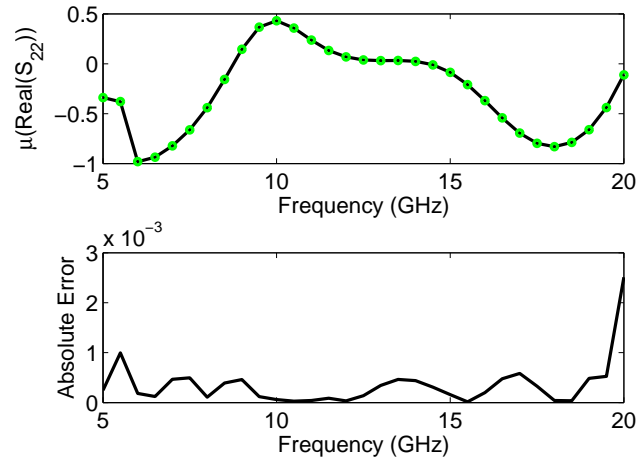
Figure 3.11: Example 3.3.2. The top plot shows a comparison between the mean of the real part of S_{22} obtained with the MC analysis (full black line) and the proposed PC-based method (green circles: (○)) for the validation frequencies. The lower plot shows the absolute error between the two values.
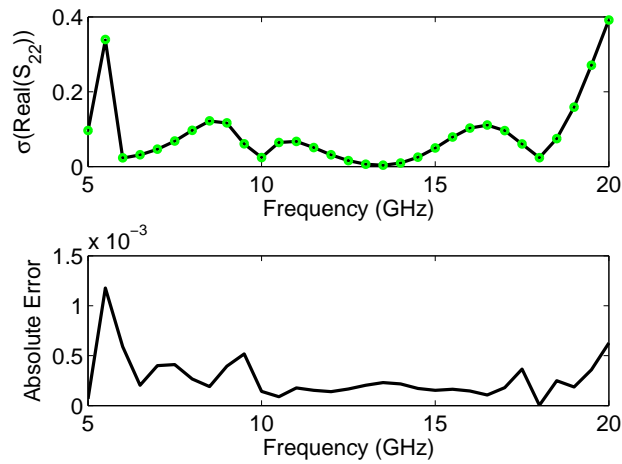
Figure 3.12: Example 3.3.2. The top plot shows a comparison between the standard deviation of the real part of S_{22} obtained with the MC analysis (full black line) and the proposed PC-based method (green circles: (○)) for the validation frequencies. The lower plot shows the absolute error between the two values.
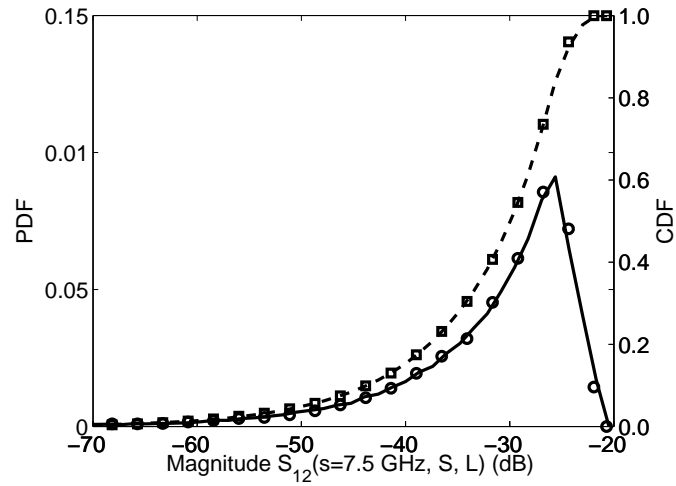
Figure 3.13: Example 3.3.2. PDF and CDF of the magnitude of S_{12} at 7.5 GHz. Full black line: PDF computed using the novel technique; Dashed black line: CDF computed using the novel technique; Circles ($\circ$): PDF computed using MC technique; Squares ($\square$): CDF computed using MC technique.
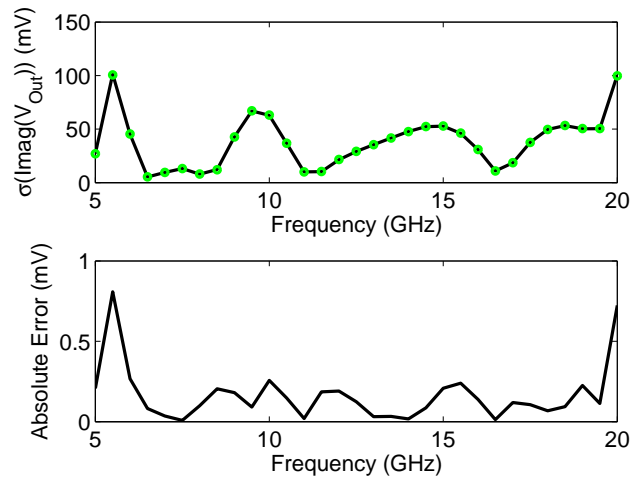
Figure 3.14: Example 3.3.2. The top plot shows a comparison between the standard deviation of the imaginary part of the voltage at the output port of the filter obtained with the MC analysis (full black line) and the proposed PC-based method (green circles: ($\circ$)) for the validation frequencies. The lower plot shows the absolute error between the two values.

References

[1] M. S. Eldred. *Recent advance in non-intrusive polynomial-chaos and stochastic collocation methods for uncertainty analysis and design.* In Proc. 50th AIAA/ASME/ASCE/AHS/ASC Structures, Structural Dynamics, and Materials Conference, Palm Springs, California, May 2009.

[2] I. S. Stievano, P. Manfredi, F. G. Canavero. *Parameters Variability Effects on Multiconductor Interconnects via Hermite Polynomial Chaos.* IEEE Trans. Compon., Packag., Manuf. Technol., 1(8):1234–1239, Aug. 2011.

[3] I. S. Stievano, P. Manfredi, F. G. Canavero. *Stochastic Analysis of Multiconductor Cables and Interconnects.* IEEE Trans. Electromagn. Compat., 53(2):501–507, May 2011.

[4] D. Vande Ginste, D. De Zutter, D. Deschrijver, T. Dhaene, P. Manfredi, F. G. Canavero. *Stochastic Modeling Based Variability Analysis of On-Chip Interconnects.* IEEE Trans. Compon., Packag., Manuf. Technol., 2(7):1182–1192, Jul. 2012.

[5] Q. Su, K. Strunz. *Stochastic circuit modelling with Hermite polynomial chaos.* IET Electronics Letters, 41(21):1163–1165, Oct. 2005.

[6] K. Strunz, Q. Su. *Stochastic formulation of SPICE-type electronic circuit simulation using polynomial chaos.* ACM Transactions on Modeling and Computer Simulation, 18(4):501–507, Sep. 2008.

[7] B. Gustavsen and A. Semlyen. *Rational approximation of frequency domain responses by Vector Fitting.* IEEE Trans. Power Del., 14(3):1052–1061, Jul. 1999.

[8] B. Gustavsen. *Improving the pole relocating properties of vector fitting.* IEEE Trans. Power Del., 21(3):1587–1592, Jul. 2006.

[9] D. Deschrijver, M. Mrozowski, T. Dhaene, and D. De Zutter. *Macromodeling of Multiport Systems Using a Fast Implementation of the Vector Fitting Method.* IEEE Microw. Wireless Compon. Lett., 18(6):383–385, Jun. 2008.

[10] D. Xiu and G.E. Karniadakis. *The Wiener-Askey Polynomial Chaos for Stochastic Differential Equations.* SIAM J. Sci. Comput., 24(2):619–644, Apr. 2002.

[11] F. Ferranti, L. Knockaert and T. Dhaene. *Parameterized S-Parameter Based Macromodeling With Guaranteed Passivity.* IEEE Microw. Wireless Compon. Lett., 19(10):608–610, Oct. 2009.

[12] F. Ferranti, L. Knockaert, T. Dhaene and Giulio Antonini,. *Passivity-Preserving Parametric Macromodeling for Highly Dynamic Tabulated Data Based on Lur'e Equations*. IEEE Trans. Microw. Theory Tech., 58(12):3688–3696, Dec. 2010.

[13] E. G. Gilbert. *Controllability and Observability in Multivariable Control Systems*. SIAM Journal on Control, 2(1):128–151, 1963.

[14] D. M. Pozar. *Microwave Engineering (Addison-Wesley Series in Electrical and Computer Engineering)*. Addison-Wesley, 1990.

[15] C. Soize and R. Ghanem. *PHYSICAL SYSTEMS WITH RANDOM UNCERTAINTIES: CHAOS REPRESENTATIONS WITH ARBITRARY PROBABILITY MEASURE*. SIAM J. SCI. COMPUT., 26(2):395–410, Jul. 2004.

[16] K. C. Gupta, R. Garg, I. Bahl, and P. Bhartia. *Microstrip Lines and Slotlines*. Artech House, Inc., Norwood, MA, 2nd edition, 1996.

4

A Comparative Study of Polynomial Chaos and Stochastic Collocation Methods for Variability Analysis of Multiport Systems

In this chapter, different state-of-the-art approach for the variability analysis are presented. In particular, the performances of the PC-based technique described in Chapter 3 are compared with respect to SC-based approaches. The proposed comparison focus on the unique features of EM system modeling. In this context, the presented study propose to build SC-based model via state-of-the art adaptive sampling schemes instead of using sparse sampling in the parameters space. This choice allows to increase the automatization of the model generation procedure, since the sampling of the parameters space is not chosen by the designer. Finally, a new SC-based method is presented that uses novel interpolation schemes based on amplitude and frequency scaling coefficients.

$\star\,\star\,\star$

D. Spina, K. Chemmangat, F. Ferranti, T. Dhaene, L. Knockaert and F. G. Canavero

Abstract Nowadays, the analysis of the effects of geometrical and electrical parameters variability on the performances of modern integrated circuits is fundamental. Design tools for the variability analysis of a circuit are highly desirable for a robust and successful design. The MC method is the standard approach for variability analysis, which gives accurate results with a straightforward implementation, but at a very high computational cost. Recently, new approaches based on the PC and SC methods have attracted a lot of attention as efficient alternatives to the computationally cumbersome MC-based techniques. This chapter presents a comparative study of three main techniques used to build stochastic models to perform variability analysis of general linear and passive multiport systems: 1) a PC-based method, 2) a SC method based on standard interpolation schemes, 3) a new SC-based method that uses novel interpolation schemes based on amplitude and frequency scaling coefficients. Pros and cons of all techniques are qualitatively and quantitatively discussed. Pertinent numerical examples are used to support the comparative analysis by means of some variability analysis results.

4.1   Introduction

Electromagnetic compatibility (EMC) and signal integrity (SI) analysis are of paramount importance for the design of the modern electronic ICs, due to the increased miniaturization and density of these devices along with the high bandwidth required for signal processing operation. In this scenario, the analysis of the effects of geometrical and electrical parameters variability on the performance of the modern ICs has become crucial in the recent years. Indeed, the variability introduced by the tolerances of the manufacturing process is a primary source of degradation of the ICs performances, since it can affect important characteristics such as coupling, delay and crosstalk.

The MC method [1] is considered the standard approach for variability analysis, thanks to its accuracy and ease of implementation. Unfortunately, the MC analysis has a slow convergence rate and it requires to perform a large number of simulations. Therefore, MC has a very high computational cost, considering that the simulations of complex systems are time consuming. Recently, several techniques [2–12] were developed to study the stochastic variations of complex systems by means of accurate and efficient stochastic macromodels as an efficient alternative to the MC-based approaches. These techniques can be divided in two groups: 1) based on the the PC expansion [2–7] and 2) based on the SC method [8–12].

As described in details in Chapter 2, the PC-based modeling approach aims at expressing a stochastic process as a series of orthogonal basis functions with suitable coefficients and gives an analytical representation of the variability of the system with respect to the random variables under consideration [13]. The tech-

niques [2–7] have a superior efficiency compared with the MC-based methods and demonstrate the flexibility of the PC expansion in performing variability analysis for different type of electrical circuit, namely lumped elements circuits [2, 3], multiconductor transmission lines [4–6] and generic linear multiport systems [7].

The basic idea of the SC approach is to approximate the unknown stochastic solution by interpolating functions in the stochastic space. The interpolation is constructed by repeatedly solving (sampling) the deterministic problem at a predetermined set of nodes in the stochastic space. This approach offers high accuracy and efficiency as the stochastic PC method as well as easy implementation as the sampling-based methods (e.g. MC approach).

In this chapter, we propose a comparative study about different PC-based and SC-based state-of-the-art techniques for the variability analysis with respect to the unique features of EM system modeling. In particular, the proposed study evaluates not only the accuracy and efficiency of the different methods in estimating system variability features, but it describes

- the order estimation and sampling strategy adopted;

- the capability to preserve the physical properties of the system under study.

- the computational cost to build the stochastic macromodel;

Indeed, using efficient sampling strategies is of paramount importance since the simulations of complex EM systems are time consuming. Performing stable time-domain simulations requires that the physical properties of stability and passivity of the stochastic macromodel are guaranteed. Finally, the compactness and computational efficiency of the stochastic macromodel are important indicators of the performances of the different variability analysis methods. In particular, the following variability analysis techniques for general linear and passive multiport systems are considered in the proposed study:

- the PC-based method discussed in [7] and presented in Chapter 3;

- a SC method based on standard interpolation schemes, named as standard SC method in what follows;

- a novel proposed SC-based approach that uses new interpolation schemes based on amplitude and frequency scaling coefficients proposed in [14, 15], named as modified SC method in what follows.

The performances of the methods listed above in estimating system variability features are compared with respect to the standard MC method.

4.2   Stochastic Collocation methods

This Section describes in details the two SC-based methods used in this comparison study for the variability analysis of general linear and passive multiport circuits. In particular, the standard SC technique used is presented in 4.2.1, while the novel SC-based method that uses novel interpolation schemes based on amplitude and frequency scaling coefficients is described in 4.2.2.

4.2.1   Standard Stochastic Collocation methods

As described in Section 2.6, SC methods are based on interpolation schemes to compute stochastic quantities. Indeed, a stochastic process $\mathbf{H}(s, \boldsymbol{\xi})$ can be expressed as (see (2.57)):

$$\mathbf{H}(s, \boldsymbol{\xi}) = \sum_{i=1}^{Q} \mathbf{H}(s, \boldsymbol{\xi}^i) L_i(\boldsymbol{\xi})$$

where s represents the Laplace variable, $\boldsymbol{\xi}$ denote the stochastic parameters and $\{L_i(\boldsymbol{\xi})\}_{n=1}^{N}$ represents the interpolation basis functions. Hence, the computational effort required for the collocation approach depends on the number of support nodes used for constructing the interpolation. Once the interpolation scheme has been selected, no estimation of the order of the basis functions is needed. As a result, the key issue for this approach is the selection of the support nodes, such that using the minimal number of nodes one achieves a good approximation.

Therefore, adaptive sampling schemes become important for SC-based approaches to reduce as much as possible the number of support nodes in the stochastic space. Recently, an interesting adaptive sampling technique based on interpolation functions has been proposed in [16]. It uses a local approach and works on local n-box regions of the design space. This creates the possibility of a tree-based implementation of the sampling algorithm, while making it portable to parallel computing platforms.

Furthermore, if the interpolation kernel functions $\{L_i(\boldsymbol{\xi})\}_{n=1}^{N}$ only depend on the stochastic space grid points and their computation does not require the solution of a linear system to impose an interpolation constraint. Therefore, interpolating systems, matrices or scalars does not make any difference for these interpolation kernel functions. Interpolation methods that belong to the general class of positive interpolation operators can be used, e.g., the piecewise multilinear and multivariate simplicial methods [17]. These interpolation schemes are able to guarantee stability and passivity over the entire stochastic space, assuming that the system solutions at the nodes $\mathbf{H}(s, \boldsymbol{\xi}^i)$ in the stochastic space are stable and passive [18, 19]. The stochastic moments can be computed by means of analytical formulas and then very efficiently, once the analytical form of the interpolation kernel functions

$\{L_i(\boldsymbol{\xi})\}_{n=1}^N$ and probability measure $W(\boldsymbol{\xi})$ has been decided, see (2.61). If the choice of the interpolation kernel functions and probability measure does not allow an analytical computation of stochastic moments, a numerical solution can be used (e.g. by MC analysis or numerical integration).

A similar interpolation-based approach has been used in [18, 19] to build parametric macromodels of multiport systems. A set of univariate rational models called *root macromodels* are interpolated at an input/output level using interpolation schemes. Parametric macromodels are multivariate models that describe the complex behavior of EM systems, which is typically characterized by the frequency (or time) and several design parameters, such as layout or substrate features. During a design process, it is important to predict the response of the system under study as a function of design parameters, such as geometrical and substrate characteristics. A typical design process includes design space optimization, exploration, sensitivity and variability analysis, and therefore it requires repeated simulations for different design parameter values. Parametric macromodels are suitable to efficiently and accurately perform these design activities, while using multiple EM simulations is often too computationally expensive due to the high computational cost per simulation.

Therefore, it is straightforward to note that parametric and stochastic macromodels share several similarities, since both categories represent models that take into account multiple design parameters. However, parametric macromodels are more general since their applications are broader.

The techniques proposed in [18, 19] combined with the sampling technique [16] are used as standard SC method in the numerical examples. The system solutions at the nodes $\mathbf{H}(s, \boldsymbol{\xi}^i)$ are modeled in a rational form and then interpolated. The order of the rational models for the nodes is selected adaptively by an error-based bottom-up approach.

4.2.2 Modified Stochastic Collocation method

Using more powerful interpolation schemes can help in reducing the number of nodes and then saving computational resources when SC-based methods are used. Recently, novel scaling interpolation methods have been proposed in [14, 15], which considerably enhances the modeling capability of standard interpolation schemes and allows to accurately model highly dynamic systems with less number of EM simulations. E.g., a stochastic quantity $\mathbf{H}(s, \boldsymbol{\xi})$ can be expressed as:

$$\mathbf{H}(s, \boldsymbol{\xi}) = \sum_{i=1}^{Q} \mathbf{H}(s, \boldsymbol{\xi}^i, L_i(\boldsymbol{\xi})) L_i(\boldsymbol{\xi}) \tag{4.1}$$

where nested interpolation schemes are used [14, 15]. A drawback of using these novel nested interpolation schemes is that an analytical computation of stochastic

moments becomes very difficult and the integrals (2.61) must be solved numerically (e.g. by MC analysis or numerical integration). However, these numerical computations remains much more efficient than a MC-based solution, since they are performed on a very efficient model. The interpolation schemes proposed in [14, 15] allow to preserve the stability and passivity of stochastic macromodels over the entire stochastic space, assuming that the system solutions at the nodes in the stochastic space are stable and passive. The technique proposed in [14, 15] combined with the adaptive sampling strategy [16] is used as modified SC method in the numerical examples. As for the standard SC approach, the order of the rational models for the nodes is selected adaptively by an error-based bottom-up approach.

4.3   Discussion

In this Section, we analyze three proposed methods for the variability analysis of multiport systems:

- the PC-based technique described in Chapter 3;

- the "standard" SC-based method described in 4.2.1;

- the "modified" SC-based method presented in 4.2.2.

The proposed study focus on the:

- accuracy and efficiency in performing the variability analysis;

- computational cost to build the stochastic macromodel;

- order estimation and sampling strategy;

- capability to preserve the physical properties of the system under study, e.g. stability and passivity.

and the estimation of system variability features obtained with the three proposed techniques is compared with respect to a standard MC method.

Stability and passivity are fundamental model properties to guarantee stable time-domain simulations (e.g. in time-domain circuit simulator such as SPICE-like solvers [20]), which are necessary to analyze the correct behavior of systems in signal integrity and EMC analysis. Stable systems have their poles in the left half-plane of the Laplace domain. Passive systems [21] cannot generate more energy than they can absorb through their electrical ports. Passivity conditions for admittance, impedance and scattering parameters can be found in [21]. Loss of model passivity implies that it is possible to find a termination circuit that drives the model to instability.

The PC method [7] presented in Chapter 3 offers a great accuracy and efficiency in performing the variability analysis with respect to the MC method, thanks to the properties of the PC expansion. It builds a stochastic macromodel of the system transfer function using the PC expansion of the corresponding state-space representation of the system. However, the choice of the number of basis functions $M + 1$ for the PC expansion and of the initial samples K in the stochastic space is not automated. The number of basis function $M + 1$ and initial samples K is chosen upfront with a-priori criteria that are not optimal. Finally, the stability and passivity of the PC-based stochastic macromodel, generated using the method of [7], are not guaranteed. Note that, preserving the passivity of PC-based macromodel of generic multiport systems is still an open problem, while it is possible to build a passive PC-based macromodel of multiconductor transmission lines starting from the PC model of the corresponding frequency independent per-unit-length parameters [22].

The SC method [18, 19] combines the efficient and accurate calculation of stochastic quantities with the possibility of using adaptive sampling schemes [16] in the stochastic space for an automated construction of stochastic models. Once the interpolation scheme has been selected, no estimation of the order of the basis functions is needed. Furthermore, the stability and passivity of the calculated stochastic macromodel can be guaranteed over the stochastic space. However, it may require a more dense initial sampling than the PC approach, leading to a higher computational time for the model construction than in the PC case. Finally, the requirement of stability and passivity may increase the computational time to build stochastic macromodels, since some passivity assessment and enforcement steps are needed for the *root macromodels* in [18, 19].

The new proposed modified SC method is based on the use of novel scaling interpolation methods [14, 15], which considerably enhances the modeling capability of standard interpolation schemes and allows to accurately model highly dynamic systems. Therefore, it requires the least dense initial sampling with respect to the other discussed stochastic methods, leading to a very efficient model construction step. As for the standard SC method, adaptive sampling schemes [16] are available for an automated initial sampling of the stochastic space. However, the calculation of stochastic quantities is less efficient with respect to the PC and standard SC methods, since a numerical solution (e.g. by Monte Carlo analysis or numerical integration) is needed to perform the variability analysis. However, these numerical computations remain much more efficient than a MC-based solution, since they are performed on a very efficient model. Finally, it is possible to guarantee stability and passivity in the calculated stochastic macromodels at the cost of an increased computational cost during the model building phase, as in the case of the standard SC method.

To summarize pros and cons of the three methods:

1. PC method

   - Pros: efficient and accurate calculation of stochastic quantities.

   - Cons:

     - the choice of the number of basis functions and initial sampling in the stochastic space is not automated. Typically, some a-priori criteria are used.
     - stability and passivity are not guaranteed over the stochastic space.

2. Standard SC method

   - Pros:

     - once the interpolation scheme has been selected, no estimation of the order of the basis functions is needed. Adaptive sampling schemes are available to automate the initial sampling in the stochastic space;
     - efficient and accurate calculation of stochastic quantities;
     - stability and passivity can be guaranteed over the stochastic space.

   - Cons: it may require a more dense initial sampling than the PC approach, then the computational time for the model construction may be higher than in the PC case. The requirement of stability and passivity over the stochastic space increases the computational time to build stochastic macromodels. Some passivity assessment and enforcement steps needed for the *root macromodels* in [18, 19] are responsible for that.

3. Modified SC method

   - Pros:

     - once the interpolation scheme has been selected, no estimation of the order of the basis functions is needed. Adaptive sampling schemes are available to automate the initial sampling in the stochastic space;
     - it requires the least dense initial sampling with respect to the other discussed methods, therefore it leads to a very efficient model construction step. As for the standard SC method, the requirement of stability and passivity over the stochastic space increases the computational time to build stochastic macromodels;
     - stability and passivity can be guaranteed over the stochastic space;

- Cons: the calculation of stochastic quantities is less efficient with respect to the PC and standard SC methods, since a numerical solution is needed (e.g. by Monte Carlo analysis or numerical integration). However, these numerical computations remains much more efficient than a MC-based solution, since they are performed on a very efficient model. As for the standard SC method, the requirement of overall stability and passivity increases the computational time to build stochastic macro-models.

4.4   Numerical results

Two pertinent numerical examples are proposed in this section and are used to support the previous comparative analysis by means of proper variability analysis results. All numerical experiments were implemented in MATLAB $2009a$ and carried out on Windows platform equipped with Intel Core2 Extreme CPU Q9300 2.53GHz and 8GB RAM.

4.4.1   System of Interconnections

In this first example, a system of interconnections has been modeled. Its structure is shown in Fig. 4.1. It consists of four coupled microstrips modeled in the frequency range $[0 - 10]$ GHz. The spacing among the lines is $S_0 = 0.1$ mm, the length of the lines is $L_0 = 10$ mm and the metal conductivity is $\sigma_0 = 4.1 \cdot 10^7$ S/m. The substrate is chosen with relative permittivity $\epsilon_{r0} = 9.6$, loss tangent $\tan \delta = 0.0002$ and thickness equal to $t_0 = 254$ μm.

To compare the performances of the different methods for the variability analysis, the scattering parameters **S** of the lines are considered as a stochastic process dependent on three different sets of independent random variables with uniform
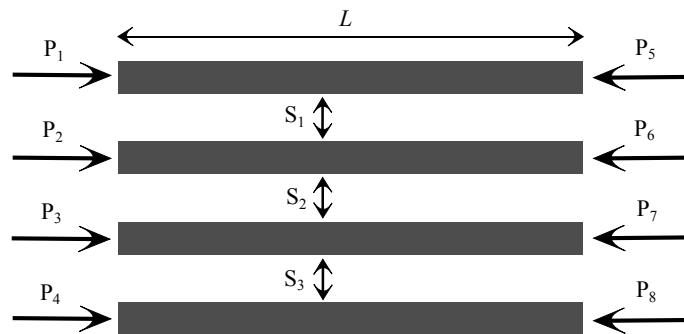

Figure 4.1: Example 4.4.1. Top view of the layout of four coupled microstrips.

PDFs: initially the variability analysis is performed with respect to the length L of the lines, then with respect to the length L and the spacing S_1, and finally with respect to the random parameters (L, S_1, S_2). In the following, the variability analysis results are shown assuming that the random variables (L, S_1, S_2) vary in a range of $\pm 10\%$ with respect to their nominal values (L_0, S_0) previously indicated. The scattering parameters are evaluated using ADS Momentum. Each method used to build a stochastic macromodel generates a corresponding sampling in the stochastic space. A standard approach of sampling the stochastic space with 10000 samples following a proper distribution has been used for the MC method.

The basis functions of the PC model are combination products of the Legendre polynomials [23] and are shown in Table 4.1 for two independent random variables, $M = 5$ and $P = 2$, and the corresponding weighting function (2.47) is:

$$W(\boldsymbol{\xi}) = \begin{cases} 2^{-N}, & |\xi_i| \leq 1, \quad i = 1, ..., N \\ 0, & elsewhere \end{cases} \tag{4.2}$$

where N is the number of random variables considered and P is the maximum order of the polynomial basis functions. For each combination of the random parameters $(L), (L, S_1), (L, S_1, S_2)$ the corresponding PC models are calculated assuming $P = 3$. Then, the corresponding number of basis functions $M + 1$ is chosen according to (2.50). The initial samples of the scattering parameters are calculated using ADS Momentum over a regular grid over the range of variation of the considered random variables, accordingly to the formula $K \approx 2 (M + 1)$ [7].

The state-space representation of the initial scattering parameters is calculated by the VF method [24–26], targeting -30 dB as maximum absolute model error between the scattering parameters and the corresponding rational model. Trying to impose a better accuracy $(< -30$ dB$)$ does not provide good results, since the VF state-space matrices become nonsmooth and noisy as functions of the stochastic parameters.

In the case of the standard [18, 19] and modified [14, 15] SC methods, the adaptive sampling algorithm [16] has chosen the stochastic space grid to build the corresponding stochastic macromodels. The rational *root macromodels* are built in a pole-residue form using the VF method. Multilinear interpolation kernels [17] are used for both SC-based approaches. The adaptive sampling scheme guarantees that the stochastic macromodels achieve an accuracy of -40 dB as maximum absolute error over the stochastic space.

In all simulations, 101 frequency samples are computed and divided in two groups: modeling samples (51 samples), used to calculate the stochastic models (PC, standard SC, modified SC), and validation samples (50 samples), used to verify the accuracy of variability analysis performed with the computed stochastic models with respect to the MC analysis performed using 10000 samples. Tables 4.2–4.4 show some comparison measures for the variability analysis for the cases

index i	i-th basis function φ_i	$<\varphi_i, \varphi_i>$
0	1	1
1	ξ_1	$\frac{1}{3}$
2	ξ_2	$\frac{1}{3}$
3	$\frac{1}{2}\left(3\xi_1^2 - 1\right)$	$\frac{1}{5}$
4	$\xi_1\xi_2$	$\frac{1}{9}$
5	$\frac{1}{2}\left(3\xi_2^2 - 1\right)$	$\frac{1}{5}$

Table 4.1: Legendre polynomials products for two independent random variables, with $M = 5$ and $P = 2$ [5].

of 1, 2 and 3 random variables respectively: the computational time and number of samples over the stochastic space needed to build the stochastic macromodel and the computational time to compute mean and standard deviation quantities. Mean and standard deviation for the PC and standard SC methods were computed analytically, while a MC analysis with 10000 samples following a proper distribution was used for the modified SC method. As previously discussed:

- the MC method is the most computationally expensive;

- the modified SC method needs the least number of samples to build a stochastic macromodel with respect to the PC and standard SC methods. Therefore, it provides the most efficient model construction step;

- the PC and standard SC methods are very efficient in computing mean and standard deviation quantities, while the modified SC method is more expensive, but still much more efficient than the MC method.

In what follows, we propose some numerical results related to the case of three independent random variables. An example of the scattering parameters variability with respect to the chosen random variables is given in Fig. 4.2.

Method	Model construction	μ and σ computation
MC		$67\ h\ 36\ min\ 40\ s$
PC	$4\ min\ 42\ s$ (11 samples)	$0.7\ s$
Standard SC	$7\ min\ 36\ s$ (13 samples)	$0.2\ s$
Modified SC	$3\ min\ 9\ s$ (5 samples)	$2\ min\ 36\ s$

Table 4.2: Example 4.4.1. Comparison Table for 1 random variable.

Method	Model construction	μ and σ computation
MC		$67\ h\ 36\ min\ 40\ s$
PC	$13\ min\ 23\ s$ (36 samples)	$8\ s$
Standard SC	$15\ min\ 53\ s$ (26 samples)	$0.55\ s$
Modified SC	$7\ min\ 49\ s$ (8 samples)	$5\ min\ 30\ s$

Table 4.3: Example 4.4.1. Comparison Table for 2 random variables.

Figs. 4.3 - 4.4 show the mean and standard deviation of the real part of the element $\mathbf{S}_{11}(s, L, S_1, S_2)$ computed by all four techniques and the corresponding absolute error:

$$Error = |Stoch_{\text{MC}} - Stoch_{\text{other method}}| \qquad (4.3)$$

between the stochastic quantities computed by the PC, standard and modified SC methods with respect to the MC analysis. The error plots show that the standard and modified SC methods are more accurate than the PC approach. Fig. 4.5 describes the PDF and the CDF of the magnitude of $\mathbf{S}_{11}(s, L, S_1, S_2)$ at the val-

Method	Model construction	μ and σ computation
MC		$67\ h\ 36\ min\ 40\ s$
PC	$32\ min\ 5\ s$ (64 samples)	$40\ s$
Standard SC	$36\ min\ 44\ s$ (40 samples)	$1.12\ s$
Modified SC	$17\ min\ 55\ s$ (14 samples)	$10\ min\ 50\ s$

Table 4.4: Example 4.4.1. Comparison Table for 3 random variables.

idation frequency 5.9 GHz using the MC and modified SC approaches. Similar results can be obtained for the other entries of the scattering matrix.

The PC method is not able to guarantee stability and passivity over the entire stochastic space, while the standard and modified SC methods do not have this drawback. We recall that a linear network described by scattering matrix $\mathbf{S}(s)$ is passive if [21]:

1. $\mathbf{S}(s^*) = \mathbf{S}^*(s)$ for all s, where "$*$" is the complex conjugate operator.

2. $\mathbf{S}(s)$ is analytic in $\Re e(s) \geq 0$.

3. $\mathbf{I} - \mathbf{S}^T(s^*)\mathbf{S}(s) \geq 0\ ; \forall s : \Re e(s) > 0$.

The third passivity condition is equivalent to the condition $\|\mathbf{S}(s)\|_\infty \leq 1$ ($\mathbf{H}_\infty$ norm) [27], i.e., the largest singular value of $\mathbf{S}(s)$ does not exceed one in the right-half Laplace plane. Due to the assumption of strict stability, the third condition can be restricted to the imaginary axis of the Laplace domain.

Figs. 4.6-4.7 show the poles and the $\mathbf{H}_\infty$ norm of the stochastic macromodels built by these three techniques for $5 \times 5 \times 5$ (L, S_1, S_2) samples on a regular grid. In this case, the stability is preserved by all methods, while passivity is guaranteed only by the standard and modified SC methods.

4.4.2 Spiral Inductor

In this second example, a spiral inductor has been modeled. Its structure is shown in Fig. 4.8 [28]. This five turn spiral inductor is modeled in the frequency range $[0-4]$ GHz. The width of the conductors W and the inner length D_{in}, shown in
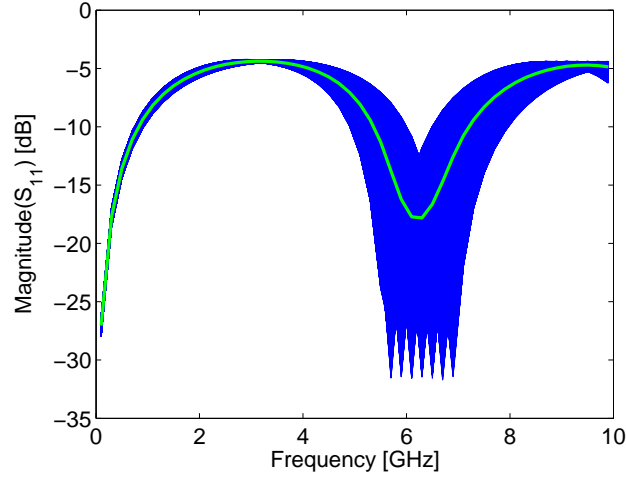
Figure 4.2: Example 4.4.1. Variability of the magnitude of $\mathbf{S}_{11}(s, L, S_1, S_2)$ with respect to the parameters (L, S_1, S_2). The blue lines are the results of MC analysis performed with ADS. The thick green line represents the corresponding mean value.

the top view of Fig. 4.8-(a), are considered as two independent random variables with Gaussian PDFs. Their nominal values are $W_0 = 10.0$ mm and $D_{\text{in}0} = 87.0$ mm. The spacing among the conductors is equal to 2 mm, while the thickness of the conductors is equal to 1 μm. A sectional view of the spiral inductor is shown in Fig. 4.8-(b) with a 5 μm silicon-dioxide substrate layer of relative permittivity $\epsilon_{r0,SiO_2} = 3.9$ and a 300 μm silicon substrate layer of relative permittivity $\epsilon_{r0,Si} = 11.9$. The conductivity of the metallic layers is equal to $\sigma_0 = 3.0 \cdot 10^7$ S/m.

To compare the performances of the different methods for the variability analysis, the admittance parameters $\mathbf{Y}$ of the spiral inductor are considered as a stochastic process dependent on W and D_{in}. In the following, the variability analysis results are shown assuming that the random variables (W, D_{in}) have a standard deviation normalized with respect to their nominal values equal to 5%. The admittance parameters are evaluated using ADS Momentum. A standard approach of sampling the stochastic space with 10000 samples following a proper distribution has been used for the MC method.

In all simulations, 41 frequency samples are computed and divided in two groups: modeling samples (21 samples), used to calculate the stochastic models (PC, standard SC, modified SC), and validation samples (20 samples), used to verify the accuracy of variability analysis performed with the computed stochastic models with respect to the MC analysis.

The basis functions of the PC model are products of the Hermite polynomials
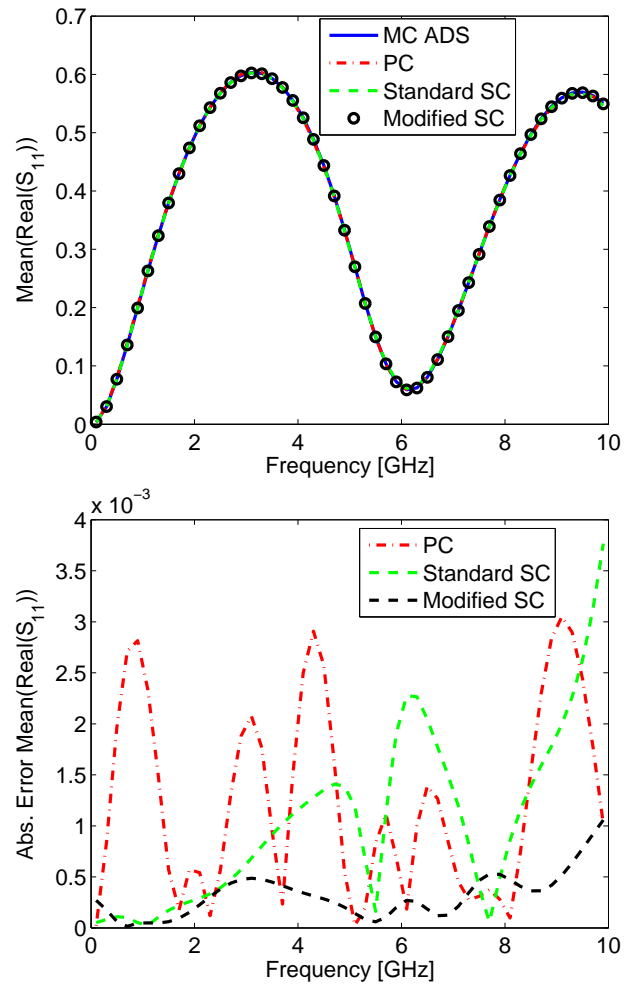
Figure 4.3: Example 4.4.1. Top: Comparison of the mean for the real part of
$\mathbf{S}_{11}(s, L, S_1, S_2)$. *Bottom: Corresponding absolute error with respect to the reference MC*
analysis.
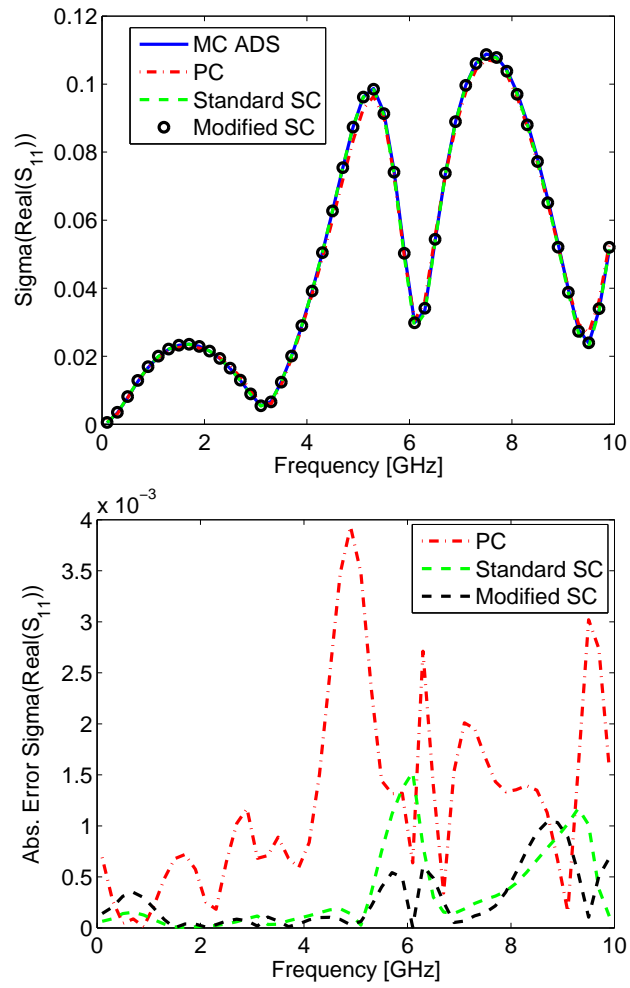
Figure 4.4: Example 4.4.1. Top: Comparison of the standard deviation for the real part of $\mathbf{S}_{11}(s, L, S_1, S_2)$. *Bottom: Corresponding absolute error with respect to the reference MC analysis.*
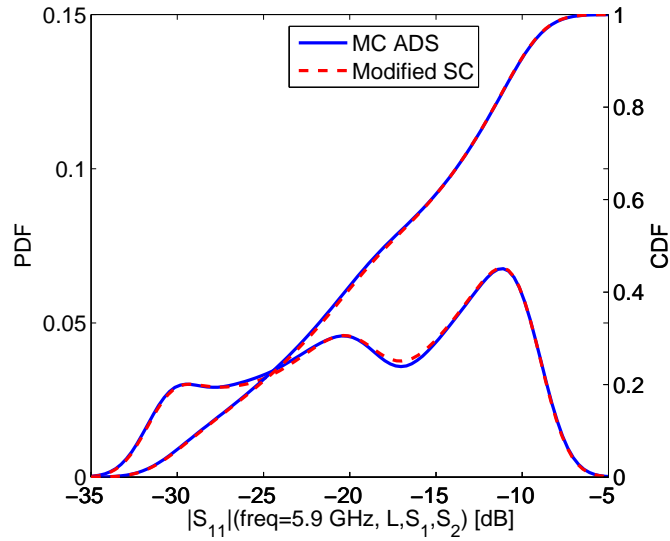
Figure 4.5: Example 4.4.1. PDF and CDF of the magnitude of $\mathbf{S}_{11}(s, L, S_1, S_2)$ at 5.9 GHz.
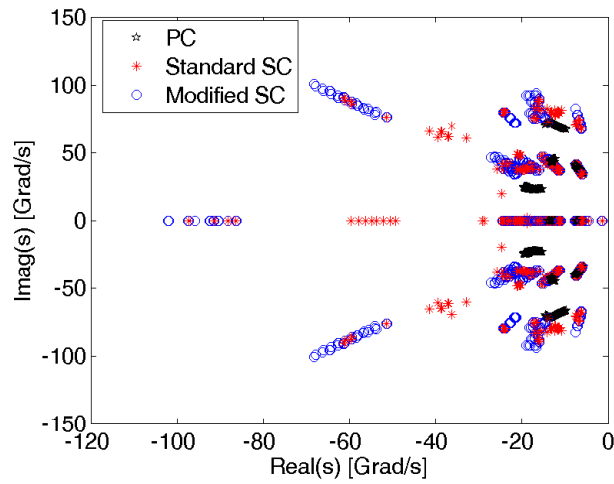
Figure 4.6: Example 4.4.1. Model poles over the stochastic space ($5 \times 5 \times 5$ (L, S_1, S_2) samples).
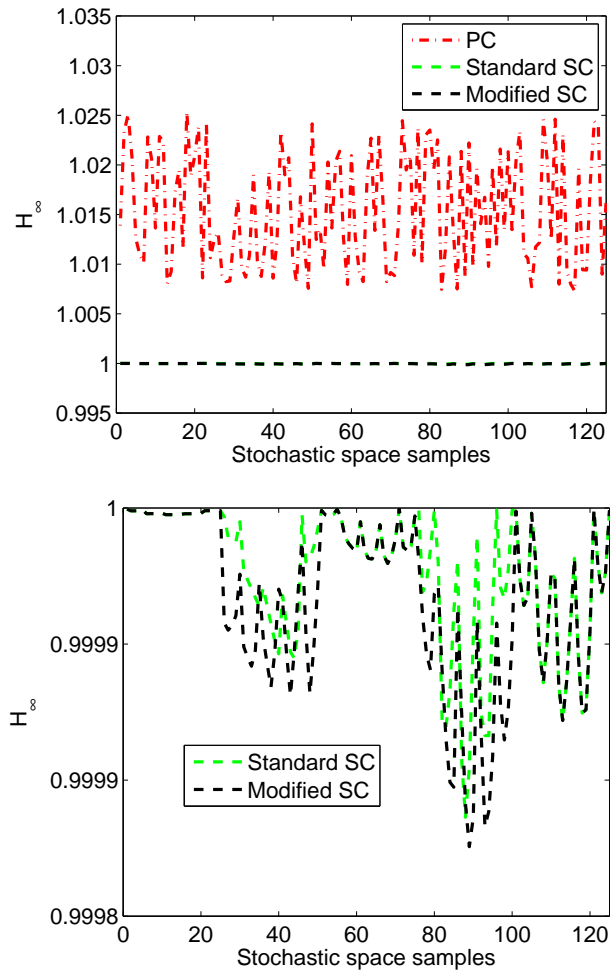
Figure 4.7: Example 4.4.1. $\mathbf{H}_\infty$ *norm over the stochastic space* $(5 \times 5 \times 5 \ (L, S_1, S_2)$ *samples).*
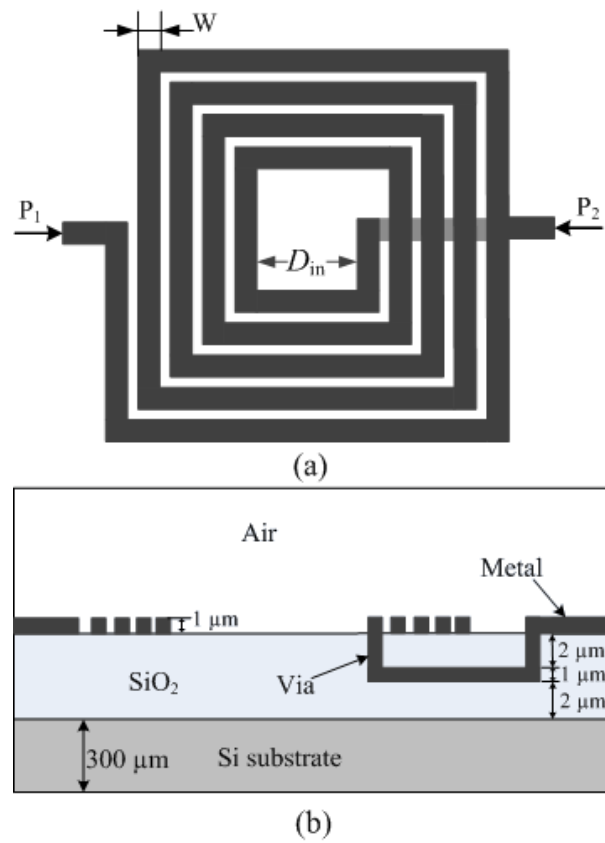
Figure 4.8: Example 4.4.2. Top (a) and sectional (b) view of the layout of the spiral inductor.

[23], as shown in Table 4.5, for two independent random variables with $M = 5$ and $P = 2$, and the corresponding weighting function (2.47) is:

$$W(\boldsymbol{\xi}) = \prod_{i=1}^{2} \frac{1}{\sqrt{2\pi\sigma_{\xi_i}^2}} e^{-0.5\left(\frac{\xi_i - \mu_{\xi_i}}{\sigma_{\xi_i}}\right)^2} \tag{4.4}$$

with normalized variables $\mu_{\xi_i} = 0$, $\sigma_{\xi_i} = 1$. The corresponding PC models are calculated assuming $P = 2$ and the corresponding number of basis function $M + 1$ is chosen according to the formula (2.50). The initial samples of the admittance parameters are calculated using ADS Momentum over a regular grid of (4×4) (W, D_{in}) samples over the ranges $[W_0 - 3\sigma_W, W_0 + 3\sigma_W]$ and $[D_{\text{in}0} - 3\sigma_{D_{\text{in}}}, D_{\text{in}0} + 3\sigma_{D_{\text{in}}}]$. The number of initial samples in the stochastic space K is chosen according to $K \approx 2(M + 1)$ [7].

index i	i-th basis function φ_i	$<\varphi_i, \varphi_i>$
0	1	1
1	ξ_1	1
2	ξ_2	1
3	$\xi_1^2 - 1$	2
4	$\xi_1\xi_2$	1
5	$\xi_2^2 - 1$	2

Table 4.5: Hermite polynomials products for two independent random variables with $M = 5$ and $P = 2$ [4].

The state-space representation of the initial admittance parameters is calculated by the VF method, targeting 0.01 as maximum weighted rms error between the admittance parameters and the corresponding rational models:

$$Error_{rms} = \sqrt{\frac{\sum_{i=1}^{N_i N_o} \sum_{k=1}^{K_s} \left| w_{Y_i}(s_k)\left(Y_{r,i}(s_k) - Y_i(s_k)\right) \right|^2}{N_i N_o K_s}} \qquad (4.5)$$

with

$$w_{Y_i}(s) = |(Y_i(s))^{-1}| \qquad (4.6)$$

where N_i,N_o are the number of input and output system ports and K_s is the number of modeling frequency samples.

In the case of the standard [18, 19] and modified [14, 15] SC methods, the rational *root macromodels* are built in a pole-residue form by means of the VF method and multilinear interpolation kernels [17] are used. The adaptive sampling algorithm [16] has chosen the stochastic space grid to build the corresponding stochastic macromodels over the ranges $[W_0 - 4\sigma_{W_0}, W_0 + 4\sigma_{W_0}]$ and $[D_{\text{in}0} - 4\sigma_{D_{\text{in}}}, D_{\text{in}0}+4\sigma_{D_{\text{in}}}]$. The adaptive sampling scheme guarantees that the stochastic macromodels achieve an accuracy of 0.01 as weighted rms error over the stochastic space. The standard and modified SC approaches use the multilinear interpolation scheme (basis functions defined locally), while the PC approach use polynomial basis functions (basis functions defined globally). Since, standard and modified SC approaches cannot rely on accurate extrapolation, as in the case of the PC approach, a larger region of the unbounded gaussian stochastic space has been sampled.

Table 4.6 shows some comparison measures for the variability analysis as in the previous example. Mean and standard deviation for the PC and standard SC methods were computed analytically, while a MC analysis with 10000 samples following a proper distribution was used for the modified SC method.

An example of the admittance parameters variability with respect to the chosen random variables is given in Fig. 4.9.
Fig. 4.10 shows the standard deviation of the real part of the element $\mathbf{Y}_{12}(s, W, D_{\text{in}})$ computed by all four techniques and the corresponding absolute error (4.3) between the stochastic quantities computed by the PC, standard and modified SC methods with respect to the MC analysis. The error plot shows that the PC and modified SC methods are more accurate than the standard SC approach.

Two important design parameters for spiral inductors are the values of the quality factor Q and inductance L, which can be expressed as a function of the admittance parameters [28]:

$$Q = -\frac{\Im m(Y_{11})}{\Re e(Y_{11})} \qquad (4.7)$$

$$L = -\frac{1}{2\pi freq}\Im m\left(\frac{1}{Y_{12}}\right) \qquad (4.8)$$

Method	Model construction	μ and σ computation
MC		$47\ d\ 4\ h\ 59\ min\ 10\ s$
PC	$1\ h\ 48\ min\ 48\ s$ (16 samples)	$0.11\ s$
Standard SC	$1\ h\ 6\ min$ (10 samples)	$0.54\ s$
Modified SC	$1\ h\ 7\ min\ 22\ s$ (10 samples)	$2\ min\ 12\ s$

Table 4.6: Example 4.4.2. Comparison Table.

Fig. 4.11 describes the PDF and the CDF of $L(s, W, D_{in})$ at the validation frequency 2.5 GHz using the MC and PC approaches. Although the stochastic models are built for admittance parameters, a good accuracy is also achieved for stochastic quantities that are functions of the admittance parameters.

4.5   Conclusions

In this chapter, we have presented a detailed comparison among three main approaches for variability analysis: 1) a PC-based method, 2) a SC method based on standard interpolation schemes, 3) a novel SC-based method that uses scaling interpolation schemes. We have used the following performance measures: 1) efficiency and accuracy in performing the variability analysis, 2) order estimation and sampling strategy, 3) computational cost to build the stochastic macromodel, 4) capability to preserve the physical properties of the system under study. Pros and cons of all techniques have been qualitatively and quantitatively discussed. In summary, the PC technique is able to accurately and efficiently compute stochastic quantities, but it lacks of automated order estimation methods, automated sampling strategies and guaranteed preservation of system properties (e.g. stability and passivity). The SC methods do not need to estimate the order of the basis functions once the interpolation schemes are selected, they can take advantage of existing adaptive sampling schemes and can guarantee system properties such as stability and passivity. The efficiency for the computation of stochastic quantities can decrease and the number of samples in the stochastic space needed to build the stochastic macromodel can increase depending on the interpolation schemes. The requirement of stability and passivity over the stochastic space increases the com-
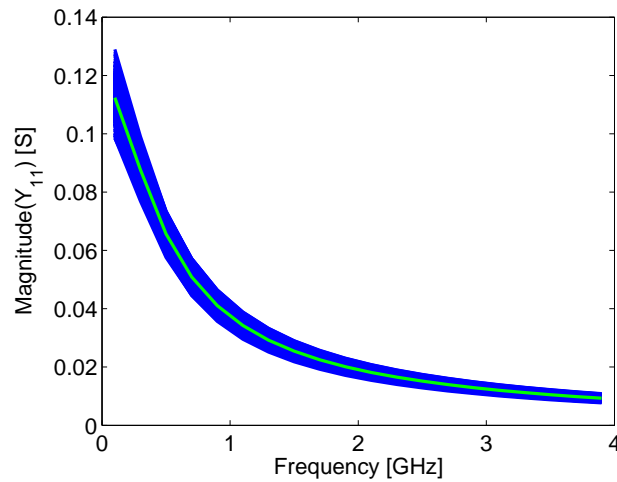
Figure 4.9: Example 4.4.2. Variability of the magnitude of $\mathbf{Y}_{11}(W, D_{\text{in}})$ with respect to the parameters (W, D_{in}). The blue lines are the results of MC analysis performed with ADS. The thick green line represents the corresponding mean value.

putational time to build stochastic macromodels by means of SC methods. Pertinent numerical examples are used to support the comparative analysis by means of proper variability analysis results.
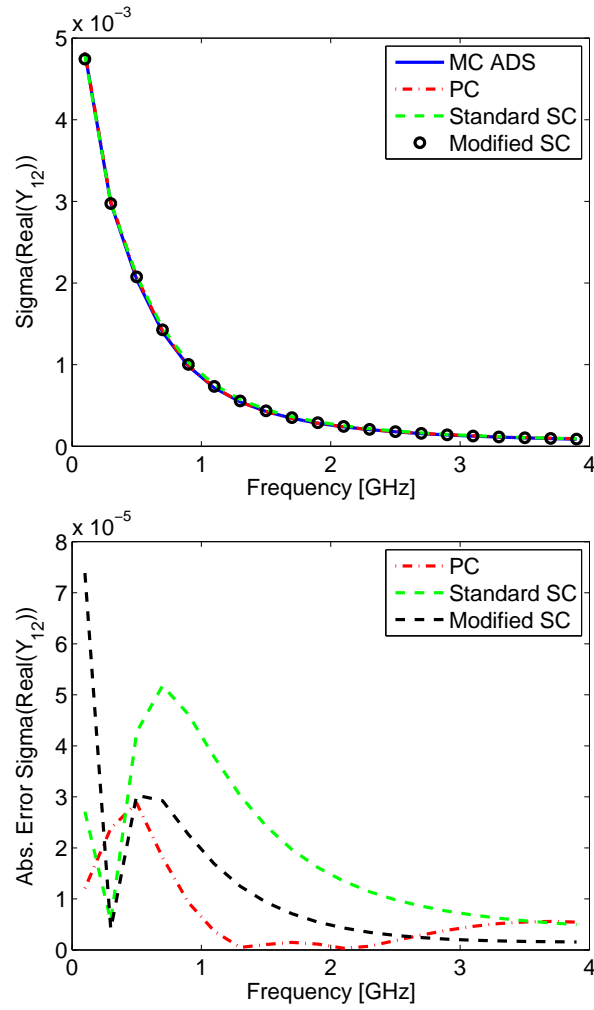
Figure 4.10: Example 4.4.2. Top: Comparison of the standard deviation for the real part of $\mathbf{Y}_{12}(s, W, D_{\text{in}})$. Bottom: Corresponding absolute error with respect to the reference MC analysis.
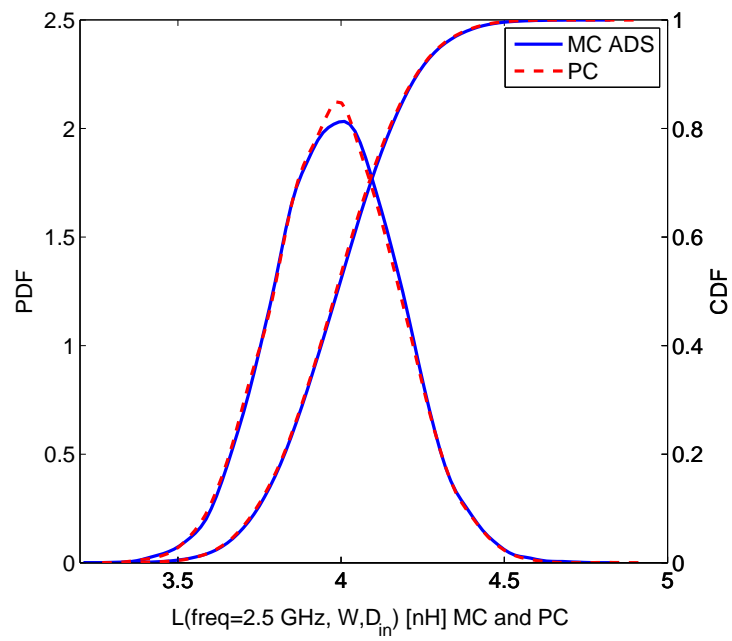
Figure 4.11: Example 4.4.2. PDF and CDF of L at 2.5 GHz.

References

[1] G. S. Fishman. *Monte Carlo: Concepts, Algorithms, and Applications.* Springer-Verlag, New York, 1996.

[2] Q. Su and K. Strunz. *Stochastic circuit modelling with Hermite polynomial chaos.* IET Electronics Letters, 41(21):1163–1165, Oct. 2005.

[3] K. Strunz and Q. Su. *Stochastic formulation of SPICE-type electronic circuit simulation using polynomial chaos.* ACM Transactions on Modeling and Computer Simulation, 18(4):501–507, Sep. 2008.

[4] I. S. Stievano, P. Manfredi, and F. G. Canavero. *Parameters Variability Effects on Multiconductor Interconnects via Hermite Polynomial Chaos.* IEEE Trans. Compon., Packag., Manuf. Technol., 1(8):1234–1239, Aug. 2011.

[5] I. S. Stievano, P. Manfredi, and F. G. Canavero. *Stochastic Analysis of Multiconductor Cables and Interconnects.* IEEE Trans. Electromagn. Compat., 53(2):501–507, May 2011.

[6] D. Vande Ginste, D. De Zutter, D. Deschrijver, T. Dhaene, P. Manfredi, and F. G. Canavero. *Stochastic Modeling Based Variability Analysis of On-Chip Interconnects.* IEEE Trans. Compon., Packag., Manuf. Technol., 2(7):1182–1192, Jul. 2012.

[7] D. Spina, F. Ferranti, T. Dhaene, L. Knockaert, G. Antonini, and D. Vande Ginste. *Variability Analysis of Multiport Systems Via Polynomial-Chaos Expansion.* IEEE Trans. Microw. Theory Tech., 60(8):2329–2338, Aug. 2012.

[8] N. Agarwal and N. R. Aluru. *Weighted Smolyak algorithm for solution of stochastic differential equations on non-uniform probability measures.* International Journal for Numerical Methods in Engineering, 85(11):1365–1389, Mar. 2011.

[9] J. S. Preston, T. Tasdizen, C. M. Terry, A. Cheung, and R. M. Kirby. *Using the Stochastic Collocation Method for the Uncertainty Quantification of Drug Concentration Due to Depot Shape Variability.* IEEE Trans. Biomedical Engineering, 56(3):609 –620, Mar. 2009.

[10] J. Silly-Carette, D. Lautru, M.-F. Wong, A. Gati, J. Wiart, and V. Fouad Hanna. *Variability on the Propagation of a Plane Wave Using Stochastic Collocation Methods in a Bio Electromagnetic Application.* IEEE Microw. Wireless Compon. Lett., 19(4):185 –187, Apr. 2009.

[11] M. A. Drissaoui, S. Lanteri, P. Leveque, F. Musy, L. Nicolas, R. Perrussel, and D. Voyer. *A Stochastic Collocation Method Combined With a Reduced Basis Method to Compute Uncertainties in Numerical Dosimetry*. IEEE Trans. Magnetics, 48(2):563 –566, Feb. 2012.

[12] J. Tao, X. Zeng, W. Cai, Y. Su, D. Zhou, and C. Chiang. *Stochastic Sparse-grid Collocation Algorithm (SSCA) for Periodic Steady-State Analysis of Nonlinear System with Process Variations*. In Proc. Design Automation Conference (ASP-DAC '07). Asia and South Pacific, pages 474–479, Jan. 2007.

[13] M. S. Eldred. *Recent advance in non-intrusive polynomial-chaos and stochastic collocation methods for uncertainty analysis and design*. In Proc. 50th AIAA/ASME/ASCE/AHS/ASC Structures, Structural Dynamics, and Materials Conference, Palm Springs, California, May 2009.

[14] F. Ferranti, L. Knockaert, and T. Dhaene. *Passivity-Preserving Parametric Macromodeling by Means of Scaled and Shifted State-Space Systems*. IEEE Trans. Microw. Theory Tech., 59(10):2394–2403, Oct. 2011.

[15] F. Ferranti, L. Knockaert, T. Dhaene, and G. Antonini. *Parametric macro-modeling based on amplitude and frequency scaled systems with guaranteed passivity*. International Journal of Numerical Modelling: Electronic Networks, Devices and Fields, 25(2):139–151, March/April 2012.

[16] K. Chemmangat, F. Ferranti, T. Dhaene, and L. Knockaert. *Tree-Based Sequential Sampling Algorithm for Scalable Macromodeling of High-Speed Systems*. In Proc. IEEE 16th Workshop on Signal and Power Integrity (SPI), May 2012.

[17] W. A. Weiser and S. E. Zarantonello. *A Note on Piecewise Linear and Multilinear Table Interpolation in Many Dimensions*. Mathematics of Computation, 50(181):253–264, Jan. 1988.

[18] F. Ferranti, L. Knockaert, and T. Dhaene. *Guaranteed Passive Parameterized Admittance-Based Macromodeling*. IEEE Trans. Adv. Packag., 33(3):623 –629, Aug. 2010.

[19] F. Ferranti, L. Knockaert, and T. Dhaene. *Parameterized S-Parameter Based Macromodeling With Guaranteed Passivity*. IEEE Microw. Wireless Compon. Lett., 19(10):608–610, Oct. 2009.

[20] L. W. Nagel. *SPICE2: A Computer Program to Simulate Semiconductor Circuits*. Electr. Res. Lab. Report ERL M520, May 1975.

[21] B. D. Anderson and S. Vongpanitlerd. *Network Analysis and Synthesis*. Prentice-Hall, Englewood Cliffs, NJ, 1973.

[22] P. Manfredi, D. Vande Ginste, D. De Zutter, and F. G. Canavero. *On the Passivity of Polynomial Chaos-Based Augmented Models for Stochastic Circuits*. IEEE Trans. Circuits Syst. I, 60(11):2998–3007, Nov. 2013.

[23] C. Soize and R. Ghanem. *PHYSICAL SYSTEMS WITH RANDOM UNCERTAINTIES: CHAOS REPRESENTATIONS WITH ARBITRARY PROBABILITY MEASURE*. SIAM J. SCI. COMPUT., 26(2):395–410, Jul. 2004.

[24] B. Gustavsen and A. Semlyen. *Rational Approximation of Frequency Domain Responses by Vector Fitting*. IEEE Trans. Power Delivery, 14(3):1052–1061, July 1999.

[25] B. Gustavsen. *Improving the pole relocating properties of vector fitting*. IEEE Trans. Power Del., 21(3):1587–1592, Jul. 2006.

[26] D. Deschrijver, M. Mrozowski, T. Dhaene, and D. De Zutter. *Macromodeling of Multiport Systems Using a Fast Implementation of the Vector Fitting Method*. IEEE Microw. Wireless Compon. Lett., 18(6):383–385, Jun. 2008.

[27] S. Boyd, L. El Ghaoui, E. Feron, and V. Balakrishnan. *Linear Matrix Inequalities in System and Control Theory*, volume 15. SIAM, Philadelphia, PA, 1994.

[28] W. Yu and J. W. Bandler. *Optimization of Spiral Inductor on Silicon using Space Mapping*. In Proc. IEEE MTT-S International Microwave Symposium Digest, pages 1085 –1088, Jun. 2006.

5

Polynomial Chaos-Based Macromodeling of Multiport Systems using an Input-Output Approach

In the previous chapter it is shown that one of the major drawbacks of the application of the PC expansion for the variability analysis of general linear and passive multiport systems is the lack of capability of preserving the physical properties of the system under study, e.g. stability and passivity. The macromodeling technique for variability analysis presented in this chapter allows to enforce the stability and check the passivity of the calculated PC-based macromodel. Furthermore, the macromodel is obtained through the application of the PC expansion at an input-output level without intermediate state-space models as for the technique presented in Chapter 3, adopting an efficient model-building procedure.

⋆ ⋆ ⋆

D. Spina, F. Ferranti, T. Dhaene, L. Knockaert, G. Antonini

Abstract An innovative technique to build stochastic frequency-domain macromodels of generic linear multiport systems is presented. The proposed method

calculates a macromodel of the system transfer function including its statistical properties, making it tailored for variability analysis. The combination of the modeling power of the VF algorithm with the PC expansion applied at an input-output level allows to accurately and efficiently describe the system variability features. Thanks to its versatility and automated order selection, the proposed technique is suitable to be applied to a large range of complex modern electrical systems (e.g. filters, interconnections) and can tackle the case of correlated random variables. The performance in terms of accuracy and computational efficiency of the proposed method are compared with respect to the standard MC analysis for two pertinent numerical examples.

5.1   Introduction

Nowadays, the analysis of the effects of geometrical or electrical parameters variability on the performance of ICs is fundamental. Indeed, many techniques [1–6], based on the PC expansion [7–11], were developed over the last years to study the stochastic variations of electrical circuits as alternative to the computationally cumbersome MC based techniques. The MC analysis is considered the standard approach for variability analysis, thanks to its robustness and ease of implementation. The drawback of MC is its slow convergence rate, that forces the designers to perform a large number of simulations to obtain reliable results. Considering that both the operative bandwidth and complexity of modern electrical systems are constantly increasing, the high computational time required by the MC analysis is a clear limitation. The PC-based techniques proposed so far allow to overcome the computational cumbersomeness of the MC-based approaches, but they were designed for specific systems: multiconductor transmission lines [1–4] or lumped elements circuits [5, 6].

Recently, a PC-based technique was presented in [12] and described in Chapter 3 that performs the variability analysis on a generic linear multiport system. This technique first builds a set of deterministic univariate frequency-domain models of the system transfer function, that can be expressed in different forms (e.g. scattering, impedance or admittance parameters), and then uses the PC expansion to perform the variability analysis. In particular, the PC expansion of the system transfer function is obtained by combining a deterministic set of system equations expressed in state-space form with the PC model of the system's state-space matrices, through the use of Galerkin projections [1–6]. This approach, while applicable to a large range of microwave systems, has a main drawback: the PC model of the system transfer function must be calculated for each frequency of interest solving a linear system. Note that, the set of frequency values of interest can be freely chosen over the frequency range of the initial set of deterministic univariate frequency-domain models of the system transfer function. Finally, despite its ac-

curacy and efficiency, the technique [12] does not offer the possibility to enforce the stability of the calculated PC-based model.

The novel approach presented in this chapter calculates a PC-based frequency-domain macromodel of a generic linear multiport system, described by its scattering parameters, which is suitable for variability analysis. Furthermore, the macromodel is obtained through the application of the PC expansion at an input-output level without intermediate state-space models as in [12], adopting an efficient model-building procedure that

- proposes an algorithm that adaptively chooses the number of basis functions of the PC model;

- it is straightforward to implement.

Finally, we propose a method to enforce the stability and check the passivity of the calculated PC-based macromodel.

The starting point of the proposed technique is the evaluation of the system scattering parameters on a discrete set of values of the frequency and the parameters involved in the variability analysis. Next, the PC model of the system transfer function for the chosen frequencies is calculated through an iterative procedure. Finally, a frequency-domain stochastic macromodel is built as weighted summation of frequency-dependent rational functions of the PC matrix coefficients by means of the VF algorithm [13, 14].

5.2 Macromodeling Strategy

5.2.1 PC modeling of system transfer function

The scattering parameters are widely used to describe the broadband frequency behavior of microwave systems. Indeed, the use of the appropriate reference impedances to all system ports overcomes the difficulties in the measurement of impedance, admittance and hybrid parameters caused by short-circuit, open-circuit, and test-circuit parasitics at microwave frequencies [15].

Also, the scattering parameters have in general a smoother and more bounded behavior with respect to the impedance, admittance and hybrid parameters. This makes the scattering parameters particularly suitable to be efficiently modeled with a PC-based approach. The reader is referred to Section 2.5 for a complete overview about the properties of the PC expansion.

Therefore, the proposed technique aims at building a PC model for the scattering parameters of a generic multiport system of the form

$$\mathbf{S}(s, \boldsymbol{\xi}) \approx \sum_{i=0}^{M} \boldsymbol{\alpha}_i(s) \varphi_i(\boldsymbol{\xi}) \tag{5.1}$$

where the matrix $\mathbf{S}$ represents the system scattering parameters and $\boldsymbol{\alpha}_i(s)$ is a univariate frequency-domain rational model of the i-th PC coefficient matrix and s is the Laplace variable. As will be demonstrated in the sequel, this goal can be achieved by

- determining the basis function $\varphi_i(\boldsymbol{\xi})$;

- deciding on the number of basis functions M (2.50);

- calculating and solving an equivalent linear system for the coefficients of the PC expansion of $\mathbf{S}$;

- calculating a rational model for each PC coefficient matrix obtained.

Without loss of generality, in the sequel we will limit our attention to stochastic processes composed by independent random variables with the corresponding PDFs included in the standard distributions. Hence, the optimal basis functions are the polynomials of the Wiener-Askey scheme. Note, however, that in the most general case of correlated random variables with arbitrary distributions, the corresponding basis functions can also be calculated using the techniques described in [7–9, 11].

The starting point of this work is the calculation of the scattering parameters $\mathbf{S}$ for a discrete set of values of the frequency $[f_l]_{l=1}^L$ corresponding to the Laplace variable $[s_l = j2\pi f_l]_{l=1}^L$ and the normalized random variables $\left[\boldsymbol{\xi}_j\right]_{j=1}^K$. Equation (5.1) can therefore be written as

$$\mathbf{S}(s_l, \boldsymbol{\xi}) \approx \sum_{i=0}^M \boldsymbol{\alpha}_i(s_l)\varphi_i(\boldsymbol{\xi}) \tag{5.2}$$

where only the coefficients $\boldsymbol{\alpha}_i(s_l)$ and the number of basis functions M must be estimated. Next, the linear regression technique [8] is used to obtain the desired PC coefficients. This approach allows to calculate the PC coefficients in (5.2) solving, for each value of the Laplace variable $[s_l]_{l=1}^L$, a least-square system [8] in the form

$$\mathbf{\Phi}\boldsymbol{\alpha} = \mathbf{R} \tag{5.3}$$

with

$$\boldsymbol{\Phi} = \begin{bmatrix} \boldsymbol{\varphi}_0\left(\boldsymbol{\xi}_1\right) & \cdots & \boldsymbol{\varphi}_M\left(\boldsymbol{\xi}_1\right) \\ \vdots & \vdots & \vdots \\ \boldsymbol{\varphi}_0\left(\boldsymbol{\xi}_K\right) & \cdots & \boldsymbol{\varphi}_M\left(\boldsymbol{\xi}_K\right) \end{bmatrix}$$

$$\boldsymbol{\alpha} = \begin{bmatrix} \boldsymbol{\alpha}_0(s_l) \\ \vdots \\ \boldsymbol{\alpha}_M(s_l) \end{bmatrix} \tag{5.4}$$

$$\mathbf{R} = \begin{bmatrix} \mathbf{S}(s_l, \boldsymbol{\xi}_1) \\ \vdots \\ \mathbf{S}(s_l, \boldsymbol{\xi}_K) \end{bmatrix}$$

and where $\boldsymbol{\alpha}$ contains the matrices of the unknown PC coefficients $[\boldsymbol{\alpha}_i(s_l)]_{i=0}^M$, the j−th row of the matrix $\boldsymbol{\Phi}$ is formed by the elements of the multivariate polynomial basis $[\varphi_i]_{i=0}^M$ evaluated in $[\boldsymbol{\xi}_j]_{j=1}^K$ multiplied by the identity matrix of the same dimension of the scattering parameters, and the matrix $\mathbf{R}$ collects the corresponding set of scattering parameters values $\mathbf{S}(s_l, \boldsymbol{\xi}_j)$ for $[\boldsymbol{\xi}_j]_{j=1}^K$.

Note that the system (5.3) must be over-determined to be solved in a least-square sense. Therefore, the number of basis functions M must be chosen to evaluate the number of initial samples K needed to solve (5.3). Since the order of expansion P is limited for practical applications [10], several techniques [1–6, 12] choose upfront the number of basis function M, according to (2.50).

We propose a fully automatic procedure, explained in Algorithm 1, to determine the minimum order of expansion P that guarantees accurate results and, therefore, the estimated number of basis functions M (2.50).

Let us assume that the basis functions up to polynomials of order P' are calculated before starting Algorithm 1. P' is chosen, see (2.50), aimed at keeping the corresponding number of basis functions $M' + 1$ limited. At this point the number of initial samples $K > M' + 1$ can be chosen. In [16] it is recommended to use a number of samples equal to the double of the basis function used, i.e., $K \approx 2\left(M' + 1\right)$.

We will now describe in detail the iterative procedure summarized in Algorithm 1. Initially, the basis functions for polynomials of order one and two, indicated in Algorithm 1 with the symbols Φ^1 and Φ^2, respectively, are selected. Next, the corresponding linear system (5.3) is solved for both PC expansion models. Following equations (2.54) and (2.55), it is now obvious to estimate the mean and the variance for the two PC models. Now, if the difference between the mean and variance of the two PC models exceeds a suitable threshold, then the PC model with polynomials up to order one is discarded and the basis functions corresponding to polynomials of order three are chosen. The procedure is repeated iteratively until the error between the mean and variance predicted by two consecutive PC

Input: Basis function up to order P': $\left[\Phi^1, \ldots, \Phi^{P'}\right]$, $\mathbf{S}(s_l, \boldsymbol{\xi}_j)$
Output: PC model of order P: $Basis_{chosen}$, $\boldsymbol{\alpha}_{chosen}$
$Basis_1 = \Phi^1$;
$Basis_2 = \Phi^2$;
$\boldsymbol{\alpha}_1$=Solve (5.3) for $Basis_1$;
$\mu_1 =$Solve (2.54) for $Basis_1$ and $\boldsymbol{\alpha}_1$;
$\sigma_1 =$Solve (2.55) for $Basis_1$ and $\boldsymbol{\alpha}_1$;
$\boldsymbol{\alpha}_2$=Solve (5.3) for $Basis_2$;
$\mu_2 =$Solve (2.54) for $Basis_2$ and $\boldsymbol{\alpha}_2$;
$\sigma_2 =$Solve (2.55) for $Basis_2$ and $\boldsymbol{\alpha}_2$;
$Error(\mu) = \frac{\mu_2 - \mu_1}{\mu_2}$
$Error(\sigma) = \frac{\sigma_2 - \sigma_1}{\sigma_2}$
$i = 2$;
$Error = error_{chosen}$;

while $Error(\mu) > Error \;||\; Error(\sigma) > Error$ **do**
    if $i < P'$ **then**
        $Basis_1 = Basis_2$;
        $\boldsymbol{\alpha_1} = \boldsymbol{\alpha_2}$;
        $\mu_1 = \mu_2$;
        $\sigma_1 = \sigma_2$;
        $Basis_2 = \Phi^{i+1}$;
        $\boldsymbol{\alpha}_2$=Solve (5.3) for $Basis_2$;
        $\mu_2 =$Solve (2.54) for $Basis_2$ and $\boldsymbol{\alpha}_2$;
        $\sigma_2 =$Solve (2.55) for $Basis_2$ and $\boldsymbol{\alpha}_2$;
        $Error(\mu) = \frac{\mu_2 - \mu_1}{\mu_2}$
        $Error(\sigma) = \frac{\sigma_2 - \sigma_1}{\sigma_2}$;
        $i = i + 1$;
    else
        end while
    end
end
if $Error(\mu) \leq Error \;\&\&\; Error(\sigma) \leq Error$ **then**
    $Basis_{chosen} = Basis_1$;
    $\boldsymbol{\alpha}_{chosen} = \boldsymbol{\alpha}_1$;

else
    $Basis_{chosen} = Basis_2$;
    $\boldsymbol{\alpha}_{chosen} = \boldsymbol{\alpha}_2$;

end

algorithm 1: Iterative procedure to build the PC model.
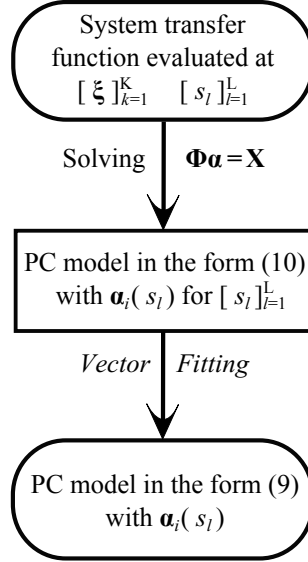
Figure 5.1: Description of the proposed modeling strategy.

models is lower than the chosen threshold. If the previous condition cannot be achieved upon calculation of the basis functions up to polynomials of order P', the PC model of order P' is chosen. It is important to notice that, in Algorithm 1 the computation of the PC coefficients corresponding to basis functions of polynomials of increasing order is not nested: a linear system in the form (5.3) must be solved for each PC model computed up to a specific order of expansion.

At this point, following the procedure described in Algorithm 1, we have calculated (5.2) for each sample $[s_l]_{l=1}^{L}$, using an iterative estimation of the expansion order and the linear regression method to calculate the PC coefficients. Next, to obtain the desired PC model in the form (5.1), the VF algorithm is applied to calculate a rational model for each PC coefficient matrix $[\alpha_i(s_l)]_{i=0}^{M}$ with $[s_l]_{l=1}^{L}$. The proposed modeling strategy is summarized in Fig. 5.1.

The technique described in this chapter is easy to implement, it can be applied to any generic linear multiport system described by its scattering parameters, and it allows to perform the variability analysis with accuracy and efficiency in the frequency-domain. It produces a macromodel of a generic multiport system in the form of a PC model, where each PC coefficient matrix is expressed with a rational model in the frequency-domain. The proposed technique only requires an initial set of samples of the system transfer function for $[s_l]_{l=1}^{L}$ and $[\boldsymbol{\xi}_j]_{j=1}^{K}$, and therefore it can be applied to a large range of microwave systems. With respect to the technique presented in [12], the novel proposed method presents several advantages:

- it proposes an algorithm for the automatic choice of the minimum order of expansion;

- it offers a simple model generation procedure (see Fig. 5.1).

- it does not require to calculate a deterministic model, e.g. state-space models as in [12], prior to the application of the PC expansion;

- it calculates a PC-based macromodel in the form of weighted summation of rational functions, therefore it is not required to solve a linear system to evaluate the obtained PC-based macromodel over a discrete set of frequencies as in [12];

It is worthwhile to notice that the proposed technique can calculate a stable frequency-domain macromodel. Indeed, the macromodel in the form (5.1) is expressed as a weighted sum of frequency-dependent rational functions. Since a weighted sum of stable frequency-dependent rational functions is also stable [17], the stability of the proposed macromodel can be ensured by calculating a stable rational model for each PC coefficient matrix $[\boldsymbol{\alpha}_i(s_l)]_{i=0}^{M}$, using the VF algorithm. Furthermore, the passivity of the proposed macromodel can be checked by means of standard techniques (see Appendix 5.5.2 for further details).

Note that, the loads can be included in the variability analysis by means of the Galerkin projections [1–6], as shown in [12].

5.3   Numerical Examples

In this Section, the proposed technique is applied to different structures. In each example, a comparison with the MC analysis is shown in order to validate the efficiency and accuracy of our novel technique. In particular, the results of the variability analysis obtained with the novel proposed method are compared with the corresponding results obtained with a MC analysis that requires a comparable computational cost as the proposed technique and with a MC analysis performed using a large set of samples.

To calculate the PC model by means of the method described in Algorithm 1, the maximum relative error between the mean and the variance of two consecutive PC models with increasing order is set to 0.01. Furthermore, the rational model of each PC coefficient matrix $[\boldsymbol{\alpha}_i(s_l)]_{i=0}^{M}$ for $[s_l]_{l=1}^{L}$, is calculated with the VF algorithm with the following relative error measure

$$Err = max_{r,c,l} \left(\frac{|\alpha_i^{rc}(s_l) - \tilde{\alpha}_i^{rc}(s_l)|}{\frac{1}{A^2 L} \sum_{r=1}^{A} \sum_{c=1}^{A} \sum_{l=1}^{L} |\alpha_i^{rc}(s_l)|} \right) \tag{5.5}$$
$$for\ r, c = 1, \ldots, A;\ l = 1, \ldots, L;$$

where the symbol $\alpha_i^{rc}(s_l)$ is the element (r, c) of the matrix $\boldsymbol{\alpha}_i(s_l)$ of size $A \times A$, where A is the number of ports, and $\tilde{\alpha}_i^{rc}(s_l)$ is the corresponding value of the rational model. The simulations are performed with MATLAB $2010a$ on a computer with an Intel(R) Core(TM) i3 processor and 4 GB RAM.

5.3.1 Hairpin Filter, 3 Independent Random Variables

In the first example, a bandpass hairpin filter of length $L = 12$ mm has been modeled within the frequency range $[1.5 - 3.5]$ GHz. Its layout is shown in Fig. 5.2. The filter conductors have width $W_1 = 0.33$ mm, while $W_2 = 0.66$ mm is the width of the conductors at the input and output port. The spacing between the port and the filter conductors is $D_1 = D_2 = 0.3$ mm and the spacing between the filter conductors is $D_3 = 1$ mm. The distance C is equal to 2.5 mm. The substrate of thickness 0.635 mm has a relative dielectric constant $\epsilon_r = 9.9$.
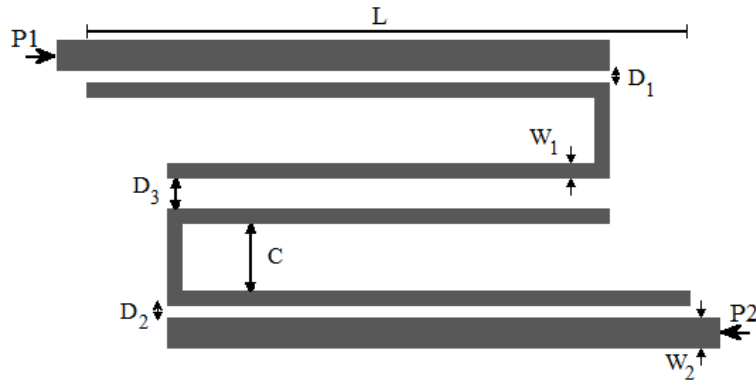
Figure 5.2: Example 5.3.1. Geometry of the bandpass hairpin filter.

Three parameters are considered as independent random variables with uniform PDFs: the spacing D_1, D_2, and D_3, varying by $\pm 10\%$ with respect to their previously indicated nominal value. The selected random variables are normalized as

$$D_1 = \mu_{D_1}(1 + \sigma_{D_1}\xi_1) \tag{5.6}$$
$$D_2 = \mu_{D_2}(1 + \sigma_{D_2}\xi_2) \tag{5.7}$$
$$D_3 = \mu_{D_3}(1 + \sigma_{D_3}\xi_3) \tag{5.8}$$

where ξ_1, ξ_2, ξ_3 are random variables with uniform PDFs over the interval $[-1, 1]$. The corresponding probability measure (2.47) is

$$W(\boldsymbol{\xi}) = \begin{cases} 2^{-N}, & |\xi_i| \leq 1, \quad i = 1, ..., N \\ 0, & elsewhere \end{cases} \tag{5.9}$$

index i	i-th basis function φ_i	$< \varphi_i, \varphi_i >$
0	1	1
1	ξ_1	$\frac{1}{3}$
2	ξ_2	$\frac{1}{3}$
3	ξ_3	$\frac{1}{3}$
4	$\xi_1\xi_2$	$\frac{1}{9}$
5	$\xi_1\xi_3$	$\frac{1}{9}$
6	$\xi_2\xi_3$	$\frac{1}{9}$
7	$\frac{1}{2}\left(3\xi_1^2 - 1\right)$	$\frac{1}{5}$
8	$\frac{1}{2}\left(3\xi_2^2 - 1\right)$	$\frac{1}{5}$
9	$\frac{1}{2}\left(3\xi_3^2 - 1\right)$	$\frac{1}{5}$

Table 5.1: Legendre polynomials products for three independent random variables, with $M = 9$ and $P = 2$.

and the optimal basis functions are products of the Legendre polynomials [11], shown in Table 5.1[1] for $M = 9$ and $P = 2$.

The filter scattering parameters are evaluated using ADS Momentum over a regular grid composed of 51 samples for the frequency and $4 \times 4 \times 4$ (D_1, D_2, D_3) samples for the geometrical parameters. The number K of initial samples for the geometrical parameters is chosen according to the relation $K \approx 2\left(M' + 1\right)$, considering a maximum number of basis function $M' = 34$ and a corresponding order $P' = 4$, according to (2.50). The frequency samples are divided in two

---

[1]Based on the fact that $\int_{-1}^{1} P_n(x)^2 dx = 2/(2n+1)$ where $P_n(x)$ are the Legendre polynomials.
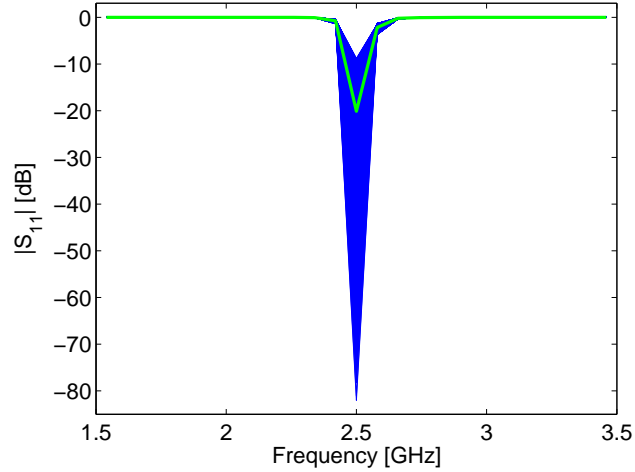
Figure 5.3: Example 5.3.1. Variability of the magnitude of S_{11}. The green thick line corresponds to the central value for (D_1, D_2, D_3), while the blue lines are the results of the MC simulations performed using 10000 (D_1, D_2, D_3) samples.

groups: modeling points (26 samples) and validation points (25 samples). Figure 5.3 shows an example of the variability of the scattering parameters with respect to the chosen random variables.

To build the rational model of the PC coefficients, the VF algorithm is used targeting 0.01 as maximum error (5.5). The PC-based model calculated with the proposed technique has $P = 3$, according to Algorithm 1, and $M = 19$, according to (2.50), and it shows an excellent accuracy and superior efficiency compared with the standard MC analysis in computing system variability features. Indeed, an example of the comparison results for the proposed technique and the MC analysis can be seen in Figs. 5.4 - 5.6, while in Table 5.2 the computational time required by the two approaches is reported. In particular, Figs. 5.4 - 5.5 show the mean and the standard deviation of the real part of S_{11} for the validation frequencies obtained with the proposed technique, a MC analysis with a comparable computational cost (performed using 64 (D_1, D_2, D_3) samples) and a MC analysis performed using 10000 (D_1, D_2, D_3) samples. It is important to notice that around the filter resonance frequency the accuracy of the MC method performed using 64 samples for the geometrical parameters is drastically reduced. Furthermore, the computation of higher order moments like the PDF and the CDF can not be performed accurately using such a reduced set of samples. Indeed, Fig. 5.6 describes the PDF and the CDF of S_{11} for the central frequency of the filter obtained with the proposed method and the MC analysis performed using a large set of samples. Finally, it is worth specifying that in Table 5.2 the total compu-

tational time of the proposed PC-based technique is split into two contributions: the time needed to calculate the initial samples over the modeling frequencies and to build the PC-based macromodel of the scattering parameters and evaluate it on the validation frequencies. Note that, the computational cost to build the PC-based macromodel shown in Table 5.2 includes the cost to compute the PC-model of the scattering parameters in the form (5.2) for all the orders $P \leq 4$ as described by Algorithm 1. Similar results can be obtained for the other entries of the scattering matrix.

Technique	Computational time
Monte Carlo Analysis (10000 samples, validation frequencies)	165 h, 3 min, 28.94 s
Monte Carlo Analysis (64 samples, validation frequencies)	63 min, 22.94 s
PC-based technique	67 min, 21.01 s
Details PC-based technique	Computational time
Initial simulations EM (64 samples, modeling frequencies)	67 min, 14.16 s
PC model scattering parameters	6.85 s

Table 5.2: Example 5.3.1. Efficiency of the Proposed PC-based Technique.

5.3.2   Distributed Microstrip Bandstop Filter, 2 Correlated Random Variables

In the second example, a distributed microstrip bandstop filter has been modeled within the frequency range $[100\,\text{Hz} - 2.5\,\text{GHz}]$. Its layout is shown in Fig. 5.7.

The filter is realized using four open stubs connected by three microstrips. The length of all the lines is $L = 4$ cm and is related to the central wavelength of the filter λ_0 as

$$L = \frac{\lambda_0}{4}$$
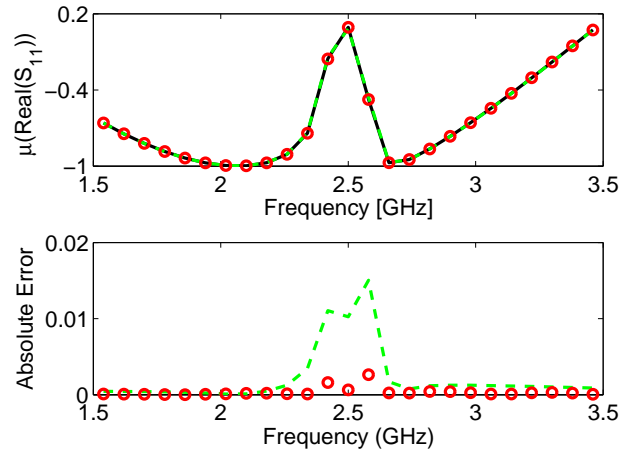
Figure 5.4: Example 5.3.1. The top plot shows a comparison between the mean of the real part of S_{11} obtained with the MC analysis performed using first 10000 (D_1, D_2, D_3) samples (full black line), then 64 (D_1, D_2, D_3) samples (dashed green line), and the proposed PC-based method (red circles: ($\circ$)) for the validation frequencies. The lower plot shows the corresponding absolute error.
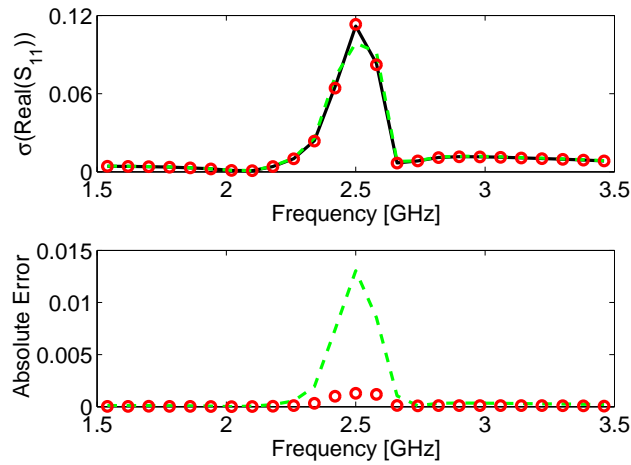
Figure 5.5: Example 5.3.1. The top plot shows a comparison between the standard deviation of the real part of S_{11} obtained with the MC analysis performed using first 10000 (D_1, D_2, D_3) samples (full black line), then 64 (D_1, D_2, D_3) samples (dashed green line), and the proposed PC-based method (red circles: ($\circ$)) for the validation frequencies. The lower plot shows the corresponding absolute error.
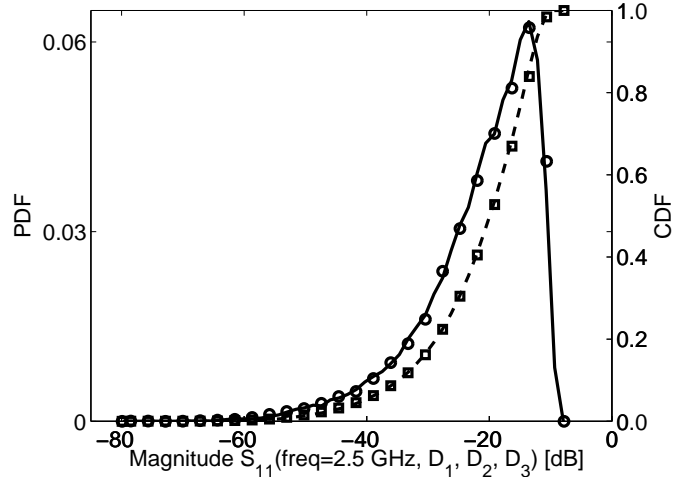
Figure 5.6: Example 5.3.1. PDF and CDF of the magnitude of S_{11} at 2.5 GHz. Full black line: PDF computed using the novel technique; Dashed black line: CDF computed using the novel technique; Circles ($\circ$): PDF computed using the MC technique; Squares ($\square$): CDF computed using the MC technique.

The substrate is $FR4$ of thickness $h = 130$ μm with a relative dielectric constant ϵ_r and a loss tangent $tan\delta$ characterized by a dispersive and causal model [18]. All the microstrips have copper conductors (conductivity $\sigma = 5.8 \cdot 10^7$ S/m) of thickness $t = 10$ μm, but with different widths. In particular the lines M_2, M_4 and M_6 have a conductor of width $w = 120$ μm; for the lines M_1 and M_7 the conductor width is $w = 20$ μm, while $w = 160$ μm for the lines M_3 and M_5.

The scattering parameters are considered as a stochastic process that depends on two correlated random variables with Gaussian PDFs: the length L of the mi-
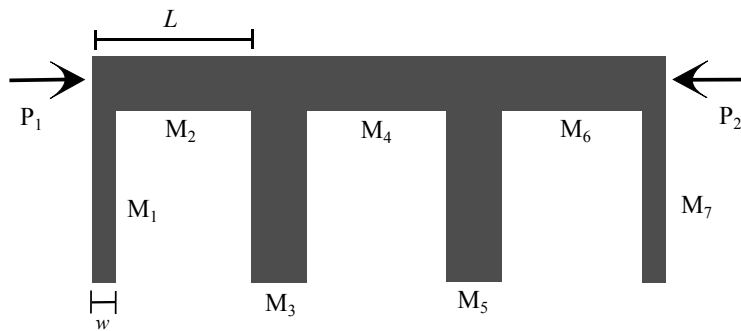
Figure 5.7: Example 5.3.2. Geometry of the distributed microstrip bandstop filter.

crostrip M_2 and the width w of the shunt M_1. Assuming a worst case analysis, the correlation coefficient is chosen equal to $\rho = 0.9$ and, for both the random variables (L, w), the normalized standard deviation is $\pm 5\%$ with respect to their nominal value, indicated in the following with the symbols L_0 for the length and w_0 for the width. The corresponding correlation matrix is

$$\mathbf{C} = \begin{bmatrix} (L_0\sigma_L)^2 & \rho L_0\sigma_L w_0\sigma_w \\ \rho L_0\sigma_L w_0\sigma_w & (w_0\sigma_w)^2 \end{bmatrix}$$

where σ_L and σ_w represent the normalized standard deviations of the length and the width, respectively. In this case $\mathbf{C}$ is positive-definite, hence the couple of random variables (L, w) follow the non-degenerate multivariate normal distribution [19]

$$W_{\boldsymbol{\eta}} = \frac{1}{2\pi det(\mathbf{C})^{\frac{1}{2}}} exp\left(-\frac{1}{2}(\boldsymbol{\eta} - \boldsymbol{\mu})^T \mathbf{C}^{-1}(\boldsymbol{\eta} - \boldsymbol{\mu})\right) \qquad (5.10)$$

where the symbol $det(\cdot)$ is used to represent the matrix determinant, while $\boldsymbol{\eta} = [L, w]^T$ and $\boldsymbol{\mu} = [L_0, w_0]^T$.

Applying the Karhunen-Loéve expansion [20], the scattering parameters can be considered as a stochastic process with respect to the pair of uncorrelated Gaussian random variables with zero mean and unit variance (ξ_1, ξ_2). In particular, the vector of correlated random variables $\boldsymbol{\eta}$ can be expressed with respect to the vector of uncorrelated random variables $\boldsymbol{\xi}$ as

$$\boldsymbol{\eta} = \boldsymbol{\mu} + \mathbf{U}\boldsymbol{\Lambda}^{\frac{1}{2}}\boldsymbol{\xi} \qquad (5.11)$$

where $\boldsymbol{\Lambda}$ is a diagonal matrix containing the eigenvalues of the correlation matrix $\mathbf{C}$ and $\mathbf{U}$ is the matrix of the corresponding eigenvectors. See Appendix 5.5.1 for further details. Therefore, due to the use of the Karhunen-Loéve expansion, it is possible to express the scattering parameters as a stochastic process that depends on the pair of uncorrelated random variables $\boldsymbol{\xi} = [\xi_1, \xi_2]^T$ and, since the variables ξ_1 and ξ_2 are Gaussian, they are also independent. Hence, the corresponding basis functions are products of the Hermite polynomials [11], as shown in Table 5.3 for $M = 5$ and $P = 2$, while the probability measure (2.47) is

$$W(\boldsymbol{\xi}) = \frac{1}{2\pi} exp\left(-\frac{1}{2}\boldsymbol{\xi}^T\boldsymbol{\xi}\right) \qquad (5.12)$$

The evaluation of the scattering parameters is performed using a quasi-analytical model [21] over a regular grid composed of 81 samples for the frequency and 8×8 samples for the geometrical parameters (L, w). Again, the number K of initial samples for the couple of geometrical parameters is chosen according to the relation $K \approx 2(M' + 1)$, considering a maximum order of expansion $P' = 6$ and a

index i	i-th basis function φ_i	$< \varphi_i, \varphi_i >$
0	1	1
1	ξ_1	1
2	ξ_2	1
3	$\xi_1^2 - 1$	2
4	$\xi_1 \xi_2$	1
5	$\xi_2^2 - 1$	2

Table 5.3: Hermite polynomials products for two independent random variables, with $M = 5$ and $P = 2$ [2].

corresponding number of basis functions $M' = 27$, according to (2.50). Next, the frequency samples are divided in two groups: modeling points (41 samples) and validation points (40 samples).

This second example represents a particular difficult structure to model since, as shown in Fig. 5.8, the random variables chosen have a high impact on the scattering parameters of the structure: the range of the stop-band frequencies is influenced by the random variables chosen and in the band-pass frequencies the magnitude of the element S_{11} has a high variability, often over -20 dB, compromising the correct behavior of the filter.

We note that, the variability analysis shown in this example cannot be performed with previous developed techniques [1–4], even if the filter is realized using only microstrips. Indeed, the techniques [1–4] employ a stochastic model of the per-unit-length parameters and the length of a line cannot be assumed as parameter for the variability analysis.

The PC model of the scattering parameters for the modeling frequencies has order $P = 5$, according to Algorithm 1, and $M = 20$, according to (2.50), while 0.01 is targeted as maximum error (5.5) between the PC coefficients and the corresponding rational models. The obtained PC-based model shows an excellent
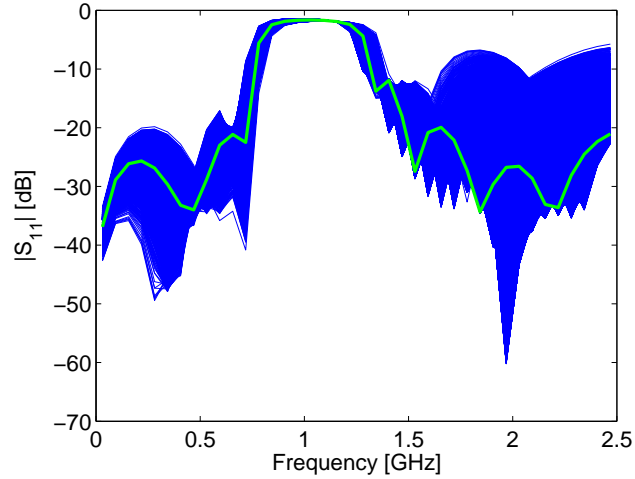
Figure 5.8: Example 5.3.2. Variability of the magnitude of S_{11}. The green thick line corresponds to the nominal value for (L, w), while the blue lines are the results of the MC simulations performed using $10000 (L, w)$ samples.

accuracy compared with the classical MC analysis in computing system variability features, as shown in Figs. 5.9 - 5.11. In particular, Figs. 5.9 - 5.10 show the mean and the standard deviation of the imaginary part of the element S_{12} for the validation frequencies computed with the proposed method, a MC analysis with the similar computational cost (performed using $64 (L, w)$ samples) and a MC analysis performed using $10000 (L, w)$ samples. It is important to notice that for this highly dynamic system the PC method offers a much higher accuracy in estimating these statistical moments than the MC analysis with the similar computational cost. Finally, Fig. 5.11 describes the PDF and the CDF of S_{11} at the frequency of 281.25 MHz. Note that similar results can be obtained for the other entries of the scattering matrix.

The proposed technique offers a great computational efficiency in addition to its accuracy; in Table 5.4 the computational time needed for the MC analysis (performed on the validation frequencies using 64 and $10000 (L, w)$ samples) and the proposed PC-based technique is reported. As in the previous example, in Table 5.4 the computational time of the new PC-based technique is explicitly divided into the time needed to calculate the initial samples and to build the polynomial model of the scattering parameters (including the computational cost to build the PC-model of the scattering parameters in the form (5.2) for all the order $P \leq 6$, as described by Algorithm 1) and evaluate it on the validation frequencies.

Figure 5.9: Example 5.3.2. The top plot shows a comparison between the mean of the imaginary part of S_{12} obtained with the MC analysis performed using first 10000 (D_1, D_2, D_3) samples (full black line), then 64 (D_1, D_2, D_3) samples (dashed green line), and the proposed PC-based method (red circles: ($\circ$)) for the validation frequencies. The lower plot shows the corresponding absolute error.

5.4   Conclusions

In this chapter, we present an innovative technique to calculate frequency-domain macromodels for efficient variability analysis of general multiport systems. It is based on the use of the PC expansion, applied at an input-output level, to describe the system variability features in combination with rational identification in the frequency-domain. The presented technique is straightforward to implement, it selects the PC expansion order automatically, and it can be applied to a large range of microwave systems. Comparisons with the standard MC approach are performed for two pertinent numerical examples, validating the accuracy and efficiency of the proposed method.

5.5   Appendix

5.5.1   Karhunen-Loéve expansion and Correlated Gaussian Random Variables

If the correlation matrix $\mathbf{C}^{N \times N}$ is symmetric and positive-definite, then it has N orthogonal eigenvectors $[\boldsymbol{u}_i]_{i=1}^N$, and can be diagonalized as

$$\mathbf{C} = \mathbf{U} \boldsymbol{\Lambda} \mathbf{U}^T \qquad (5.13)$$
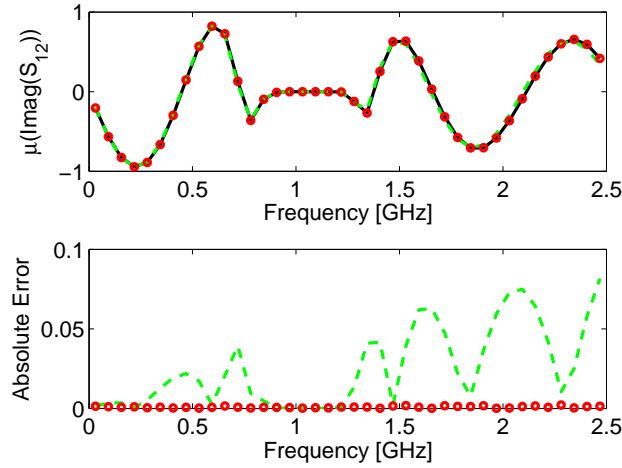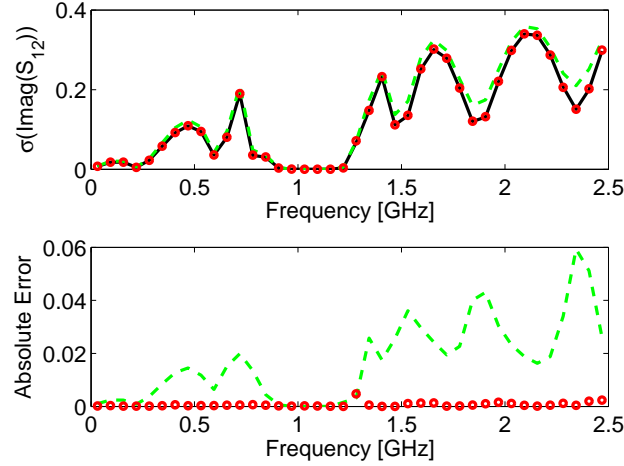
Figure 5.10: Example 5.3.2. The top plot shows a comparison between the standard deviation of the imaginary part of S_{12} obtained with the MC analysis performed using first 10000 (D_1, D_2, D_3) samples (full black line), then 64 (D_1, D_2, D_3) samples (dashed green line), and the proposed PC-based method (red circles: (○)) for the validation frequencies. The lower plot shows the corresponding absolute error.

where $\mathbf{\Lambda}$ is the diagonal matrix of the eigenvalues of $\mathbf{C}$, the symbol ^{T} indicates the matrix transpose and $\mathbf{U}$ is the orthogonal matrix defined as $\mathbf{U} = [\boldsymbol{u}_1, \dots, \boldsymbol{u}_N]$. Using (5.13) in (5.10) leads to

$$W_{\boldsymbol{\eta}} = \frac{1}{2\pi det(\mathbf{\Lambda})^{\frac{1}{2}}} exp\left(-\frac{1}{2}(\boldsymbol{\eta} - \boldsymbol{\mu})^T \mathbf{U}\mathbf{\Lambda}^{-1}\mathbf{U}^T (\boldsymbol{\eta} - \boldsymbol{\mu})\right) \qquad (5.14)$$

Therefore, for correlated Gaussian random variables that follow the non-degenerate multivariate normal distribution (5.10), the Karhunen-Loéve expansion is a simple change of variables. The joint probability density (5.14) can be written with respect to a vector of independent Gaussian random variable $\boldsymbol{x}$, with zero mean and variance equal to $[\mathbf{\Lambda}_{ii}]_{i=1}^{N}$, as

$$W_{\boldsymbol{x}} = \frac{1}{2\pi det(\mathbf{\Lambda})^{\frac{1}{2}}} exp\left(-\frac{1}{2}\boldsymbol{x}^T \mathbf{\Lambda}^{-1}\boldsymbol{x}\right) \qquad (5.15)$$

where

$$\boldsymbol{x} = \mathbf{U}^T (\boldsymbol{\eta} - \boldsymbol{\mu}) \qquad (5.16)$$

Next, the vector $\boldsymbol{x}$ can be expressed with respect to the vector of normalized Gaussian random variables $\boldsymbol{\xi}$ with zero mean and unitary variance as

$$\boldsymbol{x} = \mathbf{\Lambda}^{\frac{1}{2}}\boldsymbol{\xi} \qquad (5.17)$$

Combining (5.16) and (5.17) leads to (5.11).
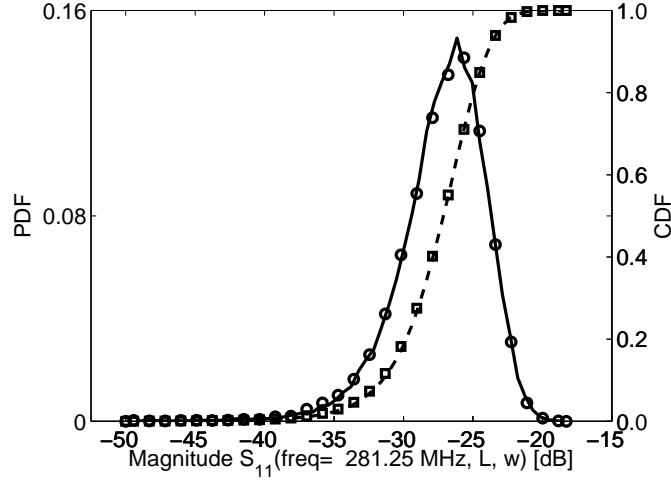
Figure 5.11: Example 5.3.2. PDF and CDF of the magnitude of S_{11} at 281.25 MHz. Full black line: PDF computed using the novel technique; Dashed black line: CDF computed using the novel technique; Circles ($\circ$): PDF computed using the MC technique; Squares ($\square$): CDF computed using the MC technique.

5.5.2   Passivity Verification of the PC-based Macromodel

The proposed technique does not guarantee the passivity of the frequency-domain macromodel in the form (5.1). However, the passivity of the proposed macromodel can be verified, since the matrix coefficients $[\boldsymbol{\alpha}_i(s)]_{i=0}^{M}$ in (5.1) are rational functions of the Laplace variable s. Hence, the coefficients $\boldsymbol{\alpha}_i(s)$ can be written as transfer functions:

$$\boldsymbol{\alpha}_i(s) = \mathbf{C}_i \left(s\mathbf{I}_i - \mathbf{A}_i\right)^{-1} \mathbf{B}_i + \mathbf{D}_i$$

where $\mathbf{I}_i$ is the identity matrix with the same dimensions as the matrix $\mathbf{A}_i$. The state space matrices $[\mathbf{A}_i, \mathbf{B}_i, \mathbf{C}_i, \mathbf{D}_i]_{i=0}^{M}$ are obtained for each $\boldsymbol{\alpha}_i(s)$ by means of system identification techniques such as VF. It should be noted that VF can enforce stability by pole flipping techniques.

Equation (5.1) can therefore be rewritten as

$$\mathbf{S}(s, \boldsymbol{\xi}) \approx \sum_{i=0}^{M} \left(\mathbf{C}_i \left(s\mathbf{I}_i - \mathbf{A}_i\right)^{-1} \mathbf{B}_i + \mathbf{D}_i\right) \varphi_i(\boldsymbol{\xi}) \tag{5.18}$$

Since (5.18) is a weighted sum of rational transfer functions, it is itself a rational transfer function, i.e.,

$$\mathbf{S}(s, \boldsymbol{\xi}) \approx \widehat{\mathbf{C}} \left(s\widehat{\mathbf{I}} - \widehat{\mathbf{A}}\right)^{-1} \widehat{\mathbf{B}}(\boldsymbol{\xi}) + \widehat{\mathbf{D}}(\boldsymbol{\xi}) \tag{5.19}$$

Technique	Computational time
Monte Carlo Analysis (10000 samples, validation frequencies)	$7\ h\ 36\ min,\ 43.7\ s$
Monte Carlo Analysis (64 samples, validation frequencies)	$2\ min,\ 55.38\ s$
PC-based technique	$3\ min\ 32.82\ s$
Details PC-based technique	Computational time
Initial simulations (64 samples, modeling frequencies)	$3\ min\ 1.36\ s$
PC model scattering parameters	$31.46\ s$

Table 5.4: Example 5.3.2. Efficiency of the Proposed PC-based Technique.

where

$$\widehat{\mathbf{A}} = blockdiagonal\left(\mathbf{A}_0, \mathbf{A}_1, \ldots, \mathbf{A}_M\right)$$

$$\widehat{\mathbf{B}}(\boldsymbol{\xi}) = \begin{bmatrix} \mathbf{B}_0\varphi_0(\boldsymbol{\xi}) \\ \mathbf{B}_1\varphi_1(\boldsymbol{\xi}) \\ \vdots \\ \mathbf{B}_M\varphi_M(\boldsymbol{\xi}) \end{bmatrix}$$

$$\widehat{\mathbf{C}} = \begin{bmatrix} \mathbf{C}_0 & \mathbf{C}_1 & \ldots & \mathbf{C}_M \end{bmatrix}$$

$$\widehat{\mathbf{D}}(\boldsymbol{\xi}) = \sum_{i=0}^{M} \mathbf{D}_i\varphi_i(\boldsymbol{\xi})$$

Here $blockdiagonal\left(\cdot\right)$ represents the blockdiagonal matrix with blocks $\left[\mathbf{A}_i\right]_{i=0}^{M}$ on the main diagonal and $\widehat{\mathbf{I}}$ is the identity matrix with the same dimensions as the matrix $\widehat{\mathbf{A}}$.

The passivity of the macromodel (5.19), and of the corresponding form (5.1), can be assessed by computing the following Hamiltonian matrix [22, 23] :

$$\begin{bmatrix} \widehat{\mathbf{A}} - \widehat{\mathbf{B}}(\boldsymbol{\xi})\widehat{\mathbf{R}}(\boldsymbol{\xi})\widehat{\mathbf{D}}(\boldsymbol{\xi})^T\widehat{\mathbf{C}} & -\widehat{\mathbf{B}}(\boldsymbol{\xi})\widehat{\mathbf{R}}(\boldsymbol{\xi})\widehat{\mathbf{B}}(\boldsymbol{\xi})^T \\ \widehat{\mathbf{C}}^T\widehat{\mathbf{S}}(\boldsymbol{\xi})\widehat{\mathbf{C}} & -\widehat{\mathbf{A}}^T + \widehat{\mathbf{C}}^T\widehat{\mathbf{D}}(\boldsymbol{\xi})\widehat{\mathbf{R}}(\boldsymbol{\xi})\widehat{\mathbf{B}}(\boldsymbol{\xi})^T \end{bmatrix} \qquad (5.20)$$

where ^{T} stands for the matrix transpose and

$$\widehat{\mathbf{R}}(\boldsymbol{\xi}) = \left(\widehat{\mathbf{D}}(\boldsymbol{\xi})^T \widehat{\mathbf{D}}(\boldsymbol{\xi}) - \mathbf{I}\right)^{-1}, \, \widehat{\mathbf{S}}(\boldsymbol{\xi}) = \left(\widehat{\mathbf{D}}(\boldsymbol{\xi})\widehat{\mathbf{D}}(\boldsymbol{\xi})^T - \mathbf{I}\right)^{-1}$$

The transfer function $\mathbf{S}(s, \boldsymbol{\xi})$ is passive if and only if the Hamiltonian matrix (5.20) does not admit purely imaginary eigenvalues. It is important to note that the Hamiltonian matrix (5.20) only depends on the normalized random variables $\boldsymbol{\xi}$. Therefore, it is always possible to identify a compact smooth region $\boldsymbol{\Xi} \subset \boldsymbol{\Omega}$ where the macromodel (5.1) is passive, if the corresponding macromodel (5.19) is passive for the values of $\boldsymbol{\xi}$ corresponding with the nominal values of the parameters under consideration, in other words for the operating point.

Note that, the passivity region $\boldsymbol{\Xi} \subset \boldsymbol{\Omega}$ corresponds with all points $\boldsymbol{\xi} \in \boldsymbol{\Omega}$ where the Hamiltonian matrix (5.20) does not admit purely imaginary eigenvalues. Equivalently, the passivity region $\boldsymbol{\Xi} \subset \boldsymbol{\Omega}$ can be found [24] by selecting the points $\boldsymbol{\xi} \in \boldsymbol{\Omega}$ where the $\mathcal{H}_\infty$ norm $\|\mathbf{S}(s, \boldsymbol{\xi})\|_\infty \leq 1.[2]$ Finally, if one wants a parameter span or closed hyper-rectangle inside the passivity region $\boldsymbol{\Xi}$, this can always be obtained, since if a point (here the operating point) is in the interior of a smooth compact region $\boldsymbol{\Xi}$, then one can always find a closed hyper-rectangle inside $\boldsymbol{\Xi}$ containing that interior point.

---

[2]Note that this proves in fact that the passivity region $\boldsymbol{\Xi}$ is smooth and compact, since norms are continuous functions of their argument and $\mathbf{S}(s, \boldsymbol{\xi})$ is by construction a continuous function of its arguments.

References

[1] P. Manfredi, I. S. Stievano, and F. G. Canavero. *Stochastic evaluation of parameters variability on a terminated signal bus*. In Proc. EMC Europe 2011, pages 362 –367, York, UK, Sep. 2011.

[2] I. S. Stievano, P. Manfredi, F. G. Canavero. *Parameters Variability Effects on Multiconductor Interconnects via Hermite Polynomial Chaos*. IEEE Trans. Compon., Packag., Manuf. Technol., 1(8):1234–1239, Aug. 2011.

[3] I. S. Stievano, P. Manfredi, F. G. Canavero. *Stochastic Analysis of Multiconductor Cables and Interconnects*. IEEE Trans. Electromagn. Compat., 53(2):501–507, May 2011.

[4] D. Vande Ginste, D. De Zutter, D. Deschrijver, T. Dhaene, P. Manfredi, and F. Canavero. *Stochastic Modeling-Based Variability Analysis of On-Chip Interconnects*. IEEE Trans. Compon., Packag., Manuf. Technol., 2(7):1182 –1192, Jul. 2012.

[5] Q. Su and K. Strunz. *Stochastic Polynomial-Chaos-Based Average Modeling of Power Electronic Systems*. IEEE Trans. Power Electron., 26(4):1167 – 1171, Apr. 2011.

[6] K. Strunz, Q. Su. *Stochastic formulation of SPICE-type electronic circuit simulation with polynomial chaos*. ACM Trans. Model. Comput. Simulation, 18(4):501–507, Sep. 2008.

[7] G. Blatman and B. Sudret. *An adaptive algorithm to build up sparse polynomial chaos expansions for stochastic finite element analysis*. Probabilistic Engineering Mechanics, 25(2):183 – 197, Apr. 2010.

[8] M. S. Eldred. *Recent advance in non-intrusive polynomial-chaos and stochastic collocation methods for uncertainty analysis and design*. In Proc. 50th AIAA/ASME/ASCE/AHS/ASC Struct., Structural Dynam., Mat. Conf., number AIAA-2009-2274, Palm Springs, California, May 2009.

[9] J. A. S. Witteveen, H. Bijl. *Modeling Arbitrary Uncertainties Using Gram-Schmidt Polynomial Chaos*. In Proc. 44th AIAA Aerosp. Sci. Meeting and Exhibit, number AIAA-2006-0896, Palm Springs, California, Jan. 2006.

[10] D. Xiu, G. E. Karniadakis. *The Wiener-Askey Polynomial Chaos for Stochastic Differential Equations*. SIAM J. Sci. Comput., 24(2):619–644, Apr. 2002.

[11] C. Soize, R. Ghanem. *PHYSICAL SYSTEMS WITH RANDOM UNCERTAINTIES: CHAOS REPRESENTATIONS WITH ARBITRARY PROBABILITY MEASURE*. SIAM J. SCI. COMPUT., 26(2):395–410, Jul. 2004.

[12] D. Spina, F. Ferranti, T. Dhaene, L. Knockaert, G. Antonini, and D. Vande Ginste. *Variability Analysis of Multiport Systems Via Polynomial-Chaos Expansion*. IEEE Trans. Microw. Theory Tech., 60(8):2329 –2338, Aug. 2012.

[13] B. Gustavsen, A. Semlyen. *Rational approximation of frequency domain responses by Vector Fitting*. IEEE Trans. Power Del., 14(3):1052–1061, Jul. 1999.

[14] D. Deschrijver, M. Mrozowski, T. Dhaene, and D. De Zutter. *Macromodeling of Multiport Systems Using a Fast Implementation of the Vector Fitting Method*. IEEE Microw. Wireless Compon. Lett., 18(6):383–385, Jun. 2008.

[15] M. Golio. *The RF and Microwave Handbook (Electrical Engineering Handbook)*. CRC Press, 2000.

[16] S. Hosder, R. W. Walters, M. Balch. *Efficient Sampling for Non-Intrusive Polynomial Chaos Applications with Multiple Uncertain Input Variables*. In Proc. 48th AIAA/ASME/ASCE/AHS/ASC Struct., Structural Dynam., Mat. Conf., number AIAA-2007-1939, Honolulu, HI, 2007.

[17] F. Ferranti, L. Knockaert, and T. Dhaene. *Guaranteed Passive Parameterized Admittance-Based Macromodeling*. IEEE Trans. Adv. Packag., 33(3):623 –629, Aug. 2010.

[18] A. R. Djordjevic̀, R. M. Biljic̀, V.D. Likar-Smiljanic̀, T.K. Sarkar. *Wideband frequency-domain characterization of FR-4 and time-domain causality*. IEEE Trans. Electromagn. Compat., 43(4):662–667, Nov. 2001.

[19] W. Bischoff. *Characterizing multivariate normal distributions by some of its conditionals*. Statistics & Probability Letters, 26(2):105 – 111, Feb. 1996.

[20] M. Loéve. *Probability Theory*. Springer-Verlag, Berlin, Germany, 4-th edition, 1977.

[21] K. C. Gupta, R. Garg, I. Bahl, and P. Bhartia. *Microstrip Lines and Slotlines*. Artech House, Inc., Norwood, MA, Norwood, MA, 2nd edition, 1996.

[22] L. Knockaert, F. Ferranti, and T. Dhaene. *Generalized eigenvalue passivity assessment of descriptor systems with applications to symmetric and singular systems*. International Journal of Numerical Modelling: Electronic Networks, Devices and Fields, 26(1):1–14, January/February, 2013.

[23] S. Grivet-Talocia and A. Ubolli. *Passivity Enforcement With Relative Error Control*. IEEE Trans. Microw. Theory Tech., 55(11):2374 –2383, Nov. 2007.

[24] F. Ferranti, L. Knockaert, and T. Dhaene. *Passivity-Preserving Interpolation-Based Parameterized Macromodeling of Scattered S-Data*. IEEE Microw. Wireless Compon. Lett., 20(3):133 –135, Mar. 2010.

6

Efficient Variability Analysis of Electromagnetic Systems via Polynomial Chaos and Model Order Reduction

So far it has been shown that PC-based macromodeling approaches are efficient and accurate in performing the variability analysis of general linear and passive multiport systems. However, it is not easy to apply the PC expansion to systems described by a large number of equations, such as the ones resulting by means of EM methods. Indeed, the use of the PC expansion would lead to an augmented system of such a high dimension that the computational cost required to solve it may compromise the efficiency of the PC expansion with respect to the MC analysis. The macromodeling technique presented in this chapter overcome this limitation thanks to a suitable combination of model order reduction and PC techniques, generating a final reduced-order model able to accurately perform stochastic computations and variability analysis.

$$\star \; \star \; \star$$

D. Spina, F. Ferranti, G. Antonini, T. Dhaene, L. Knockaert

Abstract We present a novel technique to perform the model order reduction (MOR) of multiport systems under the effect of statistical variability of geometrical or electrical parameters. The proposed approach combines a deterministic MOR phase with the use of the PC expansion to perform the variability analysis of the system under study very efficiently. The combination of MOR and PC techniques generates a final reduced-order model able to accurately perform stochastic computations and variability analysis. The novel proposed method guarantees a high-degree of flexibility, since different MOR schemes can be used and different types of modern electrical systems (e.g. filters, connectors) can be modeled. The accuracy and efficiency of the proposed approach is verified by means of two numerical examples and compared with other existing variability analysis techniques.

6.1   Introduction

Recently, the necessity of employing efficient techniques to perform the variability analysis of the modern ICs has become evident. The MC-based techniques, that represent the standard for the variability analysis due to their accuracy and ease of implementation, have the drawback of requiring a very high computational cost. In particular, the application of the MC method to complex high-speed systems analyzed by means of EM methods [1–3] is unfeasible. Indeed, EM methods usually produce very large systems of equations which are expensive to solve, and the use of the MC analysis would lead to an extremely high computational cost.

In this scenario, a reliable alternative to MC-based methods is represented by techniques based on the PC expansion [4–8], which describes a stochastic process using a base of orthogonal polynomial functions with suitable coefficients. The resulting polynomial model allows to efficiently perform the variability analysis with good accuracy, at the cost of the calculation of an augmented system [4–8]. The reader is referred to Section 2.5 for a complete overview about the properties of the PC expansion. Unfortunately, the application of the PC expansion to systems described by a large numbers of equations, such as the ones resulting by the use of EM methods, is not trivial due to the need of calculating an augmented system.

Different techniques [9–13] have proposed PC-based methodologies for the variability analysis of systems described by a large numbers of equations based on combinations of a PC expansion on the original system matrices and MOR techniques. Indeed, the MOR techniques allow to reduce the complexity of large scale models and, therefore, the computational cost of the simulations [14–16]. Recently, the techniques [11–13] propose a more general PC-based method for the variability analysis of large scale systems described by Helmholtz equations. The recently proposed methods described in [11–13] are based on the following steps:

- the evaluation of the original large system of equations over a discrete set of

points in the stochastic space, chosen using a Smolyak grid [17–19];

- the use of a deterministic MOR technique for each system of equations to generate the corresponding projection matrices;

- the calculation of the PC expansion of the original large system matrices and of the projection matrices;

- the computation of the PC coefficients of the reduced system using congruence transformations;

- the calculation of a PC-based augmented system.

Despite their accuracy and efficiency with respect to the MC-based methods, the techniques [11–13] can be expensive both in terms of memory and computational time, since they require the calculation of a PC-based model of the original large scale equations and of the projection matrices.

We propose in this chapter a novel method that follows these steps:

- the evaluation of the original large system of equations over a discrete set of points in the stochastic space, chosen using a regular grid;

- the calculation of a corresponding set of reduced order models with common order using a common compact projection matrix, following the technique [20];

- the computation of the PC expansion of the reduced models;

- the calculation of a PC-based augmented system.

This new proposed technique is able to overcome the previously mentioned limitations by first calculating a set of reduced order models with common order using a common compact projection matrix and then computing the PC expansion of the reduced models.

6.2   Stochastic Model Order Reduction

The proposed technique aims to perform the variability analysis of a generic multiport system represented by a descriptor state-space form as

$$(s\boldsymbol{C}\left(\boldsymbol{\xi}\right) + \boldsymbol{G}\left(\boldsymbol{\xi}\right))\boldsymbol{X}\left(s,\boldsymbol{\xi}\right) = \boldsymbol{B}\left(\boldsymbol{\xi}\right) \tag{6.1}$$

$$\boldsymbol{H}\left(s,\boldsymbol{\xi}\right) = \boldsymbol{L}^{T}\left(\boldsymbol{\xi}\right)\boldsymbol{X}\left(s,\boldsymbol{\xi}\right) \tag{6.2}$$

where the descriptor state-space matrices $\boldsymbol{C}, \boldsymbol{G}, \boldsymbol{B}, \boldsymbol{L}$, that depend on a vector of random variables $\boldsymbol{\xi}$, are large matrices calculated by an EM method, such as

the Partial Element Equivalent Circuit (PEEC) technique [2]. The superscript T represents the matrix transpose. The dimensionality of descriptor state-space matrices in (6.1) and (6.2) is $C \in \mathbb{R}^{Z \times Z}, G \in \mathbb{R}^{Z \times Z}, B \in \mathbb{R}^{Z \times N_p}, L \in \mathbb{R}^{Z \times N_p}$, where Z is the number of state-vector unknowns and depends on the particular EM method used to compute (6.1) and (6.2), and N_p represent the number of ports of the system. In some recent contributions [21–23], it is proven that is possible to calculate efficiently the PC expansion of the system starting from the PC expansion of the corresponding model (state-space models in [21] and transmission line models in [22, 23]). Theoretically, a similar approach could be used for systems described by equations (6.1) and (6.2). Indeed, using the PC expansion (2.56) to express the state-space matrices, the state-vector and the output in equations (6.1) and (6.2) yields

$$s \sum_{i=0}^{M} \sum_{j=0}^{M} C_i X_j(s) \varphi_i(\xi) \varphi_j(\xi) = - \sum_{i=0}^{M} \sum_{j=0}^{M} G_i X_j(s) \varphi_i(\xi) \varphi_j(\xi) + \sum_{i=0}^{M} B_i \varphi_i(\xi) \tag{6.3}$$

$$\sum_{j=0}^{M} H_j(s) \varphi_j(\xi) = \sum_{i=0}^{M} \sum_{j=0}^{M} L_i^T X_j(s) \varphi_i(\xi) \varphi_j(\xi) \tag{6.4}$$

Let us assume for the moment that the PC expansion of the state-space matrices in equations (6.3) and (6.4) is already calculated. Therefore, the only unknowns are the PC coefficient matrices of the state vector X_j and of the transfer function H_j.

The desired PC coefficient matrices can be calculated by projecting the equations (6.3) and (6.4) on each basis function $\varphi_p(\xi)$ for $p = 0, \dots, M$ (this procedure is referred as Galerkin projections [4, 22] in the PC theory). Indeed, projecting (6.3) on the basis function $\varphi_p(\xi)$ yields

$$s \sum_{i=0}^{M} \sum_{j=0}^{M} C_i X_j(s) < \varphi_i \varphi_j, \varphi_p >=$$

$$- \sum_{i=0}^{M} \sum_{j=0}^{M} G_i X_j(s) < \varphi_i \varphi_j, \varphi_p > + \sum_{i=0}^{M} B_i < \varphi_i, \varphi_p > \tag{6.5}$$

where the explicit dependency on the vector ξ is omitted, for the sake of clarity. Repeating this operation for $p = 0, \dots, M$ gives a frequency dependent linear system of the form

$$\Phi_X X_\alpha = B_\alpha \tag{6.6}$$

where $\Phi_X \in \mathbb{R}^{(M+1)Z \times (M+1)Z}$, $X_\alpha \in \mathbb{R}^{(M+1)Z \times N_p}$, and $B_\alpha \in \mathbb{R}^{(M+1)Z \times N_p}$.

To describe how it is possible to obtain equation (6.6), let us assume for simplicity that one random variable and two basis functions are used for the PC ex-

pansion. In this simplified case, equation (6.5) can be rewritten as

$$(s\boldsymbol{C}_0 + \boldsymbol{G}_0)\,\boldsymbol{X}_0\varphi_0\varphi_0 + (s\boldsymbol{C}_1 + \boldsymbol{G}_1)\,\boldsymbol{X}_0\varphi_1\varphi_0$$
$$+ (s\boldsymbol{C}_0 + \boldsymbol{G}_0)\,\boldsymbol{X}_1\varphi_0\varphi_1 + (s\boldsymbol{C}_1 + \boldsymbol{G}_1)\,\boldsymbol{X}_1\varphi_1\varphi_1 =$$
$$\boldsymbol{B}_0\varphi_0 + \boldsymbol{B}_1\varphi_1 \quad (6.7)$$

Now, thanks to the orthogonality relation (2.47), the projection of (6.7) onto the basis function φ_0 gives

$$\boldsymbol{E}_0(s)\boldsymbol{X}_0 < \varphi_0\varphi_0, \varphi_0 > + \boldsymbol{E}_1(s)\boldsymbol{X}_0 < \varphi_1\varphi_0, \varphi_0 >$$
$$+ \boldsymbol{E}_0(s)\boldsymbol{X}_1 < \varphi_0\varphi_1, \varphi_0 > + \boldsymbol{E}_1(s)\boldsymbol{X}_1 < \varphi_1\varphi_1, \varphi_0 >=$$
$$\boldsymbol{B}_0 < \varphi_0, \varphi_0 > \quad (6.8)$$

where $\boldsymbol{E}_i(s) = (s\boldsymbol{C}_i + \boldsymbol{G}_i)$ for $i = 0, 1$. The projection of (6.7) onto the basis function φ_1 yields

$$\boldsymbol{E}_0(s)\boldsymbol{X}_0 < \varphi_0\varphi_0, \varphi_1 > + \boldsymbol{E}_1(s)\boldsymbol{X}_0 < \varphi_1\varphi_0, \varphi_1 >$$
$$+ \boldsymbol{E}_0(s)\boldsymbol{X}_1 < \varphi_0\varphi_1, \varphi_1 > + \boldsymbol{E}_1(s)\boldsymbol{X}_1 < \varphi_1\varphi_1, \varphi_1 >=$$
$$\boldsymbol{B}_1 < \varphi_1, \varphi_1 > \quad (6.9)$$

Next, equations (6.8) and (6.9) can be rewritten in the form (6.6) as

$$\begin{pmatrix} \boldsymbol{\Phi}_{X00} & \boldsymbol{\Phi}_{X01} \\ \boldsymbol{\Phi}_{X10} & \boldsymbol{\Phi}_{X11} \end{pmatrix} \begin{pmatrix} \boldsymbol{X}_0 \\ \boldsymbol{X}_1 \end{pmatrix} = \begin{pmatrix} \boldsymbol{B}_0 \\ \boldsymbol{B}_1 \end{pmatrix} \quad (6.10)$$

where

$$\boldsymbol{\Phi}_{X00} = \boldsymbol{E}_0(s)\frac{< \varphi_0\varphi_0, \varphi_0 >}{< \varphi_0, \varphi_0 >} + \boldsymbol{E}_1(s)\frac{< \varphi_1\varphi_0, \varphi_0 >}{< \varphi_0, \varphi_0 >}$$
$$\boldsymbol{\Phi}_{X01} = \boldsymbol{E}_0(s)\frac{< \varphi_0\varphi_1, \varphi_0 >}{< \varphi_0, \varphi_0 >} + \boldsymbol{E}_1(s)\frac{< \varphi_1\varphi_1, \varphi_0 >}{< \varphi_0, \varphi_0 >}$$
$$\boldsymbol{\Phi}_{X10} = \boldsymbol{E}_0(s)\frac{< \varphi_0\varphi_0, \varphi_1 >}{< \varphi_1, \varphi_1 >} + \boldsymbol{E}_1(s)\frac{< \varphi_1\varphi_0, \varphi_1 >}{< \varphi_1, \varphi_1 >}$$
$$\boldsymbol{\Phi}_{X11} = \boldsymbol{E}_0(s)\frac{< \varphi_0\varphi_1, \varphi_1 >}{< \varphi_1, \varphi_1 >} + \boldsymbol{E}_1(s)\frac{< \varphi_1\varphi_1, \varphi_1 >}{< \varphi_1, \varphi_1 >}$$

$$(6.11)$$

The frequency dependent system (6.10) can now be solved for each frequency of interest, upon calculation of the scalar products in (6.11). Finally, the PC coefficients of the output $\boldsymbol{H}_j(s)$ can be computed using the PC coefficients of state vector $\boldsymbol{X}_j(s)$. Indeed, the projection of equation (6.4) onto the basis functions $\varphi_p(\boldsymbol{\xi})$, $p = 0, ..., M$, leads to

$$\boldsymbol{H}_p(s) = \sum_{i=0}^{M} \sum_{j=0}^{M} \boldsymbol{L}_i^T \boldsymbol{X}_j(s)\frac{< \varphi_i(\boldsymbol{\xi})\varphi_j(\boldsymbol{\xi}), \varphi_p(\boldsymbol{\xi}) >}{< \varphi_p(\boldsymbol{\xi}), \varphi_p(\boldsymbol{\xi}) >} \quad (6.12)$$

where all the scalar products were already calculated in order to build the matrix $\mathbf{\Phi}_X$.

However, the approach described above can not be efficiently used for systems described by equations (6.1) and (6.2). The calculation of the PC expansion (2.56) for the large matrices $\boldsymbol{C}, \boldsymbol{G}, \boldsymbol{B}, \boldsymbol{L}$, would be very expensive both in terms of memory and computational time, since each corresponding PC coefficient matrix would have the same dimension of the original matrix. Furthermore, the PC expansion of the matrices $\boldsymbol{C}, \boldsymbol{G}, \boldsymbol{B}, \boldsymbol{L}$, would lead to an augmented system in the form (6.6) of such a high dimension that the computational cost required to solve it may compromise the efficiency of the PC expansion with respect to the MC analysis.

The previously developed techniques [11–13] partially solve these issues for systems described by Helmholtz equations. Indeed, in [11–13] it is proposed to evaluate first the original large system of equations over a discrete set of points in the design space and then employ a deterministic MOR technique for each system of equations to generate the corresponding projection matrix. Then, it is calculated a PC model of the original large system matrices and of the projection matrix. It is important to notice that, following the approaches described in [11–13], all the projection matrices calculated for the initial discrete set of points must have common dimensions, otherwise it is not possible to compute the corresponding PC model of the projection matrix via numerical integration (see, for example, equation (33) in [13]). Indeed, it is not possible to calculate a summation of matrices with different dimensions. Finally, it is performed the computation of the PC coefficients of the reduced system that leads to an augmented system in a form similar to (6.6), but the overall dimension of this augmented system is drastically reduced. A compact PC expansion of the original system can be now calculated by employing standard deterministic techniques to solve the obtained augmented system. This approach is accurate and efficient with respect to the MC analysis (that has an extremely high computational cost, since it requires a huge number of simulation of the original large scale model). Furthermore, the techniques [11–13] offer the possibility to use different MOR techniques to calculate the corresponding reduced order PC models. However, the techniques [11–13] can be expensive both in terms of memory and computational time since it is required

- to calculate a PC model of the original large scale equations;

- to calculate a PC model of the projection matrices;

The novel method described in this chapter is able to overcome these limitations by first calculating a set of reduced order models with common order using a common compact projection matrix, following the technique [20], and then computing the PC expansion of the reduced system. In particular, the method described in [20] is implemented using a worst-case choice for the estimation of the reduced

model order and a global approach to build the common compact projection matrix. In the following, we will describe in details the novel proposed method.

Note that, fixing the value of the random variables $\boldsymbol{\xi} = \overline{\boldsymbol{\xi}}$ in equations (6.1) and (6.2) yields

$$\left(s\boldsymbol{C}\left(\overline{\boldsymbol{\xi}}\right) + \boldsymbol{G}\left(\overline{\boldsymbol{\xi}}\right) \right) \boldsymbol{X}\left(s, \overline{\boldsymbol{\xi}}\right) = \boldsymbol{B}\left(\overline{\boldsymbol{\xi}}\right) \tag{6.13}$$

$$\boldsymbol{H}\left(s, \overline{\boldsymbol{\xi}}\right) = \boldsymbol{L}^T\left(\overline{\boldsymbol{\xi}}\right) \boldsymbol{X}\left(s, \overline{\boldsymbol{\xi}}\right) \tag{6.14}$$

Now, it is possible to calculate an equivalent reduced order models as

$$\left(s\widehat{\boldsymbol{C}}\left(\overline{\boldsymbol{\xi}}\right) + \widehat{\boldsymbol{G}}\left(\overline{\boldsymbol{\xi}}\right) \right) \widehat{\boldsymbol{X}}\left(s, \overline{\boldsymbol{\xi}}\right) = \widehat{\boldsymbol{B}}\left(\overline{\boldsymbol{\xi}}\right) \tag{6.15}$$

$$\boldsymbol{H}\left(s, \overline{\boldsymbol{\xi}}\right) = \widehat{\boldsymbol{L}}^T\left(\overline{\boldsymbol{\xi}}\right) \widehat{\boldsymbol{X}}\left(s, \overline{\boldsymbol{\xi}}\right) \tag{6.16}$$

where the reduced order matrices, indicated with the superscript $\wedge$, can be calculated by means of a suitable projection matrix $\boldsymbol{F}$ as:

$$\widehat{\boldsymbol{C}}\left(\overline{\boldsymbol{\xi}}\right) = \boldsymbol{F}^T \boldsymbol{C}\left(\overline{\boldsymbol{\xi}}\right) \boldsymbol{F} \tag{6.17}$$

$$\widehat{\boldsymbol{G}}\left(\overline{\boldsymbol{\xi}}\right) = \boldsymbol{F}^T \boldsymbol{G}\left(\overline{\boldsymbol{\xi}}\right) \boldsymbol{F} \tag{6.18}$$

$$\widehat{\boldsymbol{B}}\left(\overline{\boldsymbol{\xi}}\right) = \boldsymbol{F}^T \boldsymbol{B}\left(\overline{\boldsymbol{\xi}}\right) \tag{6.19}$$

$$\widehat{\boldsymbol{L}}\left(\overline{\boldsymbol{\xi}}\right) = \boldsymbol{F}^T \boldsymbol{L}\left(\overline{\boldsymbol{\xi}}\right) \tag{6.20}$$

The projection matrix $\boldsymbol{F}$ can be calculated using a MOR technique, such as the Krylov-based Laguerre-singular value decomposition (SVD) [24] or passive reduced-order interconnect macromodeling algorithm (PRIMA) [25] algorithms. Therefore, it is possible to calculate for each combination of values of the random variables $\boldsymbol{\xi}$ in the stochastic space $\boldsymbol{\Omega}$ the corresponding reduced system in a descriptor state-space form. Let us suppose that we have calculated K set of reduced matrices $\left[\widehat{\boldsymbol{C}}_k, \widehat{\boldsymbol{G}}_k, \widehat{\boldsymbol{B}}_k, \widehat{\boldsymbol{L}}_k\right]_{k=1}^K$ with common dimension for the corresponding values of the random variables $[\boldsymbol{\xi}_k]_{k=1}^K$ (initial sampling) in the stochastic space $\boldsymbol{\Omega}$. To evaluate the common order for all the K reduced models that will lead to accurate results, first we calculate a reduced order model only for the set of U corner points $[\boldsymbol{\xi}_u]_{u=1}^U$ where $U \subset K$, aiming at minimizing the error with respect to the system frequency response $\boldsymbol{H}(s, \boldsymbol{\xi}_u)$ calculated with the original large dimension system matrices $\boldsymbol{C}(\boldsymbol{\xi}_u), \boldsymbol{G}(\boldsymbol{\xi}_u), \boldsymbol{B}(\boldsymbol{\xi}_u), \boldsymbol{L}(\boldsymbol{\xi}_u)$, for $u = 1, \ldots, U$. Next, we compute the corresponding set of K projection matrices of common order $\boldsymbol{F}_k$ for $k = 1, \ldots, K$. Finally, all the projection matrices calculated so far are stacked in a projection matrix as

$$\boldsymbol{F}_{Union} = \left[\boldsymbol{F}_1, \boldsymbol{F}_2, \ldots, \boldsymbol{F}_K\right] \tag{6.21}$$

The accuracy of the K reduced models with common order, which is estimated by using the U corner points, can be verified by comparing the corresponding

frequency responses with respect to the system frequency responses calculated using the K original large dimension system matrices. If, for a particular example, the desired accuracy can not be achieved by using only the U corner points for the order evaluation, it is always possible to estimate the common order using all the K initial samples. However, the choice of using corners to estimate the common order has proven to be accurate in many cases and allows to save computational time [20].

Now, it is necessary to compute a common projection matrix to be able to calculate a parametric reduced order model over the design points $[\boldsymbol{\xi}_k]_{k=1}^K$. This goal is achieved in two steps: first the SVD decomposition of the projection matrix $\boldsymbol{F}_{Union}$ is calculated as:

$$\boldsymbol{U\Sigma V}^T = svd\left(\boldsymbol{F}_{Union}\right) \tag{6.22}$$

Second, to guarantee the compactness of the common projection matrix it can be defined a common reduced order r based on the first r significant singular values, where the individuation of the desired r significant values can be performed by setting a threshold to the ratio of the singular values with respect to the largest singular value. Indeed, a common projection matrix $\boldsymbol{Q}_C$ can now be expressed as:

$$\boldsymbol{Q}_C = \boldsymbol{U}_r \tag{6.23}$$

where $\boldsymbol{U}_r$ is the matrix $\boldsymbol{U}$ resulting from the SVD decomposition (6.22) for the first r significant singular values. Hence, the desired reduced order matrices with common order can be expressed as:

$$\tilde{\boldsymbol{C}}_k\left(\boldsymbol{\xi}_k\right) = \boldsymbol{Q}_C^T \boldsymbol{C}\left(\boldsymbol{\xi}_k\right)\boldsymbol{Q}_C \tag{6.24}$$

$$\tilde{\boldsymbol{G}}_k\left(\boldsymbol{\xi}_k\right) = \boldsymbol{Q}_C^T \boldsymbol{G}\left(\boldsymbol{\xi}_k\right)\boldsymbol{Q}_C \tag{6.25}$$

$$\tilde{\boldsymbol{B}}_k\left(\boldsymbol{\xi}_k\right) = \boldsymbol{Q}_C^T \boldsymbol{B}\left(\boldsymbol{\xi}_k\right) \tag{6.26}$$

$$\tilde{\boldsymbol{L}}_k\left(\boldsymbol{\xi}_k\right) = \boldsymbol{Q}_C^T \boldsymbol{L}\left(\boldsymbol{\xi}_k\right) \tag{6.27}$$

for $k = 1, \ldots, K$, where the superscript $\sim$ represents the reduced matrices with common order.

Finally, the PC model for the matrices $\tilde{\boldsymbol{C}}, \tilde{\boldsymbol{G}}, \tilde{\boldsymbol{B}}, \tilde{\boldsymbol{L}}$ can be computed. First of all, it is necessary to calculate the basis functions $[\varphi_i]_{i=0}^M$ following the approaches indicated in Section 2.5. Without loss of generality, let us suppose that the random variables $\boldsymbol{\xi}$ are independent. Hence, the number of basis function $M + 1$ can be chosen upfront according to (2.50) considering that P can be limited between two and five [4, 21, 23] for practical applications. Finally, the PC coefficient matrices of $\tilde{\boldsymbol{C}}, \tilde{\boldsymbol{G}}, \tilde{\boldsymbol{B}}, \tilde{\boldsymbol{L}}$ of (6.24)$-$(6.27) can be calculated by means of the linear regression approach (see Section 2.5). The linear regression approach calculates the desired PC coefficients solving a suitable over-determined least-square system [7], that for

the reduced state-space matrix $\tilde{C}$ can be written as

$$\boldsymbol{\Psi}\boldsymbol{\alpha} = \boldsymbol{R} \tag{6.28}$$

where $\boldsymbol{\Psi} \in \mathbb{R}^{K\tilde{Z}\times(M+1)\tilde{Z}}$, $\boldsymbol{\alpha} \in \mathbb{R}^{(M+1)\tilde{Z}\times\tilde{Z}}$, $\boldsymbol{R} \in \mathbb{R}^{K\tilde{Z}\times\tilde{Z}}$ and $\tilde{Z}$ represents the order of the matrix $\tilde{C}$. In particular, the $k-$th row of the matrix $\boldsymbol{\Psi}$ contains the multivariate polynomial basis functions φ_i for $i = 0,\ldots,M$ evaluated in $\boldsymbol{\xi}_k$ for $k = 1,\ldots,K$ multiplied by the identity matrix of the same dimension as the matrix $\tilde{C}$. The corresponding set of values of the matrix $\tilde{C}_k(\boldsymbol{\xi}_k)$ for $k = 1,\ldots,K$ are stored in the matrix $\boldsymbol{R}$. Finally, the desired PC coefficients $\tilde{C}_i$ for $i = 0,\ldots,M$ are collected in the matrix $\boldsymbol{\alpha}$. Equation (7.12) for the each descriptor state-space matrices can be solved in a least squares sense using an element-wise, columnwise or matrix-wise approach.

Since the linear regression approach requires to solve an over-determined linear system in the form (6.28), the number of initial samples K is chosen according to the following relation [7]

$$K \approx 2\,(M+1) \tag{6.29}$$

Note that, equation (6.28) can be solved in a least squares sense using an element-wise, column-wise or matrix-wise approach.

At this point we have calculated a PC model of the reduced descriptor state-space matrices in the form (2.56). For example, the matrix $\tilde{C}(\boldsymbol{\xi})$ can be written as

$$\tilde{C}(\boldsymbol{\xi}) \approx \sum_{i=0}^{M} \tilde{C}_i \varphi_i(\boldsymbol{\xi}) \tag{6.30}$$

Finally, it is possible to write two equations in the form (6.1) and (6.2) for the reduced order descriptor state-space matrices. Applying the same procedure discussed above, it is possible to compute a frequency-dependent linear system in the form (6.6), but the overall dimension of this system is much smaller than the corresponding one related to the use of the original large scale matrices. Therefore, the PC expansion of the system transfer function can be calculated following the same procedure described above (see equations (6.7)–(6.12)).

The proposed technique is flexible, since the transfer function $\boldsymbol{H}$ of a generical multiport system can be expressed by different representations (e.g. scattering or admittance parameters), it allows to use different MOR techniques to calculate the reduced systems, and it offers a reduced computational complexity with respect to the previous approaches [11–13]. The novel proposed technique allows to perform the variability analysis of large dimension systems, such as the ones resulting from EM simulators, with accuracy and efficiency, thanks to the expression of the system transfer function as a suitable combination of PC expansion and MOR methods. Finally, the proposed method does not require to compute a PC model of the projection operator. The techniques [11–13] assume implicitly that

the projection operator as a function of the parameters chosen for the variability analysis $\boldsymbol{\xi}$ can be accurately modeled by a PC expansion. However, in the authors' experience, the calculation of a PC model of the projection operator can be prone to inaccuracies, when the system under study is quite sensitive to the parameters chosen for the variability analysis or when the range of variation of these parameters is large enough. The projection operator is computed independently for each initial sample in the stochastic space and it may not result smooth enough as a function of the stochastic parameters $\boldsymbol{\xi}$ to be accurately modeled by a PC model. Section 6.3 illustrates this aspect.

However, the proposed technique has a limitation: it can still be applied if the number of uncertain parameters is relatively large (i.e. $N = 10$), but at the cost of a loss of efficiency. Indeed, the number K of initial samples is chosen according to (6.29), and the number of basis function $M + 1$ increases rapidly with the number of uncertain parameter N, according with (2.50). Therefore, the calculation of the K initial samples of the large scale system can be expensive, and the computational costs of (6.22) and of solving the reduced system in the form (6.6) can increase as well. This limitation is originated by the formulation of the PC expansion: the number $M + 1$ of basis functions of any PC model in the form (2.56) increases rapidly with the number of uncertain parameter N, according to (2.50). Therefore, the corresponding number of $M + 1$ unknown PC coefficients that must be estimated is large.

The flowchart of the proposed approach is shown in Fig. 6.1.

6.3   Numerical Examples

In this Section, we show the results of the variability analysis performed with the proposed technique for two different structures. In each example, the random variables in the vector $\boldsymbol{\xi}$ are assumed independent and with uniform PDF. The corresponding basis functions are products of the Legendre polynomials [5]. The scalar products resulting from the use of the Galerkin projections are calculated analytically beforehand.

The validation of the accuracy and efficiency of the proposed technique is performed by means of a comparison with the results of other variability analysis techniques. The simulations are performed using Matlab R2012a on a Windows platform equipped with an Intel Core2 Extreme CPU Q9300 2.53 GHz and 8 GB RAM.

6.3.1   Transmission line

In this first example, the scattering parameters of two coupled uniform microstrip lines are considered as a stochastic process with respect to the length of the line in
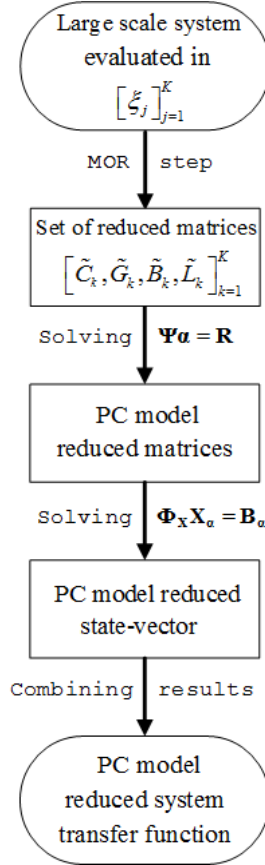
Figure 6.1: Flowchart of the proposed modeling strategy.

the frequency range $[100\,\text{kHz} - 3\,\text{GHz}]$. The cross section of the microstrip lines is shown in Fig. 6.2.

The frequency independent per-unit-length parameters of the lines are [26]

$$\boldsymbol{R}_{pul} = \begin{bmatrix} 0.2 & 0 \\ 0 & 0.2 \end{bmatrix} \frac{\Omega}{\text{m}} \tag{6.31}$$

$$\boldsymbol{L}_{pul} = \begin{bmatrix} 0.28 & 0.07 \\ 0.07 & 0.28 \end{bmatrix} \frac{\text{nH}}{\text{m}} \tag{6.32}$$

$$\boldsymbol{G}_{pul} = \begin{bmatrix} 0 & 0 \\ 0 & 0 \end{bmatrix} \frac{\text{S}}{\text{m}} \tag{6.33}$$

$$\boldsymbol{C}_{pul} = \begin{bmatrix} 0.122 & -0.05 \\ -0.05 & 0.122 \end{bmatrix} \frac{\text{pF}}{\text{m}} \tag{6.34}$$

Starting from the per-unit-length parameters, the corresponding matrices for the admittance representation are computed using the segmentation method described in [24] by dividing the lines in 1650 sections of equal length, which gives state-space matrices of order 6602. Then, these matrices are converted into the corresponding ones for the scattering representation as in [27]. The corresponding descriptor state-space representation is

$$(s\boldsymbol{C} + \boldsymbol{G})\,\boldsymbol{X}\,(s) = \boldsymbol{B} \tag{6.35}$$

$$\boldsymbol{H}\,(s) = \boldsymbol{L}^T \boldsymbol{X}\,(s) + \boldsymbol{D} \tag{6.36}$$

where the matrix $\boldsymbol{D}$ is the identity matrix of dimension $N_p \times N_p$.

It is important to notice that, the scattering parameters of the two coupled microstrips can be efficiently computed using the exact transmission line theory, therefore the variability analysis could be performed without the calculation of a large descriptor state-space model. However, the calculation of a state-space representation of order 6602 allows to verify the performances of the novel proposed method for the case in which the SVD decomposition (6.22) is computed for a very high dimension matrix. Finally, the variability analysis of the system in Fig. 6.2 is performed with respect to the length of the lines in two different ranges of variations and for different orders of the PC models. The performances of the proposed method are compared with the results of the technique [13], for the same number of initial length samples. Note that, the reduced model in the form (16) of [13] are calculated by means of the Galerkin projections instead of truncating the corresponding expansion, since the order of the PC models used in this example is greater than one.

First, the length of the lines varies within the range $[9.75 - 10.25]$ cm with a nominal value $L_0 = 10$ cm as a uniform random variable. The corresponding PC expansion is calculated using $P = 2$ and $M = 2$, according to (2.50). Therefore, the descriptor state-space form (6.35) and (6.36) is computed over a regular grid of $K = 6$ samples. The MOR technique PRIMA [25] is used to calculate the reduced order model, and a maximum absolute model error of -50 dB over 80 frequency samples is targeted to estimate the common order of the reduced models. To build
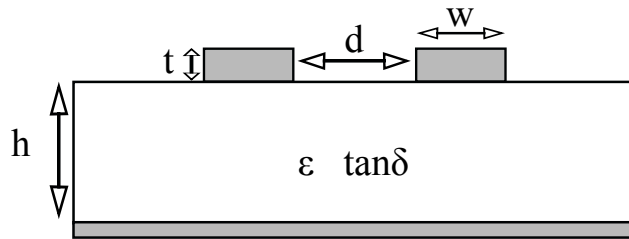

Figure 6.2: Example 6.3.1. Cross section of the coupled microstrips.

the common projector matrix, 0.0001 is chosen as threshold to individuate the first r significant singular values of the SVD decomposition in (6.22) leading to a common projection matrix $\boldsymbol{Q}_C \in \mathbb{R}^{6602 \times 64}$. Finally, K reduced models in a descriptor state-space form of order 64 are computed and modeled using PC expansions as previously discussed.

The Table 6.1 shows the total computational time of the proposed technique detailing the cost of the different operations. In particular, the element "Initial Data" in Table 6.1 represents the operation of calculating the descriptor state-space matrices for the chosen length samples and the corresponding scattering parameters for the two corner points. It is important to specify that, the latter operation takes $1h \ 11min \ 9.7s$, while the calculation of the descriptor state-space matrices for all the six length samples requires only $29min \ 24.8s$. Hence, a MC analysis performed calculating the scattering parameters using the corresponding descriptor state-space models would require approximately $281d \ 3h \ 10min \ 33.3s$, considering 10000 length samples. Therefore, to validate the results of the variability analysis for this example, the MC analysis is performed using the exact transmission line theory. The element "Projection Operator" in Table 6.1 indicates the calculation of the projection operator with common order for all the initial length samples, while the element "Reduced DSS Matrices" represents the calculation of the reduced matrices in the form $(6.24) - (6.27)$, where the symbol DSS stands for descriptor state-space. Note that, the latter operation requires only few seconds, even if the initial descriptor state-space has order 6602. Finally, the elements in the last three rows of Table 6.1 indicate the calculation of the PC model of the reduced descriptor state-space matrices using the linear regression method, the computation of the PC model of the scattering parameters solving an augmented linear system for the reduced state-space matrices in the form (6.6), and the computation of the mean and the variance of the magnitude of the scattering parameters using the corresponding PC model, respectively.

Table 6.2 shows the computational time for the variability analysis performed with the technique [13], in a similar form of Table 6.1. Again, to estimate the common order of the projection operators calculated for all the initial length samples -50 dB is assumed as maximum absolute model error. Note that, the element "PC Model Initial DSS Matrices and Proj. Op." in Table 6.2 describes the calculation through numerical integration of the PC model of the initial descriptor state-space matrices and of the projection operator.

In this case, the novel proposed method is more efficient in terms of computational time with respect to the technique [13]. Indeed, the calculation of the SVD decomposition of the projection operator (6.22) is much more efficient than the calculation of the PC model of the initial descriptor state-space matrices and projection operator required by [13], see Tables 6.1 and 6.2, even if just three PC coefficients must be estimated via numerical integration for [13].

Technique	Computational time
Proposed PC-based Method	$2\,h\,11\,min\,4.9\,s$
Detailed Description of the Computational Time	
Initial Data	$1\,h\,40\,min\,34.5\,s$
Projection Operator	$30\,min\,22.6\,s$
Reduced DSS Matrices	$3.2\,s$
PC Model Reduced DSS Matrices	$0.9\,s$
PC Model S-param	$0.8\,s$
Mean and Variance S-param	$2.9\,s$

Table 6.1: Example 6.3.1. Computational time of the proposed PC-based technique for
$L \in [9.75 - 10.25]$ cm.

Furthermore, the novel proposed PC method is much more efficient in terms of memory requirements, as shown in Table 6.3. As memory requirements we indicate the amount of Mbytes that are necessary to load a particular matrix in the computer RAM. In particular, the memory necessary to store the descriptor state-space matrices for all the initial length samples and the corresponding projection operators is the same for both the techniques, see the elements "Original DSS Matrices" and "Projection Operator" in Table 6.3, while the computation of the reduced matrices $(6.24)-(6.27)$ using the common projection operator (6.23) is much more efficient than the calculation of the PC models of the descriptor state-space matrices and of the projection operator, see elements "Common Proj. Op. (6.23) and Reduced DSS Matrices $(6.24)-(6.27)$" and "PC Model Initial DSS Matrices and Projection Operator" in Table 6.3, respectively.

Finally, the proposed PC-based stochastic model order reduction technique shows an excellent accuracy compared with the MC analysis, performed over

Technique	Computational time
PC-based Technique [13]	$2\,h\,17\,min\,0.3\,s$
Detailed Description of the Computational Time	
Initial Data	$1\,h\,40\,min\,29.6\,s$
Projection Operator	$30\,min\,18\,s$
PC Model Initial DSS Matrices and Proj. Op.	$5\,min\,54.1\,s$
PC Model Reduced DSS Matrices	$14.5\,s$
PC Model S-param	$1.1\,s$
Mean and Variance S-param	$3\,s$

Table 6.2: Example 6.3.1. Computational time of the technique [13] for
$L \in [9.75 - 10.25]$ cm.

$10000\ L$ samples, in computing system variability features, as shown in Figs. 6.3 - 6.4. In particular, Figs. 6.3 - 6.4 show the mean and standard deviation of the magnitude of the element S_{32} obtained with the MC analysis, the proposed PC method and the technique [13]. Similar results can be obtained for the other entries of the scattering matrix.

Next, the lines length is considered as a uniform random variable varying in the range $[9 - 11]$ cm. An example of the scattering parameters variability with respect to the chosen random variable is given in Fig. 6.5. The reduced order models are calculated again using the MOR technique PRIMA [25], targeting an absolute model error of -50 dB over 80 frequency samples. The common projector matrix, obtained choosing 0.0001 as threshold to individuate the first r significant singular values of the SVD decomposition in (6.22), has order $\boldsymbol{Q}_C \in \mathbb{R}^{6602 \times 72}$.

The proposed PC-based stochastic model order reduction technique is more efficient both in terms of memory and computational requirements with respect to
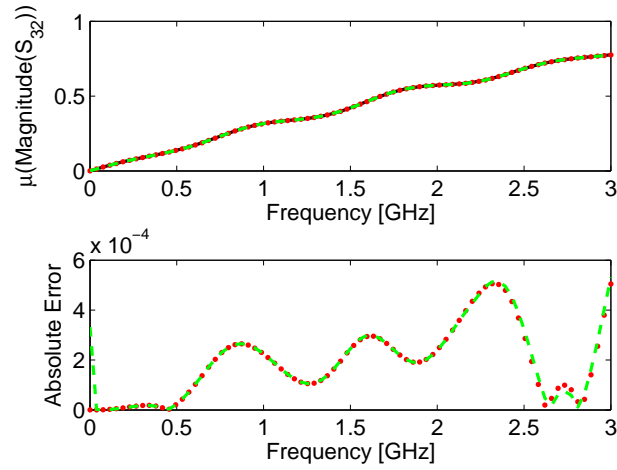
Figure 6.3: Example 6.3.1. The top plot shows a comparison between the mean of the magnitude of S_{32} obtained with the MC analysis (full black line), the proposed PC-based method (red dotted line) and the technique [13] (green dashed line). The lower plot shows the absolute error of the two PC-based variability analysis techniques with respect to the MC analysis.

Figure 6.4: Example 6.3.1. The top plot shows a comparison between the standard deviation of the magnitude of S_{32} obtained with the MC analysis (full black line), the proposed PC-based method (red dotted line) and the technique [13] (green dashed line). The lower plot shows the absolute error of the two PC-based variability analysis techniques with respect to the MC analysis.
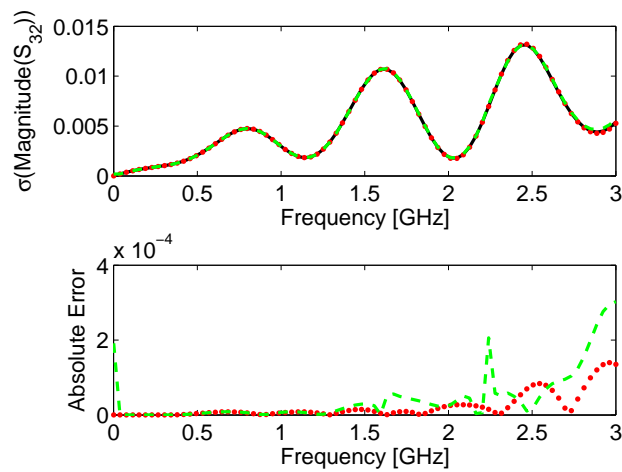
Elements	New technique	Technique [13]
Original DSS Matrices	3991.67 Mbytes	3991.67 Mbytes
Projection Operator	16.92 Mbytes	16.92 Mbytes
Common Proj. Op. (6.23) and Reduced DSS Matrices (6.24)−(6.27)	3.23 Mbytes	
PC Model Initial DSS Matrices and Projection Operator		2004.29 Mbytes
PC Model Reduced Matrices	1.58 Mbytes	1.03 Mbytes

Table 6.3: Example 6.3.1. Memory requirements of the proposed PC-based technique and of the technique [13] for $L \in [9.75 - 10.25]$ cm.

technique [13], see Tables 6.4 - 6.6, and it shows a great accuracy compared with the classical MC analysis, performed over 10000 L samples, in computing system variability features, as shown in Figs. 6.6 - 6.8. In particular, Figs. 6.6 - 6.7 show the mean and standard deviation of the magnitude of the element S_{43} obtained with the MC analysis, the proposed PC method and the technique [13]. Similar results can be obtained for the other entries of the scattering matrix.

It is important to notice that, in this case, the results of the variability analysis performed using the technique [13] are inaccurate with respect to the MC analysis performed using the transmission lines theory over 10000 L samples, see Figs. 6.6 - 6.7. Indeed the calculation via numerical integration of the PC model of the projection operator is inaccurate, see Fig. 6.9. It is worth to notice that, the calculation of the PC model of the original descriptor state-space matrices and of the projection operator is two times more expensive with respect to the previous case, see Tables 6.2 and 6.5, and it requires much more memory, see Tables 6.3 and 6.6.
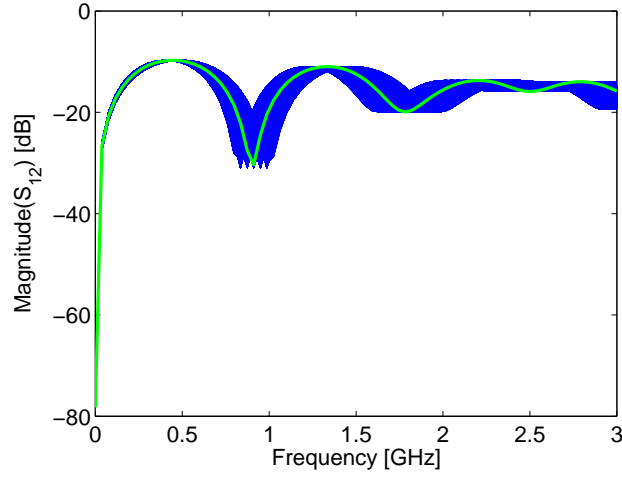
Figure 6.5: Example 6.3.1. Variability of the magnitude of S_{12} calculated for $L \in [9 - 11]$. The blue lines are the results of the MC simulations and the thick green line corresponds to the nominal value for $L_0 = 10$ cm.

Figure 6.6: Example 6.3.1. The top plot shows a comparison between the mean of the magnitude of S_{12} obtained with the MC analysis (full black line), the proposed PC-based method (red dotted line) and the technique [13] (green dashed line). The lower plot shows the absolute error of the two PC-based variability analysis techniques with respect to the MC analysis in logarithmic scale.

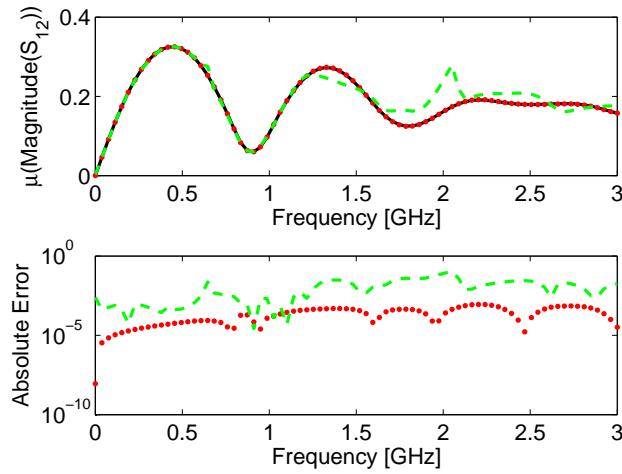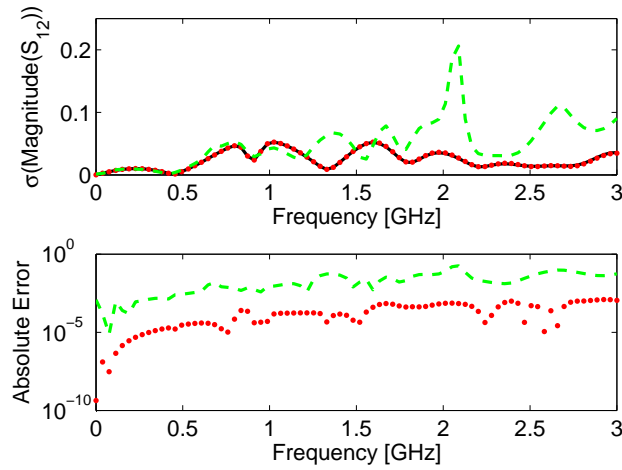*Figure 6.7: Example 6.3.1. The top plot shows a comparison between the standard deviation of the magnitude of S_{12} obtained with the MC analysis (full black line), the proposed PC-based method (red dotted line) and the technique [13] (green dashed line). The lower plot shows the absolute error of the two PC-based variability analysis techniques with respect to the MC analysis in logarithmic scale.*

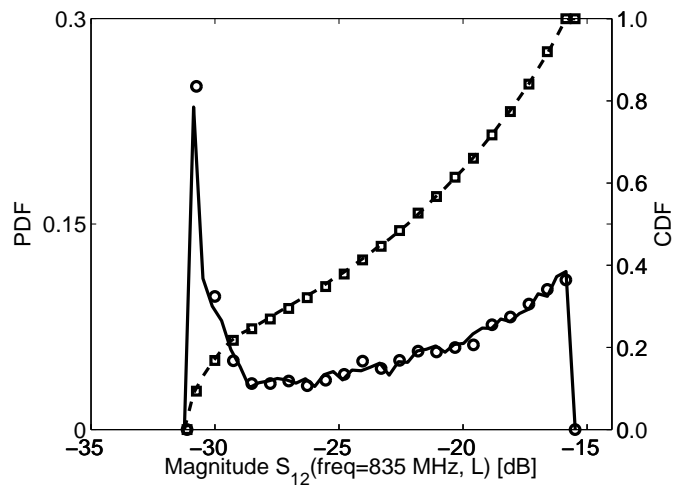*Figure 6.8: Example 6.3.1. PDF and CDF of the magnitude of S_{12} at 835 MHz. Full black line: PDF computed using the novel technique; Dashed black line: CDF computed using the novel technique; Circles ($\circ$): PDF computed using the MC technique; Squares ($\square$): CDF computed using the MC technique.*

Technique	Computational time
Proposed PC-based Method	$2\,h\,32\,min\,14.3\,s$
Detailed Description of the Computational Time	
Initial Data	$1\,h\,50\,min\,0.3\,s$
Projection Operator	$42\,min\,2.6\,s$
Reduced DSS Matrices	$4.8\,s$
PC Model Reduced DSS Matrices	$1.7\,s$
PC Model S-param	$1.5\,s$
Mean and Variance S-param	$3.4\,s$

Table 6.4: Example 6.3.1. Computational time of the proposed PC-based technique for $L \in [9-11]\,cm$.

6.3.2 Bended Conductors

In this second example, a system of three bended conductors in free space has been modeled. Its layout is shown in Fig. 6.10. The copper conductors, placed at a distance of $S_0 = 2$ mm the one from the other, have width $W_0 = 0.5$ mm and length $L_0 = 5$ mm. The copper conductivity is assumed equal to $5.8 \cdot 10^7\,S/m$.

The system admittance parameters are considered as a stochastic process first with respect to the couple of random variables (L, S) varying in a range of $\pm 10\%$ with respect to the central values previously mentioned. The admittance representation is evaluated in the frequency range $[100\,\text{kHz} - 5\,\text{GHz}]$ using the PEEC method [28] over a grid composed of 4×4 (L, S) samples for the geometrical parameters. The corresponding set of descriptor state-space matrices computed has order 2124 for each initial (L, S) sample. The Laguerre-SVD MOR technique [24] is used to calculate the reduced order models. The evaluation of the common order of the reduced models is performed assuming 0.0001 as maximum weighted rms

Technique	Computational time
PC-based Technique [13]	$2\ h\ 45\ min\ 51.2\ s$
Detailed Description of the Computational Time	
Initial Data	$1\ h\ 49\ min\ 28.4\ s$
Projection Operator	$42\ min\ 24.7\ s$
PC Model Initial DSS Matrices and Proj. Op.	$13\ min\ 11.5\ s$
PC Model Reduced DSS Matrices	$41.8\ s$
PC Model S-param	$1.3\ s$
Mean and Variance S-param	$3.5\ s$

Table 6.5: Example 6.3.1. Computational time of the technique [13] for $L \in [9-11]$ cm.

error between the admittance parameters of the reduced model and the original system over $K_s = 50$ frequency samples:

$$Error_{rms} = $$

$$\sqrt{\frac{\sum_{i=1}^{N_p^2} \sum_{k=1}^{K_s} \left| w_{Y_i}(s_k)\Big(Y_{r,i}(s_k) - Y_i(s_k)\Big)\right|^2}{N_p^2 K_s}} \tag{6.37}$$

with

$$w_{Y_i}(s) = |(Y_i(s))^{-1}| \tag{6.38}$$

The evaluation of the significant r singular values of the SVD decomposition in (6.22) is performed assuming 0.0001 as a threshold. Upon calculation of the common projection matrix (6.23), each of the K reduced order models calculated for the couple of random variables (L, S) has order 232. Finally, the set of reduced order matrices is modeled using a second order $(P = 2)$ PC expansion, giving $M = 5$ for (L, S), according to (2.50).

Elements	New technique	Technique [13]
Original DSS Matrices	5322.22 Mbytes	5322.22 Mbytes
Projection Operator	24.18 Mbytes	24.18 Mbytes
Common Proj. Op. (6.23) and Reduced DSS Matrices (6.24)−(6.27)	3.62 Mbytes	
PC Model Initial DSS Matrices and Projection Operator		2673.2 Mbytes
PC Model Reduced Matrices	2.45 Mbytes	1.48 Mbytes

Table 6.6: Example 6.3.1. Memory requirements of the proposed PC-based technique and of the technique [13] for $L \in [9 - 11]$ cm.

The results of the variability analysis obtained with the novel proposed method are compared with the corresponding ones given by the technique [13] and are validated by means of comparison with results of the MC analysis using the parameterized model order reduction technique [28]. The latter technique is a parameterized model order reduction method that guarantees the overall stability and passivity of parameterized reduced order models, by using passivity preserving interpolation schemes. In particular, first a set of reduced model with the same order are calculated assuming 0.0001 as threshold for the error measure (6.37). Then, the reduced models obtained are interpolated over the 10000 (L, S) samples used for the MC analysis. Note that, the parameterized model order reduction technique [28] is applied to the same PEEC matrices calculated for the initial (L, S) samples used for the novel proposed technique. Finally, the initial samples needed by the technique [13] are computed over a Smolyak sparse grid, composed of 29 (L, S) samples [13], while 0.0001 is assumed as maximum weighted rms error to estimate the common order of the projection operators calculated for all the initial (L, S) samples.

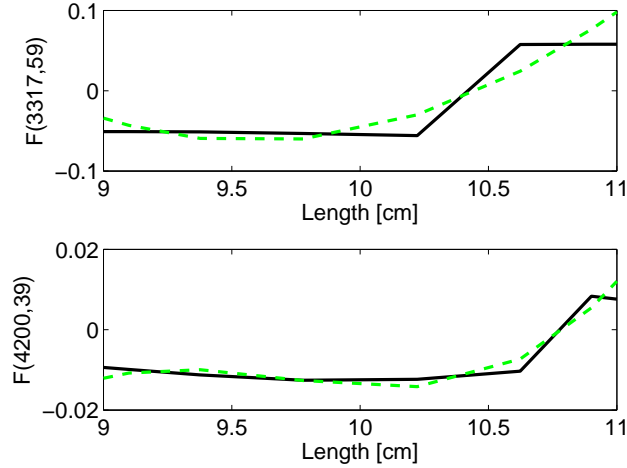The PC model of the projection operator computed by the technique [13] is

Figure 6.9: Example 6.3.1. The top plot shows a comparison between the value of the 3317th row and 59th column of the projection operator calculated for all the initial length samples (full black line) and the corresponding value obtained using the PC model of the projection operator (green dashed line). The lower plot shows the same comparison for the value of the 4200th row and 39th column of the projection operator.

not accurate, see Fig. 6.11. This leads to poor accuracy in computing the system variability features with respect to the corresponding results given by the novel proposed method and the MC analysis performed using the parameterized model order reduction technique [28], as shown in Figs. 6.12, 6.13, although the number of initial samples used to implement the technique [13] is almost the double of the ones used for the proposed PC-based method. In particular, Figs. 6.12 and 6.13 show the mean and standard deviation of the magnitude of Y_{24} calculated with respect to the random variables (L, S). Similar results can be obtained for the other entries of the admittance parameters. Furthermore, the variability analysis performed with the proposed method shows a great efficiency both in terms of memory and computational time, as shown in Table 6.7 and 6.8.

Finally, the variability analysis of the system in Fig. 6.10 is performed with respect to the set of random variables (L, S, W), varying in a range of $\pm 10\%$ with respect to the central values previously mentioned, in order to show the performances of the proposed PC method while increasing the numbers of random variables. Figure 6.14 shows an example of the system variability with respect to the chosen random variables (L, S, W). The system admittance parameters are evaluated using the PEEC method over a grid of $3 \times 3 \times 3$ (L, S, W) samples. The evaluation of the common order of the reduced models and of the r significant singular values of the SVD decomposition in (6.22) is performed with the same
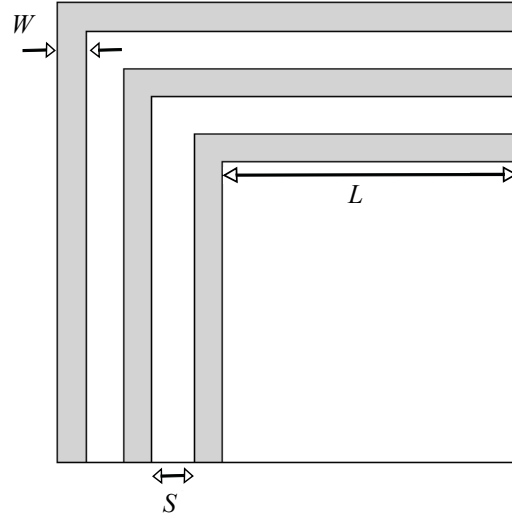
Figure 6.10: Example 6.3.2. Geometry of the system of bended conductors.

setting used in the previous case, giving reduced order models of order 328. Next, the set of reduced order matrices is modeled using a second order $(P = 2)$ PC expansion, giving $M = 9$ for (L, S, W), according to (2.50). The proposed PC-based method is compared with the MC analysis performed with the technique [28] for 100, 1000, 10000 samples.

The proposed method shows a great efficiency in computing the system variability features, as shown in Table 6.9 that compares the computational cost of the MC analysis performed with the technique [28] for 10000 samples and of the novel proposed method, and a great accuracy with respect to the corresponding analysis performed with the technique [28], as described by Figs. 6.15 - 6.17. In particular, Figs. 6.15, 6.16 show the mean and standard deviation of the magnitude of Y_{43} obtained with the proposed PC-based method and the MC analysis performed using different set of samples. Figure 6.17 describes the PDF and the CDF of the magnitude of Y_{11} at 100 kHz calculated with respect to the random variables (L, S, W) using 10000 samples for the MC results. Similar results can be obtained for the other entries of the admittance parameters.

6.4   Conclusions

In this chapter, a novel and efficient technique for stochastic model order reduction of general linear multiport systems is presented. The core of the proposed
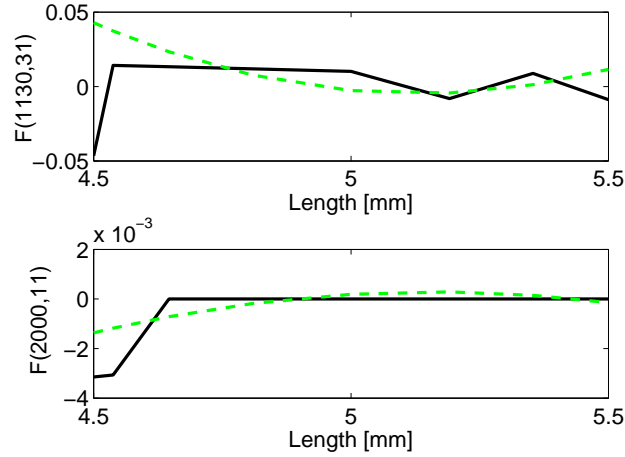
Figure 6.11: Example 6.3.2. The top plot shows a comparison between the value of the 1130*th row and* 31*th column of the projection operator calculated for all the length samples corresponding to the value of spacing* $S = 2$ *mm (full black line) and the corresponding value obtained using the PC model of the projection operator (green dashed line). The lower plot shows the same comparison for the value of the* 2000*th row and* 11*th column of the projection operator.*

technique is the application of the PC expansion to a set of reduced order system in a descriptor state-space form obtained through a MOR step. In addition to its accuracy, the proposed approach offers a great flexibility. Indeed, not only the novel method can be applied to systems whose frequency-domain transfer function can be expressed in different forms (e.g. scattering or admittance parameters), but also different MOR techniques can be used for the calculation of the reduced order system in descriptor state-space form. Two distinct pertinent numerical examples validate the accuracy and efficiency of the proposed method with respect to existing techniques concerning the calculation of system variability features.
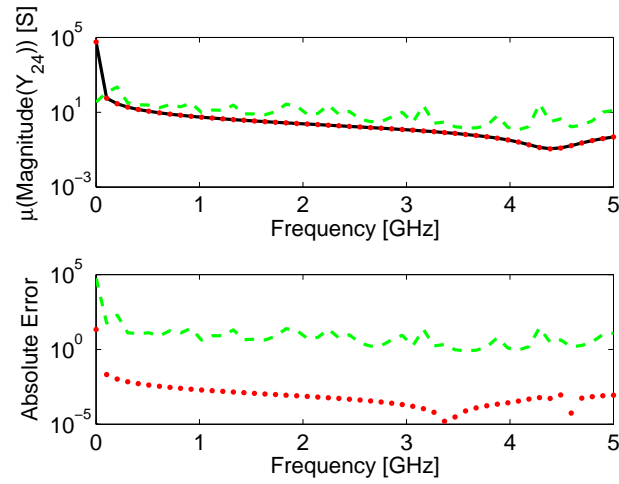
Figure 6.12: Example 6.3.2. Comparison of the mean for the magnitude of Y_{24} with respect to the couple of random variables (L, S) obtained with the MC analysis performed with the technique [28] (full black line), the technique [13] (green dashed line) and the proposed PC-based method (dotted red line).
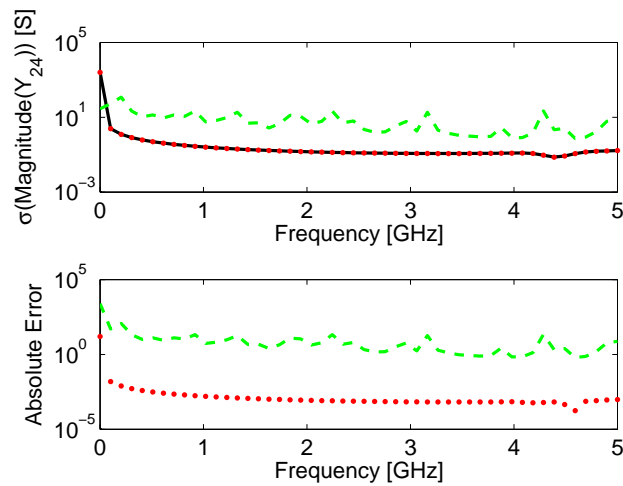
Figure 6.13: Example 6.3.2. Comparison of the standard deviation for the magnitude of Y_{24} with respect to the couple of random variables (L, S) obtained with the MC analysis performed with the technique [28] (full black line), the technique [13] (green dashed line) and the proposed PC-based method (dotted red line).

Technique	Computational time
Parameterized model order reduction [28]	$3\ h\ 19\ min\ 37.6\ s$
Technique [13]	$1\ h\ 25\ min\ 23.7\ s$
Proposed PC-based Method	$47\ min\ 15.2\ s$
Detailed Description of the Computational Time	
Initial Data	$45\ min\ 24\ s$
Projection Operator	$1\ min\ 15\ s$
Reduced DSS Matrices	$2.9\ s$
PC Model Reduced DSS Matrices	$5.7\ s$
PC Model S-param	$26\ s$
Mean and Variance S-param	$1.6\ s$

Table 6.7: Example 6.3.2. Efficiency of the proposed PC-based technique for (L, S).

Elements	New technique	Technique [13]
Original DSS Matrices	1102.45 Mbytes	1998.19 Mbytes
Projection Operator	9.33 Mbytes	16.92 Mbytes
Common Proj. Op. (6.23) and Reduced DSS Matrices (6.24)−(6.27)	17.01 Mbytes	
PC Model Initial DSS Matrices and Projection Operator		416.92 Mbytes
PC Model Reduced Matrices	5.15 Mbytes	0.31 Mbytes

Table 6.8: Example 6.3.2. Memory requirements of the proposed PC-based technique and of the technique [13] for (L, S).
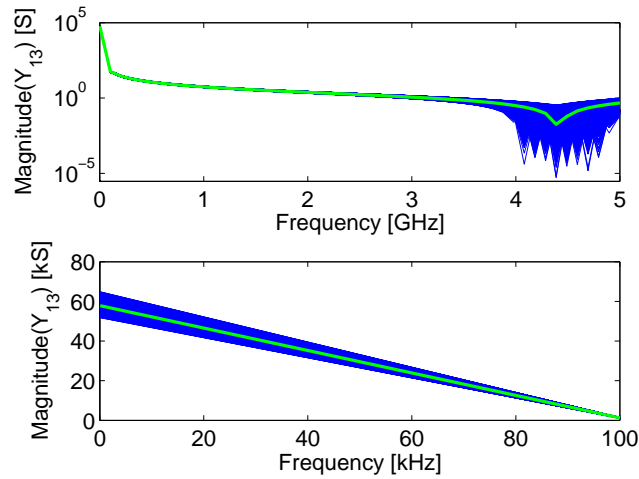
Figure 6.14: Example 6.3.2. The top plot shows the variability of the magnitude of Y_{13} with respect to the random variables (L, S, W) in the frequency range $[100\ kHz - 5\ GHz]$. The lower plot shows the variability of the magnitude of Y_{13} in the frequency range $[100\ kHz - 100\ MHz]$. In both plots, the blue lines are the results of the MC simulations and the thick green line corresponds to the nominal value for $L_0 = 5\ mm$, $S_0 = 2\ mm$ and $W_0 = 0.5\ mm$.
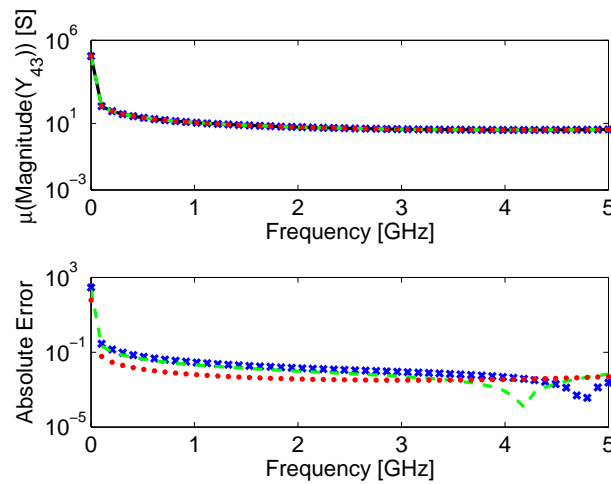
Figure 6.15: Example 6.3.2. Comparison of the mean for the magnitude of Y_{43} obtained with the MC analysis performed with the technique [28] using 10000 (full black line), 1000 (green dashed line) and 100 (blue ex $(\times)$) (L, S, W) samples and the proposed PC-based method (dotted red line).
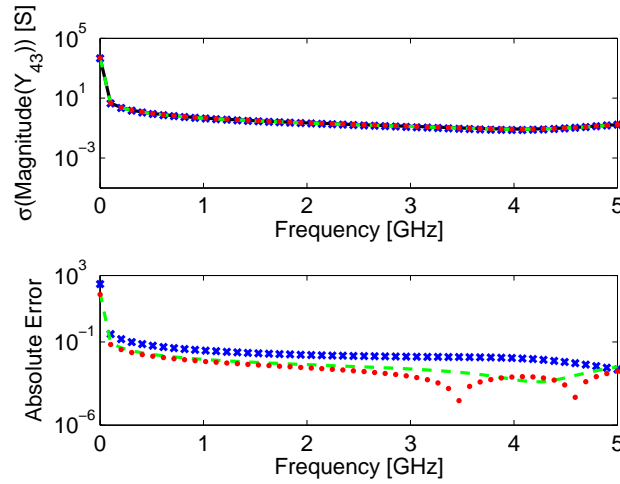
Figure 6.16: Example 6.3.2. Comparison of the standard deviation for the magnitude of Y_{43} obtained with the MC analysis performed with the technique [28] using 10000 (full black line), 1000 (green dashed line) and 100 (blue ex ($\times$)) (L, S, W) samples and the proposed PC-based method (dotted red line).
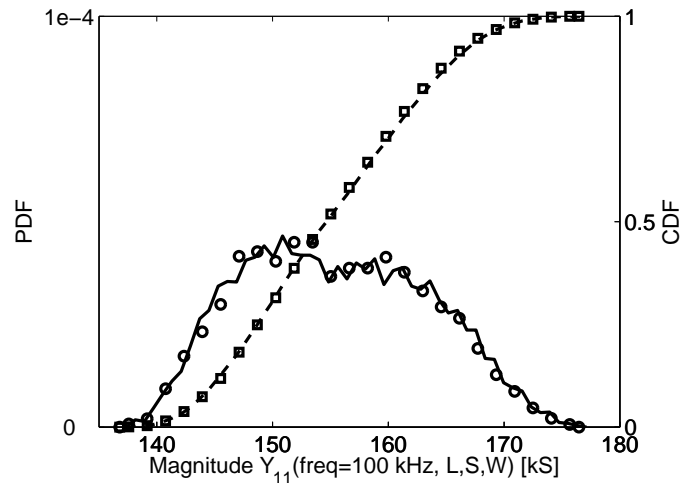
Figure 6.17: Example 6.3.2. PDF and CDF of the magnitude of Y_{11} at 100 kHz. Full black line: PDF computed using the novel technique; Dashed black line: CDF computed using the novel technique; Circles ($\circ$): PDF computed using the MC technique performed with the technique [28] ; Squares ($\square$): CDF computed using the MC technique performed with the technique [28] .

Technique	Computational time
Parameterized model order reduction [28]	$6\ h\ 1\ min\ 42.6\ s$
Proposed PC-based Method	$1\ h\ 24\ min\ 4.5\ s$
Detailed Description of the Computational Time	
Initial Data	$1\ h\ 17\ min\ 58\ s$
Calculation Projection Operator	$1\ min\ 55\ s$
Calculation Reduced DSS Matrices	$7.3\ s$
PC Model Reduced DSS Matrices	$14.2\ s$
PC Model S-param	$3\ min\ 47.9\ s$
Mean and Variance S-param	$2.1\ s$

Table 6.9: Example 6.3.2. Efficiency of the proposed PC-based technique for (L, S, W).

References

[1] R. F. Harrington. *Field Computation by Moment Methods*. Macmillan, New York, 1968.

[2] A. E. Ruehli. *Equivalent circuit models for three dimensional multiconductor systems*. IEEE Trans. Microw. Theory Tech., 22(3):216–221, Mar. 1974.

[3] J. M. Jin. *The Finite Element Method in Electromagnetics*. John Wiley and Sons, New York, 2nd edition, 2002.

[4] D. Xiu and G. E. Karniadakis. *The Wiener-Askey Polynomial Chaos for Stochastic Differential Equations*. SIAM J. Sci. Comput., 24(2):619–644, Apr. 2002.

[5] C. Soize and R. Ghanem. *PHYSICAL SYSTEMS WITH RANDOM UNCERTAINTIES: CHAOS REPRESENTATIONS WITH ARBITRARY PROBABILITY MEASURE*. SIAM J. SCI. COMPUT., 26(2):395–410, Jul. 2004.

[6] J. A. S. Witteveen and H. Bijl. *Modeling Arbitrary Uncertainties Using Gram-Schmidt Polynomial Chaos*. In Proc. 44th AIAA Aerosp. Sci. Meeting and Exhibit, number AIAA-2006-0896, Palm Springs, California, Jan. 2006.

[7] M. S. Eldred. *Recent advance in non-intrusive polynomial-chaos and stochastic collocation methods for uncertainty analysis and design*. In Proc. 50th AIAA/ASME/ASCE/AHS/ASC Struct., Structural Dynam., Mat. Conf., number AIAA-2009-2274, Palm Springs, California, May 2009.

[8] G. Blatman and B. Sudret. *An adaptive algorithm to build up sparse polynomial chaos expansions for stochastic finite element analysis*. Probabilistic Engineering Mechanics, 25(2):183 – 197, Apr. 2010.

[9] S. Vrudhula, J.M. Wang, and P. Ghanta. *Hermite Polynomial Based Interconnect Analysis in the Presence of Process Variations*. IEEE Trans. Comput.-Aided Design Integr. Circuits Syst., 25(10):2001–2011, Oct. 2006.

[10] N. Mi, S. X.-D Tan, Y. Cai, and X. Hong . *Fast Variational Analysis of On-Chip Power Grids by Stochastic Extended Krylov Subspace Method*. IEEE Trans. Comput.-Aided Design Integr. Circuits Syst., 27(11):1996–2006, Nov. 2008.

[11] P. Sumant, H. Wu, A. Cangellaris, N. Aluru. *A sparse grid based collocation method for model order reduction of finite element approximations of passive electromagnetic devices under uncertainty*. In Proc. Microwave Symposium Digest (MTT), 2010 IEEE MTT-S International, pages 1652–1655, Anaheim, California, May 2010.

[12] P. Sumant, H. Wu, A. Cangellaris, and N. Aluru. *Order reduction of finite element models of passive electromagnetic structures with statistical variability*. In Proc. URSI International Symposium on Electromagnetic Theory (EMTS), pages 688 –691, Aug. 2010.

[13] P. Sumant, H. Wu, A. Cangellaris and N. Aluru. *Reduced-Order Models of Finite Element Approximations of Electromagnetic Devices Exhibiting Statistical Variability*. IEEE Trans. Antennas Propag., 60(1):301–309, Jan. 2012.

[14] L. Knockaert, T. Dhaene, F. Ferranti, D. De Zutter. *Model order reduction with preservation of passivity, non-expansivity and Markov moments*. Systems & Control Letters, 60(1):53–61, Jan. 2011.

[15] J. Phillips, L. Daniel, L. M. Silveira. *Guaranteed passive balancing transformations for model order reduction*. IEEE Trans. CAD Integr. Circuits Syst., 22(8):1027–1041, Aug. 2003.

[16] J. Phillips, L. M. Silveira. *Poor man's TBR: a simple model reduction scheme*. IEEE Trans. CAD Integr. Circuits Syst., 24(1):43–55, Jan. 2005.

[17] V. Barthelmann, E. Novak, and K. Ritter. *High dimensional polynomial interpolation on sparse grid*. Adv. Comput. Math., 12(4):273–288, Mar. 2000.

[18] E. Novak, and K. Ritter. *High dimensional integration of smooth functions over cubes*. Numer. Math., 75(1):79–97, Nov. 1996.

[19] E. Novak, and K. Ritter. *Simple cubature formulas with high polynomial exactness*. Construct. Approx., 15(4):499–522, Oct. 1999.

[20] E. R. Samuel, F. Ferranti, L. Knockaert, and T. Dhaene. *Parameterized reduced order models with guaranteed passivity using matrix interpolation*. In Proc. IEEE 16th Workshop on Signal and Power Integrity (SPI), pages 65–68, May 2012.

[21] D. Spina, F. Ferranti, T. Dhaene, L. Knockaert, G. Antonini, and D. Vande Ginste. *Variability Analysis of Multiport Systems Via Polynomial-Chaos Expansion*. IEEE Trans. Microw. Theory Tech., 60(8):2329 –2338, Aug. 2012.

[22] D. Vande Ginste, D. De Zutter, D. Deschrijver, T. Dhaene, P. Manfredi, and F. Canavero. *Stochastic Modeling-Based Variability Analysis of On-Chip Interconnects*. IEEE Trans. Compon., Packag., Manuf. Technol., 2(7):1182 –1192, Jul. 2012.

[23] I. S. Stievano, P. Manfredi, F. G. Canavero. *Parameters Variability Effects on Multiconductor Interconnects via Hermite Polynomial Chaos*. IEEE Trans. Compon., Packag., Manuf. Technol., 1(8):1234–1239, Aug. 2011.

[24] L. Knockaert and D. De Zutter. *Laguerre-SVD reduced order modeling*. IEEE Trans. Microw. Theory Tech., 48(9):1469–1475, Sep. 2000.

[25] A. Odabasioglu, M. Celik, and L. T. Pileggi. *PRIMA: Passive reducedorder interconnect macromodeling algorithm,*. IEEE Trans. Computer-Aided Design, 17:645–654, Aug. 1998.

[26] G. Antonini. *A dyadic Green's function based method for the transient analysis of lossy and dispersive multiconductor transmission lines*. IEEE Trans. Microw. Theory Tech., 56(4):880–895, Apr. 2008.

[27] F. Ferranti, G. Antonini, T. Dhaene, and L. Knockaert. *Guaranteed Passive Parameterized Model Order Reduction of the Partial Element Equivalent Circuit (PEEC) Method*. IEEE Trans. Electromagn. Compat., 52(4):974–984, Nov. 2010.

[28] F. Ferranti, G. Antonini, T. Dhaene, L. Knockaert, and A.E. Ruehli. *Physics-Based Passivity-Preserving Parameterized Model Order Reduction for PEEC Circuit Analysis*. IEEE Trans. Compon., Packag., Manuf. Technol., 1(3):399–409, Mar. 2011.

7

Stochastic Macromodeling of Nonlinear Systems via Polynomial Chaos Expansion and Transfer Function Trajectories

In this chapter, a stochastic macromodeling technique suitable for the variability analysis of nonlinear systems is presented. It is based on the combination of the Transfer Function Trajectory method and of the PC expansion. The proposed approach can be applied to study a broad range of nonlinear systems and a hierarchical approach can be used to reduce the modeling complexity. Finally, the method allows to perform the variability analysis with good accuracy and improved efficiency compared to MC analysis.

⋆ ⋆ ⋆

D. Spina, D. De Jonghe, D. Deschrijver, G. Gielen, L. Knockaert, T. Dhaene

Abstract A novel approach is presented to perform stochastic variability analysis of nonlinear systems. The versatility of the method makes it suitable for the

analysis of complex nonlinear electronic systems. The proposed technique is a variation-aware extension of the Transfer Function Trajectory (TFT) method by means of the PC expansion. The accuracy with respect to the classical MC analysis is verified by means of a relevant numerical example showing a simulation speedup of $1777\,X$.

7.1 Introduction

The evaluation of the effects of geometrical or electrical parameter variability on the performance of modern microwave components and circuits is fundamental, due to the increasing complexity, density and bandwidth of these circuits [1, 2]. The MC method is the standard for the variability analysis due to its accuracy and robustness. It has however the clear limitation of requiring a large number of simulations. Indeed, the simulation of complex, high-speed microwave components and circuits can be expensive, in terms of both memory and computational time.

A reliable alternative to MC-based approaches is presented by the PC expansion [3–8], which describes a stochastic process as a series of orthogonal polynomials with suitable coefficients. A complete overview about the properties of the PC expansion is given in Section 2.5. The PC expansion has extensively been applied to the variability analysis of linear systems (i.e. lumped elements circuits [9, 10], multiconductor transmission lines [11–13] and generic linear multiport systems [14]). In particular, the contribution [14] (described in Chapter 3) demonstrates the accuracy and efficiency of the frequency-domain variability analysis performed while applying the PC expansion to the state-space description of the linear system under study. However, the application of the PC expansion to the variability analysis of nonlinear electronic devices so far has been limited to

- specific types of circuits (namely oscillators [15] and DC/DC converters [16]);

- the evaluation of the effects of variability of macromodels embedded in nonlinear circuits [17].

In this chapter a novel method is proposed for the variability analysis of complex nonlinear systems based on the calculation of the PC expansion of the TFT [18–20] model of the system under study, indicated below as the PC-TFT model. The proposed technique is particularly suitable to model RF nonlinear circuits thanks to the modeling power of the parametric VF algorithm [21–23] employed by the TFT method.

The calculation of the PC-TFT model requires a two-step process. At first a discrete number of TFT models is computed corresponding to a discrete set of

samples of time and of geometrical or physical parameters chosen for the variability analysis. Then the desired PC-TFT model is computed using the linear regression approach [4]. Finally, the variability analysis of the system is performed accurately and efficiently by using the PC model of the system's output, which can directly be obtained from the PC-TFT model by solving a suitable system of ordinary differential equations (ODEs) using a standard numerical method.

The proposed method offers several advantages: it can be applied to a broad range of nonlinear circuits thanks to the modeling power of the TFT; it offers the efficiency and accuracy of the PC method in performing the variability analysis; and it is suitable for the analysis of complex nonlinear circuits since a hierarchical approach can be used for the calculation of the PC-TFT model.

This chapter is structured as follows. First, an overview of the TFT trajectory method is given in Section 7.2. The time-domain stochastic macromodeling technique is described in Sections 7.3 and 7.4. A relevant numerical example is presented in Section 7.5, validating the proposed technique. Conclusions are summed up in Section 7.6.

7.2   Piecewise TFT Modeling

We consider nonlinear dynamical systems of order Z with a state-space description that arises when modeling electric circuits by modified nodal analysis (MNA):

$$\dot{\boldsymbol{g}}(\boldsymbol{x}(t)) = \boldsymbol{f}(\boldsymbol{x}(t)) + \boldsymbol{B}\boldsymbol{u}(t), \;\; \boldsymbol{y}(t) = \boldsymbol{C}^T \boldsymbol{x}(t) \tag{7.1}$$

In this chapter, $\boldsymbol{x}(t) \in \mathbb{R}^Z$ is the state vector corresponding to the node voltages and inductor currents in the circuit and $\boldsymbol{u}(t) \in \mathbb{R}^{M_i}$ are the inputs to the circuit. $\boldsymbol{g}(\cdot)$ and $\boldsymbol{f}(\cdot) \in \mathbb{R}^{Z \times Z}$ are matrix-valued functions describing the charges and currents of nonlinear components. $\boldsymbol{B} \in \mathbb{R}^{Z \times M_i}$ is a constant incidence matrix, which maps the inputs to the internal nodes of the circuit. $\boldsymbol{C} \in \mathbb{R}^{Z \times M_o}$ is the output matrix and $\boldsymbol{y}(t) \in \mathbb{R}^{M_o}$ denotes the output variables.

Trajectory piecewise (TPW) methods have proven themselves to be state-of-the-art in the field of accurate automated model generation [24, 25]. Here, the state space is covered with linear or low-order polynomial snapshots of the nonlinear system (7.1). Consequently, the nonlinear matrix functions $\boldsymbol{f}(\cdot)$ and $\boldsymbol{g}(\cdot)$ are approximated over a significant portion of the reachability space [24], [26] by a convex combination of affine functions:

$$\begin{aligned} \boldsymbol{f}(\boldsymbol{x}) &\approx \textstyle\sum_j w_j(\boldsymbol{x}) \left(\boldsymbol{A}_j \boldsymbol{x} + \mathbf{a}_j \right) \\ \boldsymbol{g}(\boldsymbol{x}) &\approx \textstyle\sum_j w_j(\boldsymbol{x}) \left(\boldsymbol{E}_j \boldsymbol{x} + \mathbf{e}_j \right) \end{aligned} \tag{7.2}$$

where A_j, E_j are the Jacobians of the linearization around $\boldsymbol{x}_j = \boldsymbol{x}(t_j)$ and $\mathbf{a}_j, \mathbf{e}_j$ are inhomogeneous offset terms. The scalar function $w_j(\boldsymbol{x})$ performs a weighted

interpolation between the samples such that $w_j(\boldsymbol{x}_j) = 1$. The idea of generating a collection of local models has also been used for the design of gain-scheduled controllers and is referred to as a quasi-linear parameter-varying (quasi-LPV) representation of the nonlinear system [26]. For robustness, the samples that are included in the quasi-LPV model need to cover the reachability space of the system. In practice, it often suffices to apply typical training signals with a large amplitude over a frequency range of interest.

The linearized matrices $\boldsymbol{A}_j$, $\boldsymbol{E}_j$ are large and sparse, so projection-based model-order reduction techniques can be applied for reducing their complexity to an order $R \ll Z$ [27, 28]. More recently, the TFT representation was proposed as a scalable version of the TPW approach that guarantuees global stability by transforming the linearized samples to the frequency domain [19]:

$$\boldsymbol{H}_j(s) = \boldsymbol{C}^T \left(s\boldsymbol{E}_j + \boldsymbol{A}_j\right)^{-1} \boldsymbol{B} \tag{7.3}$$

The above collection of transfer functions $\boldsymbol{H}_j(s)$ is parameterized in the frequency s and the state space index $j = 1, \ldots, T$, with T the number of state space samples. The resulting hyperplane is then approximated along the frequency axis with $R \ll Z$ fixed poles $diag\left(\widehat{\boldsymbol{A}}\right)$ using the parametric VF algorithm [22, 23]. Due to the non-uniqueness of the frequency-domain representation, the pole-residue form that is computed by the VF algorithm has multiple realizations which are related by similarity transform. For example, the Hammerstein and Wiener realizations respectively become:

$$\boldsymbol{H}_j(s) \approx \widehat{\boldsymbol{C}}^T(s\boldsymbol{I} - \widehat{\boldsymbol{A}})^{-1}\widehat{\boldsymbol{B}}_j \quad \text{for } j = 1, \ldots, T \tag{7.4}$$

$$\boldsymbol{H}_j(s) \approx \widehat{\boldsymbol{C}}_j^T(s\boldsymbol{I} - \widehat{\boldsymbol{A}})^{-1}\widehat{\boldsymbol{B}} \quad \text{for } j = 1, \ldots, T \tag{7.5}$$

The nonlinear functionality of the system approximation is fully embedded in the residues $\widehat{\boldsymbol{r}}_{l,k}$ by fixing the poles of the model over the entire state space. Moreover, the model is assured to be bounded-input bounded-output (BIBO) stable using a simple pole-flipping scheme [22].

In the remainder of this chapter, the TFT model (7.5) is implemented as a multi-channel Wiener system with a linear time-invariant block at the input and a nonlinear readout map. In order to capture strongly nonlinear dynamics, the nonlinear part is implemented as a piecewise combination of linear functions. Other nonlinear function approximations of the residues can be found in [18–20]. The time-domain representation of the Wiener-TFT approximation is found by piecewise integration of the residues:

$$\begin{cases} \dot{\widehat{\boldsymbol{x}}}(t) &= \widehat{\boldsymbol{A}}\widehat{\boldsymbol{x}}(t) + \widehat{\boldsymbol{B}}\boldsymbol{u}(t) \\ \widehat{\boldsymbol{y}}(t) &= \sum_j w_j(\widehat{\boldsymbol{x}}(t)) \left(\widehat{\boldsymbol{C}}_j^T \widehat{\boldsymbol{x}}(t) + \widehat{\boldsymbol{D}}_j\right) \end{cases} \tag{7.6}$$

The constant $\widehat{\boldsymbol{D}}_j$ is found by comparing the system output to the output of the model with $\widehat{\boldsymbol{D}}_j = 0$. By introducing:

$$\begin{aligned} \widehat{\boldsymbol{C}}\left(\widehat{\boldsymbol{x}}\right) &= \sum_j w_j(\widehat{\boldsymbol{x}}(t))\widehat{\boldsymbol{C}}_j^T \\ \widehat{\boldsymbol{D}}\left(\widehat{\boldsymbol{x}}\right) &= \sum_j w_j(\widehat{\boldsymbol{x}}(t))\widehat{\boldsymbol{D}}_j \end{aligned}, \tag{7.7}$$

the model (7.6) can be written compactly as:

$$\begin{cases} \dot{\widehat{\boldsymbol{x}}}(t) &= \widehat{\boldsymbol{A}}\widehat{\boldsymbol{x}}(t) + \widehat{\boldsymbol{B}}\boldsymbol{u}(t) \\ \widehat{\boldsymbol{y}}(t) &= \widehat{\boldsymbol{C}}\left(\widehat{\boldsymbol{x}}\right)\widehat{\boldsymbol{x}}(t) + \widehat{\boldsymbol{D}}\left(\widehat{\boldsymbol{x}}\right) \end{cases} \tag{7.8}$$

In the following sections, a variation-aware extension of the TFT models is developed by means of the PC theory.

7.3   Calculation of the PC-TFT Model

The goal of the proposed contribution is to model the time-domain variability of a nonlinear system that depends on a vector of random variables $\boldsymbol{\xi}$. The PC model (2.51) of the TFT description (7.8) of the nonlinear system under study (indicated as PC-TFT) can be written as:

$$\begin{cases} \dot{\widehat{\boldsymbol{x}}}(t) = & \widehat{\boldsymbol{A}}\widehat{\boldsymbol{x}}(t) + \widehat{\boldsymbol{B}}\boldsymbol{u}(t) \\ \widehat{\boldsymbol{y}}\left(t, \boldsymbol{\xi}\right) = & \sum_{i=0}^M \left(\widehat{\boldsymbol{C}}_i\left(\widehat{\boldsymbol{x}}\right)\widehat{\boldsymbol{x}}\left(t\right) + \widehat{\boldsymbol{D}}_i\left(\widehat{\boldsymbol{x}}\right)\right)\varphi_i(\boldsymbol{\xi}) \end{cases} \tag{7.9}$$

In a first step, the TFT model (7.8) of the system under study is computed over a discrete set of values of the random variables $\boldsymbol{\xi}$ and of the state space $\boldsymbol{x}(t)$, indicated as $[\boldsymbol{\xi}_r]_{r=1}^K$ and $[\boldsymbol{x}_j]_{j=1}^T$, respectively. The sampling in the state space is dictated by the training stimuli of the TFT model and does not need to be uniform [19, 24], while the samples of the random variables $\boldsymbol{\xi}$ are chosen over a regular grid in the stochastic space $\boldsymbol{\Omega}$. In particular, the number K of samples in the stochastic space is chosen according to:

$$K \approx 2\left(M + 1\right) = 2\frac{(N + P)!}{N!P!} \tag{7.10}$$

where N is the number of random variables and P is the highest degree of the polynomials used in the PC expansion. The TFT samples (7.5) that correspond to each value of $[\boldsymbol{\xi}_r]_{r=1}^K$ and $[\boldsymbol{x}_j]_{j=1}^T$ can be computed as in Section 7.2. However, it is important to choose the same set of poles for all the TFT samples (7.5) computed for all the values of $[\boldsymbol{\xi}_r]_{r=1}^K$ and $[\boldsymbol{x}_j]_{j=1}^T$. Hence, the matrices $\widehat{\boldsymbol{A}}$ and $\widehat{\boldsymbol{B}}$ of all the $K \times T$ TFT samples calculated are assumed to be constant, since they are independent from both the time and the random variables considered. Furthermore, the stability of the TFT samples computed is guaranteed by enforcing the stability

of the chosen set of poles [22]. Therefore, we have obtained a TFT model that is parameterized in the stochastic space and the state space:

$$
\begin{cases}
\dot{\widehat{\boldsymbol{x}}}(t) &= \widehat{\boldsymbol{A}}\widehat{\boldsymbol{x}}(t) + \widehat{\boldsymbol{B}}\boldsymbol{u}(t) \\
\widehat{\boldsymbol{y}}(t,\boldsymbol{\xi}) &= \widehat{\boldsymbol{C}}\left(\widehat{\boldsymbol{x}}_j, \boldsymbol{\xi}_r\right)\widehat{\boldsymbol{x}}(t) + \widehat{\boldsymbol{D}}\left(\widehat{\boldsymbol{x}}_j, \boldsymbol{\xi}_r\right)
\end{cases}
\tag{7.11}
$$

for $r = 1, \ldots, K$ and $j = 1, \ldots, T$.

Finally, the desired PC-TFT model (7.9) can be obtained by computing the corresponding PC models of the matrices $\widehat{\boldsymbol{C}}$ and $\widehat{\boldsymbol{D}}$. Once the basis functions are known, as described in Section 2.5, the PC coefficients of the matrices $\widehat{\boldsymbol{C}}$ and $\widehat{\boldsymbol{D}}$ can be found following the linear regression approach [4, 14], which leads to:

$$
\boldsymbol{\Psi}_C\left(\boldsymbol{\xi}_r\right)\boldsymbol{\alpha}_C\left(\widehat{\boldsymbol{x}}_j\right) = \boldsymbol{R}_C\left(\widehat{\boldsymbol{x}}_j, \boldsymbol{\xi}_r\right)
\tag{7.12}
$$

$$
\boldsymbol{\Psi}_D\left(\boldsymbol{\xi}_r\right)\boldsymbol{\alpha}_D\left(\widehat{\boldsymbol{x}}_j\right) = \boldsymbol{R}_D\left(\widehat{\boldsymbol{x}}_j, \boldsymbol{\xi}_r\right)
\tag{7.13}
$$

where the $r-$th row of the matrices $\boldsymbol{\Psi}_C\left(\boldsymbol{\xi}_r\right)$ and $\boldsymbol{\Psi}_D\left(\boldsymbol{\xi}_r\right)$ contains the multivariate polynomial basis functions φ_i for $i = 0, \ldots, M$ evaluated in $\boldsymbol{\xi}_r$ for $r = 1, \ldots, K$ multiplied by the identity matrix of the same dimension as the matrix $\widehat{\boldsymbol{C}}$ and $\widehat{\boldsymbol{D}}$, respectively. The corresponding set of values of the matrix $\widehat{\boldsymbol{C}}\left(\widehat{\boldsymbol{x}}_j, \boldsymbol{\xi}_r\right)$ and $\widehat{\boldsymbol{D}}\left(\widehat{\boldsymbol{x}}_j, \boldsymbol{\xi}_r\right)$ for $r = 1, \ldots, K$ and $j = 1, \ldots, T$ are collected in the matrix $\boldsymbol{R}_C\left(\widehat{\boldsymbol{x}}_j, \boldsymbol{\xi}_r\right)$ and $\boldsymbol{R}_D\left(\widehat{\boldsymbol{x}}_j, \boldsymbol{\xi}_r\right)$, respectively. Finally, $\boldsymbol{\alpha}_C\left(\widehat{\boldsymbol{x}}_j\right)$ contains the desired PC coefficients $\widehat{\boldsymbol{C}}_i\left(\widehat{\boldsymbol{x}}_j\right)$ and $\boldsymbol{\alpha}_D\left(\widehat{\boldsymbol{x}}_j\right)$ the PC coefficients $\widehat{\boldsymbol{D}}_i\left(\widehat{\boldsymbol{x}}_j\right)$ for $i = 0, \ldots, M$ and $j = 1, \ldots, T$. Note that the realization technique used to convert a pole-residue model to a state-space form has an influence on the smoothness of the matrices in (7.12), (7.13) with respect to the design parameters and, therefore, on the accuracy of the final PC model [14]. We use a Wiener realization in our approach.

It is important to notice that the stability of the computed PC-TFT model (7.9) is guaranteed if a stable set of poles is used to obtain the parameterized TFT model (7.11).

Finally, the proposed method is efficient if the number of random variables N is limited, see (7.10), and if the number of state samples T is not too high, since the total number of TFT samples to be calculated is $K \times T$. For example, when considering $N = 15$ random variables with seventh-order polynomial chaos expansion ($P = 7$), the total number of TFT models that must be calculated for each time sample is 341088, according to (7.10).

The entire flowchart of the proposed PC-TFT modeling strategy is summarized in Fig. 7.1.
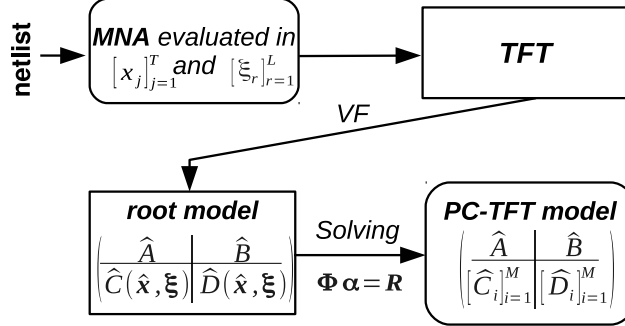
Figure 7.1: Flowchart of the proposed PC-TFT modeling strategy.

7.4 Variability Analysis of Nonlinear Systems Through PC-TFT Modeling

In the following, the efficiency and accuracy of computing the PC model of the system output, starting from the corresponding PC-TFT model (7.9), will be demonstrated. In particular, only the PC coefficients of the system output $\widehat{\boldsymbol{y}}_i$ for $i = 0, \ldots, M$ must be calculated. Indeed, equation (7.9) can be written as a system of $M + 1$ independent equations, thanks to the orthogonality relation (2.47). Projecting (7.9) on the basis function $\varphi_p(\boldsymbol{\xi})$, for $p = 1, \ldots, M$, leads to:

$$\widehat{\boldsymbol{y}}_p(t) = \widehat{\boldsymbol{C}}_p(\widehat{\boldsymbol{x}})\,\widehat{\boldsymbol{x}}(t) + \widehat{\boldsymbol{D}}_p(\widehat{\boldsymbol{x}}) \tag{7.14}$$

Hence, the PC coefficients of the system output can be calculated directly from the corresponding PC-TFT model by solving the following $M + 1$ independent systems of ODEs:

$$\begin{cases} \dot{\widehat{\boldsymbol{x}}}(t) &= \widehat{\boldsymbol{A}}\widehat{\boldsymbol{x}}(t) + \widehat{\boldsymbol{B}}\boldsymbol{u}(t) \\ \widehat{\boldsymbol{y}}_i(t) &= \widehat{\boldsymbol{C}}_i(\widehat{\boldsymbol{x}})\,\widehat{\boldsymbol{x}}(t) + \widehat{\boldsymbol{D}}_i(\widehat{\boldsymbol{x}}) \end{cases} \qquad \text{for } i = 1, \ldots, M; \tag{7.15}$$

using a standard numerical method (e.g. Backward Euler). Note that the computational cost of solving the system of ODEs (7.15) can drastically be reduced by exploiting the parallelism of these calculations. Finally, to further reduce the computational cost of solving equation system (7.15), any numerical method that employs a non-uniform sampling in the time domain can be used in such a way as to minimize the total number T' of time samples needed, while keeping the overall accuracy. Note that the set of time samples $[t_k]_{k=1}^{T'}$ depends only on the numerical method chosen to solve the system of equations (7.15) and is independent from the particular sampling of the state space used in Section 7.3 to build the PC-TFT model.

At this point, a PC model of the system output can be calculated over a discrete set of time samples as:

$$\widehat{\boldsymbol{y}}\left(t_k, \boldsymbol{\xi}\right) = \sum_{i=0}^{M} \widehat{\boldsymbol{y}}_i\left(t_k\right) \varphi_i(\boldsymbol{\xi}) \quad \text{for } k = 1, \ldots, T'; \tag{7.16}$$

The value of the PC model (7.16) can easily be computed for any time sample $t_q \neq t_k$ for $k = 1, \ldots, T'$, with $t_0 < t_k < t_{T'}$ using a numerical interpolation technique [29, 30].

The proposed methodology has several advantages. Thanks to the modeling power of the TFT method, it can be applied to study a broad range of nonlinear systems, including strongly nonlinear ones, and it offers the efficiency and accuracy of the PC expansion to determine the time-domain system variability. For example, stochastic moments like (2.54), (2.55) can be determined analytically. Furthermore, the stability of the calculated PC-TFT model can be guaranteed (see Section 7.3). Finally, the proposed technique offers a good flexibility in modeling complex nonlinear systems. Indeed, a hierarchical approach can be used: complex nonlinear systems can be divided in simpler blocks that can be modeled separately with the proposed technique.

7.5   Numerical Examples

The proposed PC-TFT model is demonstrated by modeling a RF power amplifier (PA) circuit , see Fig. 7.2. The topology of the circuit was proposed in [31] and has been implemented as a netlist description in the $I3T50$ technology for the purpose of validation of the PC-TFT technique. The circuit was stimulated by a 2 GHz RF carrier frequency.

For this PA circuit, the analog input signals are the deterministic inputs to the model. The stochastic variables are selected based upon a sensitivity screening of each stochastic variable occurring in the PA towards the output performance. This procedure yields two dominant stochastic variables ($N = 2$) that need to be included in the model for this technology, namely the variation of the threshold voltages of the input transistors. It is assumed that the stochastic variables have a normal distribution, which can be verified experimentally.

A PC model of the output mapping defined by $\widehat{C}(\cdot), \widehat{D}(\cdot)$ is computed using a fifth-order polynomial chaos expansion ($P = 5$ for accuracy reasons). Hence, the corresponding number of basis functions in the PC-TFT model is $M + 1 = 21$, according to (2.50), which leads to a minimum number of samples in the stochastic space equal to $K \approx 2\left(M + 1\right) = 42$, according to (7.10). A Wiener PC-TFT model was computed using a $7-$by-7 regular grid of the two stochastic variables $\boldsymbol{\xi}$ in a range between $\pm 4\sigma$, so $K = 49$ SPICE simulations are required for each of
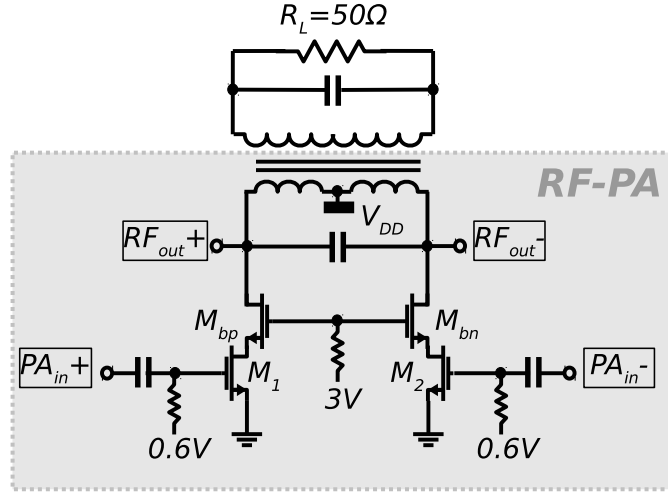
Figure 7.2: Schematic representation of the RF PA circuit.

the reference voltages. All the K initial SPICE simulations are performed for 1000 time samples. From the MNA data, 49 piecewise TFT models are computed. The computation of the 49 TFT models took $778\ s$ including the training simulations. The computation of the PC model of the output mapping $\widehat{C}_i(\cdot), \widehat{D}_i(\cdot)$ in (7.15) took $12\ s$ and the PC model (7.16) of the PA output $\widehat{y}_i$ took $1.7\ s$. All calculations were performed on a 4 GHz dual quad-core CPU with 12 GB RAM.

The time-domain response of the PA in SPICE and of the PC-TFT model are given in Fig. 7.3 for 40001 transient simulations with MC sampling of the process variations that are included in the technology data of the foundry. The models were then simulated in MATLAB and compared with circuit-level SPICE. It can be seen that, despite the output signal is highly dynamic and showing a strong nonlinear behavior, the model and the original circuit are almost indistinguishable. For the sake of clarity, the difference between both sets of waveforms is also plotted. The maximum difference never exceeds $0.2\ V$. The evaluation of the 40001 MC samples took $4088\ s$ in SPICE and only $2.3\ s$ using the PC-TFT technique. Hence, a huge simulation speedup of $1777\ X$ was achieved. Note that the SPICE simulations for the MC analysis are performed using an adaptative time step, for accuracy reasons. Hence, a post-processing step is necessary to be able to perform the variability analysis via the MC method, since the value and the number of time samples used for each MC run can be different with respect to the others. Indeed, the values of the output signal obtained via MC analysis are interpolated over the 1000 time samples used to compute the PC-TFT model. In order to present a fair comparison, the additional cost of the post-processing interpolation phase is not included in the computational time of the MC analysis.
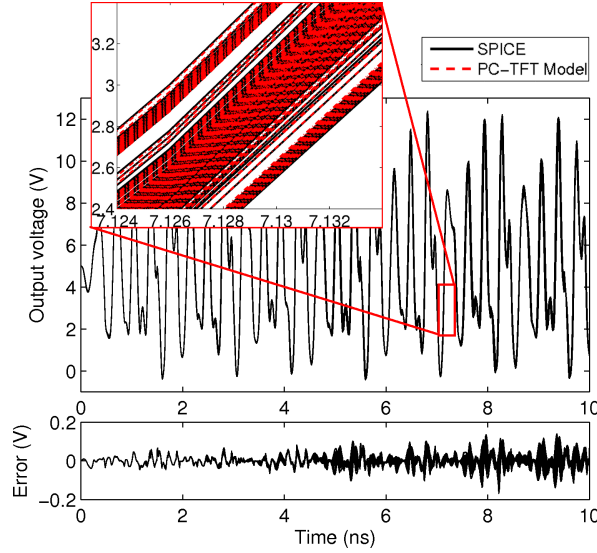
Figure 7.3: Top: time-domain waveforms of the PC circuit modeled with SPICE and the TFT model for 500 MC samples. Bottom: the difference or error between the PC-TFT model and the SPICE simulation.

More importantly, the PC-TFT model provides an analytical expression to compute stochastic moments, such as the mean μ and the variance σ^2 (see equations (2.54) and (2.55)) of the output waveforms. Hence, the mean and the standard deviation of the waveform at each time point can be calculated analytically with the PC-TFT model in $0.06\ s$.

The effectiveness of this approach is now illustrated by comparing the mean μ and the range $\mu \pm \sigma$ of the output of the PA using both the 40001 MC simulations in SPICE and using the corresponding analytical expressions of the PC-TFT model in Fig. 7.4, which has been zoomed in for the sake of visualization. Next, Fig. 7.5 shows the comparison of the standard deviation computed using the 40001 MC simulations in SPICE and using the corresponding analytical expressions of the PC-TFT model. When looking at Figs. 7.4 and 7.5, it is clear that the analytical expression is very accurate without the need for a large set of MC samples; only $K = 49$ grid samples are required for computing the PC-TFT model.

An important parameter to measure the performance of the PA considered is the total harmonic distortion (THD), defined as the ratio of the root mean square (RMS) amplitude of the higher harmonics and the fundamental harmonic when applying a 2 GHz sinusoidal input signal. The cumulative probability plot of the THD of the system is given in Fig. 7.6 for the original SPICE simulation and the PC-TFT model for 40001 MC samples. Both curves are very similar.
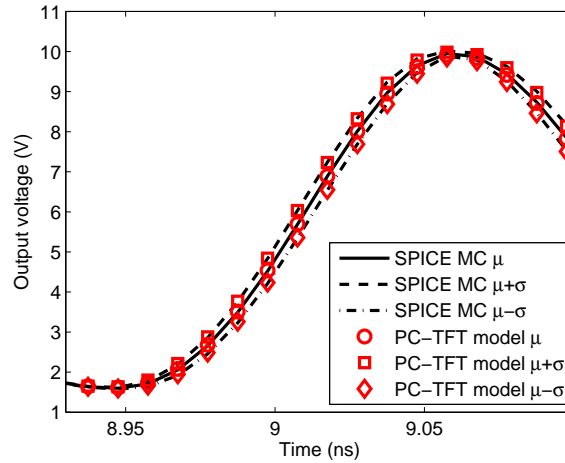
Figure 7.4: The mean μ and the range $\mu \pm \sigma$ of the output voltage of the PA circuit. The black lines are computed using 40001 Monte-Carlo simulations in SPICE. The red lines are computed analytically from the PC-TFT model.

7.6   Conclusions

This chapter has presented a novel technique for the efficient variability analysis of nonlinear systems, such as amplifiers, comparators, digital filters. It is based on the use of the polynomial chaos expansion applied to the TFT description of the system under study. The proposed approach can be applied to study a broad range of nonlinear systems and a hierarchical approach can be used to reduce the modeling complexity. Finally, the method allows to perform the variability analysis with good accuracy and improved efficiency compared to MC analysis. Comparisons with the standard MC approach have been performed for a numerical example, validating the accuracy and efficiency (i.e. a simulation speedup of $1777\,X$) of the proposed method.
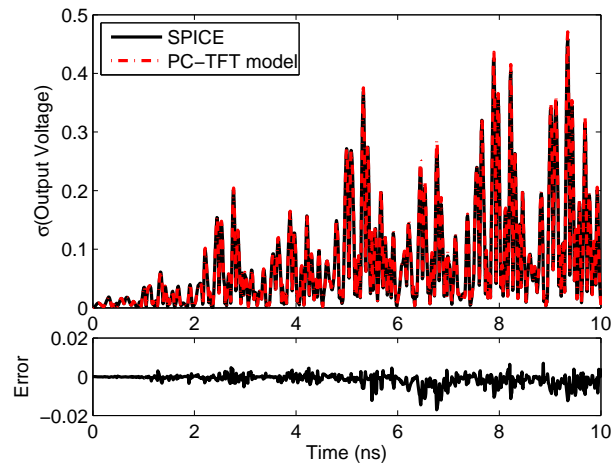
Figure 7.5: Top: standard deviation σ of the output voltage of the PA circuit over the entire time range. The black lines are computed using 40001 *MC simulations in SPICE. The red lines are computed analytically from the PC-TFT model. Bottom: the difference or error between the PC-TFT model and the SPICE simulation.*
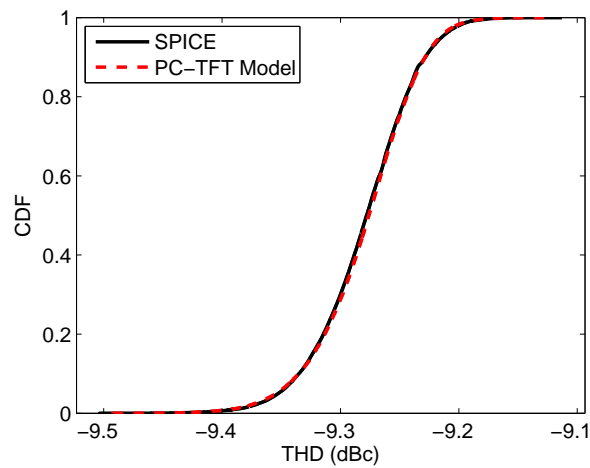

Figure 7.6: CDF of the total harmonic distortion (THD) for 40001 MC samples evaluated with a full SPICE simulation (black) and with the proposed PC-TFT model (red dashed line).

References

[1] Y. Liu and J.-S. Yuan. *CMOS RF Power Amplifier Variability and Reliability Resilient Biasing Design and Analysis.* IEEE Trans. Electron Devices, 58(2):540–546, Feb. 2011.

[2] J. S. Ochoa and A. C. Cangellaris. *Random-Space Dimensionality Reduction for Expedient Yield Estimation of Passive Microwave Structures.* IEEE Trans. Microw. Theory Tech., 61(12):4313–4321, Dec. 2013.

[3] G. Blatman and B. Sudret. *An adaptive algorithm to build up sparse polynomial chaos expansions for stochastic finite element analysis.* Probabilistic Engineering Mechanics, 25(2):183 – 197, Apr. 2010.

[4] M. S. Eldred. *Recent advance in non-intrusive polynomial-chaos and stochastic collocation methods for uncertainty analysis and design.* In Proc. 50th AIAA/ASME/ASCE/AHS/ASC Structures, Structural Dynamics, and Materials Conference, Palm Springs, California, May 2009.

[5] J. A. S. Witteveen and H. Bijl. *Modeling Arbitrary Uncertainties Using Gram-Schmidt Polynomial Chaos.* In Proc. 44th AIAA Aerospace Sciences Meeting and Exhibit, number AIAA-2006-896, Reno, Nevada, Jan. 2006.

[6] A. Papoulis. *Probability, Random Variables and Stochastic Processes.* McGraw-Hill College, 1991.

[7] C. Soize and R. Ghanem. *PHYSICAL SYSTEMS WITH RANDOM UNCERTAINTIES: CHAOS REPRESENTATIONS WITH ARBITRARY PROBABILITY MEASURE.* SIAM J. SCI. COMPUT., 26(2):395–410, Jul. 2004.

[8] D. Xiu and G. E. Karniadakis. *The Wiener-Askey Polynomial Chaos for Stochastic Differential Equations.* SIAM J. Sci. Comput., 24(2):619–644, Apr. 2002.

[9] Q. Su and K. Strunz. *Stochastic Polynomial-Chaos-Based Average Modeling of Power Electronic Systems.* IEEE Trans. Power Electron., 26(4):1167 – 1171, Apr. 2011.

[10] K. Strunz, Q. Su. *Stochastic formulation of SPICE-type electronic circuit simulation using polynomial chaos.* ACM Trans. Model. Comput. Simul., 18(4):501–507, Sep. 2008.

[11] I. S. Stievano, P. Manfredi, F. G. Canavero. *Parameters Variability Effects on Multiconductor Interconnects via Hermite Polynomial Chaos.* IEEE Trans. Compon., Packag., Manuf. Technol., 1(8):1234–1239, Aug. 2011.

[12] I. S. Stievano, P. Manfredi, F. G. Canavero. *Stochastic Analysis of Multi-conductor Cables and Interconnects*. IEEE Trans. Electromagn. Compat., 53(2):501–507, May 2011.

[13] D. Vande Ginste, D. De Zutter, D. Deschrijver, T. Dhaene, P. Manfredi, F. G. Canavero. *Stochastic Modeling Based Variability Analysis of On-Chip Interconnects*. IEEE Trans. Compon., Packag., Manuf. Technol., 2(7):1182 – 1192, Jul. 2012.

[14] D. Spina, F. Ferranti, T. Dhaene, L. Knockaert, G. Antonini, and D. Vande Ginste. *Variability Analysis of Multiport Systems Via Polynomial-Chaos Expansion*. IEEE Trans. Microw. Theory Tech., 60(8):2329 –2338, Aug. 2012.

[15] D. Lucor, C.-H. Su, and G. E. Karniadakis. *Generalized polynomial chaos and random oscillators*. Int. J. Numer. Meth. Engng., 60(3):571–596, May 2004.

[16] A. Monti, F. Ponci, and T. Lovett. *A polynomial chaos theory approach to the control design of a power converter*. In Proc. 35th Annual IEEE Power Electronics Specialists Conference (PESC), volume 6, 20-25 Jun. 2004.

[17] M. R. Rufuie, E. Gad, M. Nakhla, R. Achar. *Generalized Hermite Polynomial Chaos for Variability Analysis of Macromodels Embedded in Nonlinear Circuits*. IEEE Trans. Compon., Packag., Manuf. Technol., 4(4):673–684, Apr. 2014.

[18] D. De Jonghe, G. Gielen. *Efficient Analytical Macromodeling of Large Analog Circuits by Transfer Function Trajectories*. In Proc. IEEE/ACM International Conference on Computer-Aided Design (ICCAD), pages 91–94, 7-10 Nov. 2011.

[19] D. De Jonghe, G. Gielen. *Characterization of Analog Circuits Using Transfer Function Trajectories*. IEEE Trans. Circuits Syst. I: Regular Papers, 59(8):1796–1804, Aug. 2012.

[20] D. De Jonghe, D. Deschrijver, T. Dhaene, G. Gielen. *Extracting analytical nonlinear models from analog circuits by recursive vector fitting of Transfer Function Trajectories*. In Proc. Europe Conference & Exhibition in Design, Automation & Test (DATE), pages 1448–1453, 18-22 Mar. 2013.

[21] B. Gustavsen and A. Semlyen. *Rational approximation of frequency domain responses by Vector Fitting*. IEEE Trans. Power Del., 14(3):1052–1061, Jul. 1999.

[22] D. Deschrijver, M. Mrozowski, T. Dhaene, and D. De Zutter. *Macromodeling of Multiport Systems Using a Fast Implementation of the Vector Fitting Method*. IEEE Microw. Wireless Compon. Lett., 18(6):383–385, Jun. 2008.

[23] T. Dhaene, D. Deschrijver. *Stable Parametric Macromodeling using a Recursive Implementation of the Vector Fitting Algorithm*. IEEE Microw. Wireless Compon. Lett., 19(2):59–61, Feb. 2009.

[24] M. J. Rewieński. *A Trajectory Piecewise-linear Approach to Model-Order Reduction of Nonlinear Dynamical Systems*. PhD thesis, Massachusetts Institute of Technology, 2003.

[25] R. A. Rutenbar, G. G. E. Gielen, J. Roychowdhury. *Hierarchical Modeling, Optimization, and Synthesis for System-Level Analog and RF Designs*. Proceedings of the IEEE, 95(3):640 –669, Mar. 2007.

[26] R. Tóth. *Modeling and identification of linear parameter-varying systems*. Springer, 2010.

[27] A. Odabasioglu, M. Celik, L. T. Pileggi. *PRIMA: passive reduced-order interconnect macromodeling algorithm*. IEEE Trans. Comput.-Aided Design Integr. Circuits Syst., 17(8):645–654, Aug. 1998.

[28] J. R. Phillips, L. M. Silveira. *Poor man's TBR: a simple model reduction scheme*. IEEE Trans. Comput.-Aided Design Integr. Circuits Syst., 24(1):43–55, Jan. 2005.

[29] C. de Boor. *A Practical Guide to Splines*. Springer-Verlag, 1978.

[30] F. N. Fritsch and R. E. Carlson. *Monotone Piecewise Cubic Interpolation*. SIAM J. Numer. Anal., 17(2):238–246, Nov. 1980.

[31] B. Francois, P. Reynaert. *A fully integrated watt-level linear 900-MHz CMOS RF power amplifier for LTE-applications*. IEEE Trans. Microw. Theory Tech., 60(6):1878–1885, Jun. 2012.

8
Conclusions

8.1 General Conclusions

This PhD thesis proposes innovative PC-based or SC-based macromodeling techniques suitable for efficient and accurate variability analysis of modern high-speed ICs. In particular, the variability analysis is performed for two distinct categories of circuits: linear and passive systems and nonlinear (typically active) ones. Linear and passive systems are analyzed in the frequency-domain by computing a stochastic macromodel of their transfer function, that can be expressed by means of different representations e.g. scattering, impedance or admittance parameters, while nonlinear circuits are studied in the time-domain.

In particular, Chapter 2 gives to the reader the basic notions on probability theory as well as an overview of the state-of-the-art techniques for the variability analysis. The need for efficient and accurate macromodeling techniques tailored for the variability analysis is discussed here, since the application of the MC method for complex high-speed ICs is expensive, both in terms of memory and computational time.

In Chapter 3 is described the first data-driven stochastic macromodeling technique developed during my research activity. It is based on the calculation of root macromodels of the system transfer functions and on the PC expansion of the corresponding state-space matrices. It extends to general passive multiport circuits (such as interconnections, filters, connectors, etc.) the application of the PC expansion, previously adopted only for lumped elements and multiconductor

transmission lines.

Chapter 4 presents a comparative study of three different state-of-the-art techniques for the variability analysis of linear and passive multiport systems. In particular, the performances of the PC-based technique described in Chapter 3 are compared with respect to SC-based approaches. The proposed comparison focus on the unique features of electromagnetic system modeling. In this framework, the presented study proposes to build SC-based model via state-of-the art adaptive sampling schemes instead of using sparse sampling in the parameters space. This choice allows to increase the automatization of the model generation procedure, since the sampling of the parameters space is not chosen by the designer. Finally, a new SC-based method is presented that uses novel interpolation schemes based on amplitude and frequency scaling coefficients.

The technique described in Chapter 5 adopts a data-driven macromodeling approach based on a non-intrusive application of the PC expansion. This technique allows to enforce the stability and check the passivity of the calculated PC-based macromodel. Furthermore, the macromodel is obtained through the application of the PC expansion at an input-output level without intermediate state-space models as for the technique presented in Chapter 3, adopting an efficient model-building procedure.

Chapter 6 present a model-driven PC-based stochastic macromodeling approach suitable for the variability analysis of systems described by a large number of equations, such as the ones resulting by means of EM methods. The macromodeling technique presented in this chapter uses a suitable combination of model order reduction and PC techniques, generating a final reduced-order model able to accurately perform stochastic computations and variability analysis.

Next, a stochastic macromodeling technique suitable for the variability analysis of nonlinear systems is presented in Chapter 7. It is based on the combination of the TFT method and of the PC expansion. The proposed technique can be applied to study a broad range of nonlinear systems and offers the possibility of employing a hierarchical approach to reduce the modeling complexity. Finally, the method allows to perform the variability analysis with good accuracy and improved efficiency compared to MC analysis.

Finally, in the Appendix it is presented a technique for the parametric sensitivity analysis of multiconductor transmission lines developed in the early phase of my research.

8.2   Major Research Contributions

The work done in this PhD thesis made the following contributions in the field of efficient and accurate variability analysis of modern ICs:

- Extending to general passive multiport circuits (such as interconnections, filters, connectors, etc.) the application of the PC expansion, previously adopted only for lumped elements and multiconductor transmission lines.

- Introducing the application of adaptive sampling schemes to automatize the generation of SC-based macrodels.

- Developing innovative PC-based and SC-based macromodeling techniques suitable for the variability analysis of complex high-speed ICs. In particular, the techniques described in Chapters 3 - 6 compute stochastic macromodels suitable for the frequency-domain variability analysis of linear and passive multiport systems. The latter techniques are flexible, since they can be applied to a large range of microwave systems (e.g. filters, connectors, non-uniform transmission lines), accurate and efficient with respect to the MC analysis. Finally, the stochastic macromodeling technique described in Chapter 7 performs the time-domain variability analysis of nonlinear systems. The proposed method is accurate and efficient with respect to the MC analysis, it can be applied to study a broad range of nonlinear systems and a hierarchical approach can be used to reduce the modeling complexity.

8.3 Possible Improvements and Future Directions

8.3.1 Variability Analysis for High Number of Parameters

As discussed in Section 2.4 the MC method is accurate and robust, but has a slow convergence rate with respect to the number of simulations performed. However, the convergence rate of the MC method is independent on the number of parameters considered for the variability analysis, see (2.44). Conversely, the efficiency of PC-based and SC-based methods is influenced by the number of random parameters considered. Indeed, the number $M + 1$ of basis functions of any PC model in the form (2.56) increases rapidly with the number of uncertain parameter N, according to (2.50). Therefore, the corresponding number of $M + 1$ unknown PC coefficients that must be estimated is large. Furthermore, modeling through SC approaches (interpolation-based) the transfer function of a complex systems that depends on several parameters requires a large number of nodes, even if a sparse grid sampling strategy is adopted. Hence, the efficiency of PC-based and SC-based stochastic macromodeling strategies with respect to the MC method is greatly reduced for systems that depend on a large numbers of random parameters.

A possible approach to partially overcome this limitation is to reduce the modeling complexity. First, it is possible to screen the "important" random parameters based on their influence on the system response to be modeled adopting sensitivity analysis methods such as Morris method, Sobol method and Fast Amplitude

Screening Test (FAST) [1]. Then, using a hierarchical approach, a complex circuit can be divided in simpler blocks that can be modeled separately.

However, developing efficient PC-based and SC-based techniques for the efficient variability analysis of circuits depending on a large numbers of random parameters is still an open problem.

8.3.2   Variability Analysis for Delayed Systems

The stochastic macromodeling techniques for linear and passive systems presented in this PhD thesis are based on the hypothesis that a rational approximation in the frequency domain (see Chapters 3 - 5) or a quasi-static PEEC formulation (see Chapter 6) can be used to describe the system under study.

However, accurate modeling of electrically long systems requires a carefully consideration of the propagation delay (the time needed by an electromagnetic wave to travel from one port of the system to another one) and, if the system under study is not homogeneous, of multiple reflections that may occur during the wave propagation. Hence, the two modeling approaches described above can not be adopted. Indeed, using the VF algorithm to compute a rational model of electrically long systems

- can require a large number of poles, leading to inefficient simulations of the rational model computed [2];

- gives a nonzero response before the time-of-flight has elapsed. This effect can be the source of serious accuracy degradation in system-level simulations [2].

Furthermore, significant errors and artifacts in the modeling can occur if a quasi-static PEEC model is used to describe electrically long systems [3].

Therefore, a possible future work is to develop efficient and accurate PC-based and SC-based stochastic macromodels for electrically long systems based on modeling approaches that explicitly consider the system delays (i.e. delayed vector fitting algorithm [2]).

8.3.3   Passivity Preserving PC-based Stochastic Macromodeling

In Chapter 4 it is stated that preserving the passivity of PC-based macromodel of generic multiport systems is still an open problem. The main difficulty in preserving the passivity of a PC-based stochastic macromodel lies in the strict criteria that the polynomial basis functions must satisfy. In particular, the basis functions are orthogonal with respect to a weighting function that corresponds to the PDF of the associated random variables, when placed in a standard form [4, 5]. Due

to this property, an exponential convergence rate can be achieved [4] and analytical expressions can be used to represent stochastic moments (see 2.5). Since the choice of the polynomial basis functions depends only on the distribution of the random variables considered, the present state-of-the-art techniques can not guarantee the passivity of the PC-based model of the system transfer function in the entire stochastic space.

Conversely, SC-based method are able to compute a stable and passive macromodel in the entire stochastic space, assuming that the system solutions at the nodes in the stochastic space are stable and passive, since passivity preserving interpolation schemes can be adopted (see Chapter 4).

Recently, the technique [6] proposed an approach to compute stable and passive PC-based macromodel for multiconductor transmission lines. The core idea of the passivity proof given in [6] is based on the consideration that, for the particular case of multiconductor transmission lines with frequency independent per-unit-length parameters, the sufficient condition for the passivity is that the per-unit-length parameters matrices are positive definite. Then, in [6] it is proven that the PC model of a positive definite matrix is still positive definite if the order of the PC expansion considered is sufficiently high. However, extending the approach presented in [6] to generic multiport system is not trivial, since the formulation used in [6] is valid only in the case of multiconductor transmission lines.

References

[1] A. Boukouvalas and D. Cornford. *Screening strategies for high dimensional input spaces*. Technical report, Neural Computing Research Group, Aston University, 2007.

[2] A. Chinea, P. Triverio, S. Grivet-Talocia. *Delay-Based Macromodeling of Long Interconnects From Frequency-Domain Terminal Responses*. IEEE Trans. Adv. Packag., 33(1):246–256, Feb. 2010.

[3] F. Ferranti, M. S. Nakhla, G. Antonini, T. Dhaene, L. Knockaert, A. E. Ruehli. *Multipoint Full-Wave Model Order Reduction for Delayed PEEC Models With Large Delays*. IEEE Trans. Electromagn. Compat., 53(4):959–967, Nov. 2011.

[4] J. A. S. Witteveen and H. Bijl. *Modeling Arbitrary Uncertainties Using Gram-Schmidt Polynomial Chaos*. In Proc. 44th AIAA Aerospace Sciences Meeting and Exhibit, number AIAA-2006-0896, Palm Springs, California, Jan. 2006.

[5] D. Xiu and G. E. Karniadakis. *The Wiener-Askey Polynomial Chaos for Stochastic Differential Equations*. SIAM J. Sci. Comput., 24(2):619–644, Apr. 2002.

[6] P. Manfredi, D. Vande Ginste, D. De Zutter, and F. G. Canavero. *On the Passivity of Polynomial Chaos-Based Augmented Models for Stochastic Circuits*. IEEE Trans. Circuits Syst. I, 60(11):2998–3007, Nov. 2013.

A

Time-Domain Green's Function-Based Parametric Sensitivity Analysis of Multiconductor Transmission Lines

Variability analysis and sensitivity analysis are complementary: the first estimates the effects of the variability of geometrical or electrical parameters on the circuits performances, while the second individuates the parameters which variations have a stronger effect on the circuit performances. This Appendix describes a new parametric macromodeling technique for lossy and dispersive multiconductor transmission lines (MTLs) providing sensitivity information over the entire design space. Parametric macromodels are multivariate models describing the complex behavior of electromagnetic systems with respect to several geometrical (i.e. width or length of conductors) or electrical (i.e. dielectric permettivity) design parameters and the frequency (or time). Parametric macromodels which provide sensitivity information are well suited for design space exploration, design optimization and crosstalk analysis.

$\star\,\star\,\star$

D. Spina, F. Ferranti, G. Antonini, T. Dhaene, L. Knockaert

Abstract We present a new parametric macromodeling technique for lossy and dispersive multiconductor transmission lines. This technique can handle multiple design parameters, such as substrate or geometrical layout features, and provides time-domain sensitivity information for voltages and currents at the ports of the lines. It is derived from the dyadic Green's function of the 1-D wave propagation problem. The rational nature of the Green's function permits the generation of a time-domain macromodel for the computation of transient voltage and current sensitivities with respect to both electrical and physical parameters, completely avoiding similarity transformation and it is suited to generate state-space models and synthesize equivalent circuits, which can be easily embedded into conventional SPICE-like solvers. Parametric macromodels which provide sensitivity information are well suited for design space exploration, design optimization and crosstalk analysis. Two numerical examples validates the proposed approach in both frequency and time domain.

A.1   Introduction

The increasing demand for performance of ICs pushes operation to higher signal bandwidths, while rapid advances in manufacturing capabilities have significantly reduced the feature size and increased the density of these devices. To assist microwave designers, accurate modeling of previously neglected second order effects, such as crosstalk, reflection, delay and coupling, becomes increasingly important during circuit and system simulations. The accurate prediction of these interconnect effects is fundamental for a successful design and involves the solution of large systems of equations which are often prohibitively CPU expensive to solve [1], [2]. Furthermore, microwave designers have to make the proper trade-offs between conflicting design requirements using optimization techniques, to obtain the best possible performance considering physical effects such as reflection, crosstalk and propagation delays. For example, once the fabrication technology is decided, an optimization step is required at the early design stages to select the geometrical and material features of the structure, such as length and width of conductors, dielectric permittivity and metal conductivity, yielding the optimum electrical performance, often under stringent signal integrity and electromagnetic compatibility constraints. To perform these design activities using full electromagnetic simulations on the entire parameter space is often computationally expensive, therefore parametric macromodeling techniques that take into account design parameters in addition to frequency (or time) are needed [3], [4].

Recently, a spectral approach has been presented for the analysis of lossy and dispersive MTLs [5] and in [6] it is extended to provide a closed-form sensitivity analysis for MTLs in the frequency-domain. It is based on the computation of the closed-form dyadic Green's function of the 1-D wave propagation problem. The

major advantage of such an approach over existing techniques [7], [8] is the rational nature of the dyadic Green's function which is appropriate for time-domain macromodeling and is suitable to generate a finite state-space representation and an equivalent SPICE circuit by using standard realization [9] and circuit synthesis techniques [10]. In [3], [4] a parametric macromodeling technique for lossy and dispersive MTLs is proposed, based on the spectral approach [5]. It provides time-domain information for voltage and current at the ports of the lines, starting from the knowledge of the MTL per-unit-length (p.u.l.) parameters. In the present Appendix, the cited method is modified to perform the parametric sensitivity analysis of MTLs with respect to either geometric or physical parameters directly in the time-domain, leading to a macromodel that can be used with both linear and non linear terminations.

This Appendix is structured as follows. First, an overview of the spectral approach is given in Sections A.2. The parametric macromodeling strategy in the frequency-domain is shown in Section A.3, while the time-domain parametric sensitivity analysis is described in Section A.4. Finally, two numerical examples are presented in Section A.5, validating the proposed technique. Conclusions are summed up in Section A.6.

A.2   Spectral Modeling of MTLs

Consider a MTL of length d, with $N + 1$ conductors and $N \times N$ p.u.l. impedance matrix $\boldsymbol{Z}_{pul}(s, \boldsymbol{g})$ and $N \times N$ p.u.l. admittance matrix $\boldsymbol{Y}_{pul}(s, \boldsymbol{g})$ [11]. Assuming the quasi-transverse electromagnetic (TEM) hypothesis, the propagation of voltages and currents along the line is described by the Telegrapher's equations [11]. Using the dyadic Green's function method proposed in [5], the voltage along the uniform MTL with length d can be evaluated as

$$\begin{aligned}
\boldsymbol{V}(z, s, \boldsymbol{g}) = {} & \boldsymbol{G}(z, 0, s, \boldsymbol{g}) \left(-\boldsymbol{Z}_{pul}(s, \boldsymbol{g}) \boldsymbol{I}(0, s, \boldsymbol{g}) \right) \\
& + \boldsymbol{G}(z, d, s, \boldsymbol{g}) \left(-\boldsymbol{Z}_{pul}(s, \boldsymbol{g}) \boldsymbol{I}(d, s, \boldsymbol{g}) \right)
\end{aligned} \tag{A.1}$$

where s is the Laplace variable, $\boldsymbol{g}$ is a vector containing all the geometric or physical parameters of the MTL, while $\boldsymbol{I}(0, s, \boldsymbol{g})$ and $\boldsymbol{I}(d, s, \boldsymbol{g})$ are N-vectors containing the MTL port currents at the input and output ports, respectively. The $N \times N$ dyadic Green's function $\boldsymbol{G}(z, z', s, \boldsymbol{g})$ for uniform MTLs is written in a spectral

form as

$$G\left(z, z', s, \boldsymbol{g}\right) = -\sum_{n=0}^{\infty} \boldsymbol{\Psi}_n(s, \boldsymbol{g})^{-1} \varphi_n(z) \varphi_n(z') \qquad \text{(A.2a)}$$

$$\boldsymbol{\Psi}_n(s, \boldsymbol{g}) = \boldsymbol{\gamma}^2(s, \boldsymbol{g}) + \left(\frac{n\pi}{d}\right)^2 \boldsymbol{U} \qquad \text{(A.2b)}$$

$$\boldsymbol{\gamma}^2(s, \boldsymbol{g}) = \boldsymbol{Z}_{pul}(s, \boldsymbol{g}) \boldsymbol{Y}_{pul}(s, \boldsymbol{g}) \qquad \text{(A.2c)}$$

$$\varphi_n(z) = A_n \cos\left(\frac{n\pi z}{d}\right) \qquad \text{(A.2d)}$$

$$A_n = \sqrt{\frac{1}{d}} \text{ if } n = 0; \quad \sqrt{\frac{2}{d}} \text{ otherwise} \qquad \text{(A.2e)}$$

where $\boldsymbol{U}$ is the $N \times N$ identity matrix. Using (A.1) to calculate the voltage at the MTL ports allows to write

$$\boldsymbol{V}(s, \boldsymbol{g}) = \boldsymbol{Z}(s, \boldsymbol{g}) \boldsymbol{I}(s, \boldsymbol{g}) \qquad \text{(A.3)}$$

where $\boldsymbol{V}(s, \boldsymbol{g})$ and $\boldsymbol{I}(s, \boldsymbol{g})$ are the $2N$-vectors of the voltage and the current at the MTL ports, respectively, and the $2N \times 2N$ impedance matrix $\boldsymbol{Z}(s, \boldsymbol{g})$ can be expressed with respect to the Green's function [5] as

$$\boldsymbol{Z}(s, \boldsymbol{g}) = \sum_{n=0}^{\infty} \boldsymbol{\Psi}_n(s, \boldsymbol{g})^{-1} A_n^2 \boldsymbol{Z}_{pul}(s, \boldsymbol{g}) \boldsymbol{U}_n \qquad \text{(A.4)}$$

The symbol $\boldsymbol{U}_n$ represents the $2N \times 2N$ matrix

$$\boldsymbol{U}_n = \left[\begin{array}{cc} \boldsymbol{U} & (-1)^n \boldsymbol{U} \\ (-1)^n \boldsymbol{U} & \boldsymbol{U} \end{array} \right]$$

Referring to [5], each term of the infinite summation (A.4) is called modal impedance and is represented by the symbol $\boldsymbol{Z}_n(s, \boldsymbol{g})$. The series form of the dyadic Green's function is very general; it only assumes that the multiconductor transmission line supports the quasi-TEM mode and is uniform along the z-axis. No hypothesis has been done regarding the nature of the p.u.l. impedance $\boldsymbol{Z}_{pul}(s, \boldsymbol{g})$ and admittance $\boldsymbol{Y}_{pul}(s, \boldsymbol{g})$ matrices and, as a consequence, on the propagation constant $\boldsymbol{\gamma}^2(s, \boldsymbol{g})$. This means that skin-effect, slow-wave effect and dielectric polarization losses can be easily modeled and incorporated in transient analysis once the frequency-dependent p.u.l. parameters are available [5].

Equation (A.3) leads to an analytical expression for the voltage sensitivity with respect to the parameters $\boldsymbol{g}$ at the MTL ports

$$\widehat{\boldsymbol{V}}(s, \boldsymbol{g}) = \widehat{\boldsymbol{Z}}(s, \boldsymbol{g}) \boldsymbol{I}(s, \boldsymbol{g}) + \boldsymbol{Z}(s, \boldsymbol{g}) \widehat{\boldsymbol{I}}(s, \boldsymbol{g}) \qquad \text{(A.5)}$$

The matrix $\widehat{\boldsymbol{Z}}(s,g)$ can be written as [6]

$$
\begin{aligned}
\widehat{\boldsymbol{Z}}(s,\boldsymbol{g}) = & \sum_{n=0}^{\infty} \left(-\boldsymbol{\Psi}_n(s,\boldsymbol{g})^{-1}\right) A_n^2 \widehat{\boldsymbol{\gamma}^2}(s,\boldsymbol{g}) \boldsymbol{\Psi}_n(s,\boldsymbol{g})^{-1} \boldsymbol{Z}_{pul}(s,\boldsymbol{g}) \boldsymbol{U}_n \\
& + \sum_{n=0}^{\infty} \boldsymbol{\Psi}_n(s,g)^{-1} A_n^2 \widehat{\boldsymbol{Z}}_{pul}(s,\boldsymbol{g}) \boldsymbol{U}_n
\end{aligned}
\tag{A.6}
$$

where the propagation constant sensitivity with respect to $\boldsymbol{g}$ is

$$
\widehat{\boldsymbol{\gamma}^2}(s,\boldsymbol{g}) = \widehat{\boldsymbol{Z}}_{pul}(s,\boldsymbol{g}) \boldsymbol{Y}_{pul}(s,\boldsymbol{g}) + \boldsymbol{Z}_{pul}(s,\boldsymbol{g}) \widehat{\boldsymbol{Y}}_{pul}(s,\boldsymbol{g})
\tag{A.7}
$$

Each term of the infinite summation (A.6) can be represented with the symbol $\widehat{\boldsymbol{Z}}_n(s,\boldsymbol{g})$ since it is the sensitivity with respect to $\boldsymbol{g}$ of the corresponding modal impedance $\boldsymbol{Z}_n(s,\boldsymbol{g})$ [6].

Note that only the matrices $\boldsymbol{Z}_{pul}(s,\boldsymbol{g})$, $\boldsymbol{Y}_{pul}(s,\boldsymbol{g})$ and the corresponding derivatives with respect to parameters $\boldsymbol{g}$ (i.e., the $\widehat{\boldsymbol{Z}}_{pul}(s,\boldsymbol{g})$ and $\widehat{\boldsymbol{Y}}_{pul}(s,\boldsymbol{g})$ matrices) are required to obtain $\widehat{\boldsymbol{Z}}(s,\boldsymbol{g})$ from (A.6). While the p.u.l. parameters can be evaluated through direct measurements [12] on the MTL or using full-wave electromagnetic simulators, information on their derivatives are not *a priori* known. A key aspect of the proposed technique is to find a good approximation for the $\widehat{\boldsymbol{Z}}_{pul}(s,\boldsymbol{g})$ and $\widehat{\boldsymbol{Y}}_{pul}(s,\boldsymbol{g})$ matrices in the entire design space.

Note that relations (A.4) and (A.6) give a closed form expression for the $\boldsymbol{Z}(s,\boldsymbol{g})$ and $\widehat{\boldsymbol{Z}}(s,\boldsymbol{g})$ matrix, respectively, with respect to the p.u.l. parameters $\boldsymbol{Z}_{pul}(s,\boldsymbol{g})$ and $\boldsymbol{Y}_{pul}(s,\boldsymbol{g})$ and the corresponding sensitivity $\widehat{\boldsymbol{Z}}_{pul}(s,\boldsymbol{g})$ and $\widehat{\boldsymbol{Y}}_{pul}(s,\boldsymbol{g})$, but both expressions require to perform an infinite summation. However, only a finite number of modes is needed to model the impedance matrix and its sensitivity accurately over the frequency bandwidth of interest, as shown in [3]- [6]. Hence a mode-selection criterion must be used to calculate (A.4) and (A.6) for all the values of $\boldsymbol{g}$ in the design space.

A.3 Parametric macromodeling of MTLs

In this section, it is shown that the spectral decomposition [5], [6] allows to calculate a rational model of $\boldsymbol{Z}(s,\boldsymbol{g})$ and $\widehat{\boldsymbol{Z}}(s,\boldsymbol{g})$ for all the values of $\boldsymbol{g}$ in the design space.

To attain this goal, we start from the p.u.l. impedance and admittance matrices evaluated for a discrete set of values of the parameters $\boldsymbol{g}$ in the design space. The p.u.l. impedance and admittance are usually smooth functions with respect to frequency and physical or geometrical parameters and the corresponding matrices are symmetric, thus the initial data for the p.u.l. impedance and admittance matrices can be easily numerically interpolated leading to accurate estimation of

$Z_{pul}(s, g)$ and $Y_{pul}(s, g)$ in the entire design space with very small computational cost. The use of continuously differentiable interpolation schemes allows to obtain also the $\widehat{Z}_{pul}(s, g)$ and $\widehat{Y}_{pul}(s, g)$ matrices in the entire design space with respect to physical or geometrical parameters g of the interpolating function. Therefore, we have computed parametric macromodels of the p.u.l. parameters and corresponding sensitivities with respect to (s, g).

Next, we switch from multivariate models to univariate models fixing the value of the parameters: $g = \overline{g}$. Then, the matrices $Z(s, \overline{g})$ and $\widehat{Z}(s, \overline{g})$ can be calculated using the spectral decomposition (A.4) and (A.6), once the infinite summation of modes is truncated. Algorithm 2 describes the proposed adaptive criterion to choose the required number of modes M for the different values of the geometrical or physical parameters, indicating with $\overline{g}$ a fixed set of parameters g and with $\widehat{Z}_n(s, \overline{g})$ the corresponding sensitivity modal impedance. The adopted solution is shown only for the $\widehat{Z}(s, \overline{g})$ matrix, since a similar procedure for the impedance matrix $Z(s, \overline{g})$ is applied.

Input: $Z_{pul}(s, \overline{g})$, $Y_{pul}(s, \overline{g})$, $\widehat{Z}_{pul}(s, \overline{g})$, $\widehat{Y}_{pul}(s, \overline{g})$
Output: Number of modes M, $\widehat{Z}_M(s, \overline{g})$
$\widehat{Z}_M(s, \overline{g}) = \widehat{Z}_{prev}(s, \overline{g}) = 0$;

$n = 0$;
$M = M_{init}$;
$error = error_{chosen}$;
$rms\_error = \infty$

if $rms\_error > error$ **then**
   | **while** $n < M$ **do**
   | | $\widehat{Z}_M(s, \overline{g}) = \widehat{Z}_M(s, \overline{g}) + \widehat{Z}_n(s, \overline{g})$;
   | | $n = n + 1$;
   | **end**
   | $rms\_error = rms\_error(\widehat{Z}_M(s, \overline{g}), \widehat{Z}_{prev}(s, \overline{g}))$;
   | $M = M_{init} + M$;
   | $\widehat{Z}_{prev}(s, \overline{g}) = \widehat{Z}_M(s, \overline{g})$;
end

algorithm 2: Adaptive mode selection strategy.

The desired stable rational models for $Z(s, \overline{g})$ and $\widehat{Z}(s, \overline{g})$ are now obtained using the VF algorithm [13], [14]. Finally, the passivity of the model for the impedance matrix can be checked and enforced in a post-processing step by means of standard techniques [15], [16]. To perform design activities that need multiple simulations (e.g. design space exploration, optimization, sensitivity analysis), for

each value $\overline{g}$ of interest the parametric macromodels of the p.u.l. parameters are evaluated and the related rational macromodels of $\boldsymbol{Z}(s, \overline{g})$ and $\widehat{\boldsymbol{Z}}(s, \overline{g})$ are computed. The proposed parametric macromodeling strategy is summarized in Fig. A.1.

Note that the desired rational model for the impedance matrix could be calculated as explained in [5]. The combination of a rational model for the p.u.l. parameters with the Green's function, used to expand the solution of the Sturm-Liouville problem, allows to compute poles and residues of the impedance matrix independently for each mode, reducing the complexity of the system identification significantly. In fact, the technique described in [3], [4] first builds parametric macromodels for the p.u.l. parameters or for the modal impedance, using the Multivariate Orthonormal Vector Fitting Technique (MOVF) [17], then it combines the initial macromodels according to (A.4) to obtain the desired macromodel for the impedance matrix $\boldsymbol{Z}(s, \boldsymbol{g})$ in the entire design space. Our goal, however, it is to build a parametric macromodel also for the $\widehat{\boldsymbol{Z}}(s, \boldsymbol{g})$ matrix, to be able to perform a parametric sensitivity analysis. Using the same approach as described above for the spectral decomposition of $\widehat{\boldsymbol{Z}}(s, \boldsymbol{g})$ may be inefficient. It is easy to see that computing each mode of (A.6) is more expensive than computing a mode of (A.4). If, for each value of interest of $\boldsymbol{g}$, a large number of modes is needed to compute $\widehat{\boldsymbol{Z}}(s, \boldsymbol{g})$ in the frequency band of interest, the corresponding rational model would have a high order of poles if (A.6) is calculated starting from a rational model for the p.u.l. parameters and the corresponding sensitivities. In the proposed approach, the number of poles needed for the rational model of the matrix $\widehat{\boldsymbol{Z}}(s, \boldsymbol{g})$ depends only on its frequency behavior, leading to an efficient calculation of the spectral decomposition (A.6).

Note that the $\widehat{\boldsymbol{Z}}(s, \boldsymbol{g})$ can also be evaluated with perturbation-based techniques, since the computation of the $\boldsymbol{Z}(s, \boldsymbol{g})$ matrix can be efficiently performed using the exact transmission line theory. In both approaches an approximation is introduced in the sensitivity computation, but the p.u.l. parameters $\boldsymbol{Z}_{pul}(s, \boldsymbol{g})$ and $\boldsymbol{Y}_{pul}(s, \boldsymbol{g})$ are smoother functions with respect to physical or geometrical parameters than the MTL impedance $\boldsymbol{Z}(s, \boldsymbol{g})$, affecting the accuracy of the numerical approximation. Furthermore, the proposed macromodeling technique uses the spectral decomposition (A.6) to express the sensitivity of the MTL impedance matrix in a closed form, using a numerical approximation only for the calculation of matrices $\widehat{\boldsymbol{Z}}(s, \boldsymbol{g})$ and $\widehat{\boldsymbol{Y}}(s, \boldsymbol{g})$, while sensitivity perturbation-based techniques are prone to inaccuracies depending on the magnitude of the perturbation [18].

A.4   Time-domain parametric sensitivity analysis

The proposed technique represents both $\boldsymbol{Z}(s, \boldsymbol{g})$ and $\widehat{\boldsymbol{Z}}(\boldsymbol{s}, \boldsymbol{g})$ with a rational model for each desired value of $\boldsymbol{g}$ in the design space. The generation of the time-domain
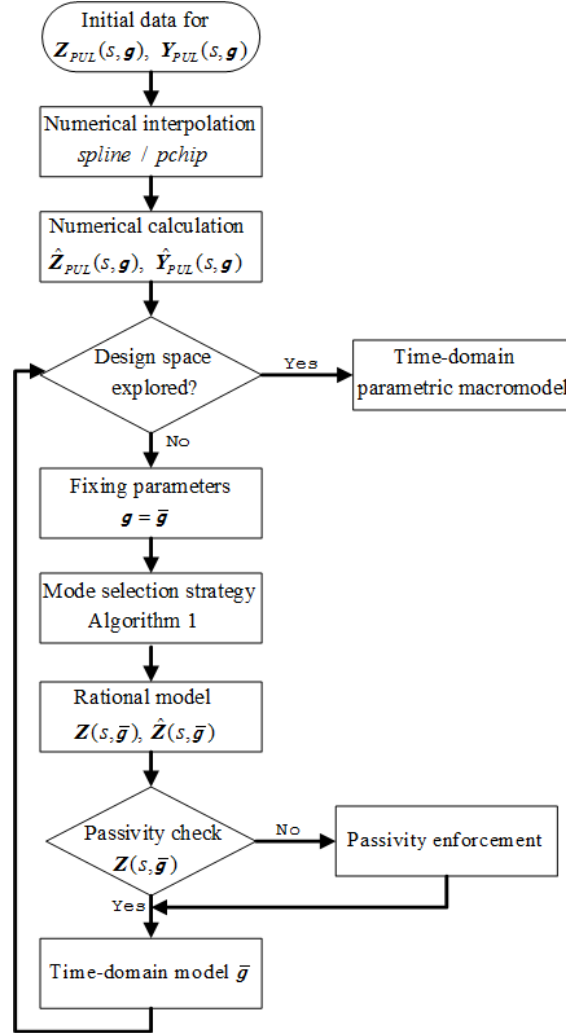
Figure A.1: Description of the parametric macromodeling strategy.

state-space equations in the Jordan form [18], [19] is straightforward. In fact, based on (A.3), it is easy to calculate the time-domain model for the voltage at the MTL ports

$$\dot{\boldsymbol{x}}(t) = \boldsymbol{A}_Z \, \boldsymbol{x}(t) + \boldsymbol{B}_Z \, \boldsymbol{i}(t) \qquad \text{(A.8a)}$$

$$\boldsymbol{v}(t) = \boldsymbol{C}_Z \, \boldsymbol{x}(t) + \boldsymbol{D}_Z \, \boldsymbol{i}(t) \qquad \text{(A.8b)}$$

Hence, based on equation (A.5), the voltage sensitivity can be represented by two different sets of state-space equations

$$\dot{\boldsymbol{x}}_1(t) = \boldsymbol{A}_{\widehat{Z}}\,\boldsymbol{x}_1(t) + \boldsymbol{B}_{\widehat{Z}}\,\boldsymbol{i}(t) \tag{A.9a}$$

$$\widehat{\boldsymbol{v}}_1(t) = \boldsymbol{C}_{\widehat{Z}}\,\boldsymbol{x}_1(t) + \boldsymbol{D}_{\widehat{Z}}\,\boldsymbol{i}(t) \tag{A.9b}$$

$$\dot{\boldsymbol{x}}_2(t) = \boldsymbol{A}_Z\,\boldsymbol{x}_2(t) + \boldsymbol{B}_Z\,\widehat{\boldsymbol{i}}(t) \tag{A.10a}$$

$$\widehat{\boldsymbol{v}}_2(t) = \boldsymbol{C}_Z\,\boldsymbol{x}_2(t) + \boldsymbol{D}_Z\,\widehat{\boldsymbol{i}}(t) \tag{A.10b}$$

where $\boldsymbol{x}(t)$, $\boldsymbol{x}_1(t)$ and $\boldsymbol{x}_2(t)$ are state-space variables, while $\boldsymbol{i}(t) = [\boldsymbol{i}_0(t)\ \ \boldsymbol{i}_d(t)]^T$ and $\widehat{\boldsymbol{i}}(t) = [\widehat{\boldsymbol{i}}_0(t)\ \ \widehat{\boldsymbol{i}}_d(t)]^T$ are the inputs [18]. Line terminations are assumed to be modeled by current sources $\boldsymbol{i}_S(t)$ and voltage-driven lumped linear and nonlinear elements that can be described by the following equation

$$\boldsymbol{i}(t) = \boldsymbol{i}_S(t) - \boldsymbol{G}\boldsymbol{v}(t) - \boldsymbol{C}\frac{d\boldsymbol{v}(t)}{dt} - \boldsymbol{f}(\boldsymbol{v}(t)) \tag{A.11}$$

where $\boldsymbol{v}(t)$ and $\boldsymbol{i}(t)$ are the port voltages and currents, matrices $\boldsymbol{G}$ and $\boldsymbol{C}$ describe linear resistive and capacitive lumped elements respectively, and $\boldsymbol{f}(\boldsymbol{v}(t))$ describes lumped nonlinear components. Calculating the derivative of (A.11) with respect to the parameters $\boldsymbol{g}$, it is possible to obtain the expression of sensitivity of the terminations

$$\widehat{\boldsymbol{i}}(t) = -\boldsymbol{G}\widehat{\boldsymbol{v}}(t) - \boldsymbol{C}\frac{d\widehat{\boldsymbol{v}}(t)}{dt} - \frac{d\boldsymbol{f}(\boldsymbol{v}(t))}{d\boldsymbol{v}(t)}\widehat{\boldsymbol{v}}(t) \tag{A.12}$$

More complex termination networks can be incorporated by using the MNA [20]. The port voltage sensitivity can be finally expressed as

$$\widehat{\boldsymbol{v}}(t) = \widehat{\boldsymbol{v}}_1(t) + \widehat{\boldsymbol{v}}_2(t) \tag{A.13}$$

Once the port currents are evaluated [18] by solving (A.8) and (A.11), state variables $\boldsymbol{x}_1$, $\boldsymbol{x}_2$ and current sensitivity are obtained through (A.9), (A.10), (A.11), (A.12) and (A.13). The port voltage sensitivities are finally recovered using (A.13).

The proposed macromodeling technique describes an uniform MTL with state-space representation in the time-domain as function of a set of physical or geometrical parameters $\boldsymbol{g}$. The macromodel gives accurate sensitivity information at the ports of the lines with respect to $\boldsymbol{g}$ and allows to include non-linear terminations during the time-domain analysis. A multistep procedure is used to calculate the state-space model for each value of the physical or geometrical parameters in the design space, see Fig. A.1, making it suitable to be used in an optimization process. Equations (A.8)–(A.13) must be solved separately for each time-domain model calculated for particular combination $\overline{\boldsymbol{g}}$ of the geometrical or physical parameters, making the proposed technique efficient if the number of parameters taken into account is limited.

A.5 Numerical Examples

In this section the presented technique is applied to different uniform MTLs. In each example the $\widehat{Z}_{pul}$ and $\widehat{Y}_{pul}$ matrices are interpolated by two polynomial techniques: *spline* and *pchip* [21], [22]. *pchip* finds values of an underlying interpolant function $P(x) \in C^1$ at intermediate points under the constraint that in each subinterval $P(x)$ is the cubic Hermite interpolant, thereby preserving shape and monotonicity of the data. *spline* returns the polynomial form of the cubic spline interpolant $S(x) \in C^2$ calculated at the data points, resulting in a not necessarily monotonic interpolation. To describe the accuracy of the parametric macromodeling strategy in the frequency-domain, for each example the maximum value of the Frobenius norm of the relative error, indicated with $RMS_{weighted}$, between the two $\widehat{Z}(s, \boldsymbol{g})$ macromodels over the validation grid and the $RMS_{weighted}$ error between the macromodel of the $\boldsymbol{Z}(s, \boldsymbol{g})$ matrix and its computation from the exact transmission line theory (TLT) will be shown. To validate the proposed method, port voltages and currents are calculated using the classic transmission line theory (TLT-IFFT) in the case of linear terminations and by means of a solver for ordinary differential equations (TLT-NLS) in the case of nonlinear terminations. The corresponding sensitivities are obtained using the perturbative approach. These signals are compared with the ones of the MTL time-domain macromodel obtained with the newly proposed method, where both the polynomial techniques *spline* and *pchip* are used to build the macromodel.

A.5.1 Three-conductors transmission line with nonlinear terminations

In the first example, two coplanar microstrips over a ground plane (length $d = 10\,cm$) with frequency-dependent p.u.l. parameters have been modeled within the frequency range $[100\,kHz - 10\,GHz]$, see Fig. A.2.
The conductors have width $w = 100\,\mu m$ and thickness $t = 50\,\mu m$. The spacing S between the microstrips varies over the design range $[100 - 500]\,\mu m$. The dielec-
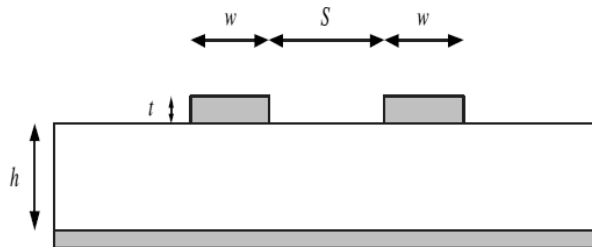

Figure A.2: Example A.5.1. Cross section of the two coupled microstrip.

Macromodel	$RMS_{weighted}$
$\boldsymbol{Z}(s, \boldsymbol{g})$ *spline*	0.0021
$\boldsymbol{Z}(s, \boldsymbol{g})$ *pchip*	0.0021
$\widehat{\boldsymbol{Z}}(s, \boldsymbol{g})$	0.0644

Table A.1: Example A.5.1. Maximum Parametric Macromodeling Error.

tric is $300 \ \mu m$ thick and it is characterized by a dispersive and lossy permittivity which has been modeled by the wideband Debye model [23]. The frequency-dependent p.u.l. parameters are evaluated using a commercial tool [24] over a reference grid of 250×20 samples, for frequency and spacing respectively, and the validation is performed over a grid of 10 spacing samples that have not been used for the generation of the macromodel. The accuracy of the parametric macro-modeling strategy is good, as can be assessed in the frequency-domain from Table A.1.

The time-domain simulations are performed with the following settings: one line is excited by a voltage pulse with amplitude $1 \ V$, rise/fall times $900 \ ps$, width $2 \ ns$, initial delay $7 \ ns$ and internal resistance $R_S = 50 \ \Omega$. The driven line is terminated on a direct biased diode. The current of the diode is given by

$$i_D(t) = I_0 \left(e^{\frac{v(t)}{V_T}} - 1 \right) \tag{A.14}$$

where $I_0 = 10 \ nA$ and $V_T = 25 \ mV$. The victim line is terminated on the near-end by $R_{NE} = 50 \ \Omega$ and on the far-end by a direct biased diode, described by (A.14). Figs. A.3 and A.4 show the accuracy of the proposed technique in the time-domain using the pchip interpolation. Similar results are obtained for the macromodel built using *spline*.

A.5.2 Coupled inverted embedded microstrip lines with frequency-dependent p.u.l. parameters and linear terminations

In this next example a three conductors transmission line (length $d = 1 \ mm$) with frequency-dependent p.u.l. parameters has been modeled within the frequency range $[0 - 200] \ GHz$, see Fig. A.5. The two inverted microstrips are embedded in a layered background medium, consisting of a doped Silicon substrate with
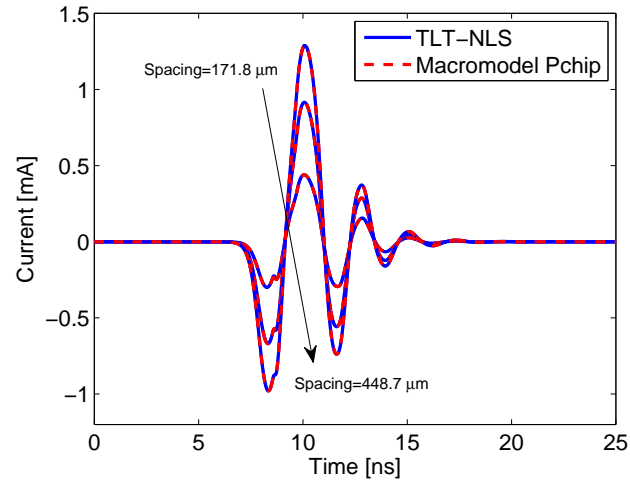
Figure A.3: Example A.5.1. Current at the input port of the victim line for
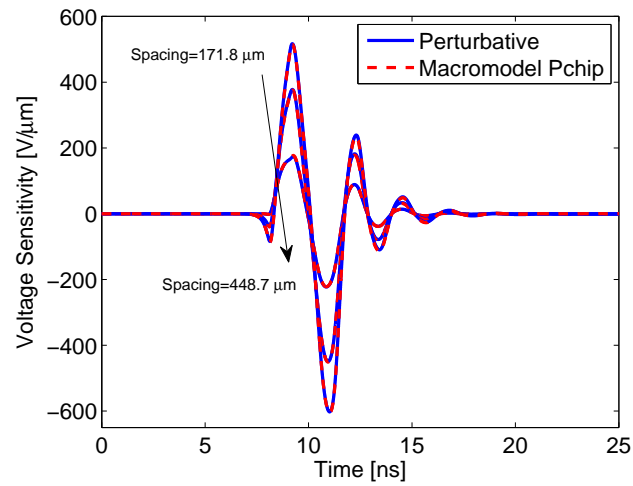$S = [171.8, \ 253.8, \ 448.7] \ \mu m.$

Figure A.4: Example A.5.1. Voltage sensitivity at the output port of the victim line for
$S = [171.8, \ 253.8, \ 448.7] \ \mu m.$

Macromodel	$RMS_{weighted}$ Spline	$RMS_{weighted}$ Pchip
$\boldsymbol{Z}(s, \boldsymbol{g})$	0.0053	0.0033
Macromodel	$RMS_{weighted}$ Spacing	$RMS_{weighted}$ Height
$\widehat{\boldsymbol{Z}}(s, \boldsymbol{g})$	0.0484	0.0059

Table A.2: Example A.5.2. Maximum Parametric Macromodeling Error.

thickness 30 μm, relative permittivity $\epsilon_r = 11.7$, conductivity $\sigma = 10 \ S/m$, and an insulator, being 11.4 μm thick SiO_2 with relative permittivity $\epsilon_r = 3.9$ and loss tangent $tan\delta = 0.001$ [25]. On the top of insulator the Aluminum ground plate of thickness 3 μm is found. The Aluminum has a conductivity of $3.77 \cdot 10^7 \ S/m$. The conductors, placed at a distance of 6.4 μm above the semiconductor, are also made of Aluminum and have width 2 μm; the spacing $S \in [1 - 6] \ \mu m$ and the height $H \in [1 - 3] \ \mu m$ of the conductors are considered design parameters in addition to frequency. The frequency-dependent p.u.l. parameters are evaluated using the technique presented in [26], [27] over a reference grid of $101 \times 11 \times 11$ samples, for frequency, spacing and height respectively. The validation is performed over a grid of 10×10 samples for spacing and height, that have not been used for the generation of the macromodel. Table A.2 shows the accuracy of the proposed technique in the frequency-domain.

One line is excited by a voltage pulse with amplitude 1 V, rise/fall times 30 ps, width 90 ps, initial delay 100 ps and internal resistance $R_S = 1 \ \Omega$. The driven line is terminated on a parallel RC load $R_L = 10 \ k\Omega$, $C_L = 1 \ pF$. The victim line is terminated on the near-end by $R_{NE} = 1 \ \Omega$ and on the far-end by a parallel RC load $R_{FE} = 10 \ k\Omega$ and $C_{FE} = 1 \ pF$. Figs. A.6 – A.8 demonstrate the high accuracy in the time-domain of the proposed method using the spline interpolation for this on-chip example that exhibits a highly dynamic behavior. Similar results are obtained for the macromodel built using *pchip*.

A.6   Conclusions

In this Appendix, an innovative parametric macromodeling approach for lossy and dispersive MTLs is presented. The dyadic Green's function of the 1-D wave propagation problem is used to compute a spectral decomposition for the voltage sensitivity and this leads to a time-domain macromodel in state-space form. Using standard realization techniques, this macromodel can be easily embedded into
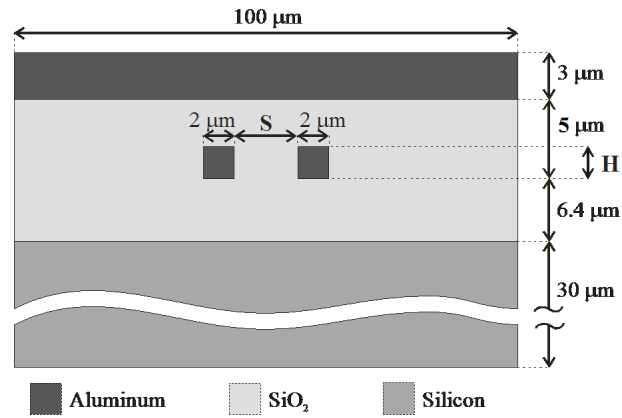
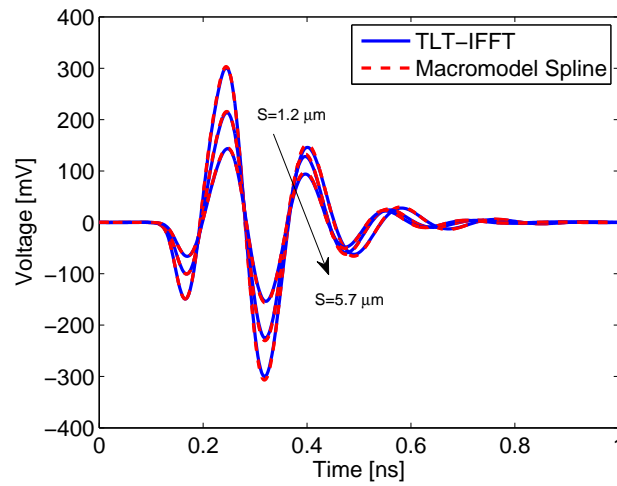*Figure A.5: Example A.5.2. Cross section of the two inverted coupled microstrip.*

Figure A.6: Example A.5.2. Voltage at the output port of the victim line for
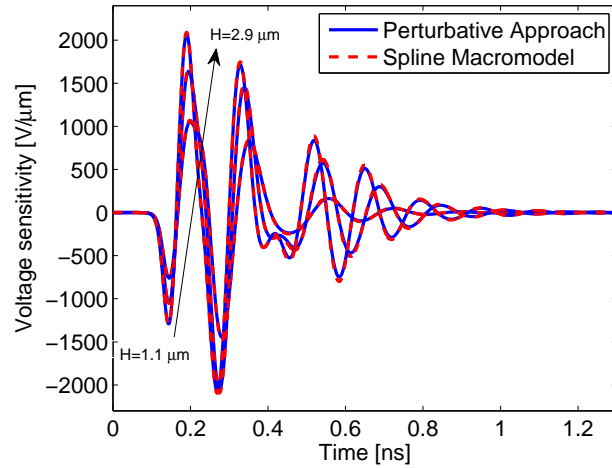$S = [1.2, \ 3.3, \ 5.7] \ \mu m \ and \ H = 2.3 \ \mu m.$

Figure A.7: Example A.5.2. Voltage sensitivity with respect to the spacing, at the input port of the victim line for $H = [1.1,\ 1.9,\ 2.9]\ \mu m$ and $S = 2.8\ \mu m$.
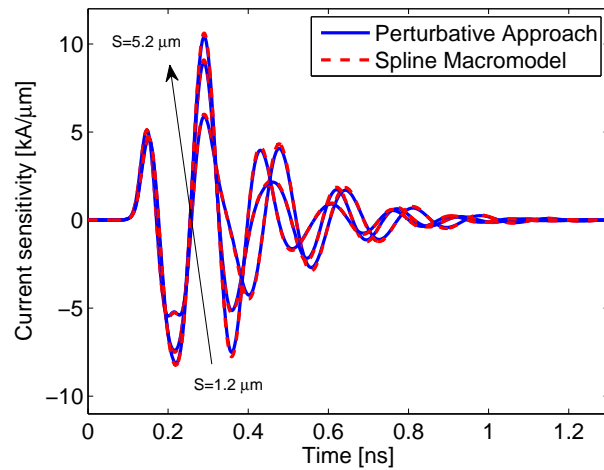

Figure A.8: Example A.5.2. Current sensitivity with respect to the height, at the input port of the driven line for $S = [1.2,\ 3.3,\ 5.2]\ \mu m$ and $H = 2.1\ \mu m$.

conventional SPICE-like solvers. Numerical interpolation of the p.u.l. parameters and evaluation, performed with numerical techniques, of the corresponding sensitivity with respect to physical or geometrical parameters, are used to calculate the spectral decomposition over the entire design space. This leads to a parametric sensitivity analysis that avoids any similarity transformation and incorporates nonlinear terminations in a straightforward way. The new proposed technique is validated by comparing the MTL port currents and voltages with classic approaches (TLT-IFFT) and (TLT-NLS). Time-domain simulations confirm reliability and robustness of the proposed method.

References

[1] A. Deutsch. *Electrical characteristics of interconnects for high-performance systems*. Proc. IEEE, 86(2):315–357, Feb. 1998.

[2] M. Nakhla and R. Achar. *Handbook on VLSI*. Boca Raton, FL: CRC, 2000.

[3] F. Ferranti, G. Antonini, T. Dhaene and L. Knockaert. *Parametric Macromodeling of Lossy and Dispersive Multiconductor Transmission Lines*. IEEE Trans. Adv. Packag., 33(2):481–491, May 2010.

[4] F. Ferranti, T. Dhaene, L. Knockaert, and G. Antonini. *Parameterized models for crosstalk analysis in high-speed interconnects*. In Proc. IEEE International Symposium on Electromagnetic Compatibility (EMC), pages 180–185, Aug. 2009.

[5] G. Antonini. *A dyadic Green's function based method for the transient analysis of lossy and dispersive multiconductor transmission lines*. IEEE Trans. Microw. Theory Tech., 56(4):880–895, Apr. 2008.

[6] G. Antonini, L. De Camillis, and F. Ruscitti. *A spectral approach to frequency-domain sensitivity analysis of multiconductor transmission lines*. IEEE Microw. Wireless Compon. Lett., pages 65–67, Feb. 2009.

[7] Jun-Fa Mao, E. S. Kuh. *Fast simulation and sensitivity analysis of lossy transmission lines by the method of characteristics*. Circuits and Systems I: Fundamental Theory and Applications, IEEE Transactions on, 44(5):391–401, May 1997.

[8] N. M. Nakhla, A. Dounavis, M. S. Nakhla, and R. Achar. *Delay-extraction-based sensitivity analysis of multiconductor transmission lines with nonlinear terminations*. IEEE Trans. Microw. Theory Tech., 53(11):3520–3530, Nov. 2005.

[9] R. Achar, M. Nakhla. *Simulation of High-Speed Interconnects*. Proc. IEEE, 89(5):693–728, May 2001.

[10] G. Antonini. *SPICE Equivalent Circuits of Frequency-Domain Responses*. IEEE Trans. Electromagn. Compat., 45(3):502–512, Aug. 2003.

[11] C. R. Paul. *Analysis of Multiconductor Transmission Lines*. John Wiley & Sons, New York, NY, second edition, 2008.

[12] L. Knockaert, D. De Zutter, F. Olyslager, E. Laermans, J. De Geest. *Recovering lossy multiconductor transmission line parameters from impedance or scattering representations*. IEEE Trans. Adv. Packag., 25(2):200–205, May 2002.

[13] B. Gustavsen and A. Semlyen. *Rational approximation of frequency domain responses by Vector Fitting*. IEEE Trans. Power Del., 14(3):1052–1061, Jul. 1999.

[14] D. Deschrijver, M. Mrozowski, T. Dhaene, and D. De Zutter. *Macromodeling of Multiport Systems Using a Fast Implementation of the Vector Fitting Method*. IEEE Microw. Wireless Compon. Lett., 18(6):383–385, Jun. 2008.

[15] B. Gustavsen. *Fast passivity enforcement for pole-residue models by perturbation of residue matrix eigenvalues*. IEEE Trans. Power Del., 23(4):2278–2285, Oct. 2008.

[16] A. Semlyen and B. Gustavsen. *A half-size singularity test matrix for fast and reliable passivity assessment of rational models*. IEEE Trans. Power Del., 24(1):pp. 345–351, Jan. 2009.

[17] D. Deschrijver, T. Dhaene and D. De Zutter. *Robust parametric macromodeling using multivariate orthonormal vector fitting*. IEEE Trans. Microw. Theory Tech., 56(7):1661–1667, Jul. 2008.

[18] G. Antonini and L. de Camillis. *Time-Domain Green's Function-Based Sensitivity Analysis of Multiconductor Transmission Lines With Nonlinear Terminations*. IEEE Microw. Wireless Compon. Lett., 19(7), Jul. 2009.

[19] C. -T. Chen. *Linear System Theory and Design, ser. Electrical and Computer Engineering*. Oxford University Press, New York, NY, 1998.

[20] C. -W. Ho, A. E. Ruehli, P. A. Brennan. *The modified nodal approach to network analysis*. IEEE Trans. Circuits Syst., 22(6):504–509, Jun. 1975.

[21] C. de Boor. *A Practical Guide to Splines*. Springer-Verlag, 1978.

[22] F. N. Fritsch and R. E. Carlson. *Monotone Piecewise Cubic Interpolation*. SIAM J. Numerical Analysis, 17:238–246, Nov. 1980.

[23] A. R. Djordjevìc, R. M. Biljìc, V. D. Likar-Smiljanìc, T.K. Sarkar. *Wideband frequency-domain characterization of FR-4 and time-domain causality*. IEEE Trans. Electromagn. Compat., 43(4):662–667, Nov. 2001.

[24] *Simbeor, Electromagnetic Simulation Environment with 3D Full-Wave Field Solver for Multi-Layered Circuits*. Simberian Inc., Seattle.

[25] D. Vande Ginste and D. De Zutter. *Influence of the trapezoidal cross-section of single and coupled inverted embedded microstrip lines on signal integrity*. In Proc. General Assembly and Scientific Symposium XXXth URSI, pages 1 –4, Aug. 2011.

[26] T. Demeester and D. De Zutter. *Quasi–TM Transmission Line Parameters of Coupled Lossy Lines Based on the Dirichlet to Neumann Boundary Operator*. IEEE Trans. Microw. Theory Tech., 56(7):1649–1660, Jul. 2008.

[27] T. Demeester, D. Vande Ginste and D. De Zutter. *Accurate Study of the Electromagnetic and Circuit Behavior of Finite Conducting Wedges and Interconnects with Arbitrary Cross–Sections*. In Proc. IEEE 19th Conference on Electrical Performance of Electronic Packaging and Systems (EPEPS), Austin, Texas, USA, pages 133–136, Oct. 2010.